Controlled synthesis of lanthanide triple-decker complexes comprising up to three different porphyrinoids

Shazia Camilla Soobrattee

This thesis is submitted in partial fulfilment of the requirements of the degree of Doctor of Philosophy at the University of East Anglia

April 2024

Declaration

The research described in this thesis is, to the best of my knowledge, original and my own work except where due reference has been made.

Shazia Camilla Soobrattee

Abstract

Sandwich double and triple decker complexes of phthalocyanine, porphyrins or a mixture of both exhibit particular π-π interactions responsible for their special physical, spectroscopic and electrochemical properties. These properties make them especially suitable for applications such as such as field effect transistors, nonlinear optical materials, sensors, molecular magnets, and multibit molecular information storage, unlike the mono-metallic macrocycle counterparts.

This thesis describes various methods for the synthesis of porphyrin-phthalocyanine-tetrabenzotriazaporphyrin triple decker complexes. These triple deckers contain either an unsymmetrical or a symmetrical dyad. The unsymmetrical dyad contains a porphyrin and a tetrabenzotriazaporphyrin molecules linked together by a flexible decyl and dodecyl chain while the symmetrical dyad consists of two tetrabenzotriazaporphrin molecules linked together by a decyl chain. Phthalocyanine and different lanthanide metals such as La, Nd, Eu, were incorporated into the sandwich structure. The synthetic challenges are discussed, and the eventual successful methods described, the 'one pot' reaction was found to be the most efficient. Spectroscopic analysis such as MALDI-TOF MS, NMR and UV-Vis were used to identify and determine the structure of the synthesised triple deckers. When La salt was used in the synthesis, the results obtained from both unsymmetrical C_{10} and C_{12} dyad were similar but differ from the known the porphyrin-phthalocyanine-porphyrin triple decker. It is found that the phthalocyanine unit is not in the middle of the sandwich and lies on the outside next to the Por unit rather than the tetrabenzotriazaporphrin unit. X-Ray crystallography analysis would give a conclusive result, however so far suitable crystals were not grown successfully. Many attempts to synthesise the La triple decker using the symmetrical dyad and phthalocyanine proved to be unsuccessful, instead, a double decker was formed. An unexpected result was obtained from the Nd triple decker synthesis where one of the fractions has its units orientated as follows porphyrin-phthalocyanine-tetrabenzotriazaporphrin, while the UV-Vis of the other fraction was similar to the newly synthesised La triple decker. The Eu triple decker has its units oriented similar to one of the fractions of Nd triple decker that is exclusively porphyrin-phthalocyanine-tetrabenzotriazaporphrin.

This thesis is dedicated to my beloved parents

Cader Soobrattee and Nassima Soobrattee

&

My sister

Farihah

Acknowledgements

This thesis would not have been possible without the guidance of the almighty God. The journey from laboratory work till writing of this thesis has been a great experience and has the contributions of many people. I have depended upon countless acts of support, generosity and guidance.

I owe sincere and earnest thankfulness to my supervisor, Professor Andrew Cammidge for his valuable and constructive suggestions throughout this project. His useful critiques and willingness to give his precious time are much appreciated. This thesis would not have been possible without his guidance and support during all the time of research and writing up of this thesis.

I am really grateful to Dr. Isabelle Fernandes for her unlimited help. She has been abundantly helpful and supported me throughout the course. I would also like to express my appreciation to Dr Chris Richard for his commitment. I also thank Dr. David Hughes for X-Ray crystallography service. I would also like to thank Dr Philip Wilson and Dr Andreas Baumeister for MALDI trainings. I also thank Dr Colin Macdonald, Dr Matthew Wallace and Dr Trey Koev for their generous time regarding NMR.

I am also grateful to the teaching, technical and administrative staff, of the school of chemistry at UEA for their help throughout my degree.

I would like to express my deepest appreciation to Dr Norah Alsaiari. Her friendship and support during the challenging times in the lab have always been motivating and helpful. I am also thankful to Dr Ahad Alsahli, Ibtesam Mashnoy, Ala Alturk and Muteb Alshammari.

I would like to extend my sincere thanks Dr Paul Mcdermott, Dr Christopher Hamilton, Dr Randa Zoqlam and Dr Leoni Palmer from the pharmacy department at UEA. In a way or another they contributed to my skills and personal developments as a teaching assistant for the undergraduates.

I would also like to thank my parents and I wish to express my greatest gratitude and without them, I would not have had the strength to complete my PhD. Their encouragement, love and support are without bounds. I would like to extend my appreciation to my sister who has helped me throughout the course and never failed to support me in the highs and lows, for having always believed in me and for being always present when needed.

Abbreviations

Ac	acetate
AcOH	Acetic acid
acac	acetylacetonate
aq	aqueous
Ar	aromatic/ aryl
br	broad
BINAP	2,2′-Bis(diphenylphosphino)-1,1′-binaphthalene
Bn	benzyl
Cat.	Catalyst
conc.	concentrated
$CDCl_3$	Deuterated chloroform
C_{10}	decane
°C	Degrees Celsius
δ	chemical shift in ppm
d	doublet
Da	Dalton
DABCO	1,4-Diazabicyclo[2.2.2]octane
DBN	1,5-diazabicyclo[4.3.0]non-5-ene
DBU	1,8-diazabicyclo[5.4.0]undec-7-ene
DCM	Dichloromethane
DD	Double decker
DDQ	2,3-Dichloro-5,6-dicyano-1,4- benzoquinone
DMAE	Dimethylaminoethanol
DMF	N, N-dimethylformamide
DMSO	Dimethylsulfoxide
DzPz	Tetradiazepinoporphyrazine
Et_2O	diethylether
eq.	equivalent
et al.	Et alii
Et	ethyl
g	Grams
h	Hours

HOMO	Highest occupied molecular orbital
HCl	Hydrochloric acid
J	Coupling value
K	Kelvin
Ln	Lanthanide
LiHMDS	Lithium hexamethyldisilazide
LUMO	Lowest unoccupied molecular orbital
m	multiplet
M (in structures)	Metal
MALDI-TOF	matrix-assisted laser desorption/ionisation-time-of-flight
Me	methyl
MeOH	Methanol
npn	Naphthalonitrile
OMe	methoxy-
min	minute(s)
mmol	millimole
m.p.	melting point
MW	Microwave
NMR	Nuclear Magnetic Resonance
o-	*ortho*
Por	porphyrin
p-	*para*
PE	Petroleum Ether
Pc	Phthalocyanine
Ph	phenyl
ppb	Parts per billion
ppm	parts per million
py	pyridine
RT	Room Temperature
s	singlet
SAP	Square-antiprismatic
SP	Square-prismatic
SMM	Single Molecule Magnets

t-Bu	tertiary butyl
t	triplet
TBDAP	TetraBenzoDiAzaPorphyrin
TBP	TetrabenzoPorphyrin
TBTAP	TetraBenzoTriazaPorphyrin
TD	Triple Decker
TCB	1,2,4-tricholorobenzene
TEA	Triethylamine
THF	Tetrahydrofuran
TFA	Trifluoroacetic acid
TLC	Thin Layer Chromatography
TPP- OH	5,10,15-tris-phenyl-20-(*p*-hydroxyphenyl) porphyrin
UV-Vis	Ultraviolet-visible
W	Watt(s)

Table of Contents

Chapter 1
Introduction

1. Introduction

1.1 Porphyrins

The word Porphyrin is derived from the Greek word *porphura* which means purple. Porphyrins are deeply pigmented organic molecules made up of linked pyrrolic units, forming a macrocycle.[1] These units are linked together by 4 unsaturated =CH-H groups known as methine. Porphyrins play an essential role in biochemical processes, they are present in chlorophyll in green plants and haemoglobin in animals.[2,3] In these biochemical processes they are involved in enzyme catalysis, oxygen transfer and storage, electron transfer and other processes.[4,5]

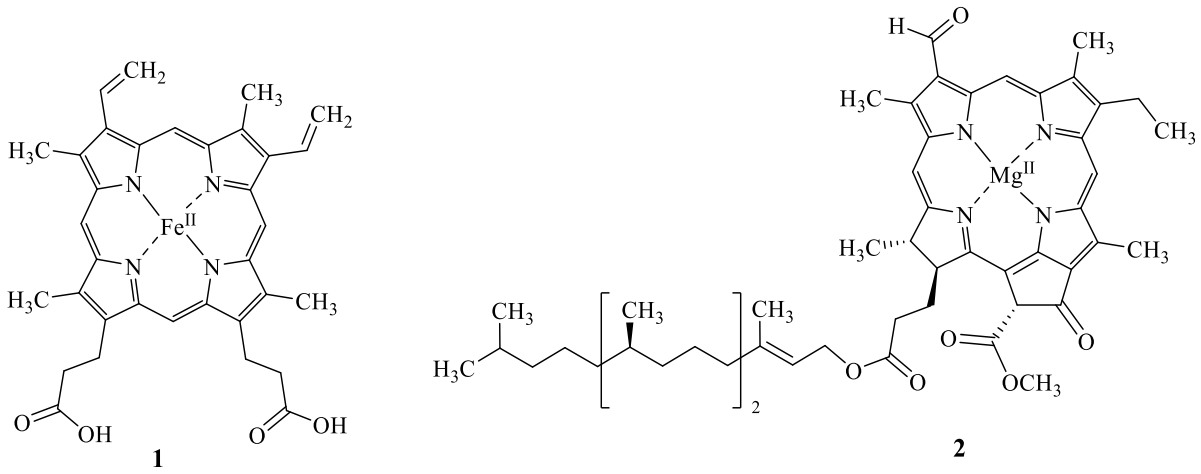

Figure 1.1: Naturally occurring porphyrins.

1.1.1 Nomenclature of Porphyrins

According to IUPAC convention, the 2, 3, 7, 8, 12, 13, 17 and 18 positions are commonly referred to as the β-positions. The α-positions on the other hand are numbered as 1, 4, 6, 9, 11, 14, 16 and 19. The positions 5, 10, 15 and 20 are identified as the *meso* positions.[6–8] The two nitrogen atoms bonded to the hydrogen atoms are positioned at 21 and 23 (figure1.2). The *meso*–substituted porphyrins are artificially made while the β-substituted porphyrin is widely present in natural products (figure 1.3).[9]

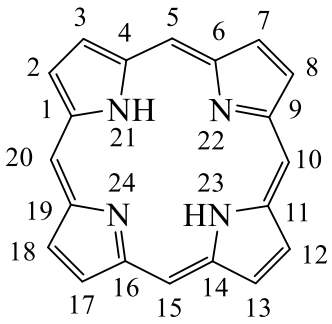

Figure 1.2: Structure of free base porphyrin (**3**) and the IUPAC numbering.

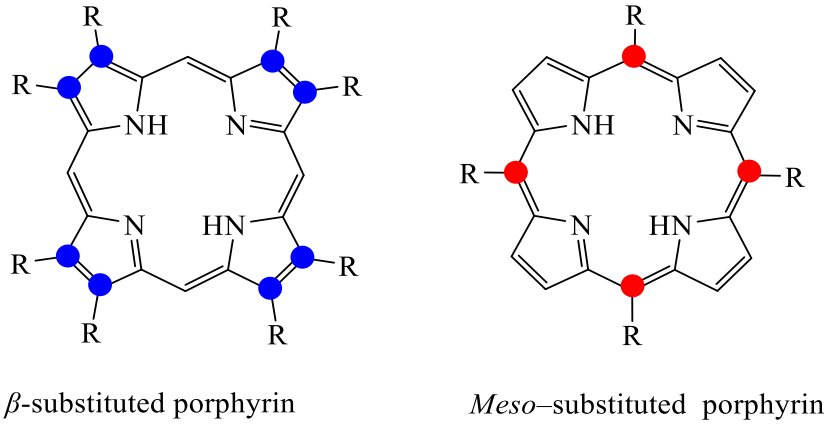

β-substituted porphyrin *Meso*–substituted porphyrin

Figure 1.3: Structure of *β*-substituted and meso-substituted porphyrins.

1.1.2 Aromaticity

The porphyrin core has a planar structure and is highly conjugated molecule and exibits many resonance forms.[10] The macrocycle is a π system of 22 π electrons of which 18 π electrons form a delocalisation system on the ring according to the Hückel rule of aromaticity (4n+2 delocalised π electrons). Some studies from ^{13}C-NMR and X-ray evidence suggest that the 16 membered ring of the 18 π electron systems is more favoured for the delocalisation pathway in the porphyrins (figure 1.4).[11]

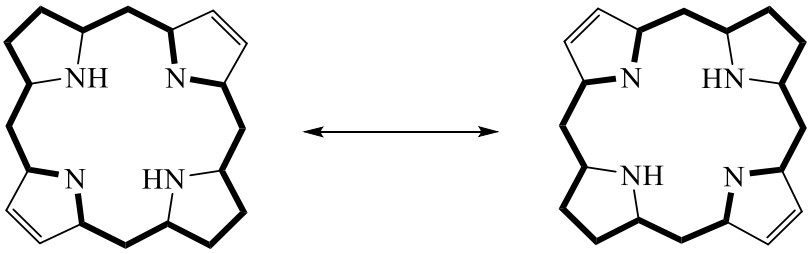

Figure 1.4: Delocalisation of 18 π electrons on the porphyrin core.

1.1.3 Synthesis of porphyrins

Inspiration from the fascinating functions of porphyrin molecules in living organisms and their ability to bind to metals led to the study of the synthetic porphyrins in 1935.[12] Rothemund investigated the synthesis of *meso*-tetrasubstituted porphyrin, by reacting acetaldehyde and pyrrole in methanol. In 1941,[13] he altered the reaction conditions by heating a mixture of pyrrole and benzaldehyde in pyridine in a sealed flask at 220 °C for 48 hours. The yield obtained for the blue crystals of the *meso*- tetraphenyl porphyrin was less than 10%, such a low yield was attributed to the severe reaction conditions. It was found that the main *meso*-substituted chlorin by-product was formed which under oxidative conditions could be converted to the product (scheme 1.1).

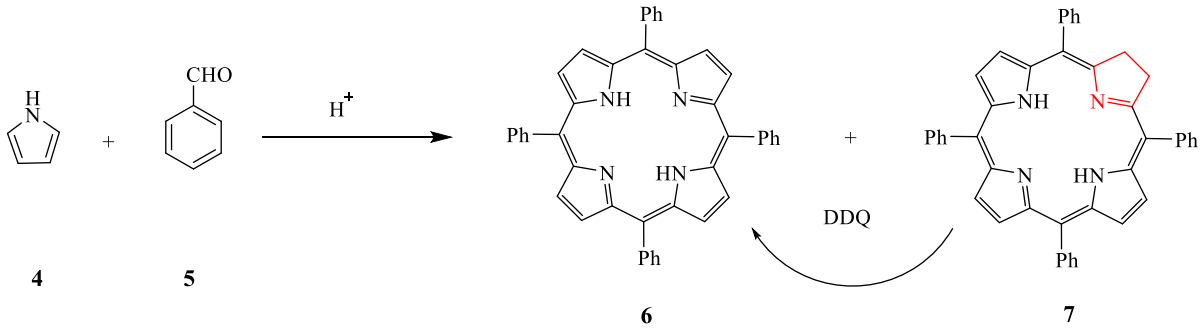

Scheme 1.1: Synthesis of 5,10,15,20-tetraphenyl porphyrin.

In 1967, the procedure to synthesise the *meso*-substituted porphyrin was modified by Adler, Longo and co-workers[14] in this alternative method the reaction was carried out in acidic conditions and in the presence of air (scheme 1.2).

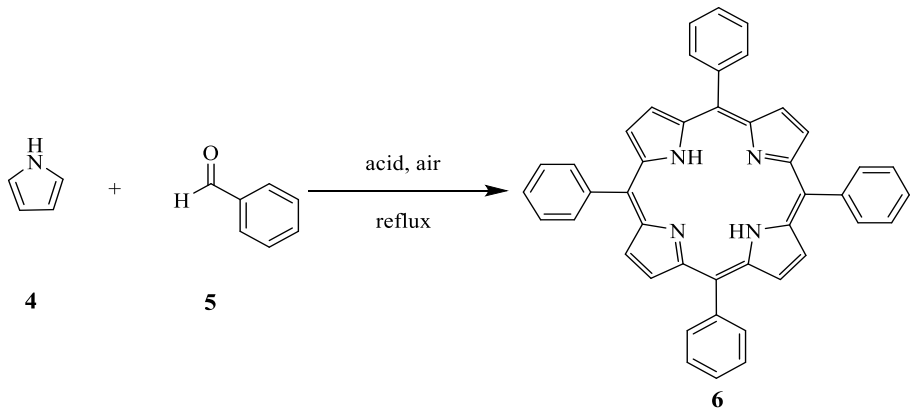

Scheme 1.2: Adler's procedure.

Different solvents and a range of concentrations of the reactants were investigated resulting in a yield of 30–40%. The concentration of the by-product chlorin was reduced compared to the Rothemund synthesis.[12] It was noticed that when the reaction was carried out in propionic acid, the reaction was faster, but a lower yield was obtained compared to acetic acid, but the product was easily crystallised in the former acid.

The Lindsey method[15] involves a 'two step- one flask' reaction for the synthesis of *meso*-substituted porphyrins. The reaction is carried out under gentle conditions such that equilibrium is achieved during the condensation reducing possible side reactions. The reaction requires a condensation of pyrrole with aldehydes in chloroform or dichloromethane in the presence of acid catalyst, TFA or boron trifloride etherate, and under inert atmosphere and room temperature (scheme 1.3). A stoichiometric amount of DDQ or *p*-chloranil is added to oxidise the initially formed porphyrinogen.[15,16]

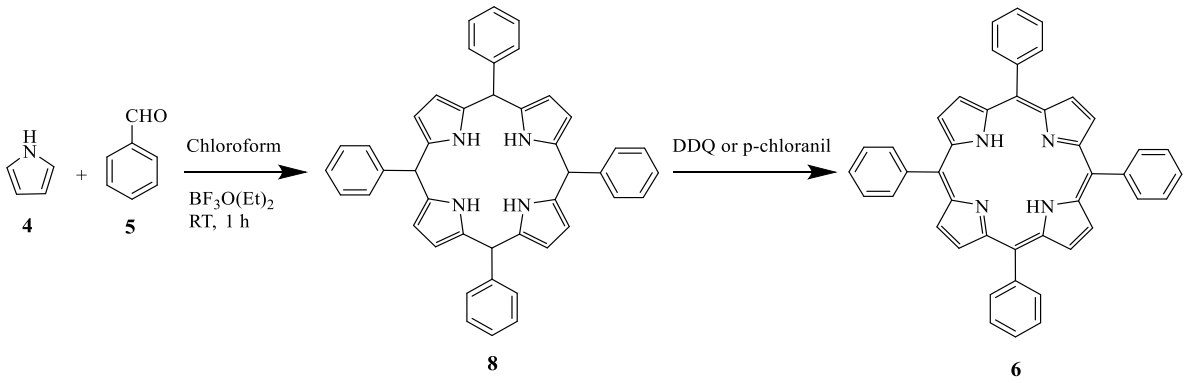

Scheme 1.3: Two-step one-flask room-temperature synthesis of porphyrins.

1.1.4 UV-Vis spectroscopy of porphyrin

As previously mentioned in the introduction about the characteristics of porphyrins, these structures are highly conjugated π-electron systems that leads to the intensity and colour of porphyrins. They are able to absorb in two distinct regions of the visible spectrum, one near the ultraviolet and the other in the mid-visible region.

Research conducted on the porphyrins has demonstrated that changes in the conjugation pathway and the symmetry of the compound would influence the UV-Vis absorption spectrum. Gouterman has presented a four-orbital model [two highest occupied π orbitals and two lowest unoccupied π* orbital] in order to decipher the absorption spectra of porphyrins. According to this theory, the absorption bands in porphyrin spectra are caused by the transition between two HOMOs and two LUMOs (figure 1.5).[17] The energies of these transitions alter in presence of substituents on the ring and the identities of the coordinating metal.

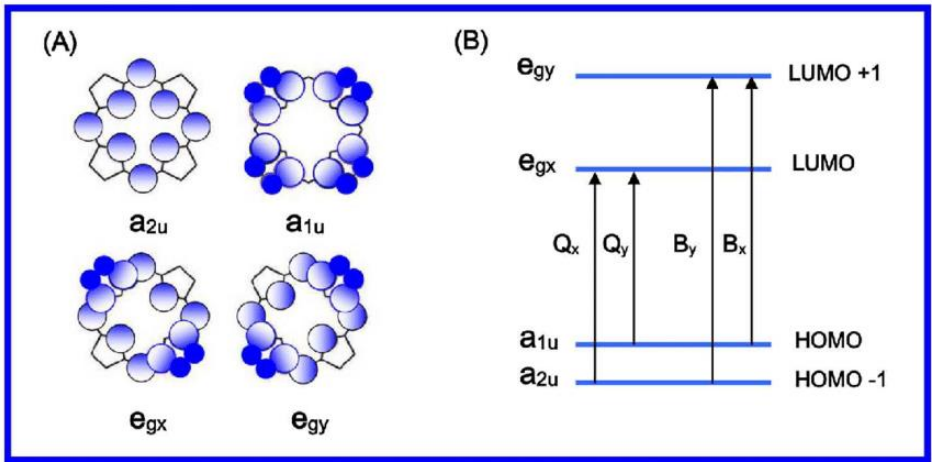

Figure 1.5: Porphyrin HOMOs and LUMOs. A) Gouterman's Orbital representation. B) Energy level transitions of the orbitals according to Gouterman's theory.

For a free base porphyrin which has a D_{2h} symmetry, its electronic absorption spectrum consists of two distinct regions. A transition from the ground state to the second excited state (S0→ S2) is called the Soret band or B band. The range of the absorption is between 380–500 nm but this depends on whether it is a *β*- or *meso*- substituted porphyrin. The second region is a weaker transition to the first excited state (S0→S1) and ranges between 500–700nm is known as the Q bands (figure 1.6).[18]

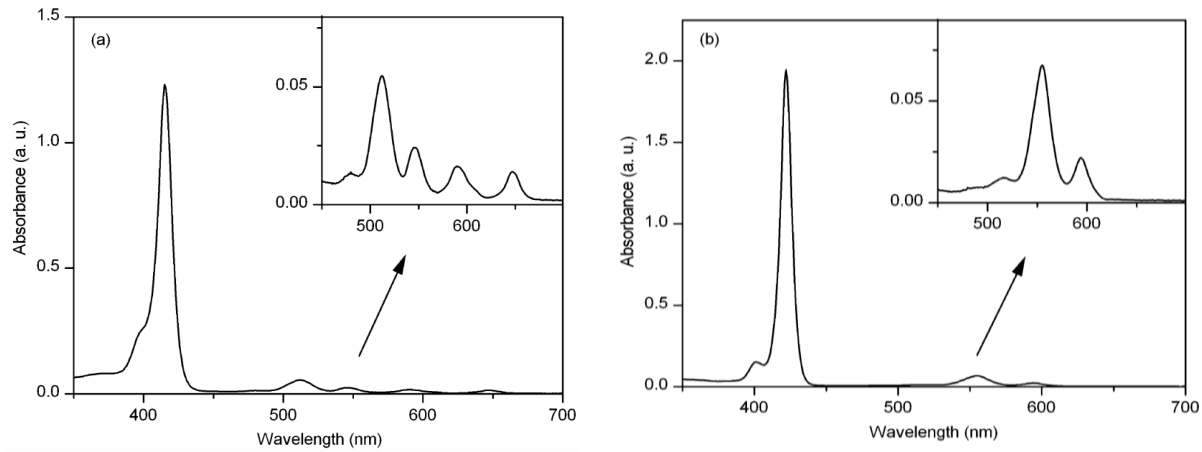

Figure 1.6: Typical UV-Vis spectra for (a) a free-base porphyrin and (b) a porphyrin–metal complex.[18]

Metalloporphyrins however simplify the UV-Vis spectrum. Two Q bands are produced instead of four Q bands as a higher D_{4h} symmetry is involved but the Soret band is barely affected.[18]

1.2 Phthalocyanine

Another analogue of these macrocyclic tetrapyrrole compounds is the phthalocyanine (Pc). In Pc, the 4 methine groups (=CH-H) from the porphyrin are replaced by 4 imine groups (-N=C) i.e the Pc contains 4 isoindole units which are linked by nitrogen atoms known as aza-bridges. Phthalocyanine is a ring system consisting of 18 π electrons which is delocalized over alternate carbon and nitrogen atoms. As a result, this delocalisation systems gives the molecule unique physical and chemical properties.[19,20]

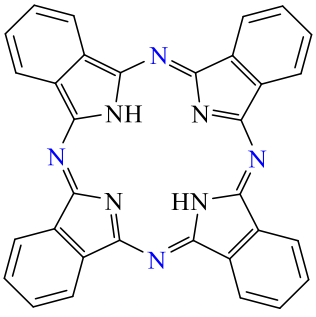

9

Phthalocyanine

Figure 1.7: Structure of Phthalocyanine (Pc).

1.2.1 Synthesis of Phthalocyanine

Phthalocyanine is prepared through the cyclotetramerization of different phthalic acid derivatives such as phthalimide, phthalic anhydride, phthalonitrile and diiminoisoindoline (scheme 1.4).[21] Phthalocyanine was first synthesised in the early 20th century by Braun and Tcherniac when *o*-cyanobenzamide was heated in ethanol, resulting in a blue substance (Pc).[22] The common method for preparation of phthalocyanines and their complexes is using phthalonitriles and by heating with a metal template, such as lithium in high boiling point solvent such as alcohols. It was found that by using phthalonitriles as precursor is that they are easy to handle and produced phthalocyanines and their complexes in good yield. Other precursors such as phthalimide and other phthalic acid derivatives often give unreliable results. This method was studied by Linstead.[23] Heating phthalonitrile with catalytic amount of DBU or DBN in the presence of metal salt resulted in Pcs or metal Pcs in high yield, while weaker bases such as piperidine and TEA gave a low yield of the compounds.[24,25]

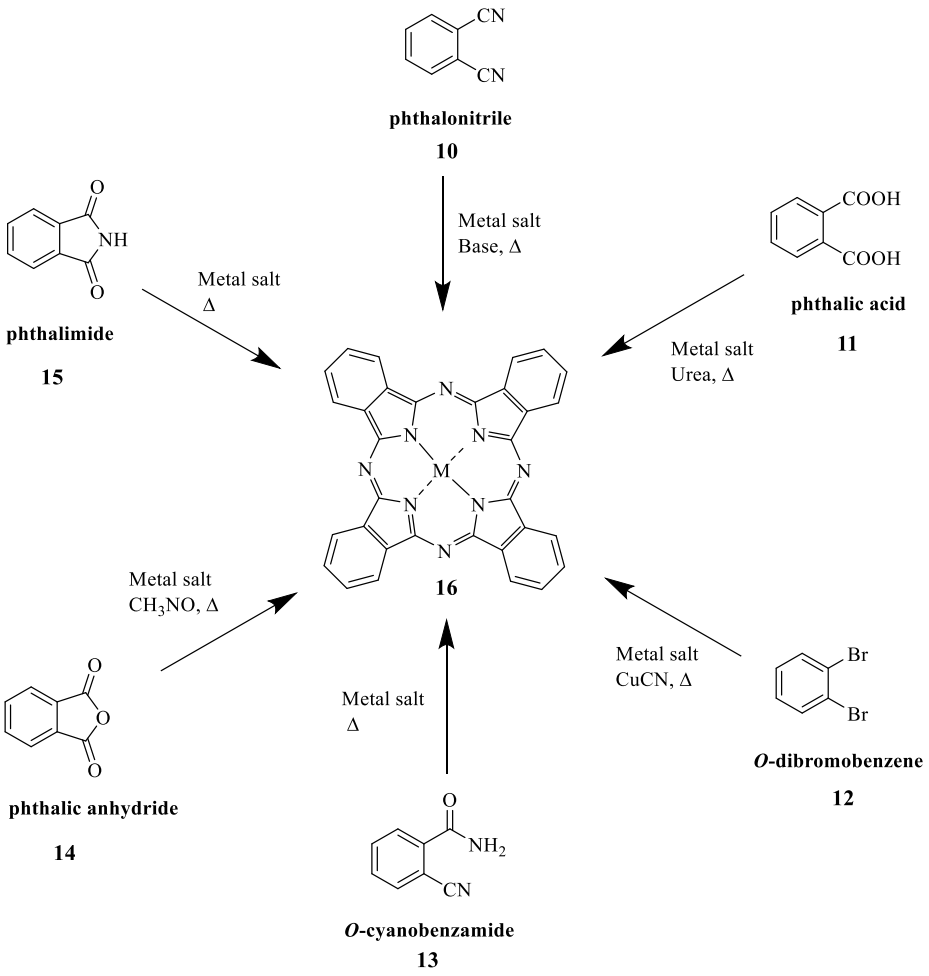

Scheme 1.4: Main synthetic routes for preparing phthalocyanines.

There are structural similarities between phthalocyanine and porphyrins and this led researchers to further investigate the physicochemical properties of Pc.[26–28] This proved to be challenging as the unsubstituted phthalocyanines are mostly insoluble in many organic solvents. To overcome this problem, chemists devised new methods to functionalise the Pc ring by introducing substituents onto the benzene ring. This caused a substantial increase in the solubility of new compounds and thus they can be analysed. A lesser studied modification involves the replacement of the imine bridging group by one or several methine moieties which lead to the formation of hybrid structures (figure 1.8).[29]

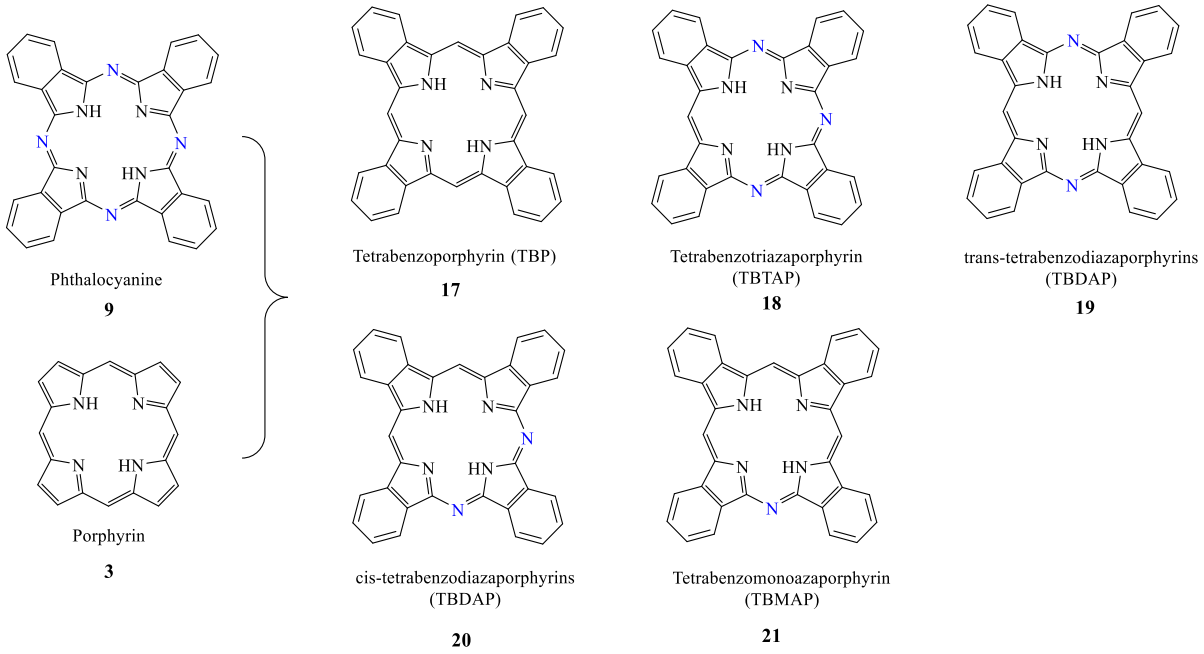

Figure 1.8: Phthalocyanine/ porphyrin hybrids.

1.3 Tetrabenzotriazaporphyrins (TBTAP)

The hybrid molecule TBTAP is structurally related to both Pc and tetrabenzoporphyrin (TBP). The only difference is that one aza-nitrogen of the Pc ring has been replaced by a methine group as shown in figure 1.9. The hybrid molecule, TBTAP combines the properties of both phthalocyanine and TBP. It combines the stability, robustness and intense long-wavelength electronic absorptions seen in phthalocyanines. In addition, the TBTAP can be functionalised at the meso-carbon which leads to a variety of possibilities that the TBTAP can undergo, further functionalisation or the ability to link to other moieties and surfaces.[29]

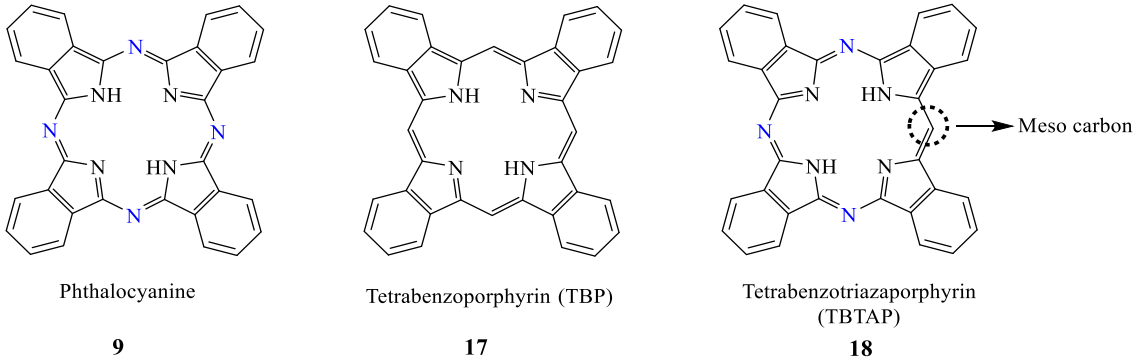

Phthalocyanine **9** | Tetrabenzoporphyrin (TBP) **17** | Tetrabenzotriazaporphyrin (TBTAP) **18**

Figure 1.9: Phthalocyanine/ porphyrin hybrids.

1.3.1 Synthesis of TBTAPs

Synthesis and isolation of TBTAP from a mixture of products proved to be very challenging, hence reviews of this molecule in literature are scarce. In 1937, Cu-TBTAP was successfully synthesised and isolated by Helberger and von Rebay.[30] Phthalonitrile (1,2-dicyanobenzene) with *o*-cyanoacetophenone in an equimolar ratio in the presence of copper (I) chloride were mixed and heated in quinoline (scheme 1.5). The resulting mixture was left to cool and upon addition of pyridine, a violet crystal of compound **22** was obtained. The authors did not report the UV-Vis spectrum of the product.

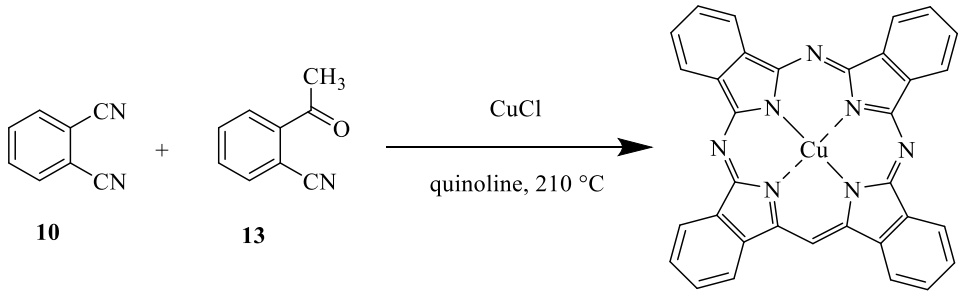

10 + **13** → **22**

Scheme 1.5: The first synthesis of Cu-TBTAP by Helberger and von Rebay.

Linstead and co-workers[31] used a modified procedure to synthesise Cu-TBTAP using the condensation product from the reaction of 1,3-diiminoisoindoline and malonic acid to yield **23** which was subsequently reacted with phthalonitrile to form the product **22** (scheme 1.6). The compound was characterised by UV-Vis spectroscopy.

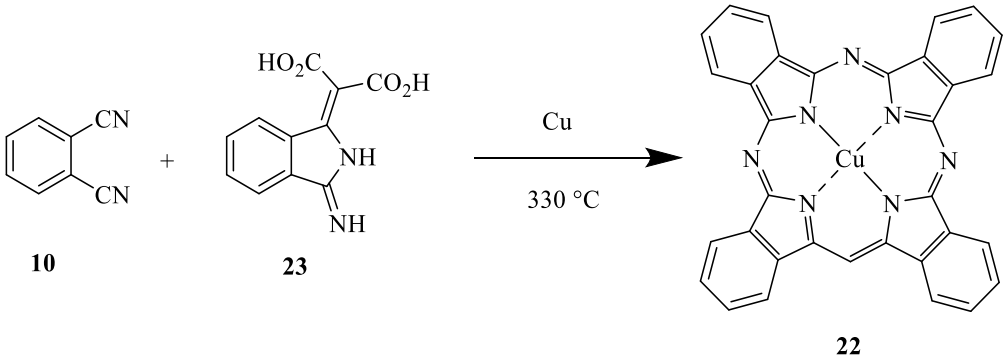

Scheme 1.6: Lindstead's synthesis of Cu-TBTAP using **23** as a precursor.

Phthalimidine acetic acid **24** or 3-methylene phthalimidine **25**, which is prepared by heating acid **24** in water at 80 °C, served as a source of methine bridge.[32] Phthalonitrile was reacted either with **25** or its carboxylic derivative **24** at 250 °C with copper salt (scheme 1.7). A 30% yield of complex **22** was achieved by Dent under similar conditions.[32] The author observed that when 3 moles of phthalonitrile, 1 mole of Phthalimidine acetic acid and 1 mole of copper chloride was used, this yielded 70 – 80% of Cu-TBTAP with small amount of copper phthalocyanine as an impurity. When a 1:3 ratio of phthalonitrile to phthalimidine acetic acid was used, the desired product (Cu-TBTAP) was not formed. Using methyl-phthalimidine acetate instead of phthalimidine acetic acid still proved to be unsuccessful.

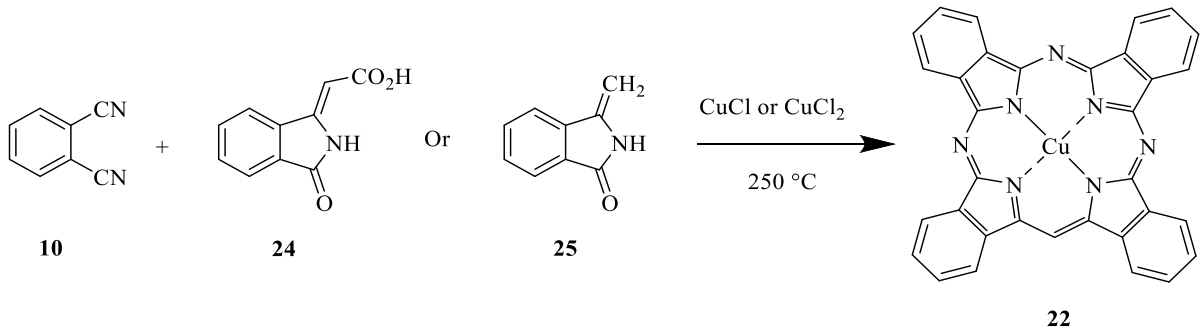

Scheme 1.7: Dent's synthesis of Cu-TBTAP using phthalimidine derivatives.

In 1939, Linstead and co-workers[23] investigated the reaction between phthalonitrile and organometallic compounds. Mg-TBTAP was synthesised in a two-step procedure. The first step involved the reaction between phthalonitrile and the organometallic reagent in low boiling ethereal solvent. The second step involved distilling off the solvent and heating the residue at 200 °C in a high boiling point solvent such as quinoline, cyclohexanol or α-naphthyl methyl

ether. Following an acid work-up, 40% yield of a green pigment was obtained (scheme 1.8). Evidences from X-ray diffraction and several quantitative oxidations, metal-free tetrabenzotriazaporphyrin **18** was identified.[23]

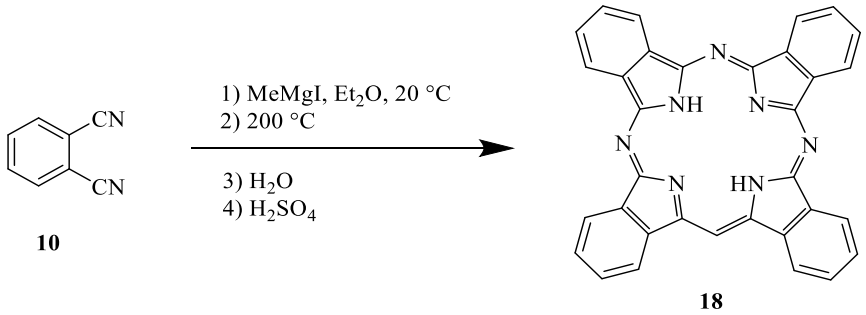

Scheme 1.8: General synthetic route for metal-free TBTAP.

Unsubstituted tetrabenzotriazaporphyrin derivatives are insoluble in organic solvents as observed by many authors. TBTAP molecules which are unsubstituted at the *meso*- carbon are partially soluble in most organic solvents. However, Mg and Cd complexes are found to be more soluble than any other metal complexes. The procedure developed by Linstead and co-workers[31]was modified so as to incorporate substituents at the *meso*-position. Magnesium complex **26** of *meso*-(p-tolyl) TBTAP derivative was formed. To afford the free ligand, complex **26** was demetallated using concentrated HCl (scheme 1.9).

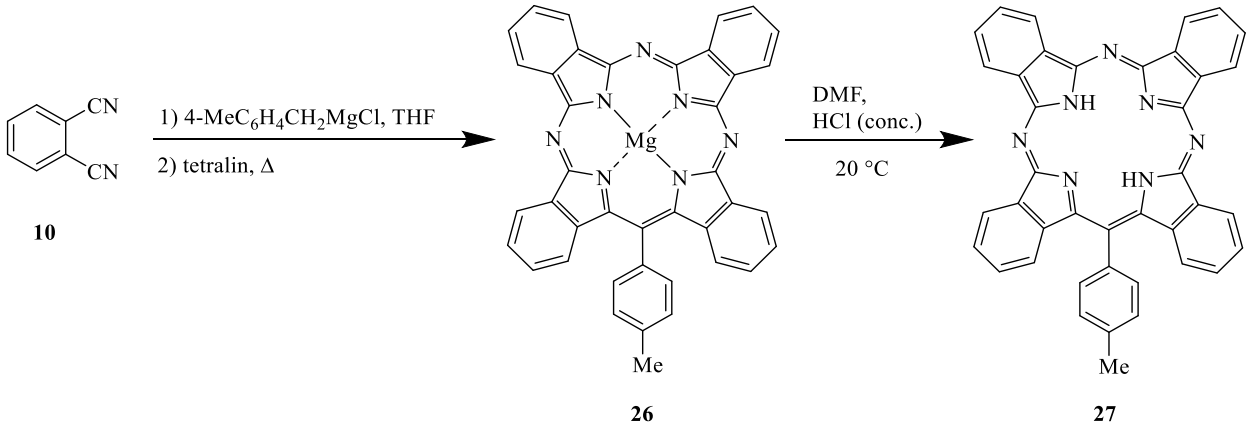

Scheme 1.9: Synthesis of the MgTBTAP-(p-tolyl) and its demetallation.

Leznoff and McKeown,[33] used various Grignard reagents in the preparation of *meso*-substituted TBTAPs from sterically hindered phthalonitriles. A 15% yield of *meso*-

phenyltetrabenzotriazaporphyrin was obtained from the reaction of phthalonitrile with benzylmagnesium chloride at 200 °C for 22 h in quinoline (scheme 1.10). Separation of the free macrocyclic ligand from unsubstituted phthalocyanine was tedious because of low solubility of the former compound in most organic solvents. However, its metallated magnesium complex can be isolated.

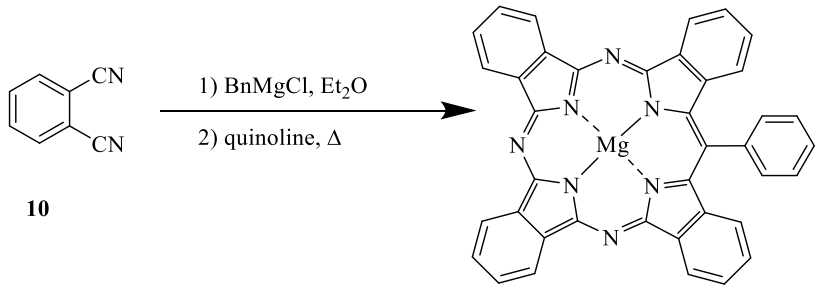

10 **28**

Scheme 1.10: Synthesis of Mg-TBTAP-Ph by Leznoff.

A modified version of the synthesis of tetrabenzotriazaporphyrins by introducing substituents with long hydrocarbon chains at the *meso*-position of the macrocycle was also carried out by Leznoff and co-workers.[34] The reaction was performed using alkyl magnesium halides and unsubstituted phthalonitrile in diethyl ether at 20 °C. The ether was eventually distilled off and the reaction mixture was subsequently heated to 120–185 °C in quinoline. The Mg complexes **29 a-d** were purified by chromatography and were finally demetallated by heating in acetic acid for 2 h and then recrystallised in toluene. Treatment of the free ligands **30 a-d** with a large excess of zinc acetate in a DMF and toluene system afforded the corresponding zinc complexes **31 a-d**. The zinc complexes were finally recrystallised from diethyl ether. The authors confirmed that introducing the alkyl substituents at the *meso*-position facilitates the purification process of both free macrocycles and their complexes (scheme 1.11).

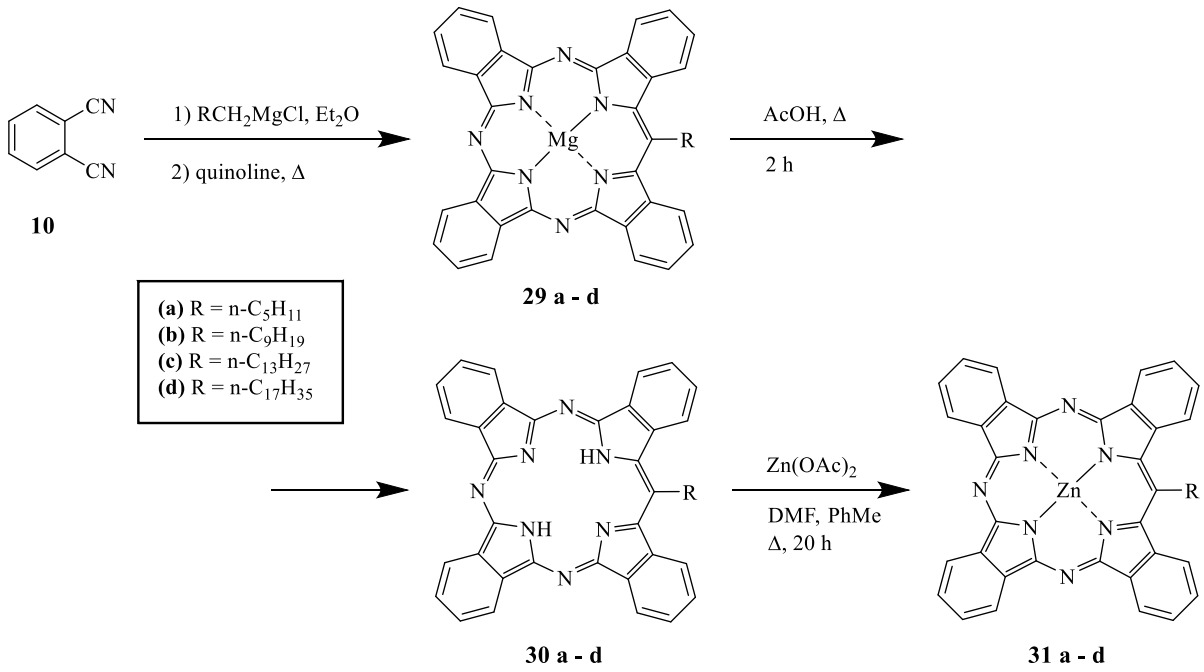

Scheme 1.11: Synthesis of meso-alkyl substituted TBTAP derivatives.

Galani and co-workers[35,36] prepared a series of Mg and Zn complexes of *meso*-substituted TBTAP. Refluxing 1,3-diiminoisoindoline **32** with a carboxylic acid which has a CH_2 group adjacent to the carboxy group and either ZnO or MgO as template agent at 290–300 °C produced a series of hybrid molecules. The yield of the tetrabenzotriazaporphyrin was less than 10%. The highly stable Zn complex bearing phenyl-substituted tetrabenzotriazaporphyrin could not be demetallated. The authors noticed that when the ratio of carboxylic acid to 1,3-diiminoisoindoline increases, the formation of complexes with more methine bridges was favoured. Complexes with more nitrogen bridges formed when the amount of carboxylic acid used is lowered. The yields of tetrabenzotriazaporphyrin derivatives **28** and **33** were 8.5% and 5%, respectively (scheme 1.12).

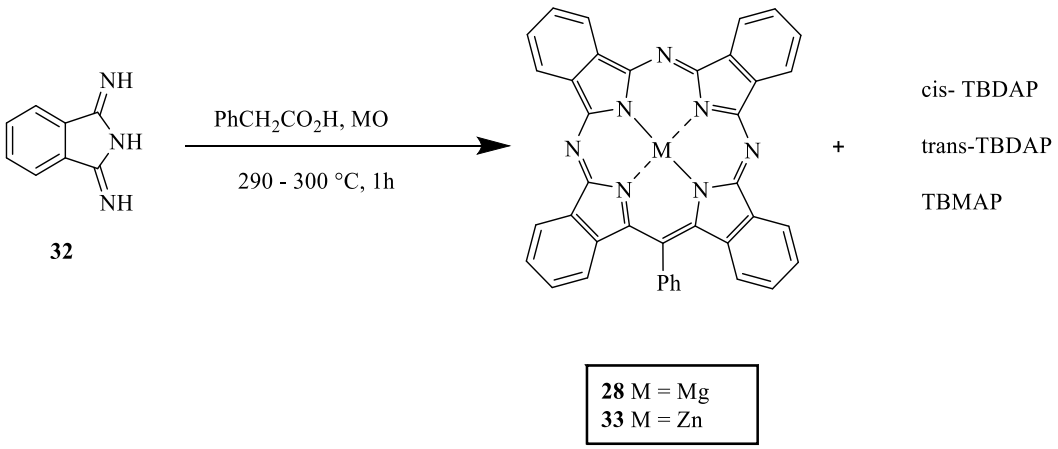

Scheme 1.12: Metal-TBTAP-Ph complexes reported by Galanin.

Galani and co-workers investigated the effects of using different aliphatic acids and the condensation of 1,3-diiminoisoindoline **32** in the presence of ZnO. These reactions yielded Zn complexes **34 a-c** and only *meso*-alkyl tetrabenzotriazaporphyrins were isolated with yields no more than 27% (scheme 1.13).[37]

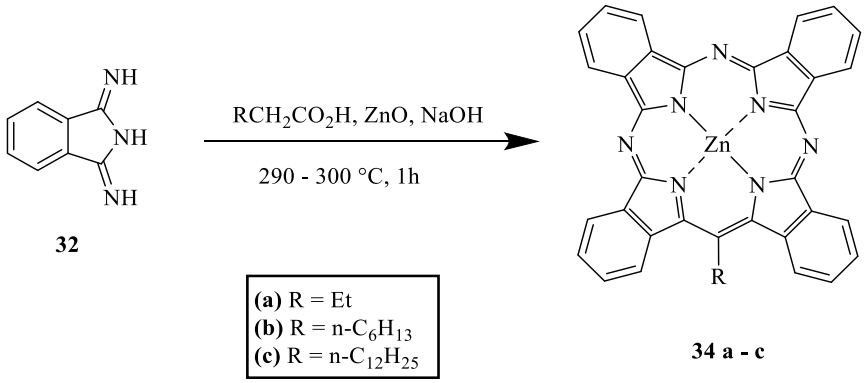

Scheme 1.13: Galanin's synthesis of meso-alkyl-TBTAPs.

In 2011, Tomilov and co-workers,[38] tried the mixed condensation of arylacetonitriles **35** with unsubstituted phthalonitrile in the presence of magnesium powder. Heating of the reaction from 240–300 °C resulted in the formation of magnesium complexes of *meso*-aryl substituted **36 a-e** with the only by-product magnesium phthalocyanine. The authors found another way of initiating the reaction through microwave irradiation of starting materials. The benefit of this process is that a higher yield of TBTAP was achieved in a short period of time. A demetallation

process involving sulfuric acid under mild conditions was employed. Under these conditions, *meso*-phenyl-substituted TBTAP was prepared in a 98% yield **37 a** (scheme 1.14).

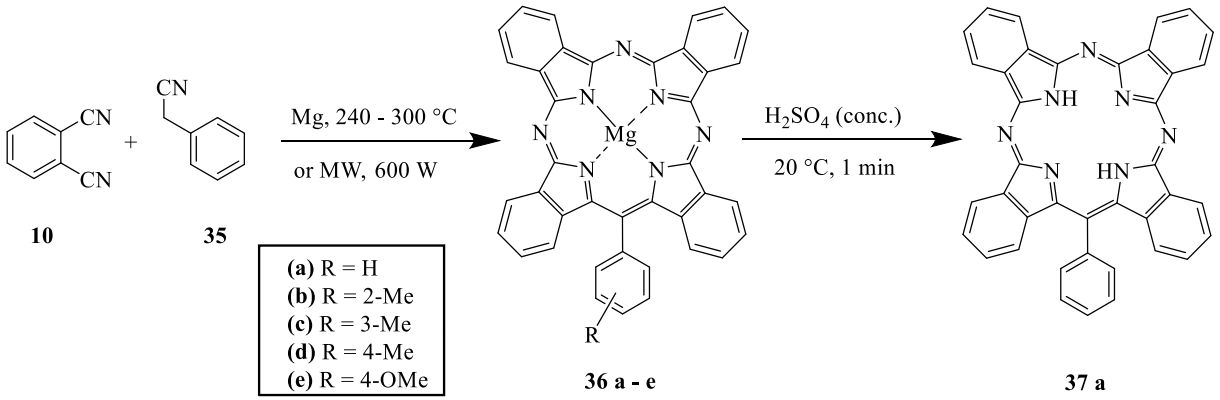

Scheme 1.14: Aryl acetonitriles for the synthesis of meso-substituted TBTAPs.

A main drawback to produce metal-free tetrabenzotriazaporphyrins from complexes containing Zn (II) as central ion is that the demetallation process proved to be unfavorable.[36] However, Tomilova and co-workers were first to report the quantitative demetallation of Zn-TBTAP under non-traditional conditions, by heating the complex **33** in an ionic liquid i.e., pyridinium hydrochloride to afford the free ligand **37 a** (scheme 1.15).[39]

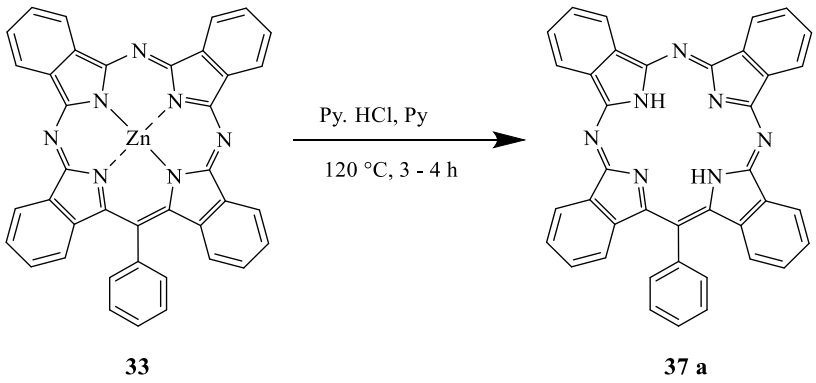

Scheme 1.15: Non-traditional conditions for ZnTBTAP-Ph demetallation.

Cammidge and co-workers[40] carried out the tetramerization of 3,6-di(n-hexyl) phthalonitrile **38 b** in n-pentanol using metallic lithium (scheme 1.16). A mixture of phthalocyanine and a dark green fraction was obtained in a ratio of 95: 5. This by-product was identified as substituted octaalkyl-tetrabenzotriazaporphyrin, np-(n-hexyl)$_8$ H_2TBTAP **39 b**. When an excess of lithium was used (from 2.1 eq to 19 eq) a better yield of TBTAP was obtained in the ratio of 77: 23

(phthalocyanine: TBTAP). Using a higher boiling point solvent such as octanol increases the formation of TBTAP (53: 47 phthalocyanine: TBTAP). The authors performed ^{13}C labelling experiment and found that the solvent used in the reaction is responsible for the introduction of methine group at the *meso*-position (scheme 1.16). Clearly, the incorporation of the ^{13}C label from the solvent involves a cleavage of the alkyl chain. Under the same conditions, the formation of TBTAP is dependent on the substituents present on the phthalonitrile. 3,6-Disubstituted phthalonitriles, **38 a, c** and **d** respectively resulted in a mixture of phthalocyanine and TBTAP. Whereas 4-tbutylphthalonitrile and 4,5-di(n-hexyl) phthalonitrile results only their corresponding phthalocyanines.

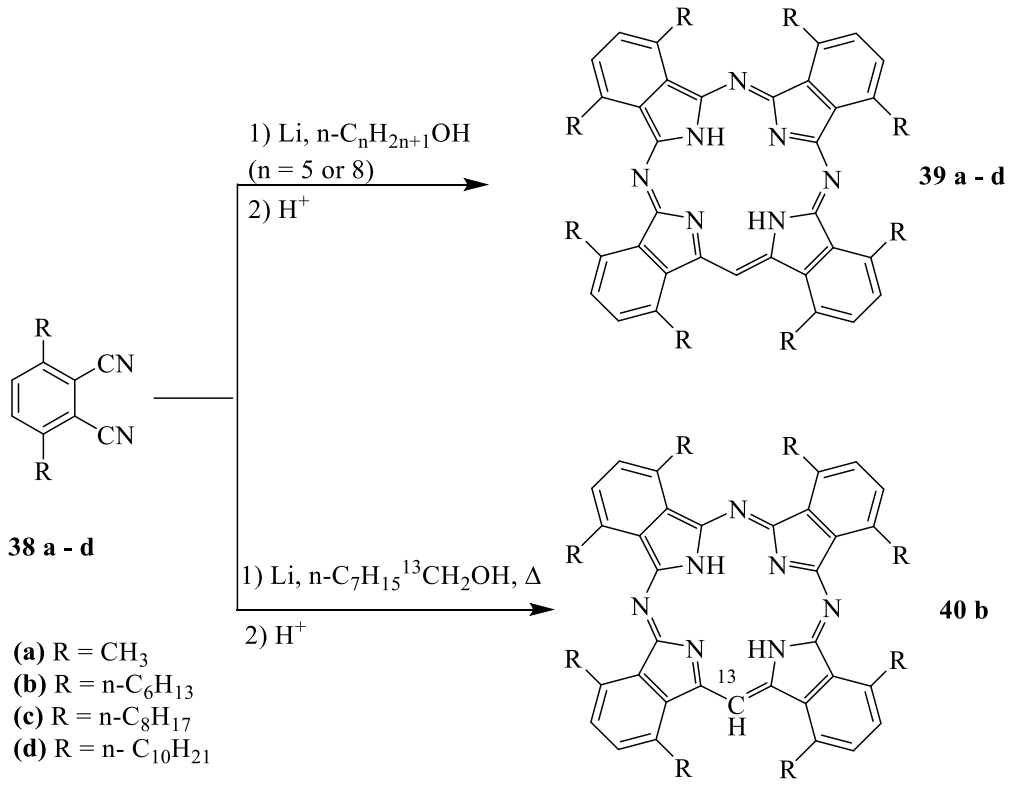

Scheme 1.16: Synthesis of np-$(alkyl)_8H_2$TBTAB complexes.

Cammidge and co-workers devised an improved version of the synthesis *meso*-phenyl substituted TBTAPs reported by Leznoff.[33] The reactions of 2-, 3- and 4-bromobenzyl magnesium chlorides (**41 a-c**) and phthalonitrile gave the corresponding macrocycles **42 a-c**. In their investigations, using quinoline as solvent, fewer impurities were present, and the complexes were more readily isolated (scheme 1.17).[41]

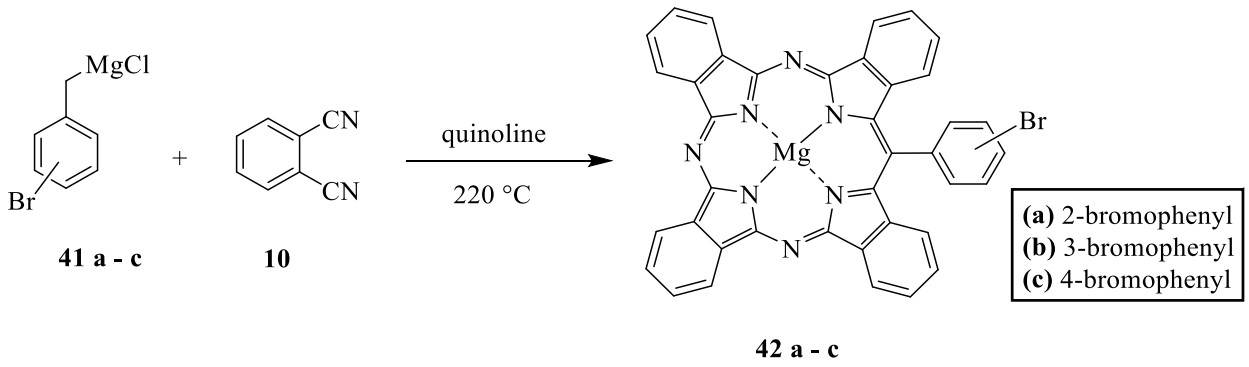

Scheme 1.17: Synthesis of Mg-TBTAP complexes from the isomeric series of bromobenzyl magnesium chlorides.

The favourable outcome from the above experiments led the researchers[42] to attempt introducing bulky substituents at the meso-position of the TBTAP macrocycle (scheme 1.18). The reactions used various organomagnesium compounds with 3,6-dihexyl phthalonitrile **38 b,** similar to Leznoff's synthesis. 3,6-Dialkyl phthalonitrile was dissolved in either ether or THF and the Grignard reagent was subsequently added. The low boiling point solvent was distilled off and finally the mixture was heated to a high temperature in quinoline in order to obtain the desired products. However, from all the trials, only unsubstituted methine derivatives of TBTAP complex was formed. Clearly substituents at the meso-position cannot be accommodated when bulky 3,6-disubstituted phthalonitriles are used.

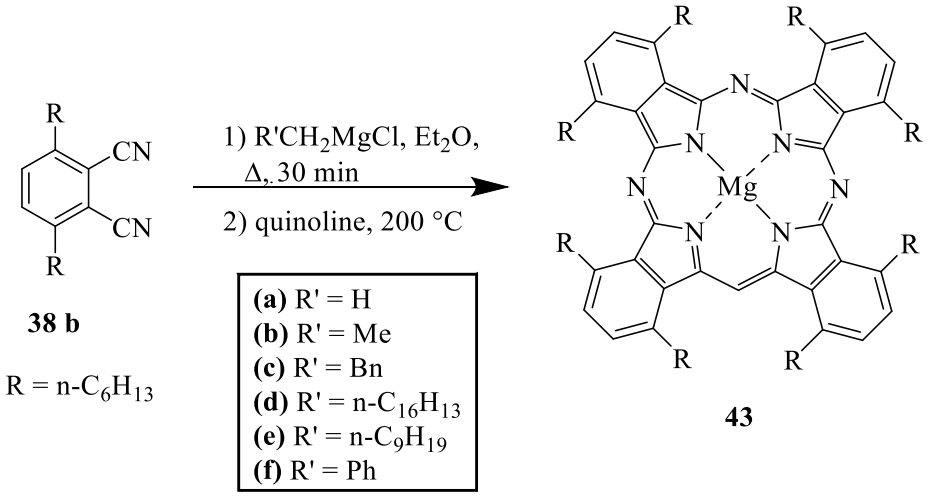

Scheme 1.18: Attempts to introduce bulky substituents at the meso-position of np-TBTAP macrocycles from various Grignard reagents.

The reaction of 4,5 dialkylphthalonitriles **44** with benzyl magnesium chloride using similar conditions produced the substituted magnesium complex **47** in low yield (scheme 1.19). This result is consistent with the data obtained by Leznoff and Mckeown, where they used various organomagnesium reagents and phthalonitriles.[42]

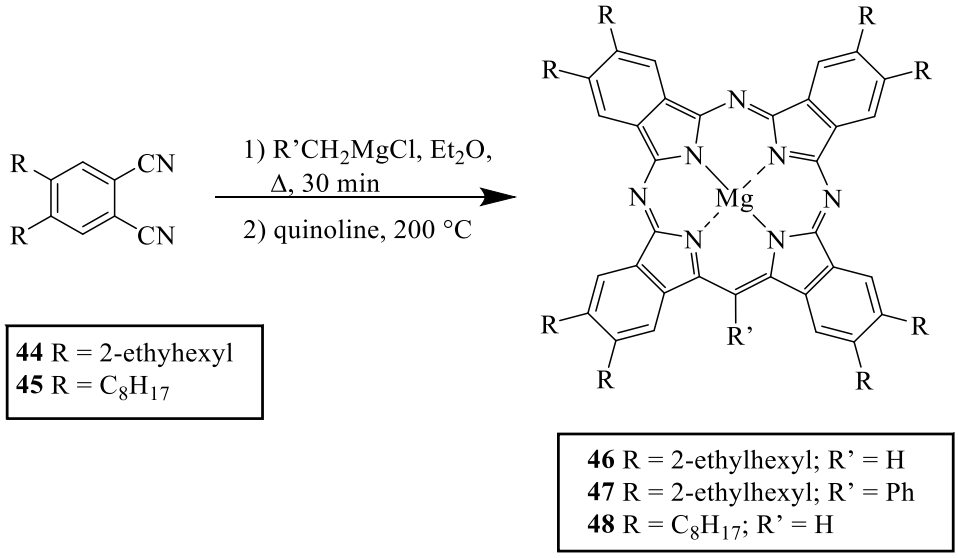

Scheme 1.19: meso-Substituted Mg-TBTAP complexes using 4,5-dialkylphthalonitriles.

Cammidge and co-workers[43] reported a modern synthetic approach for the preparation of TBTAP with a functionalized phenyl group at the *meso*-carbon. The method generated a higher yield of magnesium TBTAP and avoided the undesirable hybrid complexes. The synthesis of the magnesium TBTAP first involved the formation of the precursor aminoisoindoline by following the procedure developed by Hellal and co-workers.[44] Under microwave irradiation, the intermediate **51** was synthesized from a copper-free Sonogashira coupling between terminal aryl alkyne and 2-bromo benzimidamide hydrochloride. The amidine salt **50** was produced from the treatment of 2-bromo benzonitrile **49** with lithium bis(trimethylsilyl)amide (LiHMDS) in THF followed by quenching with isopropanol/HCl (scheme 1.20).[45]

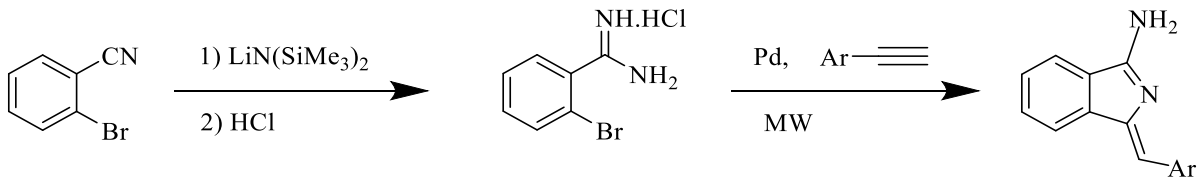

Scheme 1.20: General synthesis of aminoisoindoline.

The first attempt to synthesise the magnesium TBTAP was to react the diiminoisoindoline **32** and aminoisoindoline **51** in high boiling solvents such as quinoline, DMEA, DMF or diglyme in the presence of magnesium bromide as a template agent. The desired meso-phenyl TBTAP was formed along with magnesium phthalocyanine and self-condensation product of the aminoisoindoline **53**. This unsatisfactory result led the Cammidge group to modify the reaction synthesis and therefore they used a less reactive precursor i.e phthalonitrile rather than diiminoisoindoline **32**. This substitution gave a better outcome with an enhanced yield of 40% of the magnesium *meso*-aryl substituted TBTAP derivatives **52 a-c** (scheme 1.21).[43]

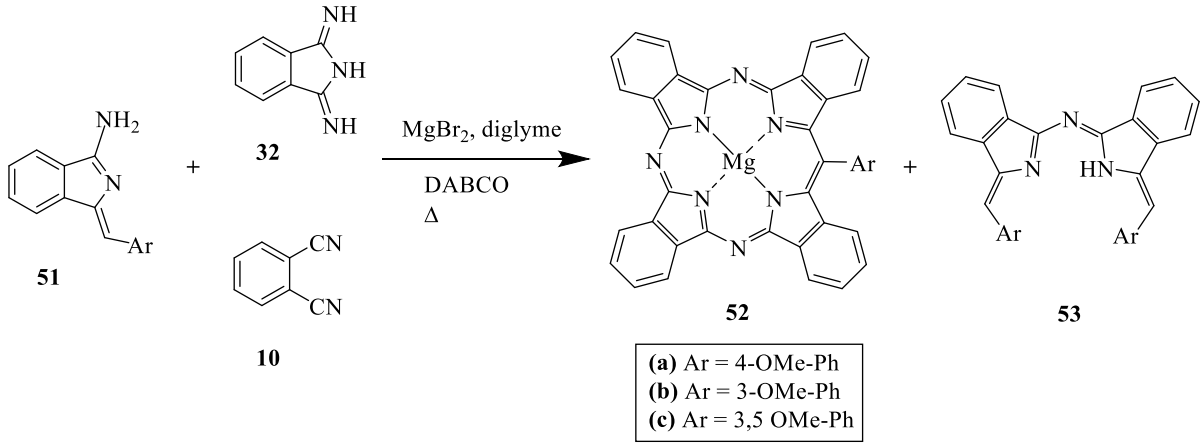

Scheme 1.21: Improved protocol for the synthesis of meso-aryl TBTAPs.

Inspired by the satisfactory results of the Cammidge group, Torres and co-workers[46] synthesised new TBTAP with an anchoring carboxy-phenyl group at the *meso*-carbon. In the presence of magnesium salt, aminoisoindoline **54** and 4-*tert*-butylphthalonitrile **55** were reacted and a 20% yield of the magnesium TBTAP **56** was obtained. During the macrocyclization reaction, the methoxy carbonyl group hydrolyses and thus no further reaction was required to form the product **56**. A transmetallation reaction was successfully carried out in the presence of zinc acetate to form the corresponding TBTAP **57** (scheme 1.22).[46]

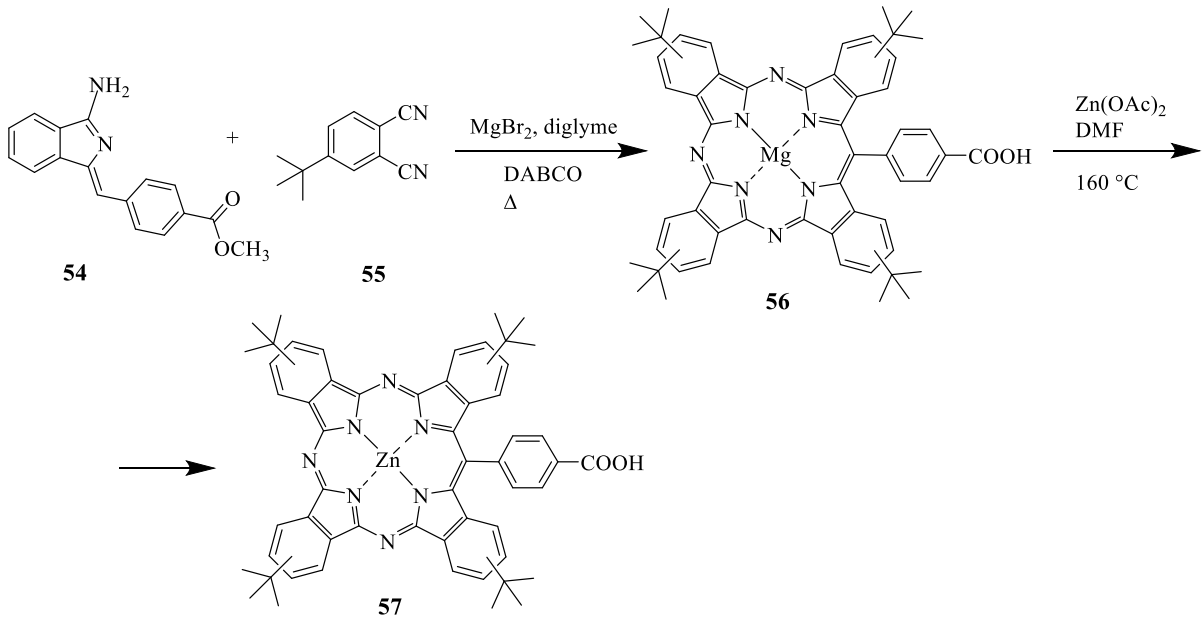

Scheme 1.22: Synthesis of TBTAP with an anchoring carboxy-phenyl group.

Further research to determine the type of hybrid molecule from the TBTAP synthesis was carried out by Cammidge and co-workers.[47,48] In the study, benzosubstituted starting materials were used. In one example, the 2,3-naphthalonitrile (**npn**) (B) and the initiator aryl-aminoisoindolene (A) were reacted to target compound **58** (an "ABBB" TBTAP). However, TBTAP **59** which was surprisingly found to be the dominant product in the reaction (scheme 1.23). The product is an Ar-ABBA TBTAP type of molecule. The outcome of the reaction can be controlled somewhat by the stoichiometric ratio of the starting materials. Research is still ongoing to understand the formation of the unexpected product **59**. As a result of the extensive π-system, red-shifted Q-band absorption at 709 and 681 nm was observed.[48]

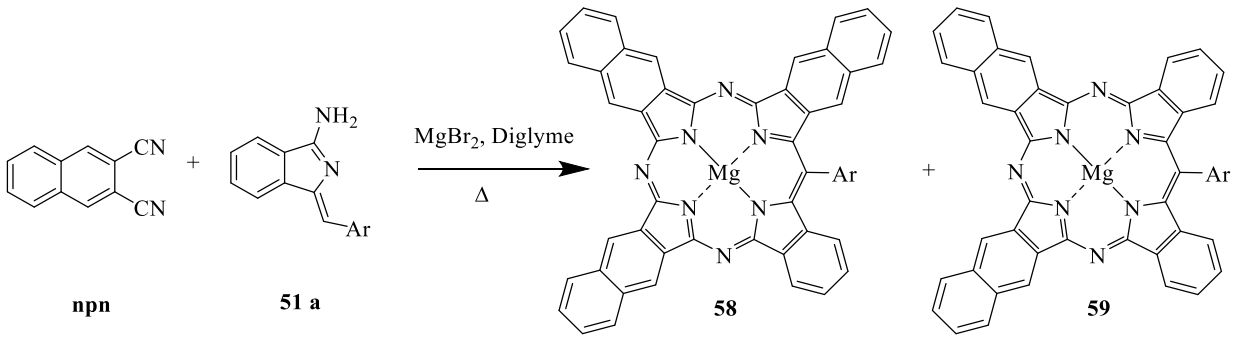

Scheme 1.23: Synthesis of TBTAP hybrid.

1.4 Metallated porphyrins

Normally porphyrins are synthesised as the free-base form and metal ions are subsequently inserted into the cavity. When a metal ion such as M^{n+} is bonded to the porphyrin H_2Por (as shown in equation below) forms $MPor^{(n-2)+}$ and the two inner imino protons are dissociated.

$$M^{n+} + PorH_2 \longleftrightarrow MPor^{(n-2)+} + 2H^+$$

Metals which meet the required criteria such as size and charge can perfectly fit into the central core of the planar macrocyclic ring system. As a result, regular metalloporphyrins are formed which are kinetically inert complexes. Such metalloporphyrins are important and play essentials roles in biological systems.[49,50] In the majority of the naturally occurring metalloporphyrins, the metal ion is located within the plane of the tetrapyrrolic ligand because they fit the size of the cavity. The radii of these metal ions range between 55–80 pm which correspond to the sphere in the porphyrin core surrounded by the four pyrrolic nitrogens (figure 1.10).

Figure 1.10: Schematic representation of regular metalloporphyrin.

It is observed that if the ionic radii of the metal ion are too large (80–90pm) to fit into the core of the macrocycle, they are outside the ligand plane, resulting in a distorted structure known as the sitting atop (SAT) metalloporphyrin (figure 1.11).

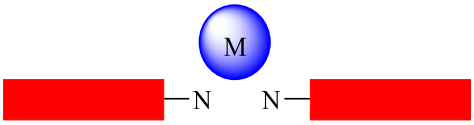

Figure 1.11: Schematic representation of SAT porphyrin.

The non-planar structures have special photochemical and photophysical features caused by the size of the metal centre.[51,52] Hence, it is possible to form sandwich type complexes with porphyrins and/or phthalocyanine (Pc). These novel structures are formed with lanthanide metals.

1.5 Sandwich type complexes

1.5.1 General introduction

Over the last few decades, there has been a huge resurgence in the study of sandwich- type complexes. The mixed (phthalocyaninato) (porphyrinato) rare earth complexes can produce a large number of homoleptic and or heteroleptic double- and triple- decker compounds which have been successfully synthesised.[53–59]

A range of metal ions can be inserted in the central core of cyclic compound such as porphyrins, phthalocyanines, napthalocyanine and other tetrapyrrole derivatives.[58,59] The nature of these tetrapyrrole ligands and the size of the metal ions directly influence the outcome of the sandwich- type structures. It is observed that lanthanides generally form stable complexes with the tetrapyrroles. These metal ions, usually in the Ln^{3+} state, however are located above the plane of the macrocycles. They act as a linker between the units of porphyrins and phthalocyanine, thereby forming double- and or triple- decker sandwich-type compounds.[56,60,61] These molecules are fascinating as they are employed in molecular machinery nanotechnology and sensors.

1.5.2 μ-oxo-nitrido-bridged dimers

Porphyrin or phthalocyanines linked together by an oxygen or nitrogen molecule commonly known as μ-oxo[62,63] or μ-nitrido[64] bridged dimers are potential candidates for designing molecular gears (figure 1.12).

The synthesis of the bridged dimers has proved to be extremely challenging with unsymmetrical core skeletons bearing diamagnetic and oxophilic metal ions. Consequently, studies on the molecular rotation of bridged dimers are rather limited.[65]

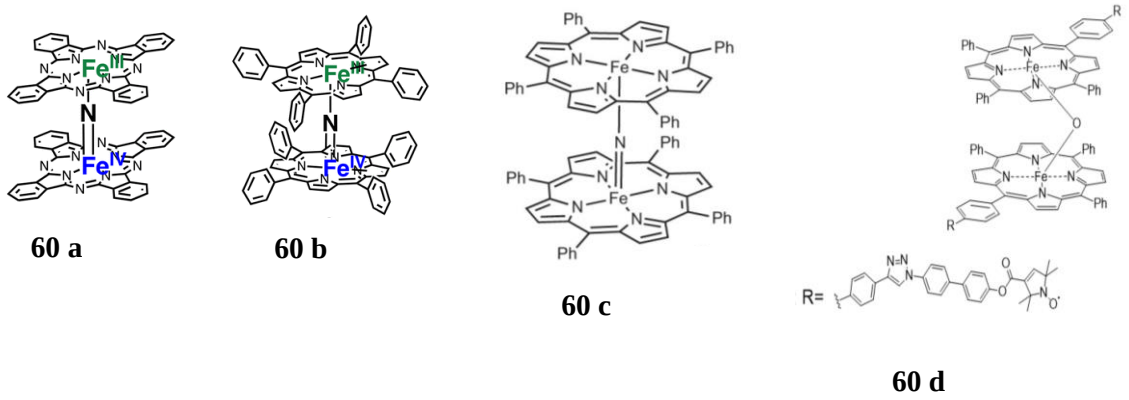

Figure 1.12: Deckers of porphyrin and phthalocyanine linked by oxygen or nitrogen.[62,65,66]

To overcome this problem, double-decker based on porphyrins, phthalocyanines and related macrocycle bridges using lanthanides metals in place of the oxygen and nitrogen are ideal candidates as they possess unique features, such as, stability, ease of synthesis, and visual responses which are easily detected by microscopy techniques.[62,67]

1.6 Synthesis of Homoleptic complexes

Generally homoleptic rare earth complexes such as double- and triple- decker compounds can be obtained via two methods. The first method involves the cyclo tetramerization of the required phthalonitriles in the presence of rare earth metal salts using an organic base like DBU. Alternatively, compounds such as Li_2Pc or H_2Pc are reacted with the metal salts in a high boiling point solvent such as octanol. Both methods resulted in the formation of double decker and a low yield of the triple decker (scheme 1.24).[68,69]

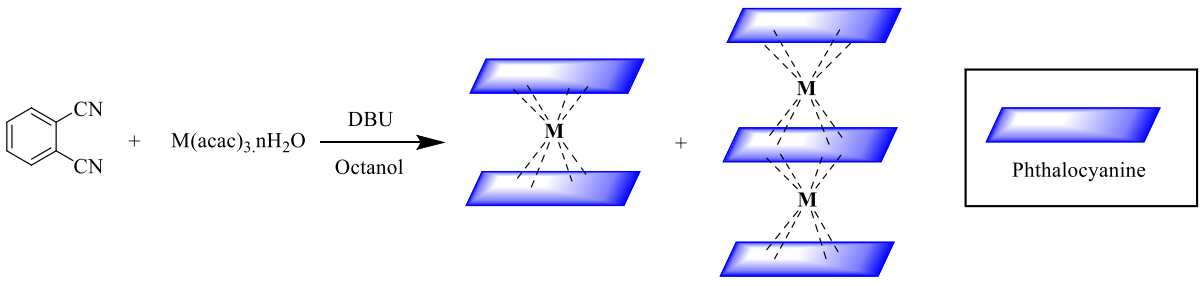

Scheme 1.24: Preparation of homoleptic double and triple decker complexes.

In the example below, Dubinina and co-workers were able to selectively synthesise and isolate double and triple decker of octaphenylphthalocyanine using terbium as rare earth metal.[70] The double decker was obtained from either the 1,2-dicyano-4,5-diphenylbenzene **62** or from the substituted phthalocyanine **61** depending on the reaction conditions. The yield of the double decker **63** product obtained from the substituted dicyano compound **62** was 26% while a yield of 64% was achieved by using the substituted phthalocyanine **61**. When the reaction temperature was increased, a mixture of double and triple deckers was obtained. The triple decker **64** was isolated in a 77% yield (scheme 1.25).

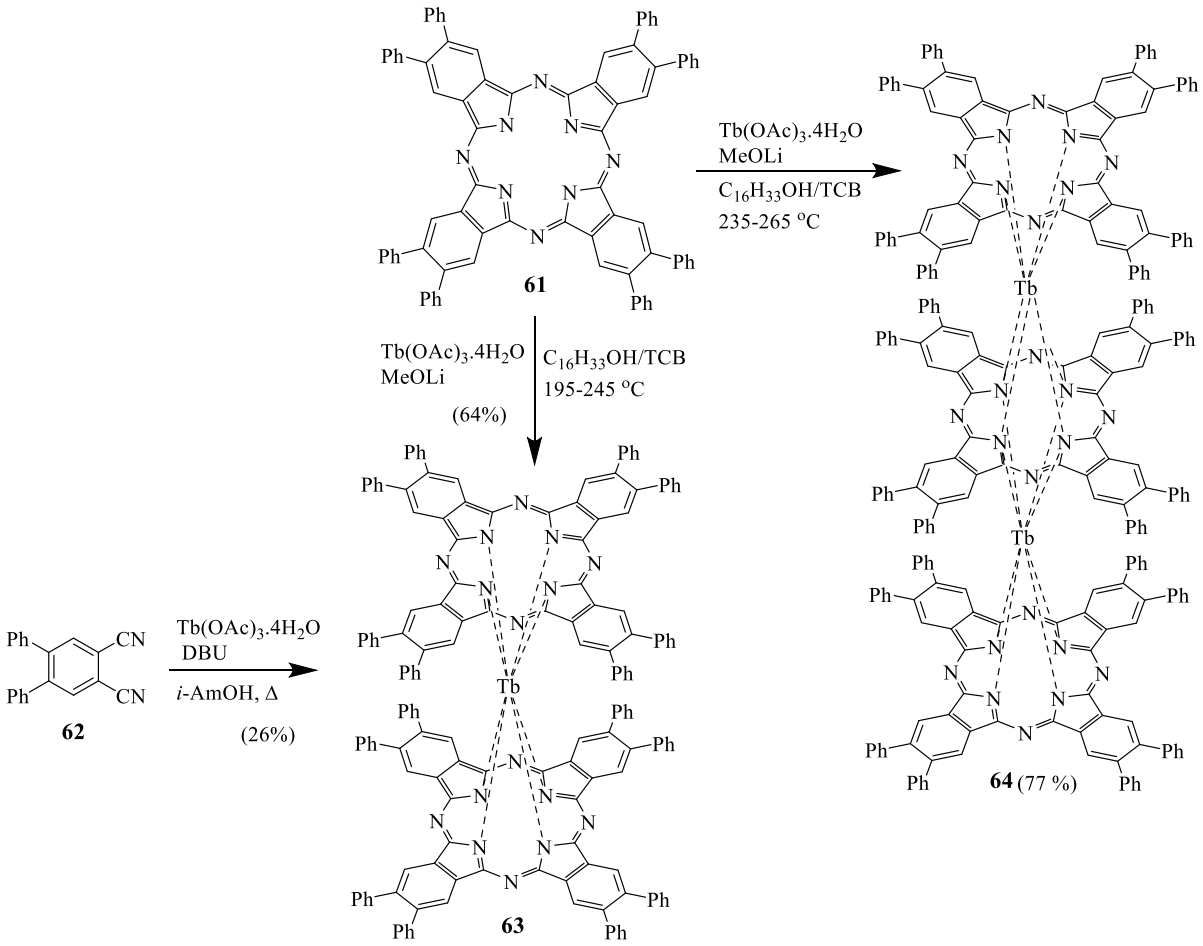

Scheme 1.25: Synthesis of terbium (III) double and triple deckers.[70]

In the following section, other chemical reactions leading to the synthesis of double and triple deckers will be described.

1.6.1 Double deckers from phthalimide

In 2021, Galani and co-workers synthesised and characterised three homoleptic bis-tetrabenzoporphyrin complexes (Gd, Er, Lu). In their approach to the synthesis of double deckers, they used an intermediate known as (*E*, *Z*)-3-((3-hydroxy-3-methyl-3*H*-isoindol-1-yl) methylene)isoindolin-1-one **65** which is obtained from the condensation reaction as per scheme below. The author claimed that the methyl moiety is derived from the acetate component. The intermediate is then made to react with the metal chloride form of Gd, Eu and Lu at a temperature of 350 °C for an hour to produce the homeleptic double deckers in yields less than 40%. MALDI-TOF analysis showed no peaks beyond 1840 Da implying that homoleptic triple deckers were not formed during the course of the reaction (scheme 1.26).[71]

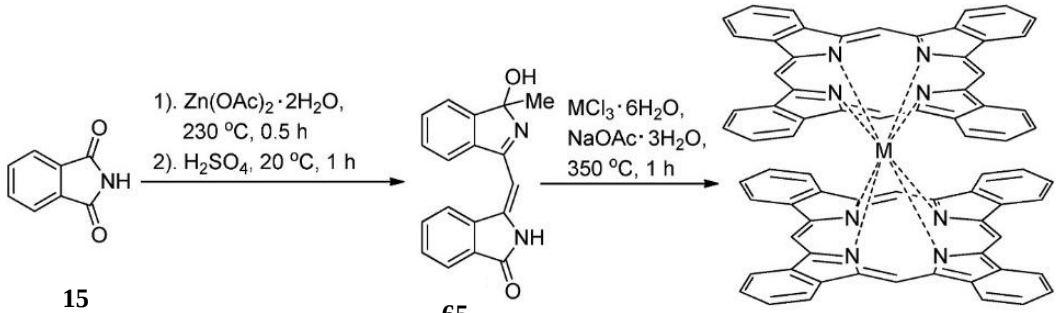

(a) M = Gd
(b) M = Eu
(c) M = Lu

Scheme 1.26: Synthesis of homoleptic double decker complex.[71]

1.7 Heteroleptic double decker from Li_2Pc

Generally the synthesis of heteroleptic double deckers can be achieved by using a preformed Li_2Pc and subsequently mixing with the other macrocycle unit to form the mixed compound.[59] The synthesis of a heteroleptic terbium double decker was achieved by Chen and co-workers.[72] Initially, $Tb(acac)_3{\cdot}nH_2O$ and $H_2\{Pc[N(C_4H_9)_2]_8\}$ were mixed in a high boiling point solvent such as octanol followed by the addition of Li_2Pc. The double decker $(Pc)Tb\{Pc[N(C_4H_9)_2]_8\}$ **68** was analysed by MALDI-TOF MS with m/z 2202 and the yield obtained was 37.9% (scheme 1.27).

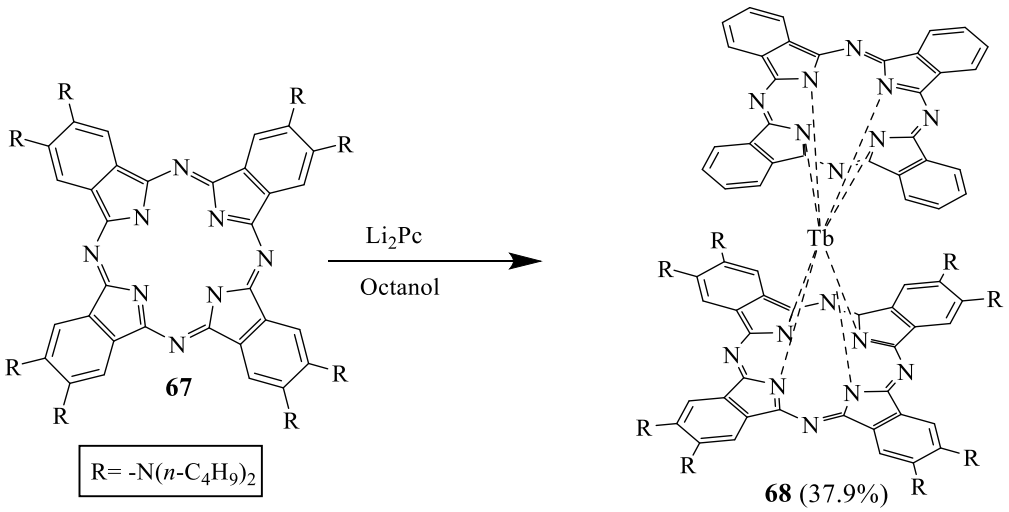

67

68 (37.9%)

Scheme 1.27: Synthesis of bis(phthalocyaninato) rare earth (III) double-decker complex**.**

1.7.1 Heteroleptic double decker from phthalimide

Galani and co-workers synthesised heteroleptic double deckers. They used an intermediate 3-[(E,Z)-{(E,Z)-3-[(1-hydroxy-1-methyl-1H-isoindol-3-yl)methylene]isoindolin-1-ylidene}methyl]-1H-iso-indol-1-one **69** obtained from the precursor phthalimide as shown in the scheme below. The intermediate was then reacted with 2-methylquinoline and 3-methyleneisoindolin- 1-one **70** in the presence of zinc oxide for 4 h and finally treated with H_2SO_4 to yield the tetrabenzoporphyrin. In a one-pot procedure, the tetrabenzoporphyrin was reacted in an excess of lanthanide chloride salts in quinoline for 2 h. An excess of phthalonitrile was then added to the mixture which was refluxed for another 4 h to yield the sandwich heteroligand complexes in 54–65% (scheme 1.28).[73]

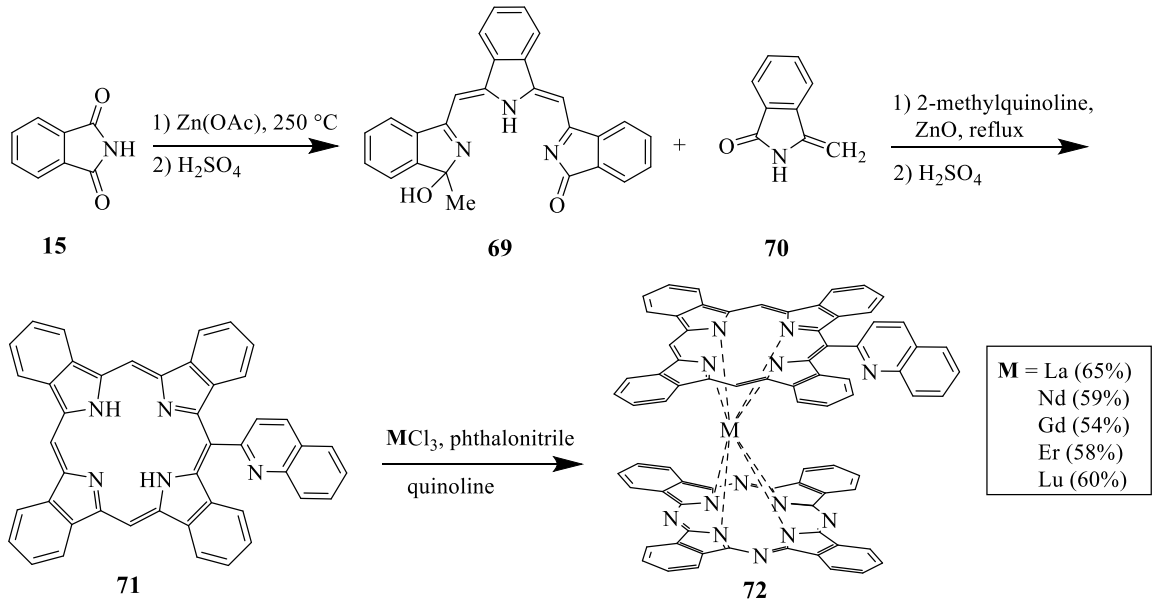

Scheme 1.28: Synthesis of heteroleptic double decker complex.[73]

1.7.2 Heteroleptic double decker with diazepine unit

In 2021, a series of new heteroleptic rare earth double decker compounds composed of electron-withdrawing tetradiazepinoporphyrazine (DzPz) and electron-donating phthalocyanine (Pc) macrocycles were designed and synthesised (scheme 1.29). The DzPz is made by fusing 1,4-diazepine heterocyclic rings and a porphyrazine core and the resulting macrocycle forms stable intermolecular interactions. Rare earth metals such as La, Eu and Lu were explored.[74]

The synthesis of the heteroleptic compounds was not straightforward and different routes were explored. Synthesis of the single-decker complexes of the DzPz consistently proved to be unsatisfactory due to the tendency of compound to form robust intermolecular contacts.[74]

Therefore, single-decker complex [^{Bu}PcLn(acac)] **73** of the Pc was prepared by following published procedure.[75] They used Lu metal as template for exploring two different strategies. In the first method, the reaction mixture of a cyclotetramerization of 1,4-diazepine-2,3-dicarbonitrile **74a** and ^{Bu}PcLu(acac) was refluxed in *n*-hexanol. This reaction resulted in the formation of the target heteroleptic double-decker and also unwanted heteroleptic triple-decker complexes of various compositions. The purification of the compound was challenging, and a 18% yield of the target product was obtained. In the second pathway, the macrocycles of ^{Bu}PcLu(acac) and $^{t\text{BuPh}}$DzPzH$_2$ **74b** were made to react in the presence of *o*-dichlorobenzene

and DBU (scheme 1.29). This gave a higher selectivity for the formation of the target compound without any of the unwanted triple decker complexes. The yield of Lu **75a** and Eu **75b** heteroleptic complexes were 62% and 42% respectively while a low yield of 10% was obtained for La complex **75c**. This low yield can be explained by the fact that during the course of the reaction, single-decker dissociates to from side products such as homoleptic complexes ($(^{t\text{BuPh}}\text{DzPz})_2\text{La}$ and $(^{\text{Bu}}\text{Pc})_2\text{La}$.[74]

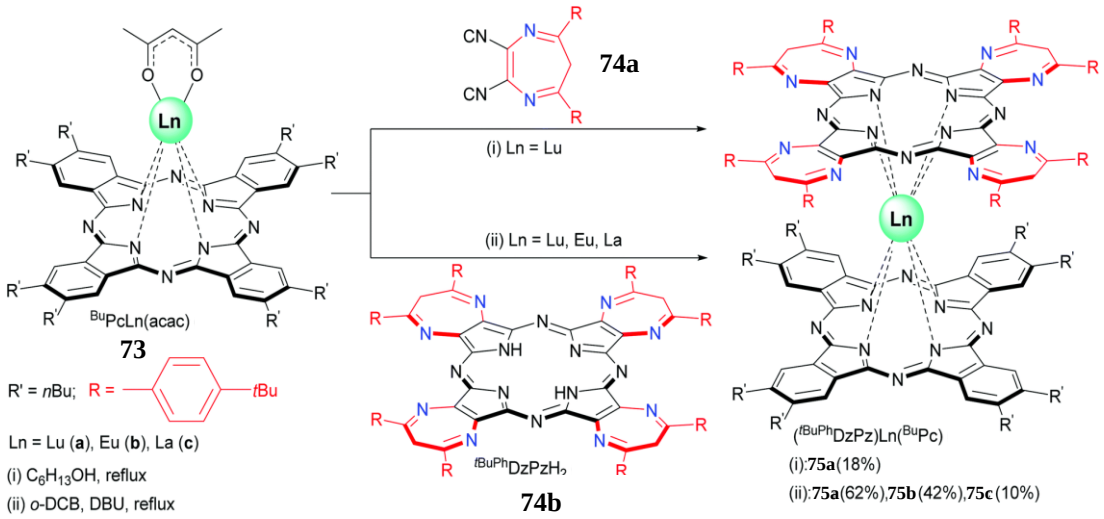

Scheme 1.29: Synthesis of heteroleptic double decker complex.[74]

The diazepine unit (see above scheme) which is attached to the porphyrazine core increases the tendency for interligand interactions in the DzPz moiety by a combination of both hydrogen bonding and π-stacking. Furthermore, based on their spectroscopic data, a dimeric compound is formed due to the outward reorientation of the diazepine unit, as shown in the model below (figure 1.13). They concluded that by changing the peripheral substituents on the cores and the Ln(III) ion, supramolecule based on intermolecular assembly can be obtained in a controlled fashion and therefore have potential applications in molecular magnets and materials based on charge transfer.

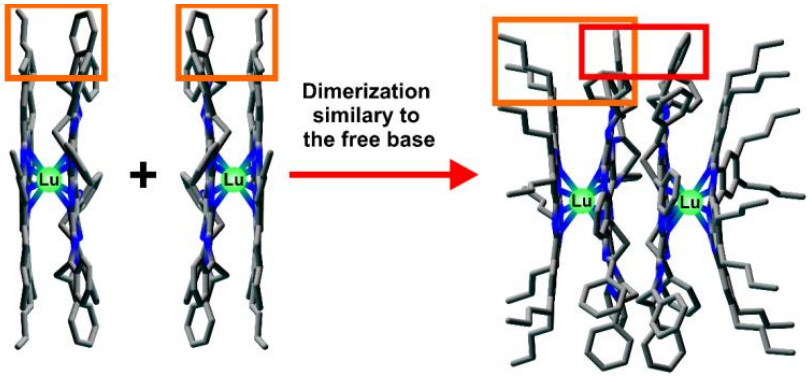

Figure 1.13: DFT-optimized structures of the heteroleptic double decker complex.[74]

1.7.3 Heteroleptic double decker with functionalised phthalocyanine

Martynov and co-workers developed and synthesised a new heteroleptic double decker of terbium bis-phthalocyanine. An ethoxy substituent is attached on the periphery of the benzene rings on the Pc and on one of the benzene ring of the Pc core, a diethylene glycol moiety with a terminal OH group and a methoxy group are attached (scheme 1.23).[76]

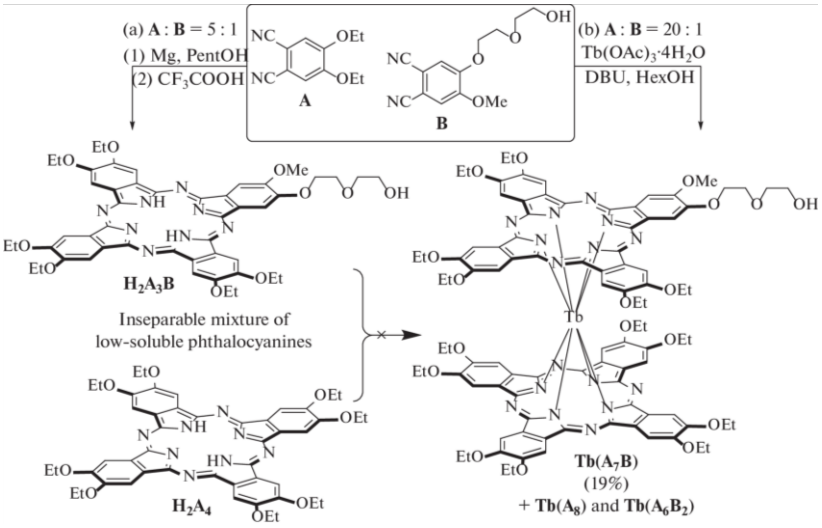

Scheme 1.30: Synthesis of heteroleptic double decker complex.[76]

Two routes to synthesise the double decker were explored. The first pathway was to condense phthalonitrile **B** with an excess of phthalonitrile **A** in the presence of magnesium metal in boiling pentanol. The metal was then removed from the resulting complexes by addition of trifluoroacetic acid to yield a mixture of phthalocyanines $H_2\mathbf{A}_x\mathbf{B}_{4-x}$, where x = 0–4. An attempt to isolate macrocycles of $H_2\mathbf{A_4}$ and $H_2\mathbf{A_3B}$ from the mixture by column chromatography was unsuccessful despite the fact that the presence of an ethoxy group on the free Pc core should

enhance the solubility. The second pathway involves condensing the phthalonitrile **A** and **B** in 1-hexanol in the presence of terbium (III) acetate and DBU. The data obtained from MALDI-TOF mass spectrometry showed that the resulting mixture contained a mixture of products that is **Tb**(**A**$_8$), **Tb**(**A**$_7$**B**), and **Tb**(**A**$_6$**B**$_2$) which were successfully isolated as they were more soluble.

In both pathways, they used an excess of phthalonitrile **A** so as to prevent the formation of compounds with more than one diethylene glycol group on the molecule.

In order to expand the potential applications of the double decker **Tb**(**A**$_7$**B**), other modifications were carried out by removing terminal OH group to an iodine atom and finally to a thioacetate moiety (scheme 1.31). The double decker with the terminal OH can be used in hybrid materials as it can be fixed on surfaces which are modified by carboxylic acid moieties as they have found in a previous study.[77] The nanoparticles of the complex containing the thioacetate moiety can be attached onto the surface of noble metals following the hydrolysis of the thioester bond (scheme 1.31).[78]

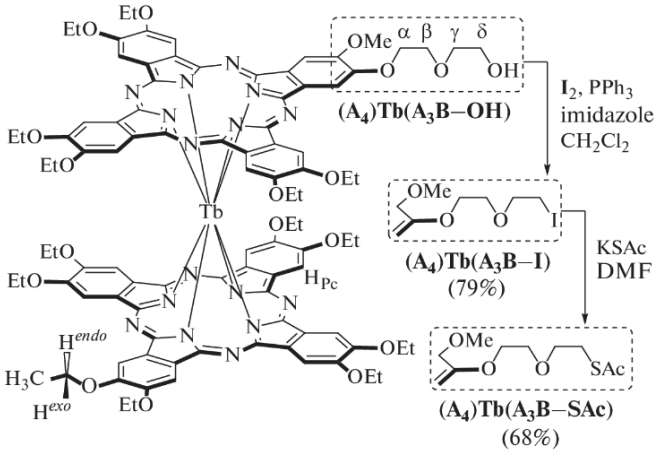

Scheme 1.31: Scheme of the functionalization of terbium (III) bis-phthalocyaninate (**A**$_4$) **Tb**(**A**$_3$**B**–OH).[76]

1.8 Synthetic methods for triple deckers

In the previous section, some of the synthetic pathways for the formation of double deckers also lead to the formation of the homoleptic triple deckers. In the following section, other methods for the selective synthesis of triple deckers will be discussed.

1.8.1 Homoleptic butoxy- and crown substituted triple deckers of phthalocyanine

In 2022, Martynov and co-workers developed a series of homoleptic butoxy- and crown substituted triple deckers of phthalocyanine (figure 1.14).[79] The authors adapted a reported synthesis of BuO- and 15C5-substituted ligands to produce Tb(III) and Y(III) trisphthalocyaninates, the reaction of $H_2[(BuO)_8Pc]$ or $H_2[(15C5)_4Pc]$ with the metal acetylacetonates in refluxing solvents such as 1-octanol or 1-chloronaphthalene yielded in 20% and 50% of the target triple-deckers after 4 hours and 1.5 hours of reaction respectively.[80,81]

Additionally, they were able to enhance the synthetic techniques, enabling quicker processes and produce higher yields of the target triple decker. The authors discovered that changing the solvent mixture of 1,2,4-trichlorobenzene (TCB) and 1-octanol to a 9:1 vol. ratio resulted in 90% and 68% yields of $\mathbf{Tb_2[(BuO)_8Pc]_3}$ and $\mathbf{Tb_2[(15C5)_4Pc]_3}$, respectively. In the case of Y(III) yields of 75% and 79% were recorded, respectively and the reaction times were shortened to half an hour.[79]

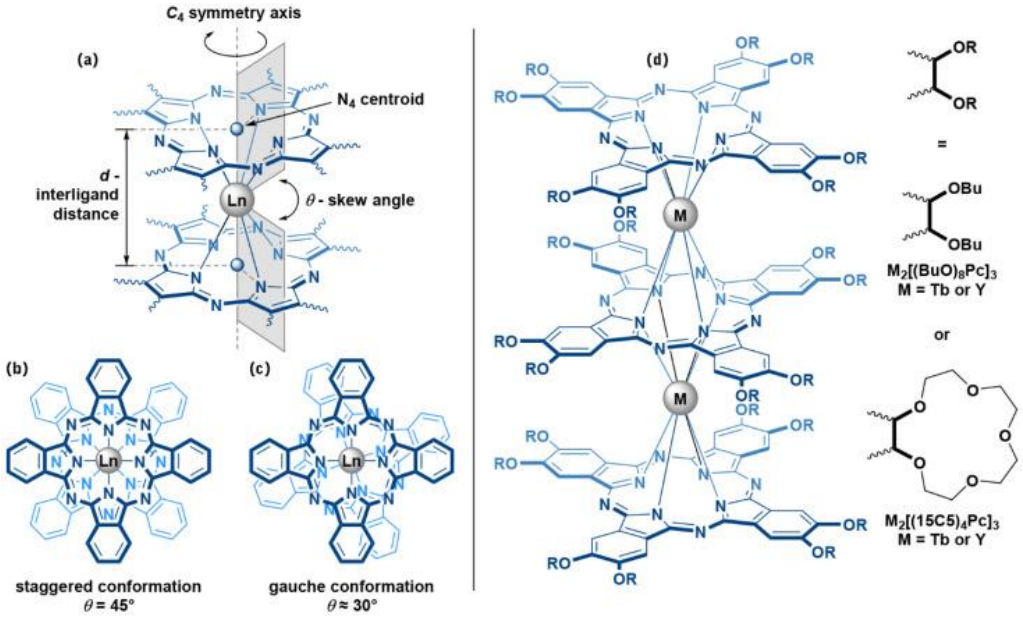

Figure 1.14: (**a**)—Structural characteristics *d* and *θ*, which determine coordination surrounding of lanthanide ion sandwiched between two Pc ligands; (**b**,**c**)—staggered (***s***-) and gauche (***g***-) conformations of Pc ligands in sandwich complexes; (**d**)—trisphthalocyaninates.[79]

Both UV-Vis spectra of triple-deckers (figure 1.15) of are 15C5- and BuO- complexes were compared as depicted in the diagram below. In the case of the BuO- substituted complex, the

data obtained from both solvents benzene and dichloromethane clearly shows a difference in the spectra with regards to the shape of the bands and the intensities. While UV-Vis spectra of the homoleptic triple decker of the 15C5- complex in both solvents showed that the shapes and positions of Q- and Soret bands were exactly the same. They concluded that the phthalocyanine cores bearing the BuO- substituents are in staggered conformations in toluene or in gauche conformations in chloroform. In contrast to the complex bearing the 15C5- substituents in both solvents, they are conformationally invariant and occurs in the staggered form.

In another investigation, they studied this phenomenon on the homoleptic Eu triple deckers of 15C5- and BuO- complexes and their observations were reproducible with the above study.[82]

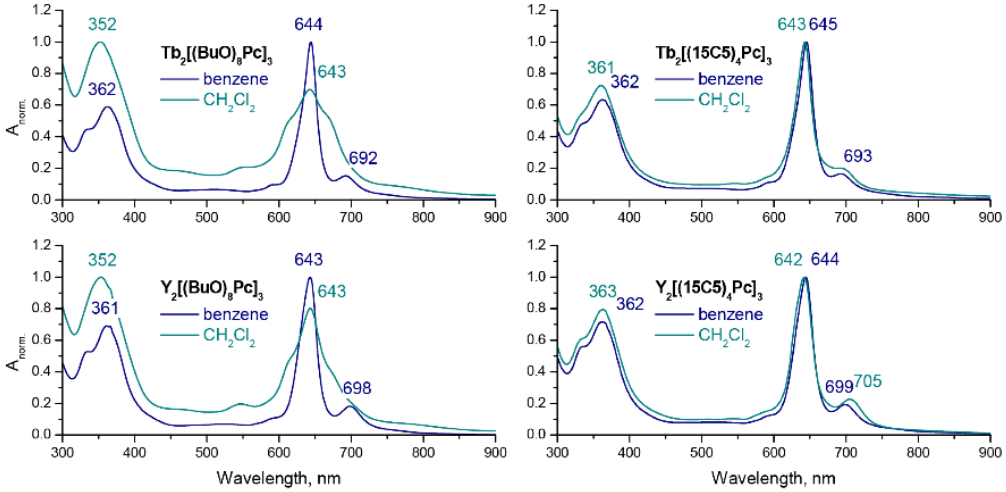

Figure 1.15: UV-Vis spectra of the homoleptic triple decker.[79]

To confirm this phenomenon in the solid state, they attempted to obtain single crystals of both homoleptic triple deckers of the BuO- and 15C5- complexes and were unsuccessful. As the complexes bearing the BuO- substituents were too soluble in both aromatic and halogenated alkanes solvents, while the 15C5- complexes were barely soluble in aromatic solvents.

1.9 Synthesis of heteroleptic triple decker complexes

In 1986, Moussavi and co-workers[83] first reported sandwich complexes of the type Ln_2Pc_2[T(4-OCH_3)Por]. There are several approaches for the synthesis of these novel structures involving porphrin and phthalocyanine.[84–86]

The so-called 'one pot' reaction is often used to synthesise these supramolecular compounds. The metals salts, H_2Por and $M(Pc)_2$ are heated under reflux in a high boiling point solvent as shown in the scheme below.

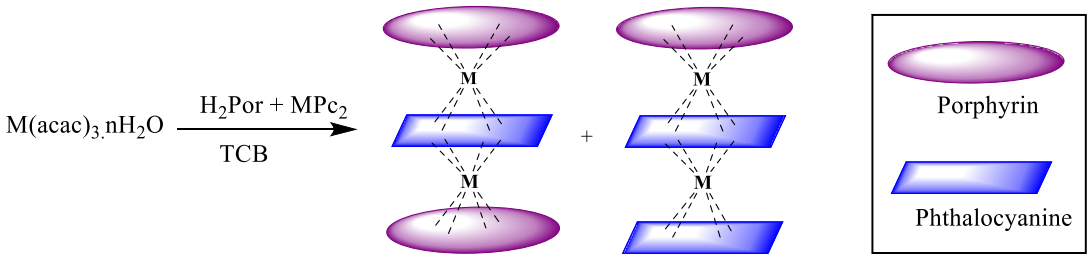

Scheme 1.32: The 'one pot' synthesis of heteroleptic triple-deckers.[87,88]

Another synthetic method known as the 'raise-by-one storey' can be carried out by reacting the $M(acac)_3.nH_2O$ and the porphyrin molecule to form a 'half-sandwich' complex, M(Por)(acac). A mixture of the heteroleptic triple deckers was obtained by the cyclo tetramerization of phthalonitrile with the M(Por)(acac). Jiang and co-workers[89] found this pathway to be particularly suitable for the preparation of heteroleptic bis(phthalocyanine) and mixed phthalocyanine and porphrin deckers complexes.

The 'raise-by-one storey' method can be used as a template to synthesise these triple deckers under different reaction conditions. Once the 'half-sandwich' complex of **M(Por)(acac)** is produced, it is added to a previously synthesised **$M(Pc)_2$** or **(Pc)M(Por)** or dilithium phthalocyanine as shown in schemes (1.33, 1.34) below. [85,90–92]

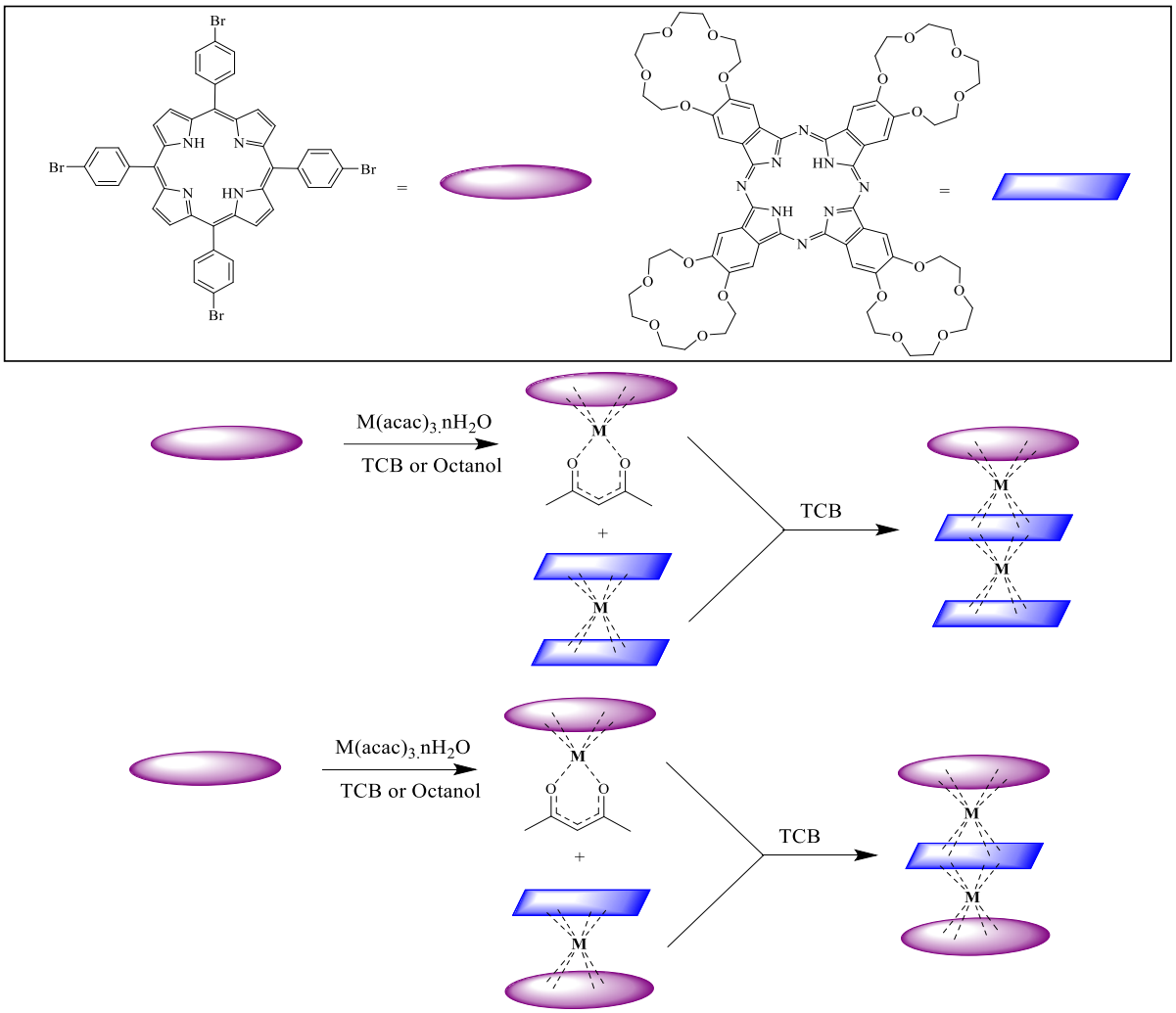

Scheme 1.33: Birin's synthesis of the heteroleptic triple deckers.[85]

It is also possible to synthesise hetero-dinuclear mixed phthalocyanine or porphyrin rare earth triple-decker compounds using the above methods.[92]

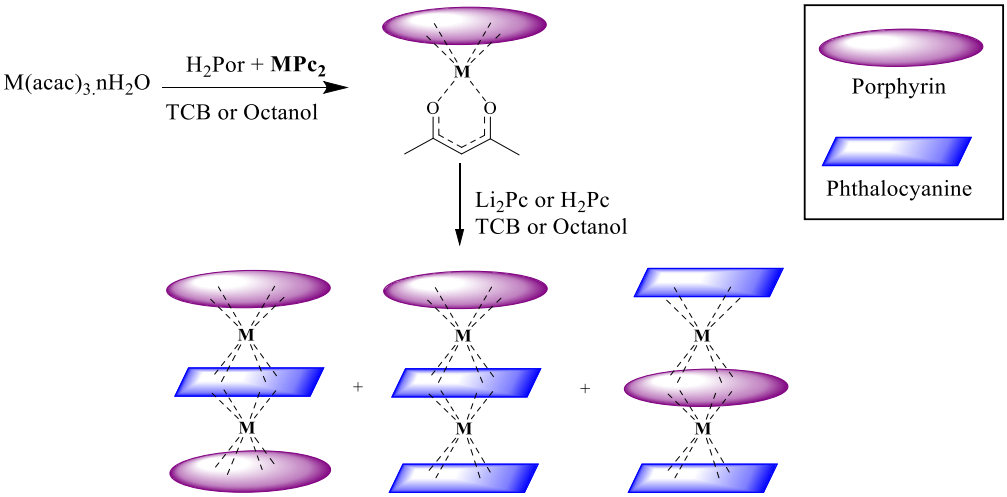

Scheme 1.341: Two steps one pot synthesis with Li_2Pc as starting material.[55,93–95]

In an investigation by Ishikawa and co- workers synthesised triple decker (figure 1.16) involving a mixture of porphyrin (H_2T(p-OMe)PP) and phthalocyanine (Pc) in the presence of the terbium ion (Tb^{3+}) which was refluxed in TCB for 12 h. After purification a 4.2% yield of the target compound **[(Pc)Tb (Pc)TbT(*p*-OMe)PP)]** was achieved. The authors did not report any scrambling nor mixing of products from the synthesis. Crystals for X-ray analysis were grown from a dichloroethane solution.[96]

As depicted in the figure 1.16, the two Pc ligands are at an angle of 45° to one another, resulting in a SAP (square-antiprismatic) coordination site. According to the authors, with the coordinating nitrogen atoms of the central Pc and those of T(*p*-OMe) PP in eclipsed positions which gave rise to a SP (square-prismatic) coordination site which is not found in double-decker complexes.

The coordination site of two terbium ions has D_{4d} symmetry with a distance of 3.6 Å. The Tb^{3+} ions in the SAP and SP and the f-f interactions between the metal ions combined two sharply different magnetic sites in the strongly coupled single-4f-ionic SMMs. This allows the molecules to exhibit a slow magnetic relaxation, characteristic of a single molecule magnet (SMM) and is clearly dependent on the geometry of the coordination site. Their results are in accordance with other reported investigations on the relationship between the twist angle and the behaviours of the SMM.[96]

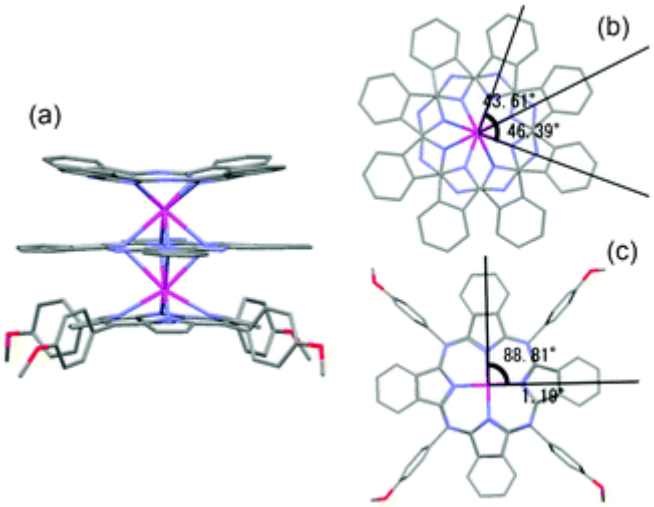

Figure 1.16: The Crystal structures of [Tb,Tb]. Views from (a) side, (b) top and (c) bottom.[96]

1.9.1 Synthesis of heteroleptic sandwich complexes using microwave procedure

Jin and co-workers attempted to synthesise Por-Pc-Pc triple decker in a high boiling point solvent such as dichlorobenzene. They adopted a raise-by-one-storey approach which was unsuccessful with bulky groups on the phthalocyanine. [84]

In a different approach, the same group used microwave activation procedure and the synthesis of a series of complexes and yields of 22–38% were achievable. Prior to the formation of the target triple decker compound, the double decker i.e **M(R$_8$Pc)$_2$** is formed first by the reacting 4-(2,5,5-trimethyl-1,3-dioxan-2-yl) phthalonitrile in the presence of the M(acac)$_3$.nH$_2$O, DBU and refluxed in pentanol. A mixture of the substituted *meso*- porphyrin and M(acac)$_3$.nH$_2$O in *o*-dichlorobenzene was irradiated in a microwave followed by the addition of the pre-made double decker. The picture below shows the summary of the reaction pathway. An advantage of this method is that the formation of undesirable macrocyclic compounds is very low and therefore the target complex was easily isolated (scheme 1.35).[84]

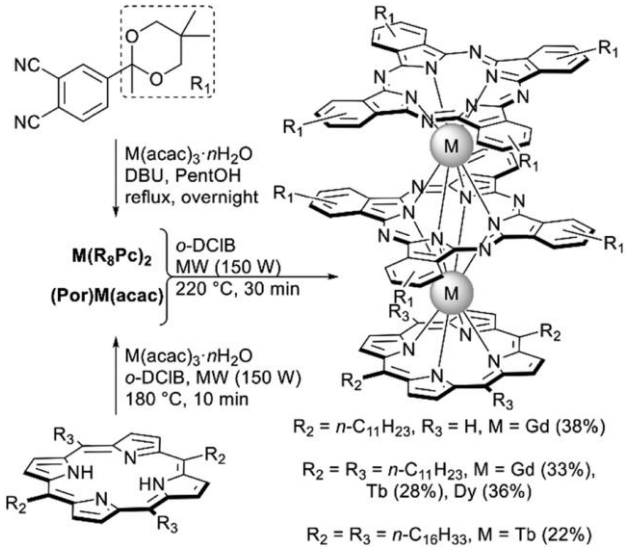

Scheme 1.35: Microwave-mediated synthesis of lanthanide porphyrin/phthalocyanine triple-deckers with bulky substituents.[84]

1.9.2 Heteroleptic butoxy- and crown substituted triple deckers of phthalocyanine.

In the previous section, Martynov and co-workers' synthesis of homoleptic butoxy- and crown substituted triple deckers of phthalocyanine using rare earth metals such as terbium, europium and ytterium was described. However, they were unable to get any crystals for the X-ray analysis due to solubility of the compounds. To overcome this problem, a more successful

investigation was carried out whereby they combined both types of phthalocyanine cores (i.e BuO- and 15C5-) resulting in single heteroleptic triple decker, [**B4**]**M**[**B4**]**M**[**C4**] (scheme 1.35).[97] Novel heteroleptic triple-decker complexes of yttrium (III) and terbium (III) were prepared.[97]

Initially, the crown substituted phthalocyanine and the metal acetylacetonate were mixed together in only TCB to yield the monophthalocyaninates **[C4]M**(acac) as an intermediate. This intermediate was then made to react with the pre-formed double decker of the butoxy phthalocyanine (scheme 1.36). This procedure resulted in a low yield of the target triple decker while homoleptic triple decker of the intermediate **M2[C4]3** was formed preferentially. An alternative pathway was followed which involves the addition of the pre-formed double decker to the crown phthalocyanine and $M(acac)_3 \cdot nH_2O$ in a mixture of TCB and n-octanol. Careful monitoring of the reaction using UV spectroscopy showed that the reaction is completed in 10 minutes. The yields of the triple decker complexes of Y(III) and Tb (III) were 66% and 58% respectively.[97] The complexes were easily isolated from the unreacted **M[B4]2** and the homoleptic side product **M2[C4]3** due to the combination of nonpolar BuO- and polar 15C5-groups.

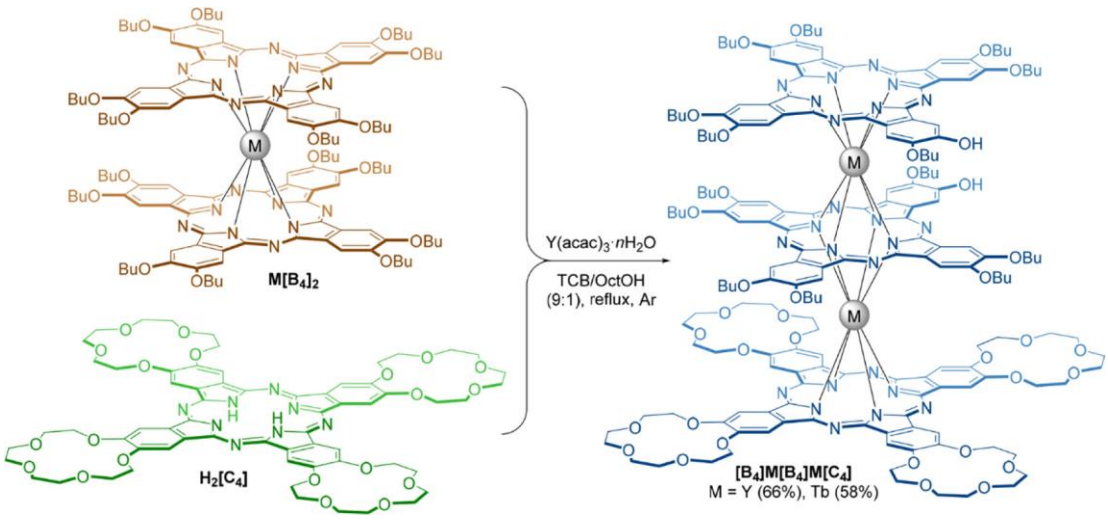

Scheme 1.36: Synthesis of heteroleptic triple decker complex.[97]

Single crystals of [**B4**]**M**[**B4**]**M**[**C4**] were successfully grown and upon X-ray analysis, the authors found out that the Pc ligands were in a staggered conformation giving rise to both metal ions in a square-antiprismatic environment when solvated with toluene. However, when solvated with dichloromethane only one of the metal ions (which is in between the Pc ligands bearing the BuO- and the crown substituents) is in a square-antiprismatic environment and the

other metal ion holding the Pc ligands bearing BuO- substituents changed to a gauche conformation as depicted in the figure 1.17. ^{1}H-NMR analysis also confirmed that these conformations are maintained in the solution. As the symmetry of the triple decker changes from staggered to gauche, therefore, one can manipulate the magnetic characteristics of the lanthanide trisphthalocyaninates by means of solvation-induced conformational switching.[97]

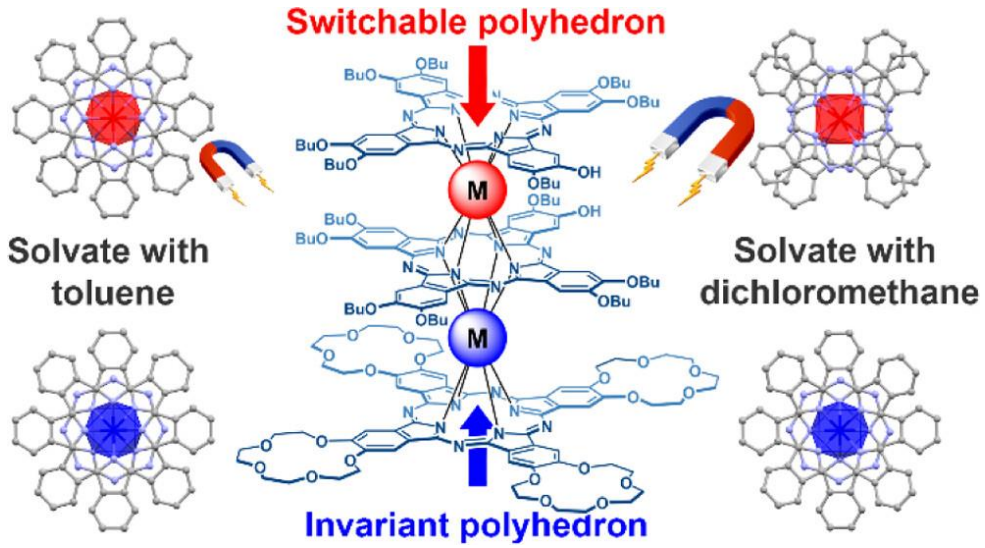

Figure 1.17: Coordination surrounding the lanthanide ion sandwiched between two Pc ligands; staggered and gauche conformations of Pc ligands in sandwich complexes.

1.9.3 Heteroleptic crown substituted and unsubstituted phthalocyanine triple deckers

The heteroleptic triple decker (scheme 1.36) was synthesised by refluxing the metal-free tetra-15-crown-5-phthalocyanine, lanthanum bisphthalocyaninate La $(Pc)_2$ and terbium(III) acetylacetonate in 1-chloronaphthalene and the yield of the target compound **(Pc)Tb[(15C5)$_4$Pc]Tb(Pc)** was 19%.[98] Complex, **[(15C5)$_4$Pc]M[(15C5)$_4$Pc]M(Pc)** resulted in a 38% yield. They followed the "raise-by-one-storey" technique whereby the target heteropletic triple decker complex was synthesised by adding another deck to the double-decker complex **[(15C5)$_4$Pc]Tb(Pc)**. This synthesis was carried out in refluxing solvents of a mixture of TCB and OcOH for 10 minutes. After purification, target compound was isolated in 80% yield (scheme 1.37).[99]

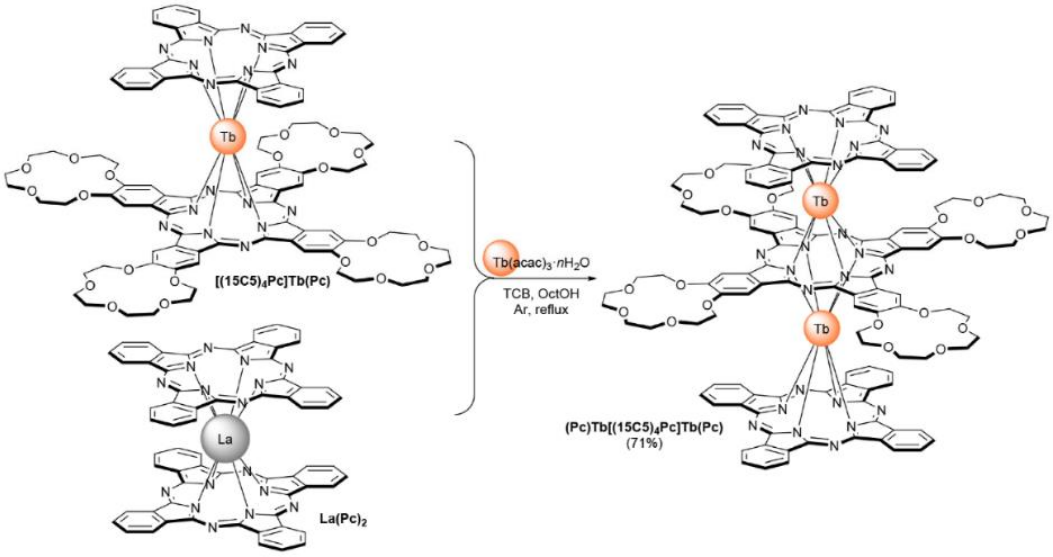

Scheme 1.37: Synthesis of heteroleptic triple decker complex.[99]

The choice of using the crown substituted phthalocyanine is based primarily on their previous studies on SMM of the heterometallic triple decker complex of **[(15C5)$_4$Pc]M*[(15C5)$_4$Pc]M(Pc)** where M and M* is Tb or Y.[57] In this complex, **(Pc)Tb[(15C5)$_4$Pc]Tb(Pc)**, both metals are arranged in an asymmetric heteroleptic configuration, which the authors stated would lead to improved SMM characteristics.

Crystals of **(Pc)Tb[(15C5)$_4$Pc]Tb(Pc**) were grown from a solution of *o*-dichlorobenzene and *n*-hexane (figure 1.18). From the crystallographic data, the Tb–Tb distance was 3.46 Å which is shorter than the sum of the Van der Waals radii of the two terbium atoms corresponding to 4.74 Å. A twist angle of 42.6° was measured between the outer and inner decks which is consistent with the value they obtained with a previous study, confirming a D_{4d} symmetry. This angle is in the range of other double-deckers of terbium (III) phthalocyanines which exhibits SMM behaviour.[98]

They studied the magnetic susceptibility of **(Pc)Tb[(15C5)$_4$Pc]Tb(Pc)** and the data revealed the presence of ferromagnetic coupling between the two Tb^{III} ions and the short Tb-Tb distance contributes to an enhancement of f-f interactions.[99]

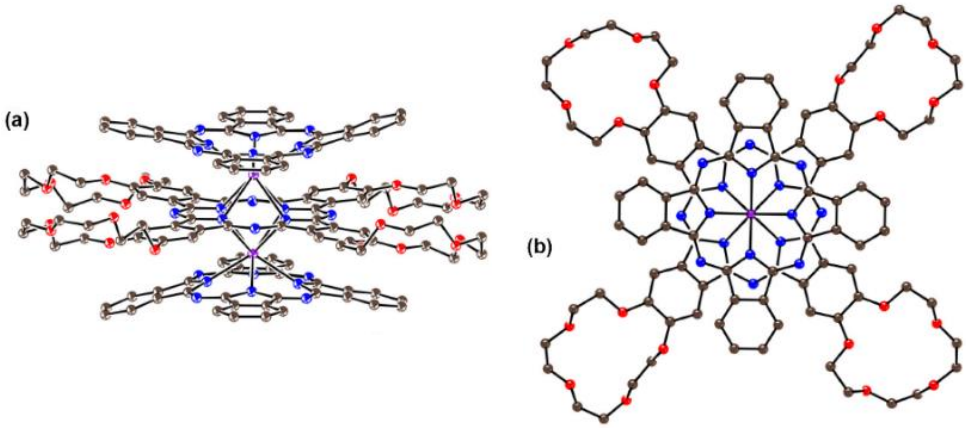

Figure 1.18: X-ray crystal structure of heteroleptic triple decker complex **(Pc)Tb[(15C5)$_4$Pc]Tb(Pc)**. Views from (a) side, (b) top.[99]

1.10 Heteroleptic Heteronuclear Tb (III) and Y (III) Trisphthalocyaninates

In the previous studies, Martynov and co-workers were investigating the effects of:

1) changing the heteroleptic ligand in the presence of the same metal
2) changing the heterometallic ions in the presence of the same ligand.

The same authors further investigated the effects of changing both the metal and the ligand in heterometallic heteroleptic complex. Two new compounds with Tb(III) and Y(III) with phthalocyanine core bearing BuO- [**B**] and 15C5- [**C**] as substituents were synthesised.

The synthesis of **[B$_4$]M[B$_4$]M*[C$_4$]** (where M ≠ M* are Tb or Y) complex was carried out in a stepwise procedure. The initial step involved the synthesis the homoleptic double decker unit of **M[B$_4$]$_2$**.[97] In the second step the butoxy substituted **M[B$_4$]$_2$** phthalocyanine, where M is either Tb or Y, was mixed with the metal-free of 15C5- substituted phthalocyanine H$_2$**[C$_4$]** and with the other metal acetylacetonate M*(acac)$_3$·nH$_2$O (where M* = Y or Tb) in boiling solvent mixture of 1,2,4-trichlorobenzene and 1-octanol. The target complexes were isolated and purified from unreacted starting double-deckers and the sole by-product homonuclear trisphthalocyaninates **M*$_2$[C$_4$]$_3$**. The yields of **[B$_4$]Y[B$_4$]Tb[C$_4$]** and **[B$_4$]Tb[B$_4$]Y[C$_4$]** were 65% and 74% respectively (scheme 1.38).[100]

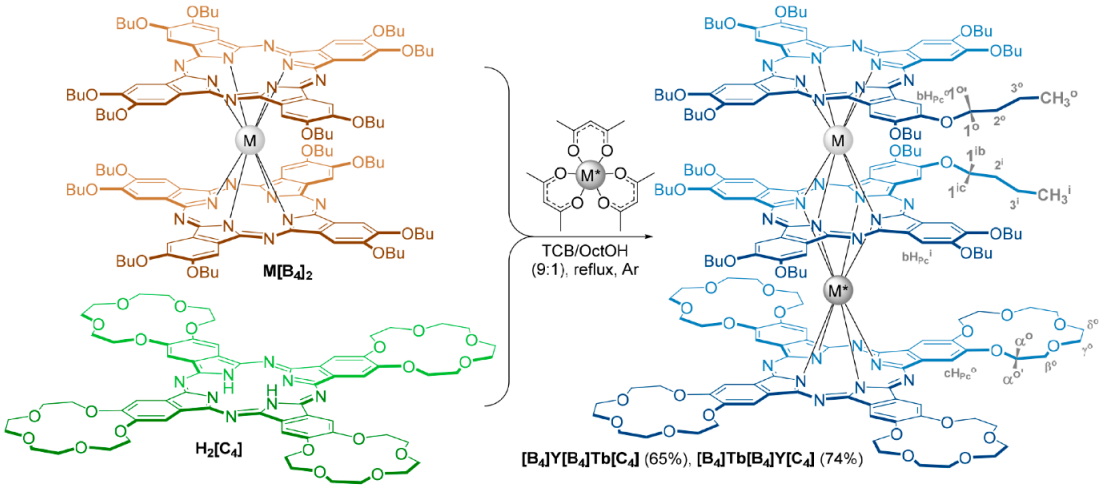

Scheme 1.38: Synthesis of heterometallic heteroleptic triple decker complex.[100]

The complexes were characterised by UV-vis in a halogenated and aromatic solvents such as dichloromethane and toluene respectively. Both complexes displayed less intense Soret and N-bands at 362 and 293 nm and well-resolved intense Q-bands at 643 and 696 nm in toluene. The spectra of the complexes in CH_2Cl_2, showed differences in the Soret and N-bands with a decrease in the intensity of the Q-bands as shown in the figure 1.19.

To account for the above differences in spectra, the authors proposed that these complexes are switched by solvation whereby in the conformers where both metal centres are square antiprismatic, is stabilised in toluene. In CH_2Cl_2 however, the metal centres M and M* are in a distorted prismatic and antiprismatic environment, respectively.

The above results are consistent with their previous work. The ^{1}H-NMR spectra of the complexes **[B$_4$]Y[B$_4$]Tb[C$_4$]** and **[B$_4$]Tb[B$_4$]Y[C$_4$]**, showed signals distributed over a wide range of chemical shifts due to paramagnetic nature of the Tb^{3+} ion. The magnetic susceptibility is sensitive to the switching conformation in the presence of Tb(III) ions. These outcomes open up a new avenue for manipulating the magnetic properties of phthalocyanine-containing lanthanide complexes.[100]

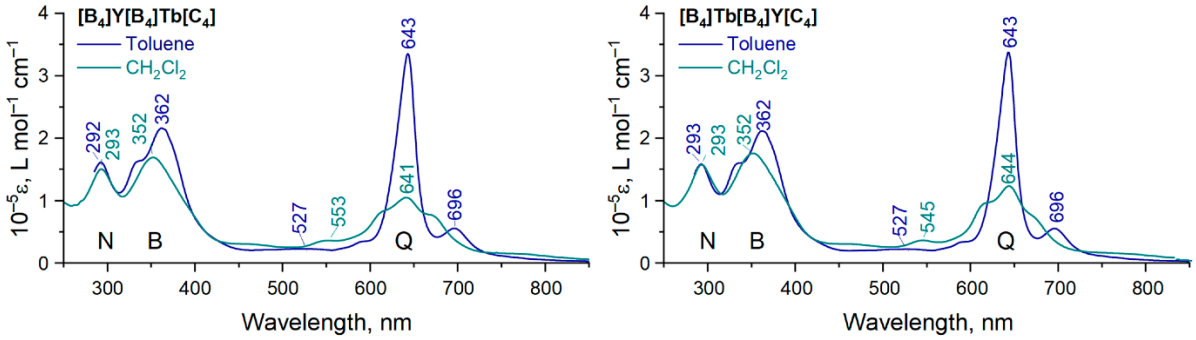

Figure 1.19: UV-Vis spectra of the triple decker complex.[100]

1.10.1 Heteroleptic heteronuclear porphyrin and phthalocyanine triple decker complex

Jiang and co-workers synthesised heteroleptic heterometallic triple decker using octa(phenoxyl)phthalocyanine, $Pc(OPh)_8$ and *meso*-tetrakis(4-chlorophenyl)porphyrin, TClPP with dysprosium and or yttrium as the spin carrier.[101]

Synthesis of the target triple decker **(TClPP)M[Pc(OPh)$_8$]M′[Pc(OPh)$_8$]** where M–M′ = Dy–Dy, Y–Dy, Dy–Y was achieved in a stepwise procedure. Initially the single decker complex of M(TClPP)(acac) was obtained by mixing the metal-free porphyrin (**76**) with the $[M(acac)_3]\cdot nH_2O$. This intermediate (**77**) was then added to a preformed bis(phthalocyaninato) rare-earth complex [Pc(OPh)$_8$]M′[Pc(OPh)$_8$] in boiling TCB for 4 h. After purifications, the yields of 50%, 43%, 75% were recorded for the complexes of **(TClPP)Dy[Pc(OPh)$_8$]Dy[Pc(OPh)$_8$]**, **(TClPP)Y[Pc(OPh)$_8$]Dy[Pc(OPh)$_8$]**, **(TClPP)Dy[Pc(OPh)$_8$]Y[Pc(OPh)$_8$]** respectively (scheme 1.39).[101] The authors did not report any scrambling nor mixing of products from the synthesis.

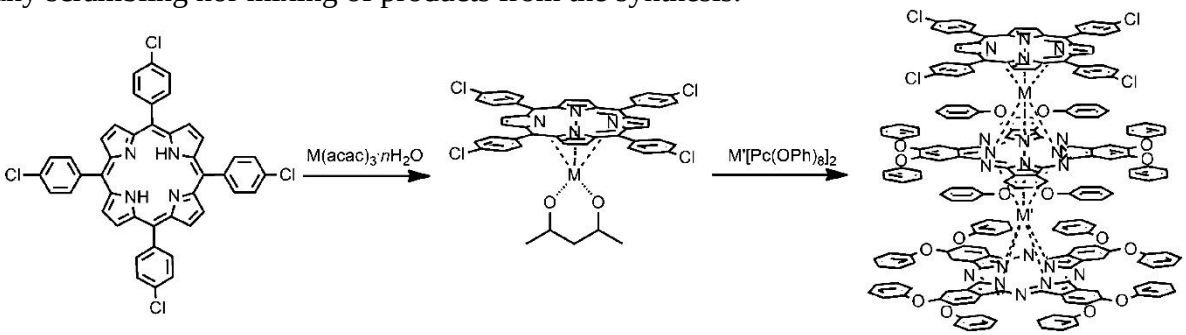

76 **77** **78**

Scheme 1.39: Synthesis of heteroleptic triple decker complex.[101]

Crystals for X-ray crystallographic analysis of the three triple deckers were grown from a solution of methanol and chloroform. The short distance between M-M′ in all the three complexes was 3.586(3)–3.605(3) Å which results in a magnetic dipolar interaction. The twist angle between the outer porphyrin and the inner phthalocyanine ligand was found to be 9.64–9.90°, adopting a more (pronounced) distorted square-antiprism (SAP) geometry. While the angle between the two phthalocyanine cores was 25.12–25.30° giving rise to a distorted SAP octa coordination geometry as depicted in the figure 1.20.

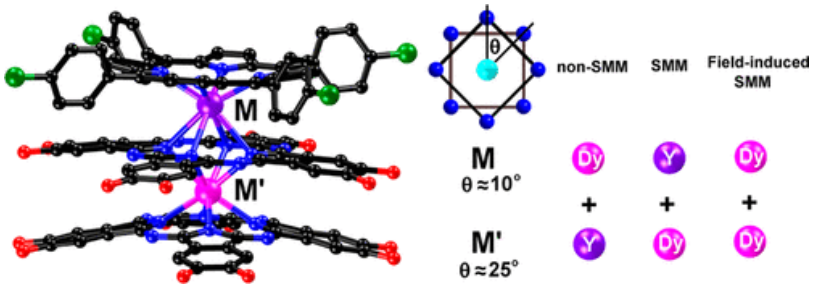

Figure 1.20: Molecular structure of the complex and the twist angle around the two metals.[101]

The same authors then investigated the magnetic properties of the three complexes to determine whether the effects of the coordination geometry around the metal ion and the f–f interaction between the two metal ions have an impact on the magnetic susceptibility. They found that when the sandwich system of Dy−Dy, Y−Dy, and Dy−Y were subjected to magnetic field-induced SMM, SMM, and non-SMM respectively, the coordination geometry of the spin carrier gave rise to the magnetic properties and not the f–f interaction between the metal ions.[101]

1.11 Supramolecular deckers

In recent years, there has been a huge interest to develop multi-decker compounds that is, quadruple-, quintuple-, sextuple- decker types of compounds using rare-earth metals.[102–105]

In 2021, Jiang and co-workers[103] designed and synthesised a sextuple-decker complex composing of heteroleptic phthalocyanine heterometallic samarium–cadmium compound, **[(Pc)Sm(Pc)Cd(Pc*)Cd(Pc*)Cd(Pc)Sm(Pc)] 79** where Pc and Pc* are unsubstituted phthalocyanine and 2,3,9,10,16,17,23,24-octakis(*n*-pentyloxy)phthalocyanine as depicted in the picture below. A preformed double decker, Pc-Sm-Pc[106] was added to a mixture of $Cd(OAc)_2 \cdot 2H_2O$ and H_2Pc^* in TCB. After purification and recrystallisation, a dark-blue crystal of the product was formed in a 15% yield (figure 1.21).

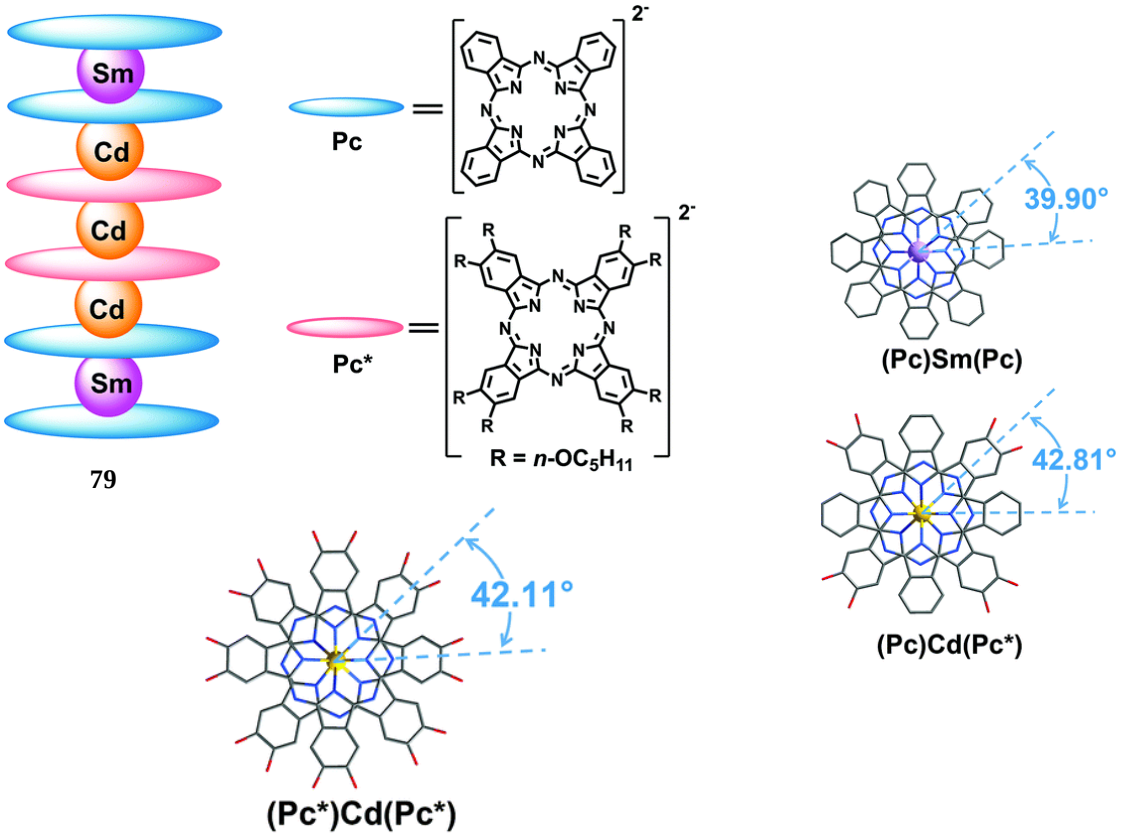

Figure 1.21: Molecular model of sextuple-decker complex **79** and angles between the ligands.[103]

The authors found that for the (Pc)Cd(Pc), (Pc)Cd(Pc*) and (Pc*)Cd(Pc*) subunits in complex **79**, the rotation angles between the adjacent phthalocyanines are 39.90°, 42.81° and 42.11°, respectively. This suggests that the ligands surrounding the metal ions Sm and Cd are in square-antiprismatic polyhedron. The intrinsic conjugated nature of the complex **79** has led the researchers to investigate in both the solution and gel glass forms of this complex and they showed third-order nonlinear optical properties.

1.11.1 Supramolecule from a dimerization of triple decker

In 2020, Martynov and co-workers first reported a single-crystal X-ray diffraction crystallographic characterization of a supramolecule composed of two heteroleptic crown-substituted trisphthalocyaninates.[107]

In order to design this supramolecule, the triple decker **[(15C5)$_4$Pc]Y(Pc)Y(Pc)]**, which consists of two phthalocyanine units and a crown substituted phthalocyanine is first synthesised followed by the addition of potassium tetraphenylborate resulting in a dimerization product. The resulting compound is a six decker with four rare earth metal ions without any additional

bridging groups at the core. Dark blue crystals were formed by using gradual diffusion of a $KBPh_4$ solution in acetonitrile into a solution of **[(15C5)$_4$Pc]Y(Pc)Y(Pc)]** in a solvent mixture of chloroform and 20% methanol (scheme 1.40).

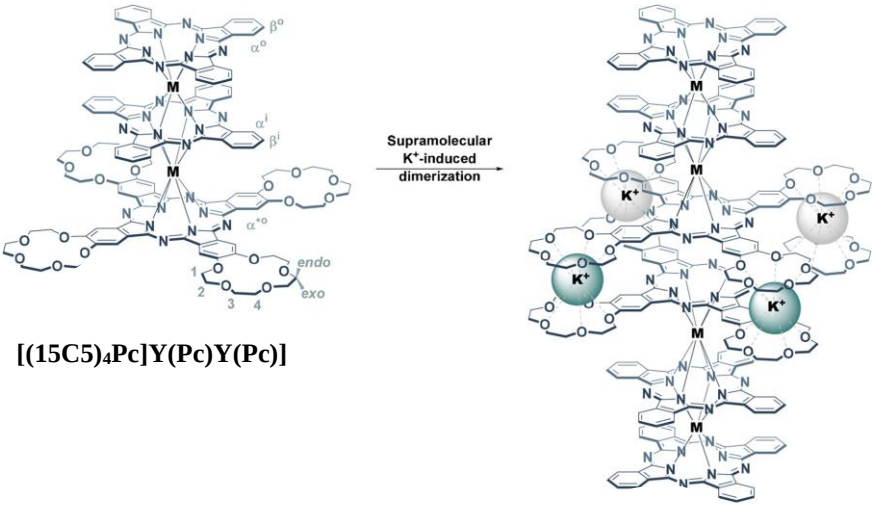

Scheme 1.40: Synthesis of the dimerise product from **[(15C5)$_4$Pc]Y(Pc)Y(Pc)]**.[107]

The X-ray crystallography data (figure 1.22) of the dimerisation product showed, the distance between Y···Y distance was 3.485(2) Å, which is similar to other reported homonuclear triple decker of phthalocyanine with M···M distance of 3.5 Å.[57,108] This distance is essential for the strong ferromagnetic coupling between the metal ions. The intramolecular distance between Y1···Y1′ was found to be 13.174(2) Å. The outcome of their study is that this dimeric compound can be potentially used in supramolecular magnetic materials.[107]

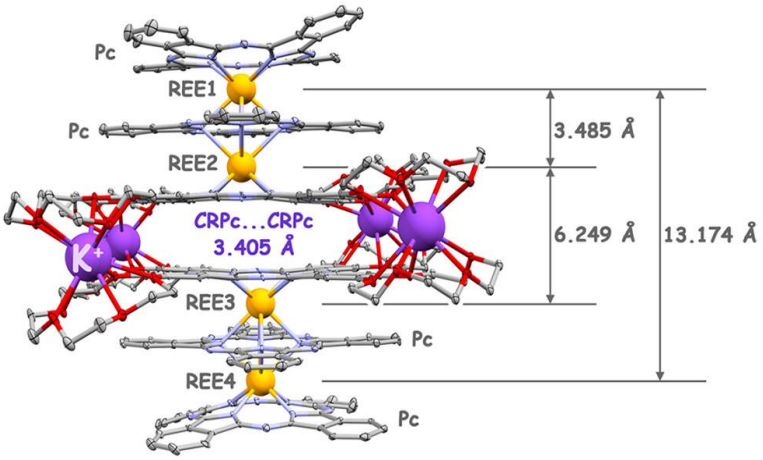

Figure 1.22: Molecular structure of the dimerised product.[107]

1.12 Sandwich complexes of TBTAP

In 2013, Pushkarev and co-workers[39] were the first to report sandwich-type complexes bearing tetrabenzotriazaporphyrin ligands. The group successfully synthesised homoleptic (Ph-TBTAP)$_2$Lu **80 a**, (Ph-TBTAP)$_2$Eu **80 b**, and heteroleptic (tetrabenzotriazaporphyrinato) (phthalocyaninato) lutetium derivative (Ph-TBTAP)LuPc **81 a**, (Ph-TBTAP)EuPc **81 b**, in good yields. Prior to the formation of these double deckers, the preformed zinc *meso*-phenyl TBTAP was demetallated to form the free ligand which then underwent a complexation reaction with M(III) acetylacetonate in a high boiling point solvent such as n-hexadecanol to yield the homoleptic double decker. During the course of the reaction, the authors isolated a small quantity of the Eu triple decker sandwich **82** (figure 1.23). They found that the yield of the triple decker significantly increased upon changing the concentration, increasing the temperature and using a higher equivalent of the Ln (III) salts.[109] The heteroleptic dyad was obtained by reacting the metal-free *meso*-phenyl TBTAP with preformed lutetium mono phthalocyanine in 1, 2, 4 trichlorobenzene (scheme 1.41).

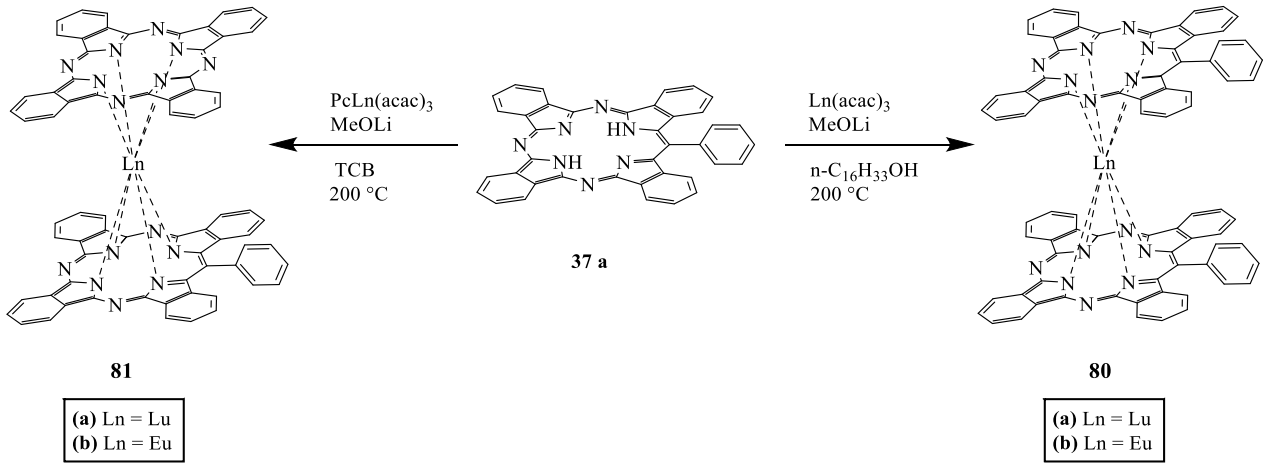

Scheme 1.41: Homo- and heteroleptic lutetium double-decker complexes based on *meso*-phenyl-tetrabenzotriazaporphyrin.[109]

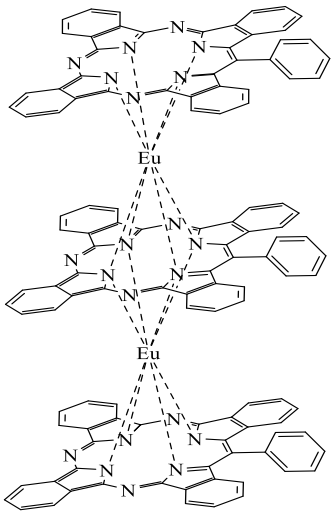

82

Figure 1.23: Isolated triple decker as a by-product from the synthesis of **80b**.[109]

The synthesis of the sandwich type deckers of TBTAP are very limited in literature. Therefore, there is a need to expand the scope on the synthesis of such compounds.

1.13 Applications

The design and synthesis of the rare earth double- and triple- decker complexes with porphyrin and/ or phthalocyanine macrocycles have potential applications in material science and some applications have been mentioned in the previous sections. The intramolecular π- π interactions and f-f interactions of the metal ions have contributed to their optical, spectroscopic, physical, electrical and electrochemical properties. Previously synthesised sandwich triple-deckers showed a remarkable number of redox states with reversible electrochemistry and possess low oxidation potentials. Because of these outstanding characteristics, they have potential use in multibit molecular information storage, areas of sensors, molecular magnets, field effect transistors nonlinear optical materials and nanomaterials.[61,69]

1.13.1 Single-molecule magnets (SMM)

Certain molecules have been found to store individual pieces of data and can be used in high density data storage. A single-molecule magnet (SMM) consists of small molecules and each molecule behaves as an individual superparamagnet and provides the ultimate limit for data storage.[110] Compared to traditional recording media, molecule-based media would afford much

greater storage densities. The distinctive property of SMMs is the occurrence of magnetic hysteresis at low temperature, so that each molecule behaves as a tiny magnet.

Metals from the lanthanides series contain electrons occupying the f orbitals. Such metals possess high magnetic susceptibilities which are the origin of their behaviour. Dysprosium to erbium is classified as the middle-late lanthanides and were found to have the highest magnetic susceptibilities. Among the series of Ln^{3+} ions, Dy^{3+} and Tb^{3+} are arguably the ions of choice for preparing high-performance SMMs.[69,101]

1.13.2 Organic solar cells

Organic solar cells (OSCs) have gained much attention over the past two decades due to their potential to produce flexible, inexpensive and lightweight devices.

Porphyrin and phthalocyanines macrocycles have been extensively studied in terms of their ability to absorb and donate electrons for OSCs. Multi-decker molecules of porphyrins and phthalocyanines are characterised by the presence of their extensive π–π interactions which can enhance electron delocalization and charge transport making them suitable for OSCs. Unfortunately, there has been a serious lack of studies on photovoltaic cells produced from deckers of phthalocyanines and porphyrins in literature. Solar cells which are manufactured from phthalocyanine deckers may use their unique electronic and optical properties including broadband absorption at a wavelength higher than 700 nm and high carrier mobility make these complexes suitable for photovoltaic applications.[69,111]

Wang and co-workers investigated the potential capabilities of two previously synthesised double **83** and triple decker **84** complexes in OSCs (figure 1.24).[112,113] Results from the optical characterization show that broad band light harvesting is possible with these materials. The performance of these cells was found to be highly dependent on the relevant decker structures, the morphology of the active layers, and the cell structures.[114]

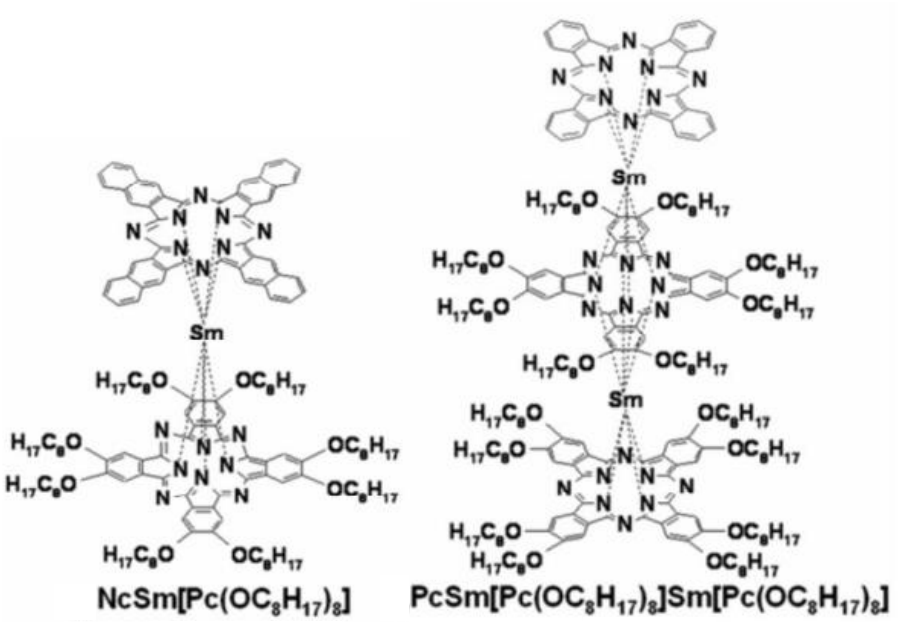

83 **84**

Figure 1.24: Heteroleptic double and triple deckers.[112]

For example, Li and co-workers have designed and synthesised a series of highly soluble sandwich-type protonated mixed (porphyrinato)(phthalocyaninato) double-decker complexes (**85–91**) (figure 1.25) bearing different rare earth metal centres. Their results demonstrated that such complexes were suitable in the development of new photovoltaic materials with broadband light harvesting capabilities.[115]

The complexes synthesised were used as broadband absorbers and electron donors. As for the electron acceptor component, the authors used N,N-bis(1-ethylhexyl)-3,4:9,10-perylenebis(dicarbox-imide) (PDI) or [6,6]-phenyl-C_{61} butyric acid methyl ester (PCBM). The authors found that the solar cells in which the PDI was incorporated had a higher power conversion efficiency. The results from their study showed that on a cell area of 0.36 cm^2 a 0.82% efficiency was reported when europium double decker was used while a lower efficiency of 0.59% was recorded for lutetium double decker. The authors are still investigating other complexes in order to achieve a higher efficiency.

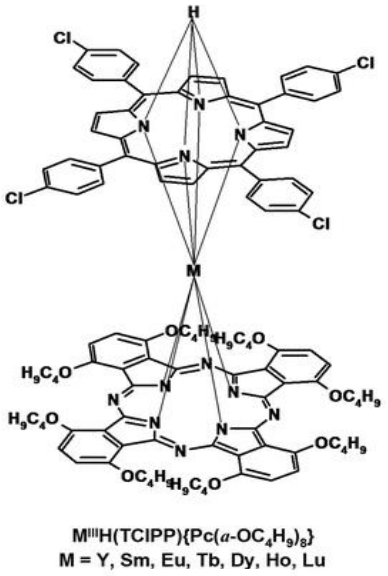

85- 91

Figure 1.25: Mixed (porphyrinato)(phthalocyaninato) double-decker.

1.13.3 Detection of NO_2, NH_3 and H_2S using sensor based on europium-decker complexes

Over the last few years, scientists have been focusing on the development of high performance and precision gas sensors to detect hazardous gases such as H_2S, NO_2, NH_3. Available devices used inorganic semiconducting materials which only worked at high temperatures. Therefore, it is essential to develop cheap, light weight organic semiconductors with easier mouldability of molecular properties, and solution processability and can work at low temperatures.

In 2023, Chen and co-workers synthesised 3 heteroleptic and homoleptic europium double deckers bearing tetradiazepinoporphyrazine and or phthalocyanine molecules. They obtained [$^{n\text{Bu}}$Pc]$_2$Eu **92**, [$^{t\text{BuPh}}$DzPz][$^{n\text{Bu}}$Pc]Eu **73 b** and [$^{t\text{BuPh}}$DzPz]$_2$Eu **93** (figure 1.26).[116]

To produce the nanostructures of the compounds they used a solution-based method, known as the quasi-Langmuir-Shäfer (QLS), which led to a well-ordered film.

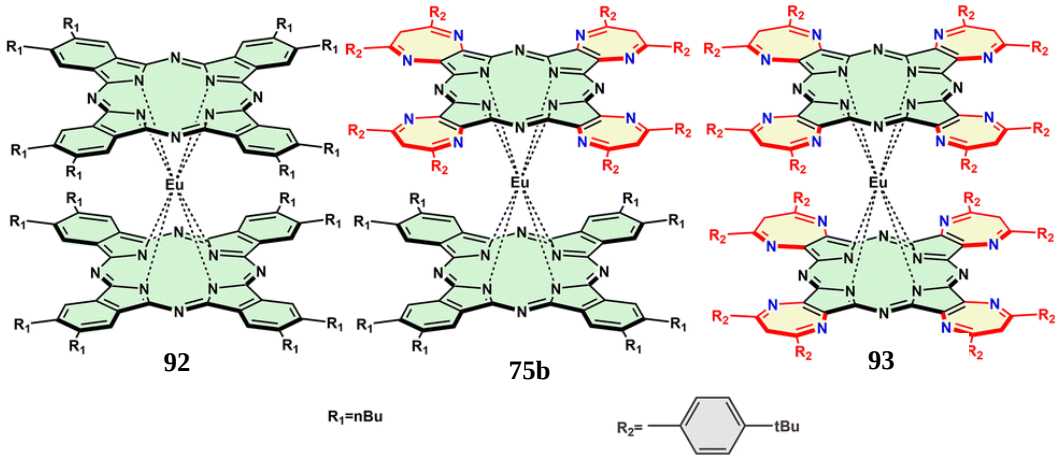

Figure 1.26: Molecular structures of [$^{n\text{Bu}}$Pc]$_2$Eu **92**, [$^{t\text{BuPh}}$DzPz][$^{n\text{Bu}}$Pc]Eu **75b** and [$^{t\text{BuPh}}$DzPz]$_2$Eu **93**.[116]

The three stable double deckers were exposed to the three gases, NO_2, NH_3, H_2S at room temperature and their conductivity responses were monitored. They found out that at sub-ppm level, compound **92** responded to NO_2 and NH_3, compound **75 b** gave a response to the three gases while compound **93** responded to NO_2 and H_2S. Of all the three double deckers, compound [$^{t\text{BuPh}}$DzPz][$^{n\text{Bu}}$Pc]Eu **75b** gave an excellent sensing response to the three gases with good sensitivities for NO_2, NH_3, and H_2S. An ultra-low concentration of 20 ppb, 1 ppm, 100 ppb were detected for the three gases NO_2, NH_3 and H_2S respectively with a quick response time of 1 min for compound **75b**.

The same group reported two Eu triple deckers (**94** and **95**), one of which bears an electron withdrawing group such as trifluoroethoxy while the other has an electron donating group such as an alkoxy or polyoxyethylene at the periphery position of the Pc ring (figure 1.27). These groups were introduced to play an important role in adjusting their HOMO and LUMO levels for the application of ambipolar organic semiconductors. Both compounds had a higher detection limit of 0.1 ppm, 3 ppm, 5 ppm for NO_2, NH_3, H_2S respectively. A good sensitivity was recorded for NO_2, NH_3, H_2S when Eu triple deckers **94** was used. However, the compounds had a longer recovery time of 2 min and 12 min for **94** and **95** respectively as compared to the above double deckers.[117]

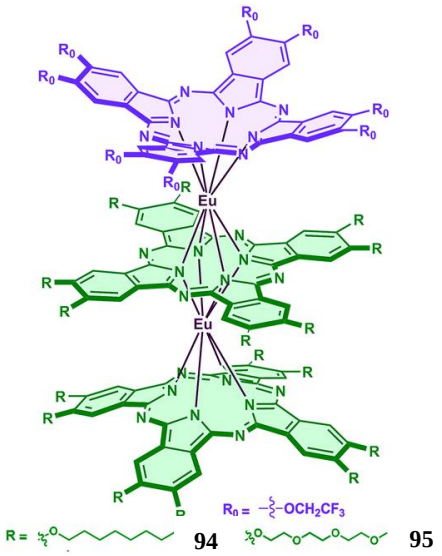

Figure 1.27: Molecular structures of triple-decker $Eu_2[Pc(OC_8H_{17})_8]_2[Pc(OCH_2CF_3)_8]$ **94** and $Eu_2\{Pc[(OC_2H_4)_3OCH_3]_8\}_2[Pc(OCH_2CF_3)_8]$ **95**.[117]

Jiang and co-workers synthesised double decker $Eu[Pc(SC_2H_5)_8]_2$ (**Pc-1**), and triple decker $Eu_2[Pc(SC_2H_5)_8]_3$ (**Pc-2**), of ethylthio-substituted phthalocyaninato europium (III) complexes and their dimer was obtained by combining with double- and/or triple-decker (figure 1.28).[118]

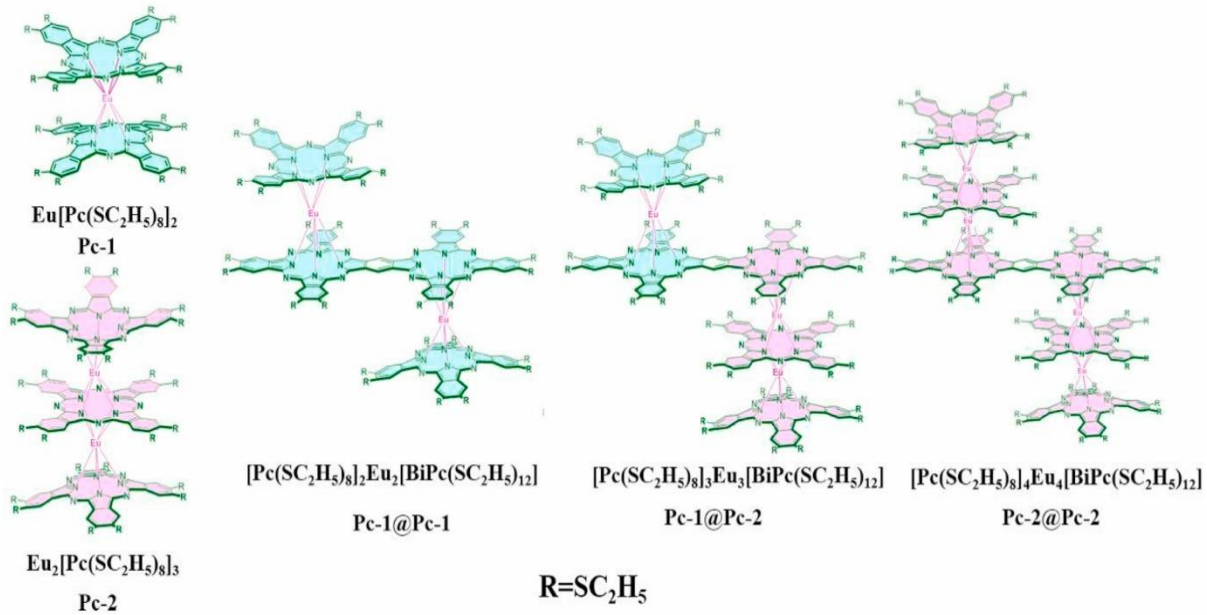

Figure 1.28: Schematic molecular structures of **Pc-1**, **Pc-2**, **Pc-1@Pc-1**, **Pc-1@Pc-2** and **Pc-2@Pc-2**.[118]

The **Pc-2@Pc-2** has an extended π-conjugation and among the five compounds it was found to be oxidized easily, as a result, it is more sensitive to NO_2 detection, and it was 4 times higher

than **Pc-1**. They found the sensitivity (in % ppm^{-1}) increases in the order of **Pc-1** < **Pc-2** < **Pc-1@Pc-1** < **Pc-1@Pc-2** < **Pc-2@Pc-2** for NO_2, and **Pc-1@Pc-2** < **Pc-1** < **Pc-1@Pc-1** < **Pc-2@Pc-2** < **Pc-2** for NH_3. A high sensitivity for NO_2 and NH_3 for the complexes **Pc-2@Pc-2** and **Pc-2** were recorded respectively. The limit of detection for NO_2 and NH_3 were 10 ppb and 0.48 ppm respectively. Of all the complexes, films of **Pc-2@Pc-2** and **Pc-2** were the best gas sensors for organic semi-conductors at room temperature. The results obtained from five recycling tests of less than 2 min exposure time were reproducible and stable towards 100 ppb of NO_2 gas and 4 ppm of NH_3.

The authors then attempted to use these complexes for the potential detection of gases such as H_2S and CO_2. They reported that no distinct responses were recorded, and they suggested that this observation is probably due to their weaker electron-donating ability than NH_3.[118]

1.13.4 Molecular gears

Molecular machines play an important role in many biological processes. They respond in a very controlled manner to a specific external stimulus with high precision and efficiency.[119,120] In the last few decades, many researches have been focusing on design and synthesis of supramolecular machines with a high degree of precision into controlling the motions at the molecular level involving functionalised porphyrin units.[120–124] Synthesis of molecules bearing many motions which are linked and synchronised at the same time is proving to be extremely challenging and progress in this field has proved to be very slow.

In 2023, Nishino and co-workers designed a molecular gearing compound consisting of cerium (IV) double-decker of a functionalised porphyrin molecule with triptycene units (figure 1.29).[125] Using variable temperature ^{1}H-NMR measurement, the dynamic behaviour was studied from 213–373 K. The data obtained from the ^{1}H-NMR at room temperature reveals that the 3,5-dibutoxyphenyl and the porphyrin rings are not rotating while the triptycenes move freely. At 213 K, the peaks broadened, suggesting that the rotational speed of triptycenes was slower and was closer to the NMR timescale. A study of the rotational behaviour between the porphyrin molecules was studied. The peaks corresponding to protons at the β-position on the pyrrole unit of the porphyrin did not alter at 373 K implying that the relative angle of two porphyrins coordinating to the Ce ions was maintained even at high temperature and Ce(**L**)$_2$ has

a high activation energy for intra-ligand rotation. The data obtained from the NMR analysis clearly shows that the rotation of both the engaged triptycenes and porphyrins rotation were independent of each other. The authors are still investigating the possibility of using these molecules in molecular gear devices.[125]

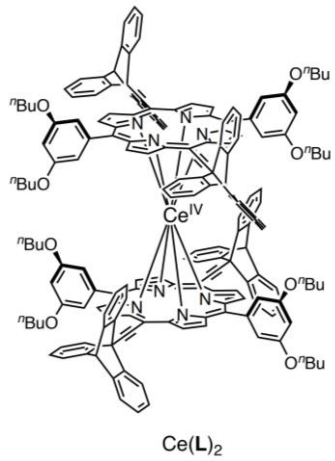

Figure 1.29: Cerium double decker complex.[125]

References

(1) Cornils, B.; Herrmann, W. A.; Weinheim, V. C. H. Colorful Catalysts. *Adv. Mater.* **1997**, *9* (15), 571. – 675.

(2) Lesage, S.; Hao Xu; Durham, L. The Occurrence and Roles of Porphyrins in the Environment: Possible Implications for Bioremediation. *Hydrological Sciences Journal/Journal des Sciences Hydrologiques* **1993**, *38* (4), 343–354.

(3) Ptaszek, M. Rational Design of Fluorophores for in Vivo Applications. *Prog Mol Biol Transl Sci* **2013**, *113*, 59–108.

(4) Zhang, R.; Warren, J. J. Recent Developments in Metalloporphyrin Electrocatalysts for Reduction of Small Molecules: Strategies for Managing Electron and Proton Transfer Reactions. *ChemSusChem*. Wiley-VCH Verlag January 7, 2021, pp 293–302.

(5) Zhang, W.; Lai, W.; Cao, R. Energy-Related Small Molecule Activation Reactions: Oxygen Reduction and Hydrogen and Oxygen Evolution Reactions Catalyzed by Porphyrin- and Corrole-Based Systems. *Chem Rev* **2017**, *117* (4), 3717–3797.

(6) Karlson, P. The Nomenclature of Tetrapyrroles. *J Clin Chem Clin Biochem* **1981**, *19* (1), 43–47.

(7) Moss, G. P. Nomenclature of Tetrapyrroles (Recommendations 1986). *Pure and Applied Chemistry* **1987**, *59* (6), 779–832.

(8) Moss, G. P. Nomenclature of Tetrapyrroles. *Eur J Biochem* **1988**, *178* (2), 277-328.

(9) Rothemund, P. A New Porphyrin Synthesis. The Synthesis of Porphin. *Journal of the American Chemical Society* **1936**, *58* (4), 625–627.

(10) Falk, J. E. *Porphyrins and Metalloporphyrins*; 1975; Vol. 2.

(11) Kadish, K. M.; Smith, K. M.; Guilard, R. *The Porphyrin Handbook, Volume 1*; 2000; Vol. 1.

(12) Rothemund, P. Formation of Porphyrins from Pyrrole and Aldehydes. *J Am Chem Soc* **1935**, *57* (10), 2010–2011.

(13) Rothemund, P.; Menotti, A. R. Porphyrin Studies. IV. 1 The Synthesis of α, β, γ, δ-Tetraphenylporphine. *J Am Chem Soc* **1941**, *63* (1), 267–270.

(14) Adler, A. D.; Longo, F. R.; Shergalis, W. Mechanistic Investigations of Porphyrin Syntheses. I. Preliminary Studies on Ms-Tetraphenylporphin. *J Am Chem Soc* **1964**, *86* (15), 3145–3149.

(15) Lindsey, J. S.; Schreiman, I. C.; Hsu, H. C.; Kearney, P. C.; Marguerettaz, A. M. Rothemund and Adler-Longo Reactions Revisited: Synthesis of Tetraphenylporphyrins under Equilibrium Conditions. *J Org Chem* **1987**, *52* (5), 827–836.

(16) Lindsey, J. S.; MacCrum, K. A.; Tyhonas, J. S.; Chuang, Y. Y. Investigation of a Synthesis of Meso-Porphyrins Employing High Concentration Conditions and an Electron Transport Chain for Aerobic Oxidation. *J Org Chem* **1994**, *59* (3), 579–587.

(17) Gouterman, M. Spectra of Porphyrins*. *J Mol Spectroscopy* **1961**, *6*, 138–163.

(18) Rio, Y.; Rodríguez-Morgade, M. S.; Torres, T. Modulating the Electronic Properties of Porphyrinoids: A Voyage from the Violet to the Infrared Regions of the Electromagnetic Spectrum. *Org Biomol Chem* **2008**, *6* (11), 1877–1894.

(19) De La Torre, G.; Claessens, C. G.; Torres, T. Phthalocyanines: Old Dyes, New Materials. Putting Color in Nanotechnology. *Chemical Communications* **2007**, No. 20, 2000–2015.

(20) De La Torre, G.; Vázquez, P.; Agulló-López, F.; Torres, T. Materials Phthalocyanines and Related Compounds: Organic Targets for Nonlinear Optical Applications. *J. Mater. Chem* **1998**, *8* (8), 1671–1683.

(21) Sakamoto, K.; Ohno-Okumura, E. Syntheses and Functional Properties of Phthalocyanines. *Materials* **2009**, *2* (3), 1127–1179.

(22) García-Sánchez, M. A.; Rojas-González, F.; Menchaca-Campos, E. C.; Tello-Solís, S. R.; Quiroz-Segoviano, R. I. Y.; Diaz-Alejo, L. A.; Salas-Bañales, E.; Campero, A. Crossed and Linked Histories of Tetrapyrrolic Macrocycles and Their Use for Engineering Pores within Sol-Gel Matrices. *Molecules* **2013**, *18* (1), 588–653.

(23) Barrett P A.; Linstead R P.; Tuey G A P.; Robertson M J. Phthalocyanines and Related Compounds. Part XV. Tetrabenztriaxaporphin: Its Preparation from Phthalonitrile and a Proof of Its Structure. *J Chem Soc* **1939**, 1809–1820.

(24) Tomoda, H.; Saito, S.; Shiraishi, S. Synthesis of Metallophthalocyanines from Phthalonitrile with Strong Organic Bases. *Chem Lett* **1983**, *12*, 313–316.

(25) Tomoda, H.; Saito, S.; Ogawa, S.; Shiraishi, S. Synthesis of Phthalocyanines from Phthalonitrile with Organic Strong Bases. *Chemistry Letters* **1980**, *9*, 1277–1280.

(26) Waring, D. R. *Heterocyclic Dyes and Pigments. In Comprehensive Heterocyclic Chemistry*; Elsevier Inc: Oxford, 1984.

(27) Milaeva, E. R.; Speier, G.; Lever, A. B. P.; Leznoff, C. C.; Lever, A. B. P. *The Phthalocyanines, Properties and Applications.*; Wiley, 1992.

(28) Leznoff, C. C. *Phthalocyanines: Properties and Applications*; VCH publishers, 1989.

(29) Kalashnikov, V. V; Pushkarev, V. E.; Tomilova, L. G. Tetrabenzotriazaporphyrins: Synthesis, Properties and Application. *Russian Chemical Reviews* **2014**, *83* (7), 657–675.

(30) Helberger, J. H.; Von Rebay, A. Action of Cuprous Cyanide on O-Haloacetophenone. II. *Justus Liebigs Ann. Chem* **1397**, *531*, 279–287.

(31) Barrett P A.; Linstead R P.; Rundall F G.; Tuey G A P. Phthalocyanines and Related Compounds. Part XIX. Tetrabenzporphyrin, Tetrabenzomonazaporphyrin and Their Metallic Derivatives. *Journal of the Chemical Society (Resumed)* **1940**, 1079–1092.

(32) Dent, C. E. Preparation of Phthalocyanine-like Pigments Related to the Porphyrins. *J. Chem. Soc* **1938**, 1–6.

(33) Leznoff, C. C.; McKeown, N. B. Preparation of Substituted Tetrabenzotriazaporphyrins and a Tetranaphthotriazaporphyrin: A Route to Mono-Meso-Substituted Phthalocyanine Analogs. *J Org Chem* **1990**, *55* (7), 2186–2190.

(34) Tse, Y.-H.; Goel, A.; Hu, M.; Lever, A. B. P.; Leznoff, C. C.; Van Lier, J. E. Electrochemistry and Spectroelectrochemistry of Substituted Tetrabenzotriazaporphine. *Can J Chem* **1993**, *71* (5), 742–753.

(35) Galanin, N. E.; Kudrik, E. V; Shaposhnikov, G. P. Synthesis and Properties of Meso-Phenyl-Substituted Tetrabenzoazaporphins Magnesium Complexes. *Russian Journal of Organic Chemistry* **2002**, *38* (8), 1200–1203.

(36) Galanin, N. E.; Kudrik, E. V; Shaposhnikov, G. P. Meso-Phenyltetrabenzoazaporphyrins and Their Zinc Complexes. Synthesis and Spectral Properties. *Russ J Gen Chem* **2005**, *75* (4), 651–655.

(37) Galanin, N. E.; Kudrik, E. V; Shaposhnikov, G. P. Synthesis and Properties of Meso-Alkyltetrabenzotriazaporphyrins and Their Zinc Complexes. *Russ J Gen Chem* **2004**, *74* (2), 282–285.

(38) Kalashnikov, V. V; Pushkarev, V. E.; Tomilova, L. G. A Novel Synthetic Approach to 27-Aryltetrabenzo [5, 10, 15] Triazaporphyrins. *Mendeleev Communications* **2011**, *21* (2), 92–93.

(39) Pushkarev, V. E.; Kalashnikov, V. V; Trashin, S. A.; Borisova, N. E.; Tomilova, L. G.; Zefirov, N. S. Bis(Tetrabenzotriazaporphyrinato) and (Tetrabenzotriazaporphyrinato) (Phthalocyaninato) Lutetium(III) Complexes-Novel Sandwich-Type Tetrapyrrolic Ligand Based NIR Absorbing Electrochromes. *Dalton Transactions* **2013**, *42* (83), 12083–12086.

(40) Cammidge, A. N.; Cook, M. J.; Hughes, D. L.; Nekelson, F.; Rahman, M. A Remarkable Side-Product from the Synthesis of an Octaalkylphthalocyanine: Formation of a Tetrabenzotriazaporphyrin. *Chemical Communications* **2005**, No. 7, 930–932.

(41) Alharbi, N.; Díaz-Moscoso, A.; Tizzard, G. J.; Coles, S. J.; Cook, M. J.; Cammidge, A. N. Improved Syntheses of Meso-Aryl Tetrabenzotriazaporphyrins (TBTAPs). *Tetrahedron* **2014**, *70* (40), 7370–7379.

(42) Cammidge, A. N.; Chambrier, I.; Cook, M. J.; Hughes, D. L.; Rahman, M.; Sosa-Vargas, L. Phthalocyanine Analogues: Unexpectedly Facile Access to Non-Peripherally Substituted Octaalkyl Tetrabenzotriazaporphyrins, Tetrabenzodiazaporphyrins, Tetrabenzomonoazaporphyrins and Tetrabenzoporphyrins. *Chemistry - A European Journal* **2011**, *17* (11), 3136–3146.

(43) Díaz-Moscoso, A.; Tizzard, G. J.; Coles, S. J.; Cammidge, A. N. Synthesis of Meso-Substituted Tetrabenzotriazaporphyrins: Easy Access to Hybrid Macrocycles. *Angewandte Chemie - International Edition* **2013**, *52* (41), 10784–10787.

(44) Hellal, M.; Cuny, G. D. Microwave Assisted Copper-Free Sonogashira Coupling/5-Exo-Dig Cycloisomerization Domino Reaction: Access to 3-(Phenylmethylene)Isoindolin-1-Ones and Related Heterocycles. *Tetrahedron Lett* **2011**, *52* (42), 5508–5511.

(45) Dalai, S.; Belov, V. N.; Nizamov, S.; Rauch, K.; Finsinger, D.; De Meijere, A. Access to Variously Substituted 5,6,7,8-Tetrahydro-3H-Quinazolin-4-Ones via Diels-Alder Adducts of Phenyl Vinyl Sulfone to Cyclobutene-Annelated Pyrimidinones. *European J Org Chem* **2006**, No. 12, 2753–2765.

(46) Tejerina, L.; Yamamoto, S.; López-Duarte, I.; Martínez-Díaz, M. V.; Kimura, M.; Torres, T. Meso-Substituted Tetrabenzotriazaporphyrins for Dye-Sensitized Solar Cells. *Helv Chim Acta* **2020**, *103* (8).

(47) Faeza Hamad Alkorbi. Synthesis of Uniquely Functionalised Tetrabenzotriazaporphyrins, University of East Anglia, 2020.

(48) Alkorbi, F.; Díaz-Moscoso, A.; Gretton, J.; Chambrier, I.; Tizzard, G. J.; Coles, S. J.; Hughes, D. L.; Cammidge, A. N. Complementary Syntheses Giving Access to a Full Suite of Differentially Substituted Phthalocyanine-Porphyrin Hybrids. *Angewandte Chemie - International Edition* **2021**, *60* (14), 7632–7636.

(49) Kawamura, K.; Igarashi, S.; Yotsuyanagi, T. Catalytic Activity of Noble Metal Ions for the Degradation of 5,10,15,20-Tetrakis(4-Sulfonatophenyl)Porphine in the Presence of Oxidizing Agent, and Its Application to the Determination of Ultra Trace Amounts of Ruthenium. *Microchimica Acta* **2011**, *172* (3–4), 319–326.

(50) Martirosyan, G. G.; Azizyan, A. S.; Kurtikyan, T. S.; Ford, P. C. Low Temperature NO Disproportionation by Mn Porphyrin. Spectroscopic Characterization of the Unstable

Nitrosyl Nitrito Complex MnIII(TPP)(NO)(ONO). *Chemical Communications* **2004**, *4* (13), 1488–1489.

(51) Fleischer, E. B.; Wang, J. H. The Detection of a Type of Reaction Intermediate in the Combination of Metal Ions with Porphyrin. *J Am Chem Soc* **1960**, *82*, 3498–3502.

(52) Barkigia, K. M.; Fajer, L. J.; Adler, L. A. D.; Williams, G. J. B. *"Roof'' Porphyrin";* 1980; Vol. 19.

(53) Liu, C.; Yang, W.; Zhang, Y.; Jiang, J. Quintuple-Decker Heteroleptic Phthalocyanine Heterometallic Samarium - Cadmium Complexes. Synthesis, Crystal Structure, Electrochemical Behavior, and Spectroscopic Investigation. *Inorg Chem* **2020**, *59* (23), 17591–17599.

(54) Akabane, T.; Ohta, K.; Takizawa, T.; Matsuse, T.; Kimura, M. Discotic Liquid Crystals of Transition Metal Complexes, 54: Rapid Microwave-Assisted Synthesis and Homeotropic Alignment of Phthalocyanine-Based Liquid Crystals. *J Porphyr Phthalocyanines* **2017**, *21*, 476–492.

(55) Lu, G.; Li, J.; Jiang, X.; Ou, Z.; Kadish, K. M. Europium Triple-Decker Complexes Containing Phthalocyanine and Nitrophenyl-Corrole Macrocycles. *Inorg Chem* **2015**, *54* (18), 9211–9222.

(56) Lu, G.; Li, J.; Yan, S.; Zhu, W.; Ou, Z.; Kadish, K. M. Synthesis and Characterization of Rare Earth Corrole-Phthalocyanine Heteroleptic Triple-Decker Complexes. *Inorg Chem* **2015**, *54* (12), 5795–5805.

(57) Holmberg, R. J.; Polovkova, M. A.; Martynov, A. G.; Gorbunova, Y. G.; Murugesu, M. Impact of the Coordination Environment on the Magnetic Properties of Single-Molecule Magnets Based on Homo- and Hetero-Dinuclear Terbium(III) Heteroleptic Tris(Crownphthalocyaninate). *Dalton Transactions* **2016**, *45* (22), 9320–9327.

(58) Chan, W. L.; Xie, C.; Lo, W. S.; Bünzli, J. C. G.; Wong, W. K.; Wong, K. L. Lanthanide-Tetrapyrrole Complexes: Synthesis, Redox Chemistry, Photophysical Properties, and Photonic Applications. *Chem Soc Rev* **2021**, *50* (21), 12189–12257.

(59) Martynov, A. G.; Horii, Y.; Katoh, K.; Bian, Y.; Jiang, J.; Yamashita, M.; Gorbunova, Y. G. Rare-Earth Based Tetrapyrrolic Sandwiches: Chemistry, Materials and Applications. *Chem Soc Rev* **2022**, *51* (22), 9262–9339.

(60) Mironov, A. F. Porphyrin Complexes with Lanthanides. *Russian Chemical Reviews* **2013**, *82* (4), 333–351.

(61) Zhang, P.; Guo, Y. N.; Tang, J. Recent Advances in Dysprosium-Based Single Molecule Magnets: Structural Overview and Synthetic Strategies. *Coordination Chemistry Reviews* **2013**, *257*, 1728–1763.

(62) Abdullin, D.; Fleck, N.; Klein, C.; Brehm, P.; Spicher, S.; Lützen, A.; Grimme, S.; Schiemann, O. Synthesis of μ 2 -Oxo-Bridged Iron(III) Tetraphenylporphyrin–Spacer–Nitroxide Dimers and Their Structural and Dynamics Characterization by Using EPR and MD Simulations. *Chemistry - A European Journal* **2019**, *25* (10), 2586–2596.

(63) Oniwa, K.; Shimizu, S.; Shiina, Y.; Fukuda, T.; Kobayashi, N. A μ-Oxo Hetero Dimer of Silicon Phthalocyanine and Naphthalocyanine. *Chemical Communications* **2013**, *49* (75), 8341–8343.

(64) Yamada, Y.; Miwa, Y.; Toyoda, Y.; Phung, Q. M.; Oyama, K. I.; Tanaka, K. Evaluation of CH4 Oxidation Activity of High-Valent Iron-Oxo Species of a μ-Nitrido-Bridged Heterodimer of Iron Porphycene and Iron Phthalocyanine. *Catal Sci Technol* **2023**, *13* (6), 1725–1734.

(65) Iwanaga, O.; Fukuyama, K.; Mori, S.; Song, J. T.; Ishihara, T.; Miyazaki, T.; Ishida, M.; Furuta, H. Ruthenium(Iv) N-Confused Porphyrin μ-Oxo-Bridged Dimers: Acid-Responsive Molecular Rotors. *RSC Adv* **2021**, *11* (40), 24575–24579.

(66) Kudrik, E. V.; Afanasiev, P.; Alvarez, L. X.; Dubourdeaux, P.; Clémancey, M.; Latour, J. M.; Blondin, G.; Bouchu, D.; Albrieux, F.; Nefedov, S. E.; Sorokin, A. B. An N-Bridged High-Valent Diiron-Oxo Species on a Porphyrin Platform That Can Oxidize Methane. *Nat Chem* **2012**, *4* (12), 1024–1029.

(67) Otsuki, J.; Komatsu, Y.; Kobayashi, D.; Asakawa, M.; Miyake, K. Rotational Libration of a Double-Decker Porphyrin Visualized. *J Am Chem Soc* **2010**, *132* (20), 6870–6871.

(68) Jiang, J.; Liu, R. C. W.; Mak, T. C. W.; Chan, T. W. D.; Ng, D. K. P. Synthesis, Spectroscopic and Electrochemical Properties of Substituted Bis (Phthalocyaninato) Lanthanide (III) Complexes. *Polyhedron* **1997**, *16* (3), 515–520.

(69) Jiang, J.; Ng, D. K. P. A Decade Journey in the Chemistry of Sandwich-Type Tetrapyrrolato-Rare Earth Complexes. *Acc Chem Res* **2009**, *42* (1), 79–88.

(70) Dubinina, T. V.; Belousov, M. S.; Maklakov, S. S.; Chernichkin, V. I.; Sedova, M. V.; Tafeenko, V. A.; Borisova, N. E.; Tomilova, L. G. Phenyl-Substituted Terbium(III) Single- and Multiple-Decker Phthalocyaninates: Synthesis, Physicochemical Properties and Peculiarities of Self-Assembly in Solid Phase. *Dyes and Pigments* **2019**, *170*.

(71) Koptyaev, A. I.; Galanin, N. E.; Travkin, V. V.; Pakhomov, G. L. Bis-Tetrabenzoporphyrinates of Rare Earths: Effective Template Synthesis, Optical,

Electrochemical Properties and Conductivity in Thin Films. *Dyes and Pigments* **2021**, *186*, 108984.

(72) Chen, Y.; Ma, F.; Chen, X.; Dong, B.; Wang, K.; Jiang, S.; Wang, C.; Chen, X.; Qi, D.; Sun, H.; Wang, B.; Gao, S.; Jiang, J. A New Bis(Phthalocyaninato) Terbium Single-Ion Magnet with an Overall Excellent Magnetic Performance. *Inorg Chem* **2017**, *56* (22), 13889–13896.

(73) Koptyaev, A. I.; Bazanov, M. I.; Galanin, N. E. Synthesis and Properties of Heteroligand Sandwich Complexes of Lantanides Containing 5-(Quinolin-2-Yl)Tetrabenzoporphyrin and Phthalocyanine Chromophores. *Russian Journal of Organic Chemistry* **2020**, *56* (5), 788–796.

(74) Tarakanova, E. N.; Tarakanov, P. A.; Simakov, A. O.; Furuyama, T.; Kobayashi, N.; Konev, D. V.; Goncharova, O. A.; Trashin, S. A.; De Wael, K.; Sulimenkov, I. V.; Filatov, V. V.; Kozlovskiy, V. I.; Tomilova, L. G.; Stuzhin, P. A.; Pushkarev, V. E. Synthesis and Characterization of Heteroleptic Rare Earth Double-Decker Complexes Involving Tetradiazepinoporphyrazine and Phthalocyanine Macrocycles. *Dalton Transactions* **2021**, *50* (18), 6245–6255.

(75) Pushkarev, V. E.; Breusova, M. O.; Shulishov, E. V; Tomilov, Y. V; Zelinsky, N. D. Selective Synthesis and Spectroscopic Properties of Alkyl-Substituted Lanthanide(III) Mono-, Di-, and Triphthalocyanines. *Russ Chem Bull* **2005**, *54* (9), 2087–2093.

(76) Yagodin, A. V.; Kormshchikov, I. D.; Martynov, A. G.; Gorbunova, Y. G.; Tsivadze, A. Y. Synthesis and Functionalization of Unsymmetrical Terbium(III) Bis-Phthalocyaninates, Promising Components of Hybrid Magnetic Materials. *Russian Journal of Inorganic Chemistry* **2023**, *68* (9), 1125–1132.

(77) Oluwole, D. O.; Yagodin, A. V; Mkhize, N. C.; Sekhosana, K. E.; Martynov, A. G.; Gorbunova, Y. G.; Aslan.; Sivadze, Y. T.; Bello Nyokong, T. First Example of Nonlinear Optical Materials Based on Nanoconjugates of Sandwich Phthalocyanines with Quantum Dots. *Chemistry – A European Journal* **2017**, *23* (12), 2820–2830.

(78) Shokurov, A. V.; Yagodin, A. V.; Martynov, A. G.; Gorbunova, Y. G.; Tsivadze, A. Y.; Selektor, S. L. Octopus-Type Crown-Bisphthalocyaninate Anchor for Bottom-Up Assembly of Supramolecular Bilayers with Expanded Redox-Switching Capability. *Small* **2022**, *18* (2), 2104306.

(79) Martynov, A. G.; Polovkova, M. A.; Gorbunova, Y. G.; Tsivadze, A. Y. Redox-Triggered Switching of Conformational State in Triple-Decker Lanthanide Phthalocyaninates. *Molecules* **2022**, *27* (19), 6498.

(80) Katoh, K.; Kajiwara, T.; Nakano, M.; Nakazawa, Y.; Wernsdorfer, W.; Ishikawa, N.; Breedlove, B. K.; Yamashita, M. Magnetic Relaxation of Single-Molecule Magnets in an External Magnetic Field: An Ising Dimer of a Terbium(III)-Phthalocyaninate Triple-Decker Complex. *Chemistry - A European Journal* **2011**, *17* (1), 117–122.

(81) Martynov, A. G.; Polovkova, M. A.; Kirakosyan, G. A.; Zapolotsky, E. N.; Babailov, S. P.; Gorbunova, Y. G. 1H NMR Spectral Analysis of Structural Features in a Series of Paramagnetic Homoleptic Binuclear Triple-Decker Phthalocyaninato Lanthanide Complexes. *Polyhedron* **2022**, *219*, 115792.

(82) Alexander G. Martynov; Alexey V. Yagodin; Kirill P. Birin; Yulia G. Gorbunova; Aslan Yu. Tsivadze. Solvation-Induced Switching of the Conformational State of Alkoxy- and Crown-Substituted Trisphthalocyaninates Studied by UV-Vis and 1H-NMR Spectroscopy. *J Porphyr Phthalocyanines* **2023**, *27*, 414–422.

(83) Moussavi, M.; De Cian, A.; Fischer, J.; Weiss, R. (Porphyrinato)Bis(Phthalocyaninato)Dilanthanide(III) Complexes Presenting a Sandwich Triple-Decker-like Structure. *Inorg Chem* **1986**, *25* (13), 2107–2107.

(84) Jin, H. G.; Jiang, X.; Kühne, I. A.; Clair, S.; Monnier, V.; Chendo, C.; Novitchi, G.; Powell, A. K.; Kadish, K. M.; Balaban, T. S. Microwave-Mediated Synthesis of Bulky Lanthanide Porphyrin-Phthalocyanine Triple-Deckers: Electrochemical and Magnetic Properties. *Inorg Chem* **2017**, *56* (9), 4864–4873.

(85) Birin, K. P.; Gorbunova, Y. G.; Tsivadze, A. Y. Efficient Scrambling-Free Synthesis of Heteroleptic Terbium Triple-Decker (Porphyrinato)(Crown-Phthalocyaninates). *Dalton Transactions* **2012**, *41* (32), 9672–9681.

(86) Birin, K. P.; Abdulaeva, I. A.; Poddubnaya, A. I.; Gorbunova, Y. G.; Tsivadze, A. Y. Heterocycle-Appended Lanthanum(III) Sandwich-Type (Porphyrinato) (Phthalocyaninates). *Dyes and Pigments* **2020**, *181*, 108550.

(87) Lu, G.; Chen, Y.; Zhang, Y.; Bao, M.; Bian, Y.; Li, X.; Jiang, J. Morphology Controlled Self-Assembled Nanostructures of Sandwich Mixed (Phthalocyaninato)(Porphyrinato) Europium Triple-Deckers. Effect of Hydrogen Bonding on Tuning the Intermolecular Interaction. *J Am Chem Soc* **2008**, *130* (35), 11623–11630.

(88) Lu, J.; Deng, Y.; Zhang, X.; Kobayashi, N.; Jiang, J. Optically Active Mixed (Phthalocyaninato)(Porphyrinato) Rare Earth Triple-Decker Complexes. Synthesis, Spectroscopy, and Effective Chiral Information Transfer. *Inorg Chem* **2011**, *50* (6), 2562–2567.

(89) Bian, Y.; Wang, R.; Jiang, J.; Lee, C.-H.; Wang, J.; Ng, D. K. P. Synthesis, Spectroscopic Characterisation and Structure of the First Chiral Heteroleptic Bis (Phthalocyaninato) Rare Earth Complexes. *Chemical communications* **2003**, *10*, 1194–1195.

(90) Gross, T.; Chevalier, F.; Lindsey, J. S. Investigation of Rational Syntheses of Heteroleptic Porphyrinic Lanthanide (Europium, Cerium) Triple-Decker Sandwich Complexes. *Inorg Chem* **2001**, *40* (18), 4762–4774.

(91) Bai, M.; Bao, M.; Ma, C.; Arnold, D. P.; Choi, M. T. M.; Ng, D. K. P.; Jiang, J. New Dimeric Supramolecular Structure of Mixed (Phthalocyaninato)(Porphyrinato)Europium(III) Sandwiches: Preparation and Spectroscopic Characteristics. *J Mater Chem* **2003**, *13* (6), 1333–1339.

(92) Chabach, D.; De Cian, A.; Fischer, J.; Weiss, R.; Bibout, M. E. M. Mixed-Metal Triple-Decker Sandwich Complexes with the Porphyrin/Phthalocyanine/Porphyrin Ligand System. *Angewandte Chemie International Edition* **1996**, *35* (8), 898–899.

(93) Sun, X.; Li, R.; Wang, D.; Dou, J.; Zhu, P.; Lu, F.; Ma, C.; Choi, C. F.; Cheng, D. Y. Y.; Ng, D. K. P.; Kobayashi, N.; Jiang, J. Synthesis and Characterization of Mixed Phthalocyaninato and Meso-Tetrakis(4-Chlorophenyl)Porphyrinato Triple-Decker Complexes - Revealing the Origin of Their Electronic Absorptions. *Eur J Inorg Chem* **2004**, No. 19, 3806–3813.

(94) Gryko, D.; Li, J.; Diers, J. R.; Roth, K. M.; Bocian, D. F.; Kuhr, W. G.; Lindsey, J. S. Studies Related to the Design and Synthesis of a Molecular Octal Counter. *J Mater Chem* **2001**, *11* (4), 1162–1180.

(95) Padmaja, K.; Youngblood, W. J.; Wei, L.; Bocian, D. F.; Lindsey, J. S. Triple-Decker Sandwich Compounds Bearing Compact Triallyl Tripods for Molecular Information Storage Applications. *Inorg Chem* **2006**, *45* (14), 5479–5492.

(96) Sakaue, S.; Fuyuhiro, A.; Fukuda, T.; Ishikawa, N. Dinuclear Single-Molecule Magnets with Porphyrin-Phthalocyanine Mixed Triple-Decker Ligand Systems Giving SAP and SP Coordination Polyhedra. *Chemical Communications* **2012**, *48* (43), 5337–5339.

(97) Martynov, A. G.; Sinelshchikova, A. A.; Dorovatovskii, P. V.; Polovkova, M. A.; Ovchenkova, A. E.; Birin, K. P.; Kirakosyan, G. A.; Gorbunova, Y. G.; Tsivadze, A. Y. Solvation-Induced Conformational Switching of Trisphthalocyanates for Control of Their Magnetic Properties. *Inorg Chem* **2023**, *62* (26), 10329–10342.

(98) Martynov, A. G.; Zubareva, O. V.; Gorbunova, Y. G.; Sakharov, S. G.; Nefedov, S. E.; Dolgushin, F. M.; Tsivadze, A. Y. Diphthalocyaninatolanthanum as a New

Phthalocyaninato-Dianion Donor for the Synthesis of Heteroleptic Triple-Decker Rare Earth Element Crown- Phthalocyaninato Complexes. *Eur J Inorg Chem* **2007**, No. 30, 4800–4807.

(99) Faraonov, M. A.; Martynov, A. G.; Polovkova, M. A.; Khasanov, S. S.; Gorbunova, Y. G.; Tsivadze, A. Y.; Otsuka, A.; Yamochi, H.; Kitagawa, H.; Konarev, D. V. Single-Molecule Magnets Based on Heteroleptic Terbium(III) Trisphthalocyaninate in Solvent-Free and Solvent-Containing Forms. *Magnetochemistry* **2023**, *9* (2), 36.

(100) Martynov, A. G.; Birin, K. P.; Kirakosyan, G. A.; Gorbunova, Y. G.; Tsivadze, A. Y. Site-Selective Solvation-Induced Conformational Switching of Heteroleptic Heteronuclear Tb(III) and Y(III) Trisphthalocyaninates for the Control of Their Magnetic Anisotropy. *Molecules* **2023**, *28* (11), 4474.

(101) Kan, J.; Wang, H.; Sun, W.; Cao, W.; Tao, J.; Jiang, J. Sandwich-Type Mixed Tetrapyrrole Rare-Earth Triple-Decker Compounds. Effect of the Coordination Geometry on the Single-Molecule-Magnet Nature. *Inorg Chem* **2013**, *52* (15), 8505–8510.

(102) Lu, G.; Kong, X.; Wang, H.; Chen, Y.; Wei, C.; Chen, Y.; Jiang, J. A Sandwich-Type Tetrakis(Phthalocyaninato) Europium-Cadmium Quadruple-Decker Complex: Structural, Spectroscopic, OFET, and Gas Sensing Properties. *New Journal of Chemistry* **2019**, *43* (39), 15763–15767.

(103) Liu, C.; Yang, W.; Wang, J.; Ding, X.; Ren, H.; Chen, Y.; Xie, Z.; Sun, T.; Jiang, J. A Sextuple-Decker Heteroleptic Phthalocyanine Heterometallic Samarium-Cadmium Complex with Crystal Structure and Nonlinear Optical Properties in Solution and Gel Glass. *Dalton Transactions* **2021**, *50* (39), 13661–13665.

(104) Horii, Y.; Damjanović, M.; Ajayakumar, M. R.; Katoh, K.; Kitagawa, Y.; Chibotaru, L.; Ungur, L.; Mas-Torrent, M.; Wernsdorfer, W.; Breedlove, B. K.; Enders, M.; Veciana, J.; Yamashita, M. Highly Oxidized States of Phthalocyaninato Terbium(III) Multiple-Decker Complexes Showing Structural Deformations, Biradical Properties and Decreases in Magnetic Anisotropy. *Chemistry - A European Journal* **2020**, *26* (39), 8621–8630.

(105) Liu, C.; Yang, W.; Zhang, Y.; Jiang, J. Quintuple-Decker Heteroleptic Phthalocyanine Heterometallic Samarium - Cadmium Complexes. Synthesis, Crystal Structure, Electrochemical Behavior, and Spectroscopic Investigation. *Inorg Chem* **2020**, *59* (23), 17591–17599.

(106) Wang, H.; Kobayashi, N.; Jiang, J. New Sandwich-Type Phthalocyaninato-Metal Quintuple-Decker Complexes. *Chemistry - A European Journal* **2012**, *18* (4), 1047–1049.

(107) Martynov, A. G.; Polovkova, M. A.; Berezhnoy, G. S.; Sinelshchikova, A. A.; Dolgushin, F. M.; Birin, K. P.; Kirakosyan, G. A.; Gorbunova, Y. G.; Tsivadze, A. Y. Cation-Induced Dimerization of Heteroleptic Crown-Substituted Trisphthalocyaninates as Revealed by X-Ray Diffraction and NMR Spectroscopy. *Inorg Chem* **2020**, *59* (13), 9424–9433.

(108) Ishikawa, N.; Otsuka, S.; Kaizu, Y. The Effect of the F-f Interaction on the Dynamic Magnetism of a Coupled 4f8 System in a Dinuclear Terbium Complex with Phthalocyanines. *Angewandte Chemie - International Edition* **2005**, *44* (5), 731–733.

(109) Pushkarev, V. E.; Kalashnikov, V. V.; Tolbin, A. Y.; Trashin, S. A.; Borisova, N. E.; Simonov, S. V.; Rybakov, V. B.; Tomilova, L. G.; Zefirov, N. S. Meso-Phenyltetrabenzotriazaporphyrin Based Double-Decker Lanthanide(III) Complexes: Synthesis, Structure, Spectral Properties and Electrochemistry. *Dalton Transactions* **2015**, *44* (37), 16553–16564.

(110) Gabarró-Riera, G.; Aromí, G.; Sañudo, E. C. Magnetic Molecules on Surfaces: SMMs and Beyond. *Coord Chem Rev* **2023**, *475*, 214858.

(111) Chen, Y.; Su, W.; Bai, M.; Jiang, J.; Li, X.; Liu, Y.; Wang, L.; Wang, S. High Performance Organic Field-Effect Transistors Based on Amphiphilic Tris(Phthalocyaninato) Rare Earth Triple-Decker Complexes. *J Am Chem Soc* **2005**, *127* (45), 15700–15701.

(112) Wang, R.; Li, Y.; Li, R.; Cheng, D. Y. Y.; Zhu, P.; Ng, D. K. P.; Bao, M.; Cui, X.; Kobayashi, N.; Jiang, J. Heteroleptic Rare Earth Double-Decker Complexes with Naphthalocyaninato and Phthalocyaninato Ligands. General Synthesis, Spectroscopic, and Electrochemical Characteristics. *Inorg Chem* **2005**, *44* (6), 2114–2120.

(113) Liu, W.; Jiang, J.; Pan, N.; Arnold, D. P. *Octakis(Octyloxy)Phthalocyaninato] Rare Earth(III) Triple-Deckers: Synthesis and Spectroscopic Characterization*; 2000; Vol. 310.

(114) Wang, Q.; Li, Y.; Yan, X.; Rathi, M.; Ropp, M.; Galipeau, D.; Jiang, J. Organic Photovoltaic Cells Made from Sandwich-Type Rare Earth Phthalocyaninato Double and Triple Deckers. *Appl Phys Lett* **2008**, *93* (7).

(115) Li, Y.; Bian, Y.; Yan, M.; Thapaliya, P. S.; Johns, D.; Yan, X.; Galipeau, D.; Jiang, J. Mixed (Porphyrinato)(Phthalocyaninato) Rare-Earth(III) Double-Decker Complexes for

Broadband Light Harvesting Organic Solar Cells. *J Mater Chem* **2011**, *21* (30), 11131–11141.

(116) Kong, X.; Tarakanova, E. N.; Du, X.; Tomilova, L. G.; Chen, Y. Discrimination and Detection of NO2, NH3 and H2S Using Sensor Array Based on Three Ambipolar Sandwich Tetradiazepinoporphyrazinato/Phthalocyaninato Europium Double-Decker Complexes. *Mater Adv* **2023**, *4* (6), 1515–1522.

(117) Liu, S.; Wang, H.; Wang, X.; Li, S.; Liu, H.; Chen, Y.; Li, X. Diverse Sensor Responses from Two Functionalized Tris(Phthalocyaninato)Europium Ambipolar Semiconductors towards Three Oxidative and Reductive Gases. *J Mater Chem C Mater* **2019**, *7* (2), 424–433.

(118) Wei, C.; Lu, G.; Guo, C.; Lv, X.; Tang, X.; Liu, Q.; Cai, X.; Chen, Y.; Jiang, J. Ethylthio-Substituted Sandwich Phthalocyaninato Europium (III) Semiconductors for Sensing NO2 and NH3: Effect of the Extended π-Conjugate Systems on Tuning the Conductivity and Sensing Behavior. *Org Electron* **2021**, *93*, 106151.

(119) Stoddart, J. F. Mechanisch Verzahnte Moleküle (MIMs) – Molekulare Shuttle, Schalter Und Maschinen (Nobel-Aufsatz). *Angewandte Chemie* **2017**, *129* (37), 11244–11277.

(120) Ogi, S.; Ikeda, T.; Wakabayashi, R.; Shinkai, S.; Takeuchi, M. A Bevel-Gear-Shaped Rotor Bearing a Double-Decker Porphyrin Complex. *Chemistry - A European Journal* **2010**, *16* (28), 8285–8290.

(121) Gisbert, Y.; Abid, S.; Bertrand, G.; Saffon-Merceron, N.; Kammerer, C.; Rapenne, G. Modular Synthesis of Pentaarylcyclopentadienyl Ru-Based Molecular Machines: Via Sequential Pd-Catalysed Cross Couplings. *Chemical Communications* **2019**, *55* (97), 14689–14692.

(122) Abid, S.; Gisbert, Y.; Kojima, M.; Saffon-Merceron, N.; Cuny, J.; Kammerer, C.; Rapenne, G. Desymmetrised Pentaporphyrinic Gears Mounted on Metallo-Organic Anchors. *Chem Sci* **2021**, *12* (13), 4709–4721.

(123) Gisbert, Y.; Abid, S.; Kammerer, C.; Rapenne, G. Molecular Gears: From Solution to Surfaces. *Chemistry - A European Journal* **2021**, *27* (47), 12019–12031.

(124) Erbland, G.; Abid, S.; Gisbert, Y.; Saffon-Merceron, N.; Hashimoto, Y.; Andreoni, L.; Guérin, T.; Kammerer, C.; Rapenne, G. Star-Shaped Ruthenium Complexes as Prototypes of Molecular Gears. *Chemistry - A European Journal* **2019**, *25* (71), 16328–16339.

(125) Nishino, T.; Fukumura, M.; Katao, S.; Yasuhara, K.; Rapenne, G. Multiply Engaged Molecular Gears Composed of a Cerium(Iv) Double-Decker of a Triptycene-Functionalized Porphyrin. *Dalton Transactions* **2023**, *52* (34), 11797–11801.

Chapter 2
Results and Discussion

2. Results and Discussion

2.1 Introduction to the aim of the project

The potential application of both double and triple deckers in molecular devices has recently led to a big leap in research involved in their synthesis. Inspired by the work of Birin and co-workers,[1] the Cammidge group[2] has attempted to synthesise a bis-double decker heteroleptic structure from a linked porphyrin and phthalocyanine derivatives. This experiment failed to produce the desired compound; instead triple-decker with porphyrin-phthalocyanine-porphyrin was predominantly formed as shown in scheme 2.1.[3]

The Cammidge group reported several complexes of lanthanide-bridged heteroleptic porphyrin–phthalocyanine–porphyrin triple decker assemblies. It was found that the linking chain length between the two porphyrins was crucial. For example, hexyl chain was first used but this did not result in the formation of the triple decker. Successful results were obtained when the chain length was increased.[2]

Refluxing the porphyrin dyad **2.1**, phthalocyanine and lanthanum acetylacetonate in a high boiling point solvent (octanol) produced two products and no starting materials were detected. Separation and analysis of the mixture revealed the formation of bis-triple decker **2.7** and the bridged triple-decker **2.2**. Excess of phthalocyanine led to the formation of **2.7**, whereas one equivalent of phthalocyanine produced only compound **2.2**.

Based on this successful outcome, different salts from the lanthanide series with decreasing ionic radii were selected. Assembly and isolation of the praseodymium **2.3**, neodymium **2.4**, samarium **2.5** and europium **2.6** TDs were formed following the procedure mentioned above (radii Pr^{3+} = 99 pm, Nd^{3+} = 98 pm, Sm^{3+} = 96 pm, Eu^{3+} = 95 pm). The pure triple deckers obtained gave absorption spectra characteristic of TDs. It was found that the desired triple deckers could be isolated with ions of atomic radii greater than 94 pm whereas small ions such as Tb (92 pm), Dy (91 pm) and Yb (87 pm) failed to produce the desired product, which implies that there is a cut-off point for stability in the constrained assemblies.[3]

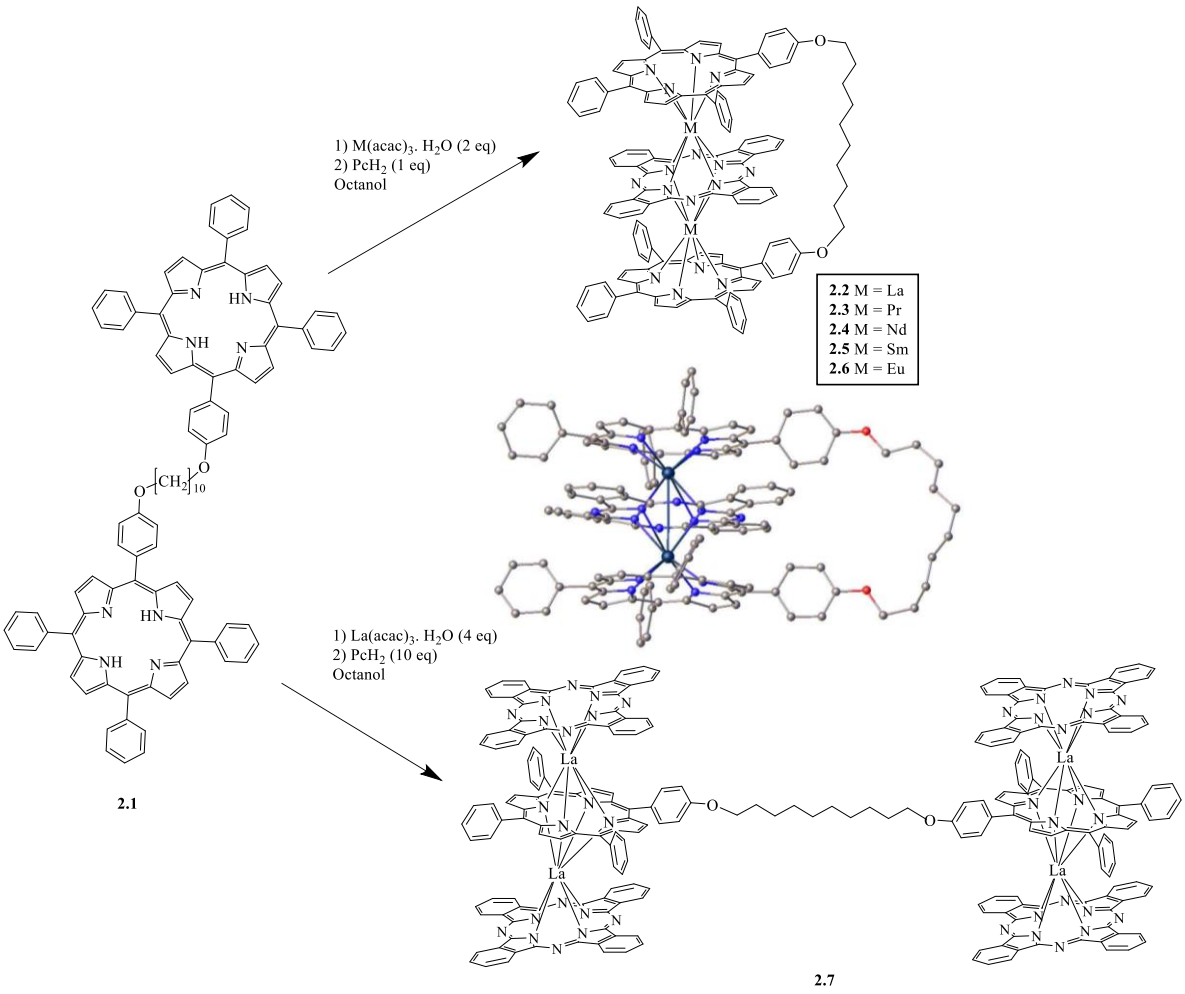

Scheme 2.1: Reported synthesis of the triple and bis-triple decker.[3]

Based on the successful synthesis of the La, Pr, Sm and Eu triple deckers, the Cammidge group now aimed at synthesising triple deckers using different dyads. The goal of this project is to expand the scope into the development of new materials which can be used in the production of advanced electronic devices such as optoelectronics and magnetic devices.

Our main objective was to design and synthesise TDs from two types of dyads,

(i) an unsymmetrical dyad bearing a TBTAP and a porphyrin molecule

(ii) a symmetrical dyad i.e with two TBTAP molecules

Lanthanide metals such as La, Nd and Eu will be incorporated into the sandwich structure. The desired dyad can be obtained by linking the molecules by long alkyl chain such as a decane chain as depicted in the scheme below (scheme 2.2).

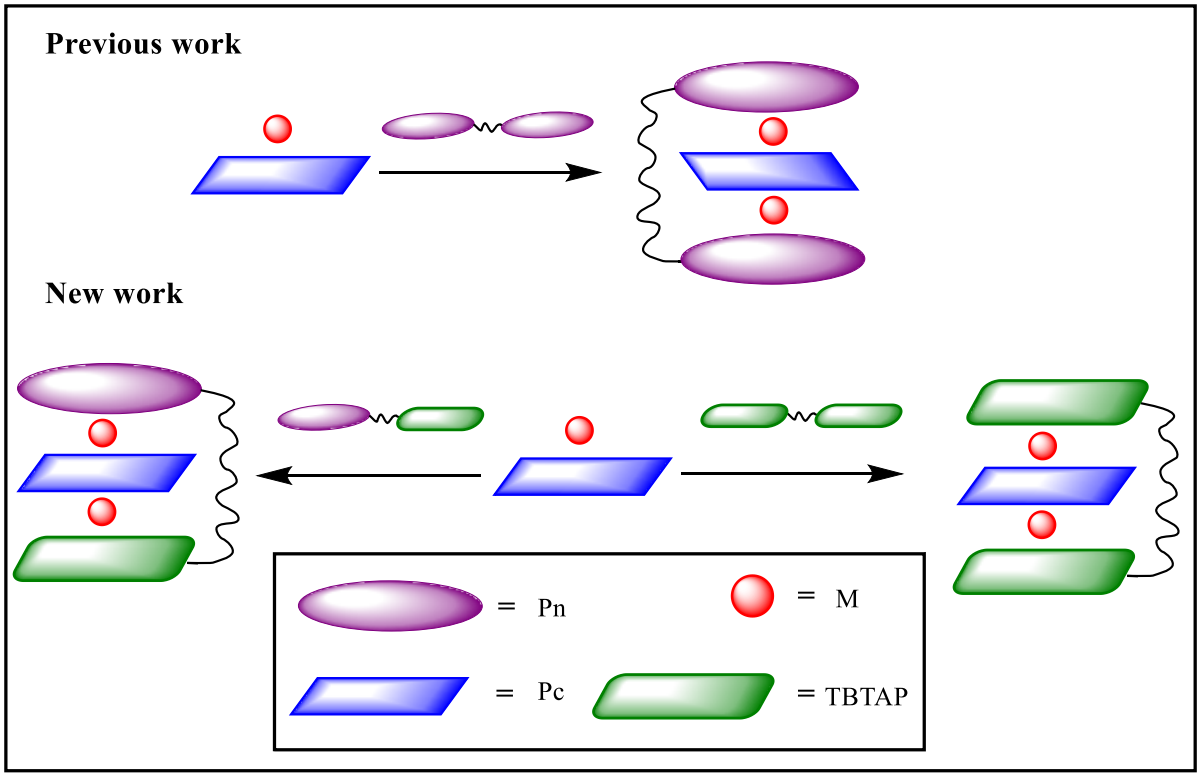

Scheme 2.2: Novel heteropletic complexes from symmetrical and unsymmetrical dimers.

In both precursors, the tetrabenzotriazaporphyrin (TBTAP) and the porphyrin designed for this experiment have a hydroxy phenyl group at the meso carbon to which the alkyl chain will be attached to form the symmetrical and unsymmetrical dyads (figure 2.1).

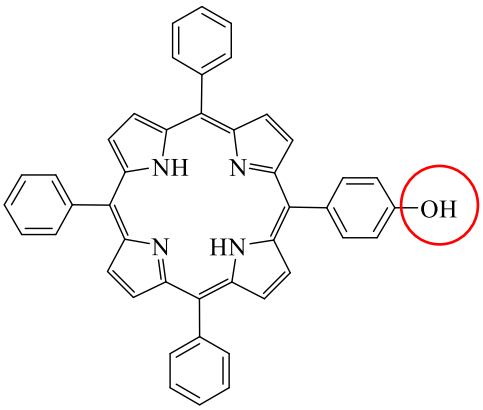

2.8

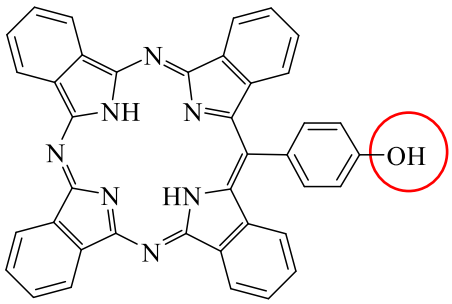

2.9

Figure 2.1: The key precursors, TPP-OH **2.8** and TBTAP-OH **2.9** bearing single linking points.

2.2 Proposed synthetic route to yield TBTAP-OH 2.9

The scheme below shows a proposed synthetic route to yield the target compound TBTAP-OH.

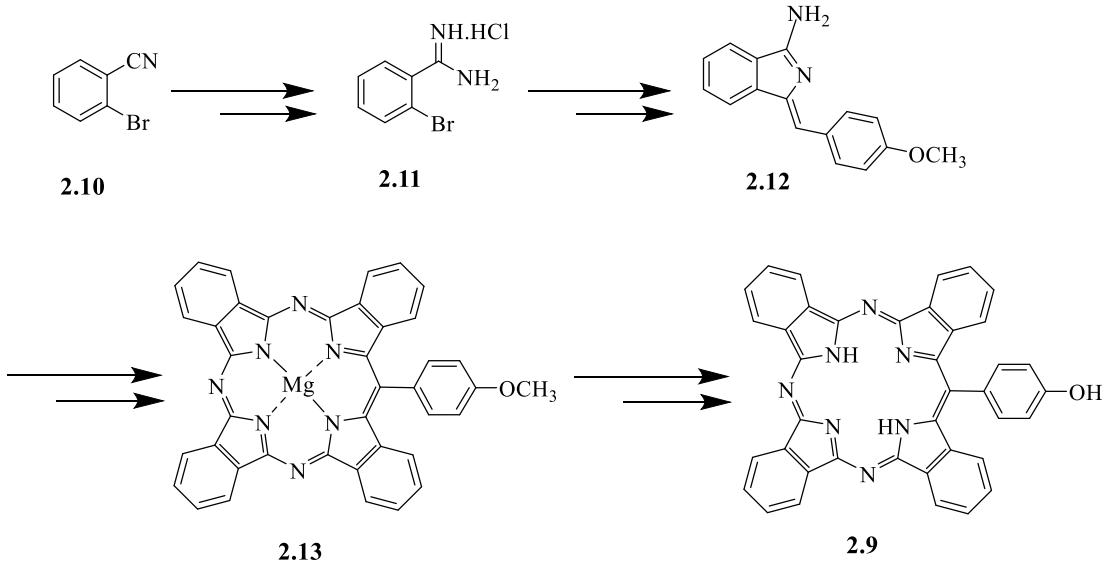

Scheme 2.3: Proposed synthetic route to yield TBTAP-OH.

Prior to the synthesis of the TBTAP bearing a methoxy phenyl group at the meso-position **2.13**, the precursor 2-bromobenzimidamide hydrochloride **2.11** was synthesised following the procedure developed by Dalai *et al*.[4] The synthesis of the amidine salt was achieved by the addition of lithium bis(trimethylsilyl)amide (LiHMDS) to a solution of 2-bromobenzonitrile **2.10** in THF at room temperature. After 4 hours, the reaction mixture was quenched with a mixture of isopropanol and HCl, precipitating the desired product as an HCl salt. The product was filtered off and an off-white solid was obtained in a 94% yield (scheme 2.4). The identity of the product was confirmed by ^{1}H-NMR spectroscopy as the desired amidine **2.11** (figure 2.2).

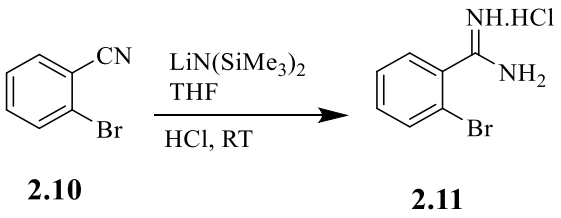

2.10 **2.11**

Scheme 2.4: Synthesis of amidine **2.11**.

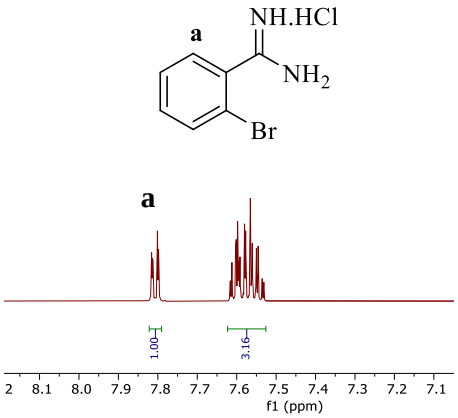

Figure 2.2: ^{1}H-NMR spectrum of amidine salt **2.11** (500 MHz, MeOD, 25 °C).

2.3 Synthesis of Aminoisoindoline

Aminoisoindoline **2.12** was synthesised following the procedure developed by Hellal and Cuny.[5] The amidine salt **2.11**, was treated with 4-methoxyphenylacetylene **2.14** using a palladium catalyst under microwave irradiation (scheme 2.5). After workup a 50% yield of the desired compound was obtained.

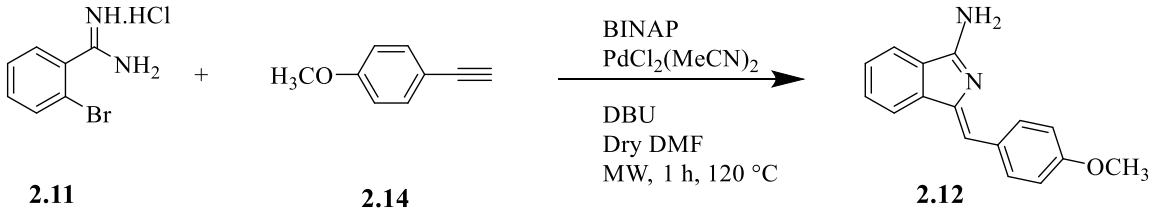

Scheme 2.5: Synthesis of aminoisoindoline **2.12**.

From the ^{1}H-NMR spectrum, the peak around 6.75 ppm is characteristic of the proton of the alkene group which integrates to 1. The peak around 3.83 ppm is due to the methoxy peak which integrates to 3 (figure 2.3).

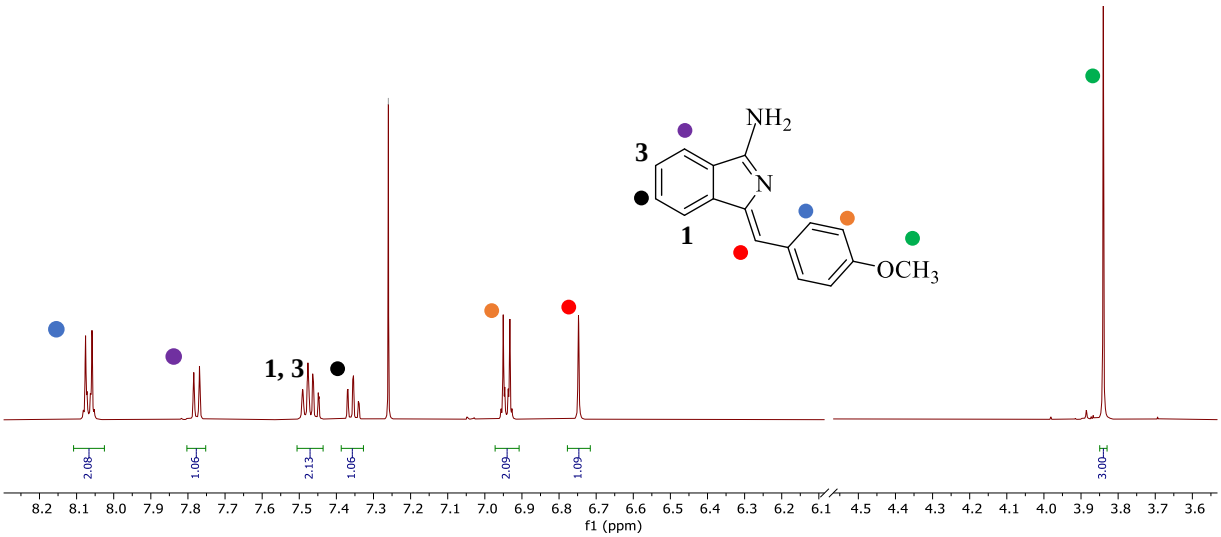

Figure 2.3: ^{1}H-NMR spectrum of (Z)-1-(4-methoxybenzylidene)-1H-isoindol-3-amine **2.12** (500 MHz, $CDCl_3$, 25 °C).

2.4 Synthesis of Mg-TBTAP-OMe

The next step was to synthesise the TBTAP compound via two separate pathways as per scheme 2.6.

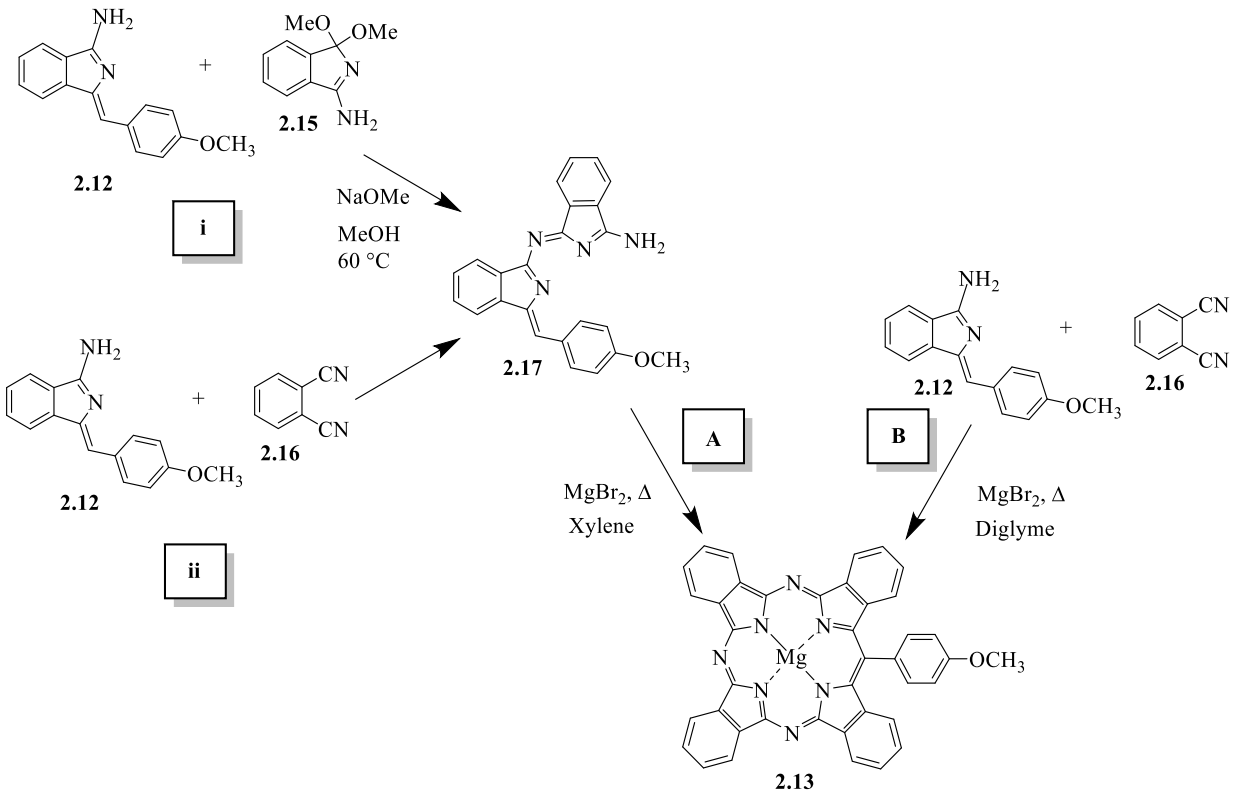

Scheme 2.6: Proposed synthetic pathways A and B to yield Mg-TBTAP-OMe **2.13**.

The first attempt to synthesise Mg-TBTAP-OMe **2.13**, by pathway A as per scheme 2.6 produced an intermediate **2.17** to which magnesium bromide in a high boiling point solvent such as xylene was added.

2.4.1 Synthesis of Intermediate 2.17

The first attempt to produce the intermediate **2.17** involved the synthesis of dimethoxyaminoisoindoline **2.15**.[7] Compound **2.15** was prepared by stirring phthalonitrile **2.16** and sodium methoxide (NaOMe) in methanol at room temperature. After 2 h, the precipitate was filtered off and washed several times with cold methanol. A white powder in a 57% yield was obtained. Intermediate **2.17** was prepared as shown in scheme 2.7. A mixture of aminoisoindoline **2.12**, NaOMe and dimethoxyaminoisoindoline **2.15** was dissolved in methanol and the resulting mixture was refluxed. The procedure was repeated using different amount and times as per table 2.1.

The isolation and purification of the intermediate **2.17** was carried out as follows: the precipitate was filtered off and washed with cold MeOH. The resulting residue was collected and purified by column chromatography using DCM → DCM: AcOEt (1:1) → AcOEt as solvent gradient. The fractions containing the desired product were combined and the solvent was removed under reduced pressure. An orange-brown solid was collected.

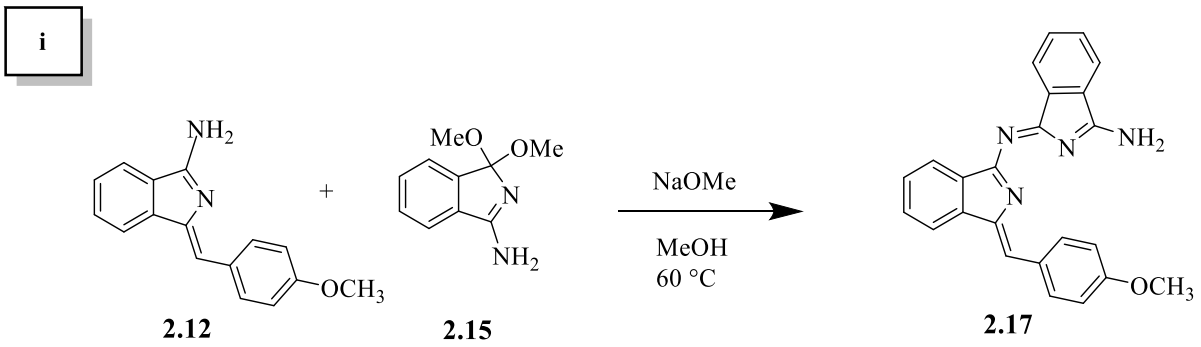

2.12 **2.15** **2.17**

Scheme 2.7: Synthesis of intermediate **2.17** using dimethoxyaminoisoindoline **2.15**.

Table 2.1: Attempted conditions for synthesis of dimer via Method (i).[a]

Entry	Solvent	Time (h)	Yield (%)[b]
1	MeOH	Overnight	20
2	MeOH	2	14

3	MeOH	4	10
4	MeOH	6	24
5	Dry MeOH	6	12
6[c]	Dry MeOH	6	25

[a]Reactions conditions: Aminoisoindoline (1.02 mmol), dimethoxyaminoisoindoline (1.15 mmol) NaOMe (1.53 mmol), solvent (5 mL). [b]Isolated yield. [c]A total of 3 mmol of dimethoxyaminoisoindoline used, added in portions.

The synthesis of the intermediate **2.17** from dimethoxyaminoisoindoline **2.15** is straightforward but the yield is poor (Table 2.1, entry 1-6). Therefore, the reaction was repeated by using a less reactive starting material, phthalonitrile, under different conditions, following method (ii) as depicted in scheme 2.8. In a typical reaction, the aminoisoindoline **2.12**, phthalonitrile **2.16** and NaOMe were mixed in methanol and the resulting mixture was refluxed. The results are summarised in table 2.2. After the required time interval, the isolation and purification was carried out using the same procedure as above.

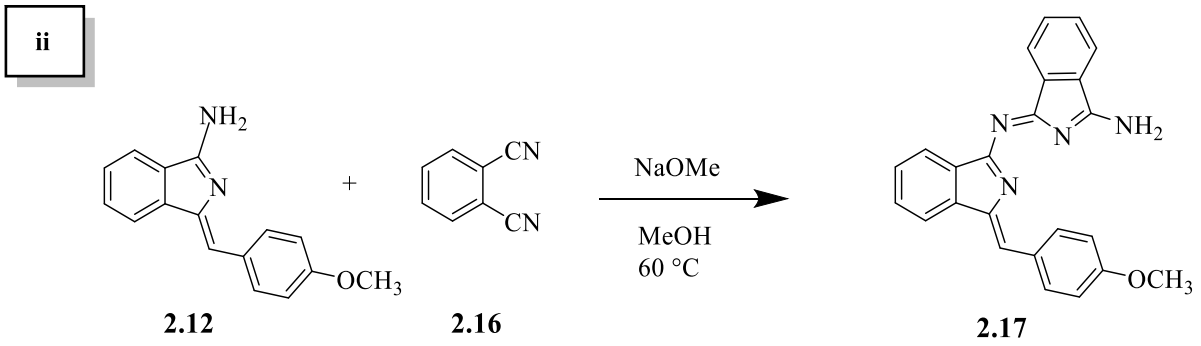

2.12 **2.16** **2.17**

Scheme 2.8: Synthesis of intermediate **2.17** using phthalonitrile **2.16**.

Table 2.2: Attempted conditions for synthesis of dimer via Method (ii).[a]

Entry	Solvent	Time (h)	Yield (%)[b]
1	MeOH	Overnight	20
2[c]	MeOH	Overnight	10
3[d]	MeOH	4	9
4[e]	MeOH	4	30
5[f]	MeOH	2	40
6[d]	Dry MeOH	4	10
7[e]	Dry MeOH	2	47
8	Ethanol	2	12

9	THF	3	5

[a]Reactions conditions: Aminoisoindoline (0.40 mmol), phthalonitrile (0.40 mmol), NaOMe (0.61 mmol), volume of solvent (5 mL). [b]Isolated yield. [c]Reaction was heated at 80 °C in a sealed tube. [d]Diluted conditions used. [e]A total of 1.0 mmol of phthalonitrile used, added in portions. [f]Excess of phthalonitrile (1.8 mmol).

Phthalonitrile **2.16** as starting material instead of dimethoxyaminoisoindoline **2.15** gave a better yield as indicated in table 2.2. In more diluted conditions (Table 2.2, entry 3, 6) the reaction is unfavourable towards the formation of intermediate. At higher temperatures and longer periods of time, the 'trimer' **2.18** (scheme 2.9) is formed in preference to the dimer (Table 2.2, entry 2) as the solution turns more brownish. A MALDI-TOF MS analysis on the brown solution confirmed the formation of the trimer **2.18** with a peak at 611 m/z. After 1 hour (Table 2.2, entry 4, 7) TLC analysis of the reaction showed the presence of unreacted aminoisoindoline. The presence of unreacted aminoisoindoline, the dimer **2.17** and the trimer **2.18** in the reaction mixture indicated that there is an equilibrium between the starting materials and the product **2.17**.[6]

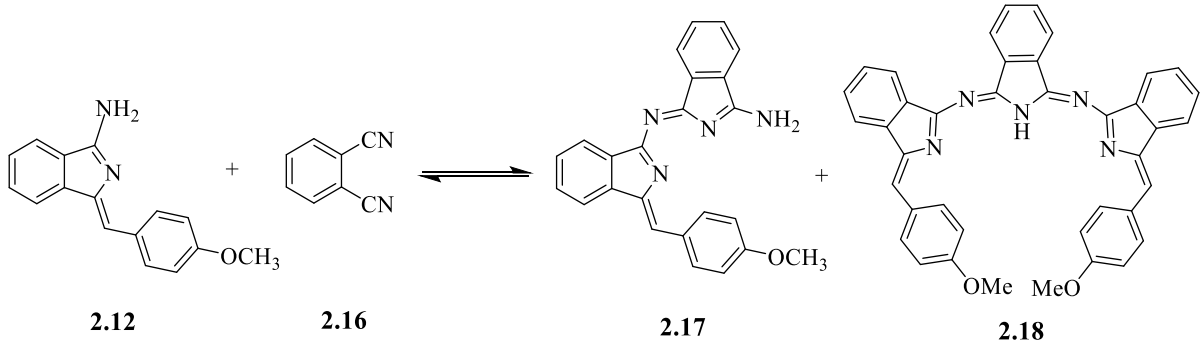

2.12 **2.16** **2.17** **2.18**

Scheme 2.9: Equilibrium between starting materials and products.

When an excess of phthalonitrile (Table 2.2, entry 4, 5, 7) is used in the reaction mixture, the yield of the intermediate improved, this also resulted in the formation of a dark blue compound, phthalocyanine.

In an attempt to increase the yield of the product, the reaction was carried out in other solvents (Table 2.2, entry 8 and 9). Solvents such as THF and ethanol did not improve the yield of the dimer. A higher yield of the product was obtained when the reaction was performed under dry conditions (Table 2.2, entry 7). It should be noted that in both methods (i) and (ii), the reactions are dependent on temperature, volume of solvent used and the reaction time. Therefore, the synthesis of the dimer is preferentially carried out using phthalonitrile instead of

dimethoxyaminoisoindoline at a temperature of 60 °C in dry methanol over a 2 hour period (Table 2.2, entry 7).

The isolation and purification of the intermediate **2.17** were carried out using the same technique discussed above. The ^{1}H-NMR spectrum confirmed the formation of the intermediate is shown in figure 2.5. The singlet at 7.25 ppm and 3.80 ppm corresponds to the proton on the alkene and the methoxy group respectively. The assignment of the protons are concordant with the structure.

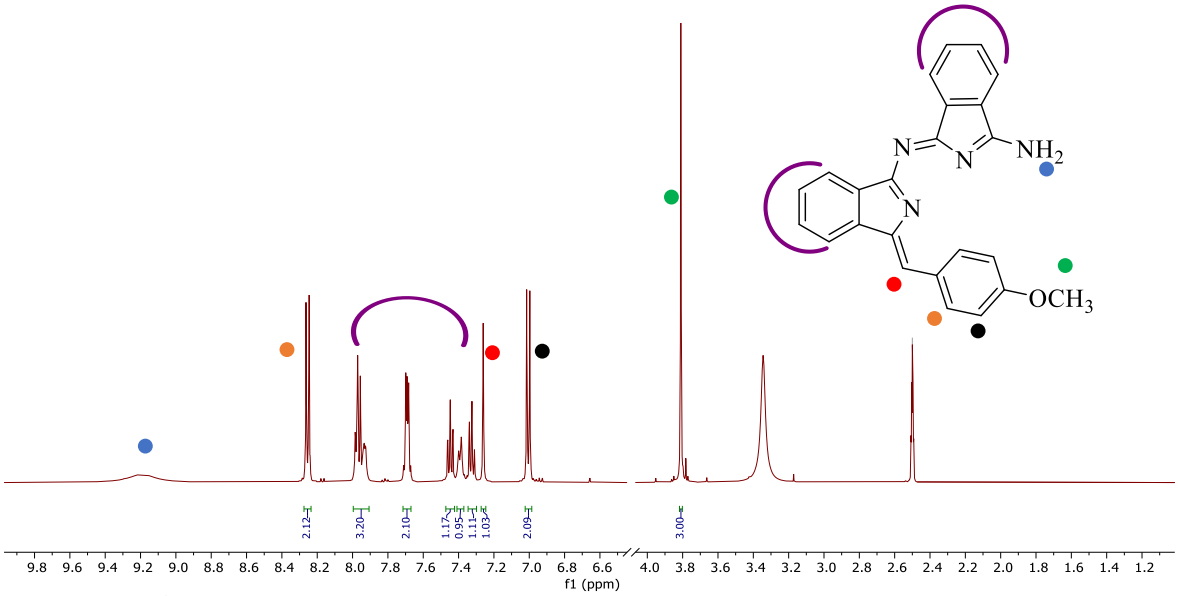

Figure 2.5: ^{1}H-NMR spectrum of intermediate **2.17** (500 MHz, DMSO-d_6).

2.4.2 Synthesis of Mg-TBTAP-OMe from the dimer/intermediate.

After the successful synthesis of the intermediate, the next step was to investigate the synthetic methods to yield the Mg-TBTAP-OMe **2.13** (scheme 2.9).

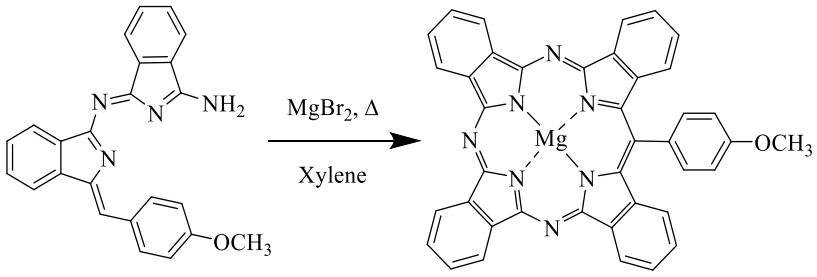

2.17 **2.13**

Scheme 2.9: Synthesis of Mg-TBTAP-OMe **2.13** from intermediate **2.17**.[6]

The 'one pot' method was used, whereby the intermediate **2.17** and $MgBr_2$ were mixed in xylene, the mixture was refluxed under an inert atmosphere. The results are summarised in table 2.3.

Table 2.3: Attempted conditions for the synthesis of Mg-TBTAP-OMe **2.13** from **2.17**.[a]

Entry	Time (h)	Yield (%)[b]
1	Overnight	10
2	9	33
3[c]	9	12
4	6	27
5[d]	9	30

[a]Reactions conditions: Dimer (0.21 mmol), $MgBr_2$ (0.32 mmol), volume of xylene (3 mL). [b]Isolated yield. [c] Volume of xylene (6 mL). [d]Volume of xylene (2 mL).

The yield of the Mg-TBTAP-OMe is found to be dependent on concentration of xylene used as per table 2.3. A more concentrated solution of xylene (Table 2.3, entry 3) resulted in a better yield of Mg-TBTAP-OMe.

The isolation and purification of the Mg-TBTAP-OMe was carried out as follows: the solvent was removed under a stream of nitrogen and the reaction mixture was allowed to cool to room temperature. A mixture of DCM: MeOH was added to the reaction mixture and was finally sonicated. The crude was purified using two flash column chromatographies. The first column was carried out using DCM and a red fraction, the aminoisoindoline dimer **2.19** was eluted. A mixture of DCM: Et_3N (20:1), and DCM: THF: Et_3N (10:1:4) was used to separate the next green-blue fraction. Unreacted phthalocyanine remained on the baseline. All the fractions containing the green-blue material were combined and subjected to a second column, using a mixture of PE: THF: MeOH (10:3:1) as an eluent, a green and blue fractions were obtained. A TLC analysis of the green and blue fractions confirmed the presence of Mg-TBTAP-OMe **2.13** and Mg-Pc **2.20** respectively when tested against reference compounds (scheme 2.10). Finally, a recrystallisation from acetone and ethanol yielded the title product.

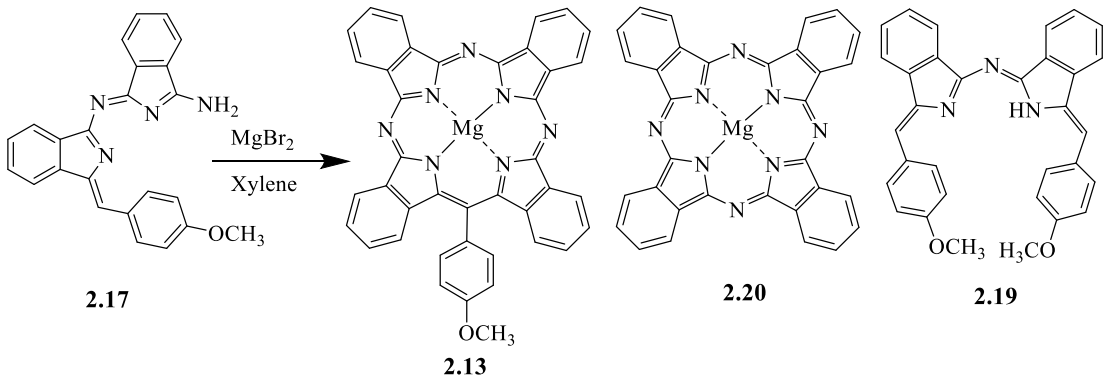

Scheme 2.10: Synthesis of Mg-TBTAP-OMe **2.13** and by-products.

The traditional method of synthesising *meso*-substituted TBTAP was revisited in order to establish the reproducibility of the reaction conditions and in an attempt to increase the yield of the product as illustrated in scheme 2.11 pathway B.[8]

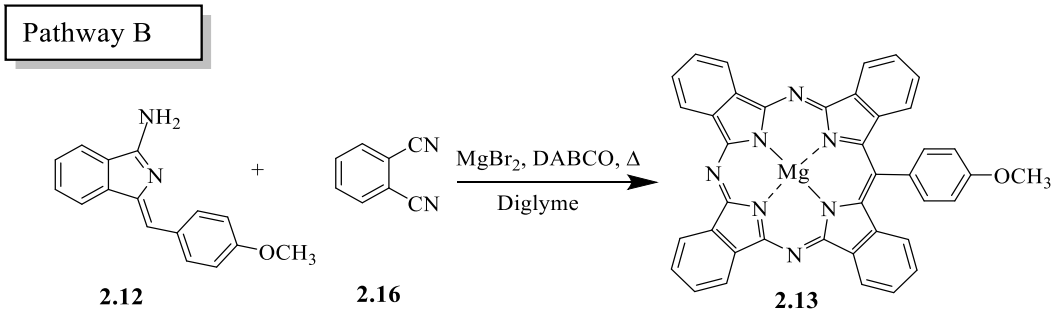

Scheme 2.11: Synthesis of Mg-TBTAP-OMe **2.13** through Pathway B.

Using the established procedure, a mixture of phthalonitrile **2.16** and $MgBr_2$ in diglyme was heated for 10 min under an inert atmosphere.[8] A solution containing phthalonitrile **2.16** and aminoisoindoline **2.12** in dry diglyme was added to the above mixture using a syringe pump. After 1 hour, another solution of phthalonitrile **2.16** and DABCO in diglyme was gradually added over a 1 h period using a syringe pump. The mixture changed from colourless to deep green/blue. After heating for a few minutes, a deeper green mixture was eventually obtained. After 3 h, TLC analysis showed red, green and blue spots corresponding to aminoisoindoline dimer **2.19**, Mg-TBTAP-OMe **2.13** and Mg-Pc **2.20** respectively. Mg-Pc **2.20** was the dominant product with a yield of 49%, and the Mg-TBTAP-OMe **2.13** was isolated with a yield of 13% after following the above procedure for isolation and purification.

In an attempt to increase the yield of Mg-TBTAP-OMe **2.13**, a '1 pot' synthesis was performed in which aminoisoindoline **2.12**, phthalonitrile **2.16** and $MgBr_2$ were mixed together in different dry solvents under different conditions as per table 2.4 and was refluxed under an inert atmosphere.

Table 2.4: Attempted conditions for the '1-pot' synthesis of Mg-TBTAP-OMe **2.13**.[a]

Entry	Solvent	Time (h)	Yield (%)[b]
1	Diglyme	overnight	20
2[c]	Diglyme	3	20
3	Diglyme	3	17
4	Diglyme	6	37
5[d]	Diglyme	6	33
6	Diglyme	12	34
7[d]	Xylene	3	12
8[d,e]	Xylene	6	18
9[d]	Xylene	18	13
10[d,e]	Xylene	18	19

[a]Reactions conditions: Aminoisoindoline (0.70 mmol), phthalonitrile (2.03 mmol), $MgBr_2$ (1.02 mmol), volume of solvent (2 mL). [b]Isolated yield. [c]DABCO used in synthesis. [d]Reaction was heated at a mantle temperature of 170 °C. [e]Diluted conditions used.

When xylene was used, (Table 2.4, entry 8-9) the yield of product was lower. Of all the pathways attempted, the 'one pot' procedure in which the starting materials, aminoisoindoline **2.12**, phthalonitrile **2.16** and the metal template $MgBr_2$ in the absence of DABCO gave the best result (Table 2.4, entry 4). The by-products aminoisoindoline dimer **2.19**, Mg-Pc **2.20** and phthalocyanine were present.

The ^{1}H-NMR spectrum of the product corresponded to the reported structure **2.13** and is shown in figure 2.6.[9] There are two protons as doublet at 9.60 ppm and four protons as multiplet in range from 9.53–9.50 ppm. The aromatic protons on the methoxy phenyl ring appear as doublets at 8.05 and 7.52 ppm with a total integration of 4. At 4.20 ppm the peak of the methoxy group appears as a singlet.

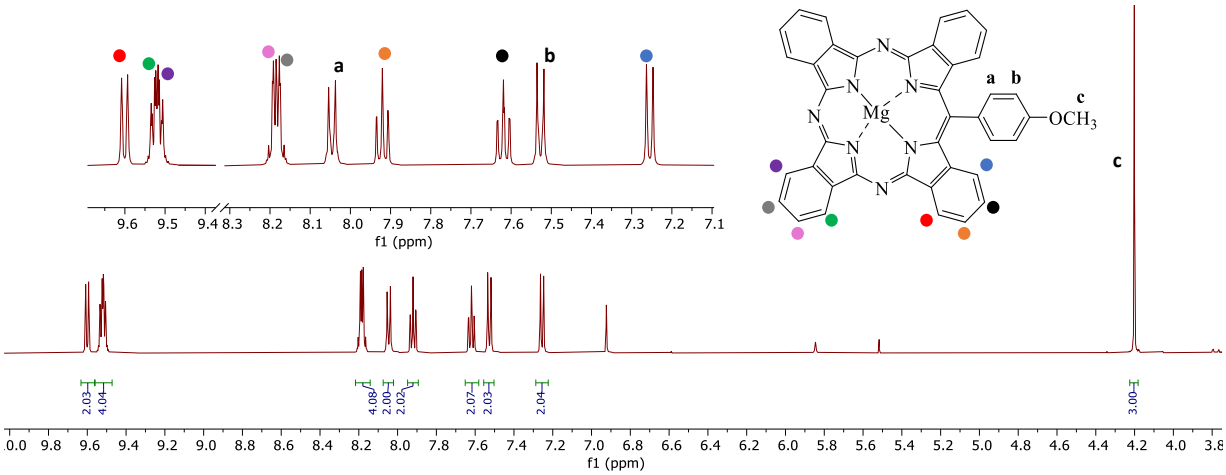

Figure 2.6: ^{1}H-NMR spectrum of Mg-TBTAP-OMe **2.13** with an expanded scale of the aromatic region (500 MHz, THF-d_8, 25 °C).

2.5 Zinc TBTAP-OMe

In an attempt to increase the yield of the TBTAP-OMe, other metals were investigated using the 'one-pot' method. The same methodology was applied as in (Table 2.4, entry 4) in the synthesis of the Zn-TBTAP-OMe and the results are summarised in table 2.5.

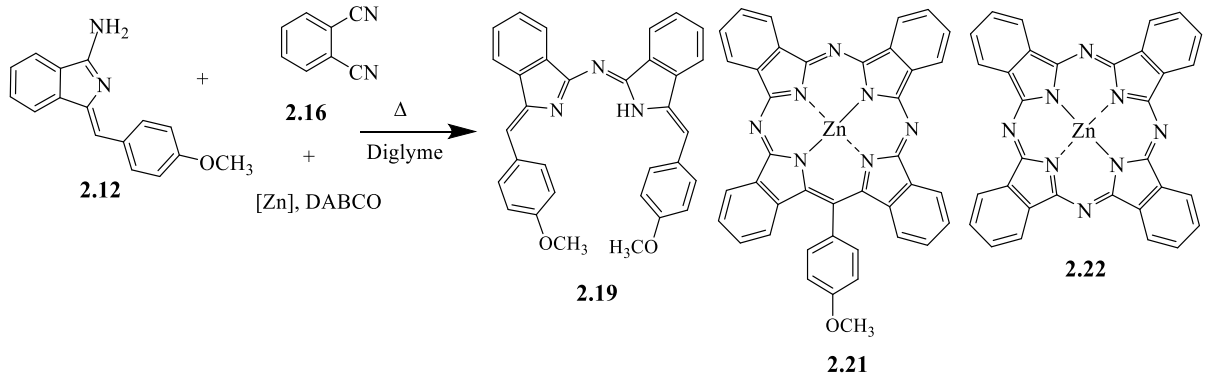

Scheme 2.12: Synthesis of Zn-TBTAP-OMe **2.21** using different zinc salts.

Table 2.5: Different Zinc salts for the synthesis of Zn-TBTAP-OMe **2.21**.[a]

Entry	Metal salts	Yield (%)[b]
1	$ZnCl_2$	5
2	$ZnBr_2$	4
3	Anhydrous $ZnCl_2$	4
4	Anhydrous $ZnBr_2$	5
5	Anhydrous $Zn(CH_3CO_2)_2$	5

6	ZnO	0

[a]Reactions conditions: Aminoisoindoline (0.20 mmol), phthalonitrile (0.60 mmol), [Zn] (0.40 mmol), Volume of diglyme (2 mL). [b]Isolated yield.

The crude mixture was analysed by MALDI-TOF MS and peaks at 483, 681and 576 m/z was observed corresponding to aminoisoindoline dimer **2.19**, Zn-TBTAP-OMe **2.21** and Zn-Pc **2.22** respectively (scheme 2.12). After isolation and purifications, the yields obtained were poorer compared to the magnesium salt. Zinc oxide did not produce any Zn-TBTAP-OMe, therefore the procedure using zinc salts was abandoned.

2.6 Synthesis of Mg-TBTAP-OH

Once the Mg-TBTAP-OMe **2.13** had been successfully synthesised, demethylation and demetallation steps of the Mg-TBTAP-OMe **2.13** were carried out in order to produce the TBTAP-OH **2.9**, a precursor to the symmetrical and unsymmetrical dyads. Boron tribromide, (BBr_3) was chosen as a demethylating reagent (scheme 2.13) and it can also remove the magnesium from the central core to form the target compound, TBTAP-OH **2.9**. The Mg-TBTAP-OMe **2.13** was dissolved in dry DCM followed by the slow addition of BBr_3 solution. The reaction was continuously monitored by MALDI-TOF-MS for several days and peaks at 641, 627, 619 and 605 m/z were found corresponding to Mg-TBTAP-OMe **2.13**, Mg-TBTAP-OH **2.23**, TBTAP-OMe **2.24** and TBTAP-OH **2.9** respectively (figure 2.7). The purification of this mixture by column chromatography was difficult due to lack of solubility in solvents such as DCM, EtOAc and THF.

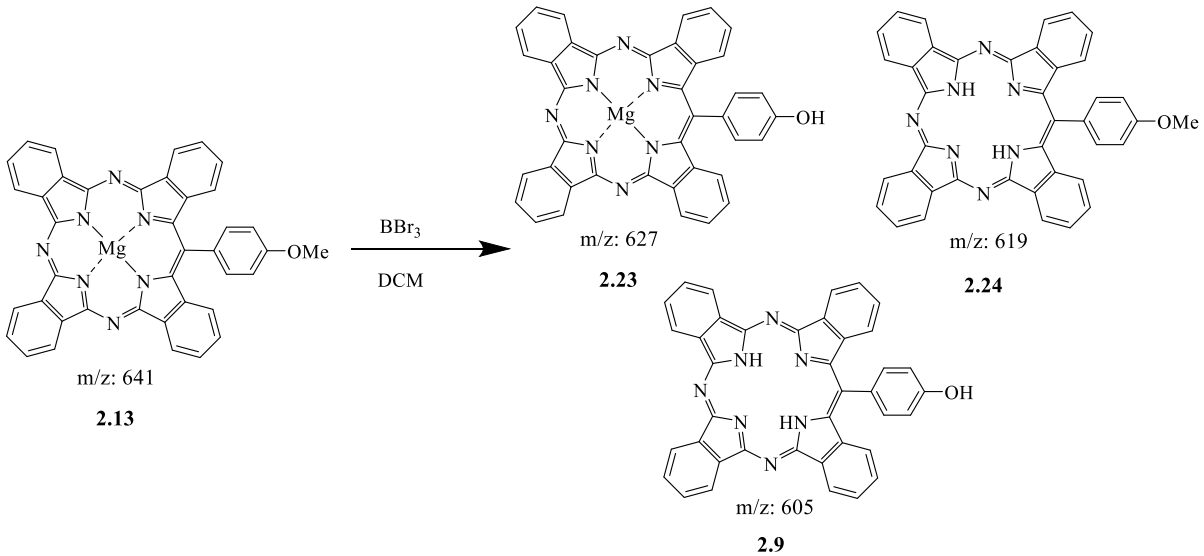

Scheme 2.13: Attempted demethylation of Mg-TBTAP-OMe using BBr_3.

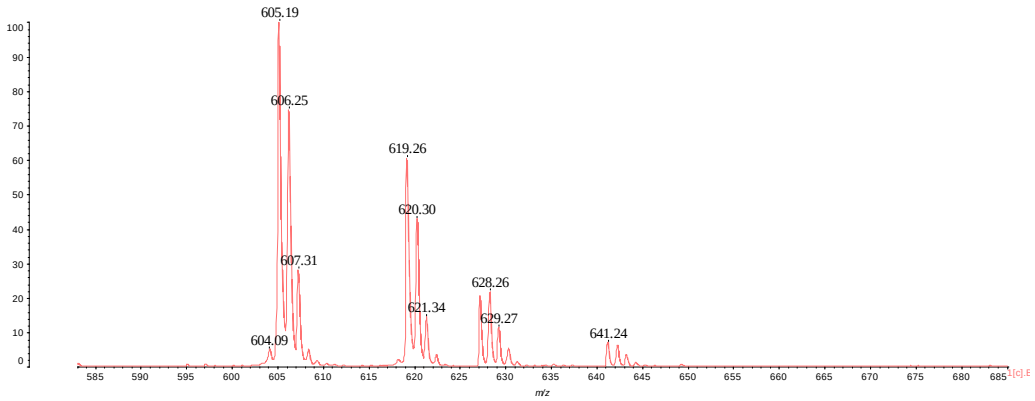

Figure 2.7: MALDI-TOF MS spectrum of crude product.

The known method was then carried out by using magnesium iodide (MgI_2) as a demethylating reagent (scheme 2.14).[9] The Mg-TBTAP-OMe **2.13** and MgI_2 was heated at 150 °C in dry toluene in a sealed-tube, overnight and the mixture was analysed by MALDI-TOF MS and TLC. Only a single peak at 627 m/z corresponding to Mg-TBTAP-OH **2.23** was obtained suggesting that the starting material was fully used-up. Then MeOH was added to the reaction vessel and was stirred at room temperature for 30 min. The solvents were removed under vacuum and the crude solid was finally purified by column chromatography using PE: THF: MeOH (10:3:1) as eluent. The purification was easier as the compound was soluble in organic solvents. A recrystallisation was achieved by acetone and methanol as solvent system to yield the title green compound.

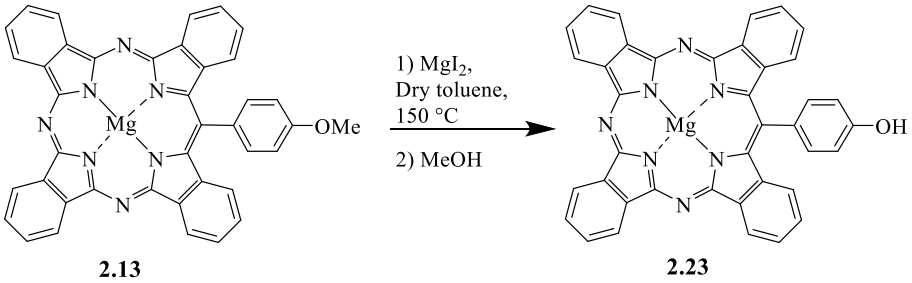

Scheme 2.14: Demethylation of Mg-TBTAP-OMe **2.13** using MgI_2.

2.7 Synthesis of Unsymmetrical dyad

Synthesis of the triple decker (target compound) involves an initial stage in which the unsymmetrical dyad has to be synthesised. The unsymmetrical dyad consists of a molecule of TBTAP and TPP with a bridging alkyl chain as depicted in the figure 2.8.

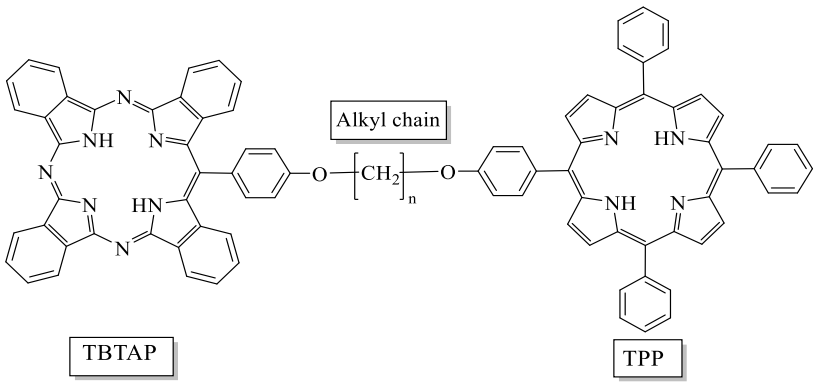

Figure 2.8: Unsymmetrical dyad.

2.7.1 Demetallation of Mg-TBTAP-OH 2.23

In the first step, a demetallation of the Mg-TBTAP-OH **2.23** was achieved by treating the sample with concentrated sulfuric acid and then ice-cold water was added. A green precipitate was obtained. The precipitate was filtered off and washed with MeOH. MALDI-TOF MS analysis revealed the formation of TBTAP-OH **2.9** and an 80% yield was obtained (scheme 2.15).[10] The resulting peak from the MALDI-TOF MS showed 605 m/z for TBTAP-OH **2.9** (figure 2.9).

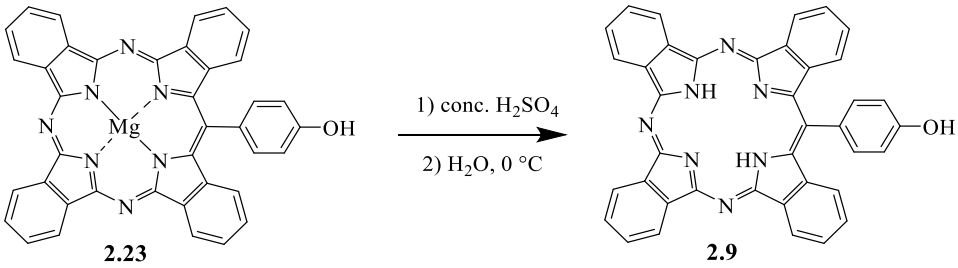

Scheme 2.15: Demetallation of Mg-TBTAP-OH **2.23** to yield TBTAP-OH **2.9**.

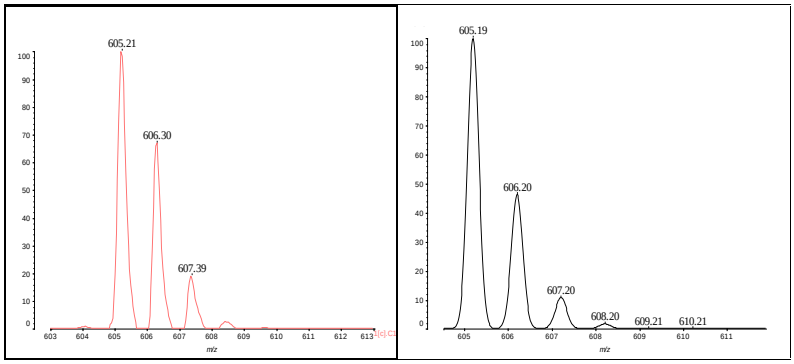

Figure 2.9: MALDI-TOF MS spectrum of TBTAP-OH **2.9** with its theoretical prediction.

2.7.2 Synthesis of TPPOH

The second step involves the synthesis of alkylating TPP-OH. Unsymmetrical tetraphenylporphyrin TPP-OH **2.8** was synthesised using a modified version of Adler's methodology,[11] using the ratio of reagents shown in the scheme below (scheme 2.16).

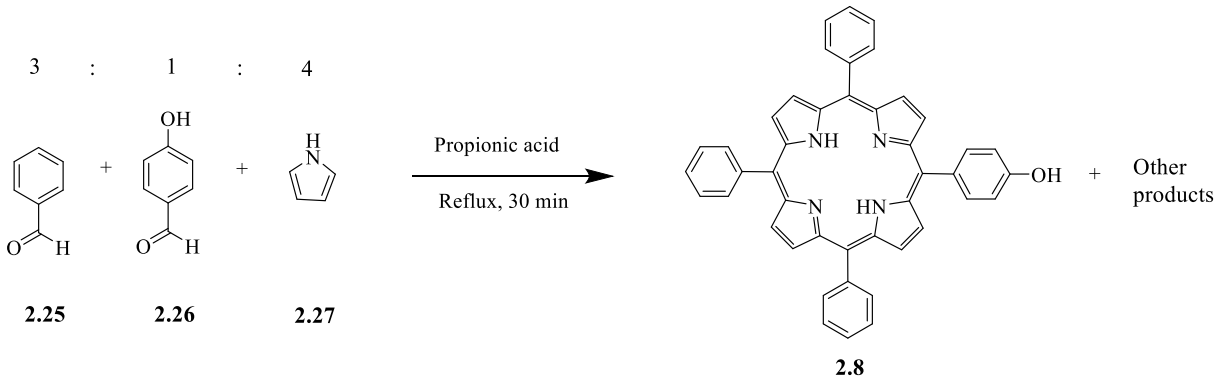

2.25 **2.26** **2.27** **2.8**

Scheme 2.16: Synthesis of unsymmetrically substituted porphyrin **2.8** (TPPOH).[3]

Benzaldehyde **2.25**, 4-hydroxy benzaldehyde **2.26** and propionic acid were mixed together and heated to reflux. Freshly distilled pyrrole **2.27** was added dropwise to the mixture which was further refluxed for 30 min. The mixture was allowed to cool, and methanol was added. The crude was left to precipitate overnight in the fridge. The mixture of porphyrins was filtered off, and most of the side products were left in the solution. The crude product was purified on a silica gel column using a mixture of THF and petroleum ether as eluent. The desired fraction was collected and after a recrystallisation from DCM: MeOH, the monohydroxy porphyrin **2.8** was obtained in a 3.6% yield.

The ^{1}H-NMR spectrum of TPP-OH **2.8** is more complex compared to TPP **2.28** (figure 2.11) as there are more peaks in the aromatic region. This is because the monohydroxy-porphyrin **2.8** is no longer symmetrical; it also shows the broad signal from the OH group at the para position with a chemical shift of 5.01 ppm. The aromatic protons on the hydroxy phenyl ring appears at 8.08 and 7.22 ppm with a total integration of 4. The shielded imino protons of the macrocycle resonate at around –2.77 ppm which is caused by the ring current effect (figure 2.11).

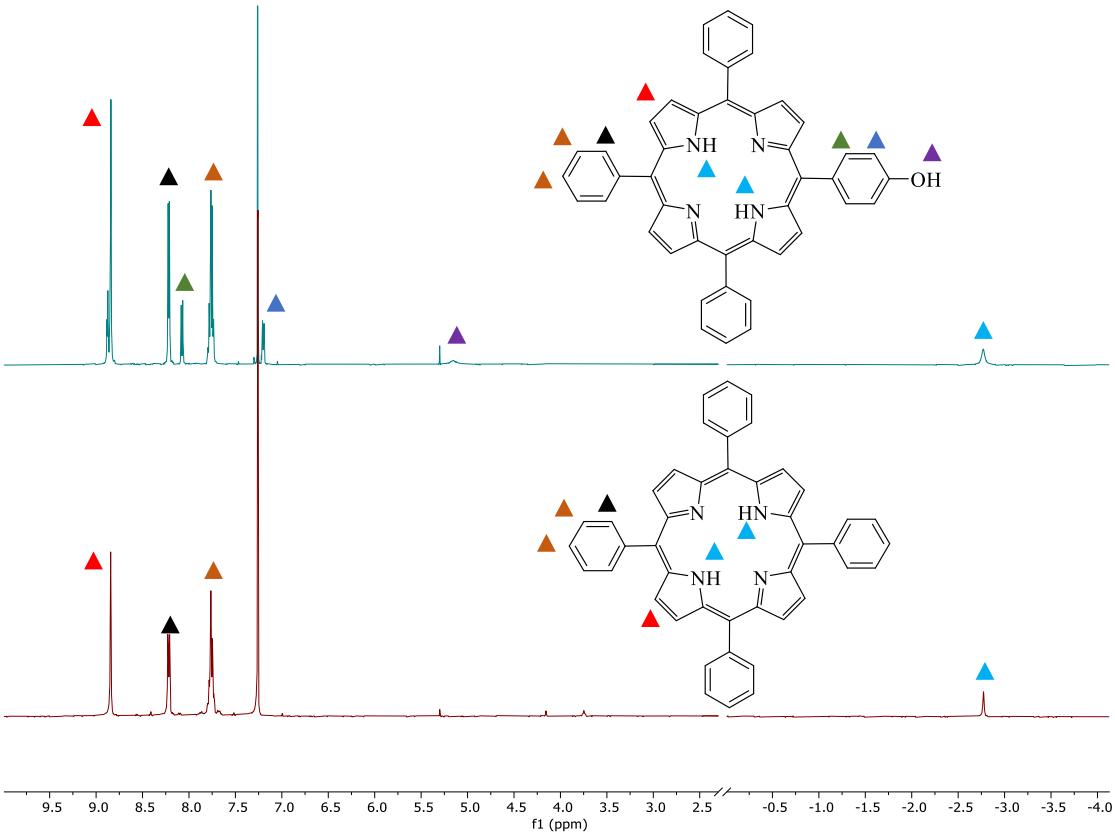

Figure 2.11: ^{1}H-NMR spectra: Top TPP-OH **2.8**, bottom of TPP **2.28** (400 MHz, $CDCl_3$, 25 °C).

2.7.3 Synthesis of the mono-alkylated TPPO- C_{10}-Br 2.29

The next step was to synthesise the mono-alkylated TPP-O-C_{10}-Br **2.29** by reacting the TPP-OH **2.8** with an excess of 1,10 dibromodecane in the presence of K_2CO_3 and DMF at room temperature as reported by the Cammidge group (scheme 2.17).[2] The product was purified by column chromatography and a recrystallisation from DCM: MeOH gave the TPP-O-C_{10}-Br **2.29** in 49% yield.

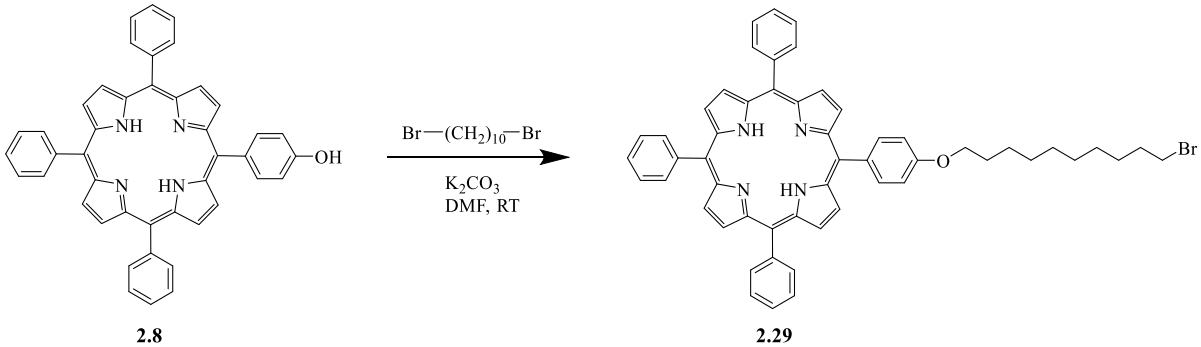

Scheme 2.17: Synthesis of TPP-O- C_{10}-Br **2.29**.

The ^{1}H-NMR spectrum shown in figure 2.12 confirmed the presence of TPP-O-C$_{10}$-Br **2.29**. The 2 sets of triplet peaks at around 4.22 ppm and 3.35 ppm corresponding to the protons of the -OC*H*$_2$- and -C*H*$_2$-Br respectively.

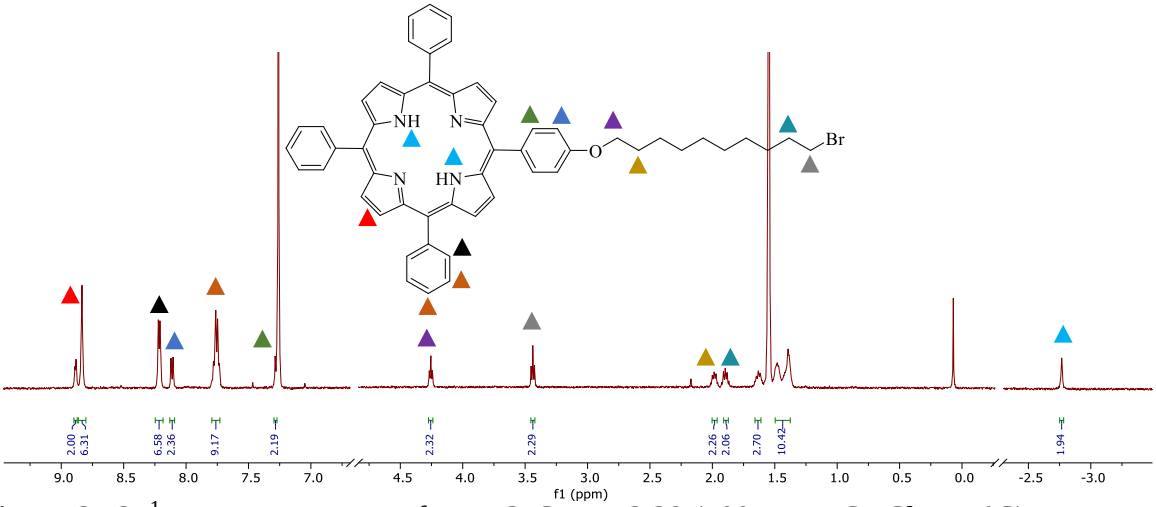

Figure 2.12: ^{1}H-NMR spectrum of TPP-O-C$_{10}$-Br **2.29** (500 MHz, $CDCl_3$, 25 °C).

2.7.4 Synthesis of unsymmetrical dyad 2.30 using TBTAP-OH 2.9

The next step was to produce the unsymmetrical dyad **2.30**. The demetallated TBTAP-OH **2.9** and TPP-O-C$_{10}$-Br **2.29** in a 1:1 ratio was reacted in the presence of K_2CO_3 (scheme 2.18) at room temperature. Two solvents were tested, acetone and DMF. The reaction was left to stir overnight.

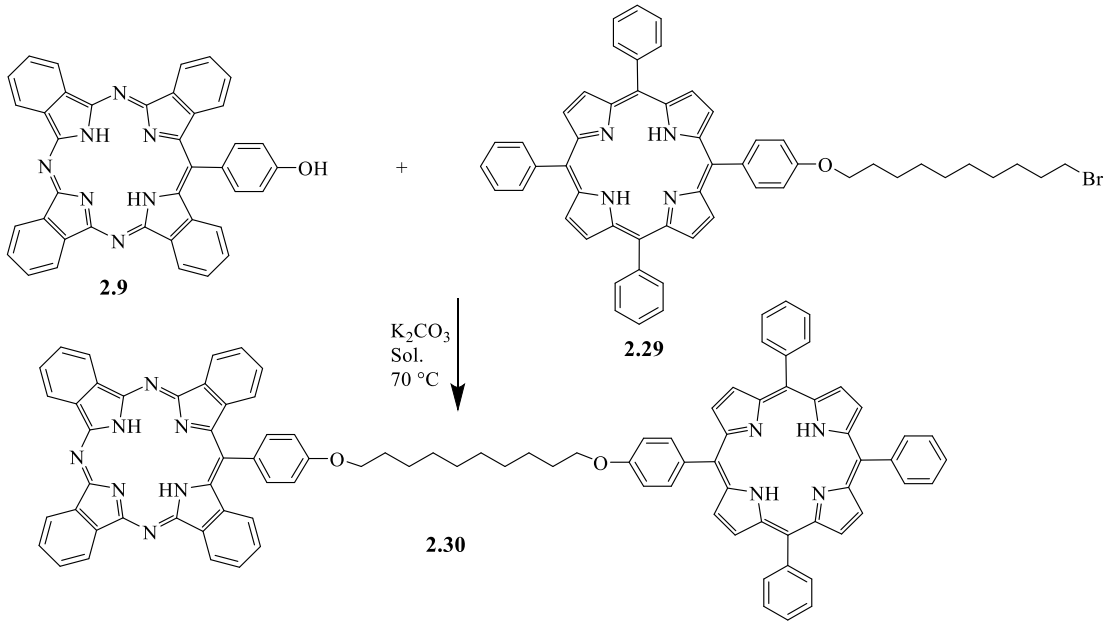

Scheme 2.18: Synthesis of unsymmetrical dyad **2.30**.

TLC analysis revealed the absence of new spots. Both reactions were heated to 70 °C in a sealed tube and was left to stir overnight. TLC analysis for the DMF reaction showed a faint new spot had formed. This sample was then subjected to MALDI-TOF MS analysis which confirmed the formation of the desired product with a peak at 1376 m/z along with peaks for the starting materials TBTAP-OH **2.9** and TPP-O-C_{10}-Br **2.29**. However, the reaction performed in acetone showed no formation of product and hence this reaction was abandoned. The reaction with DMF was left to stir for longer with continuous monitoring. After 10 days the DMF reaction was stopped when no TPP-O-C_{10}-Br **2.29** could be detected on TLC. The crude product was then purified by column chromatography. However, the purification of the product was tedious and lengthy as the sample stuck on the silica although various polar organic solvents were used such as THF, MeOH and EtOAc. The product was MALDI-TOF MS tested and a peak at 1376 m/z confirming the presence of TBTAP-O-C_{10}-O-TPP **2.30** (figure 2.13). Only trace amount of the product was obtained.

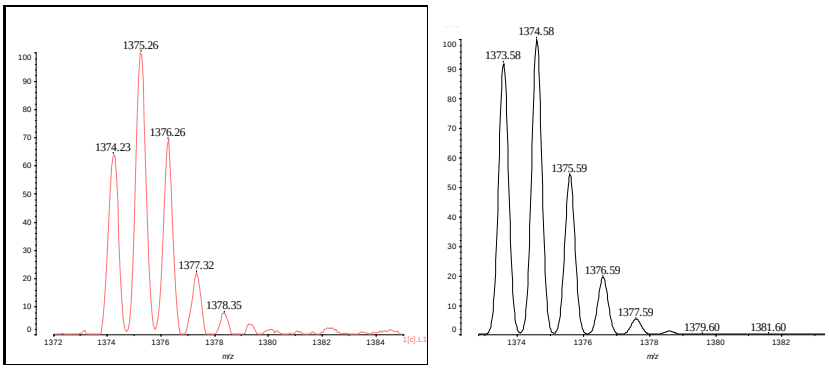

Figure 2.13: MALDI-TOF MS spectrum of dyad **2.30** with its theoretical prediction.

From literature, it is known that working with the demetallated form of TBTAP is always time consuming.[12] Therefore, this way of making the unsymmetrical dyad was abandoned. Instead, a new procedure was attempted in which the demetallation step was left until last.

After the difficulty of producing the unsymmetrical dyad in a quantitative yield, two alternative synthetic pathways were investigated (scheme 2.19).

In method A, mono-alkylated Mg-TBTAP-O-C_{10}-Br **2.31** is made, followed by the addition of TPP-OH in the presence of base, K_2CO_3 (scheme 2.19). In method B, mono-alkylated TPP-O C_{10}-Br **2.29** is produced and was then reacted with Mg-TBTAP-OH in the presence of base, K_2CO_3 (scheme 2.19).

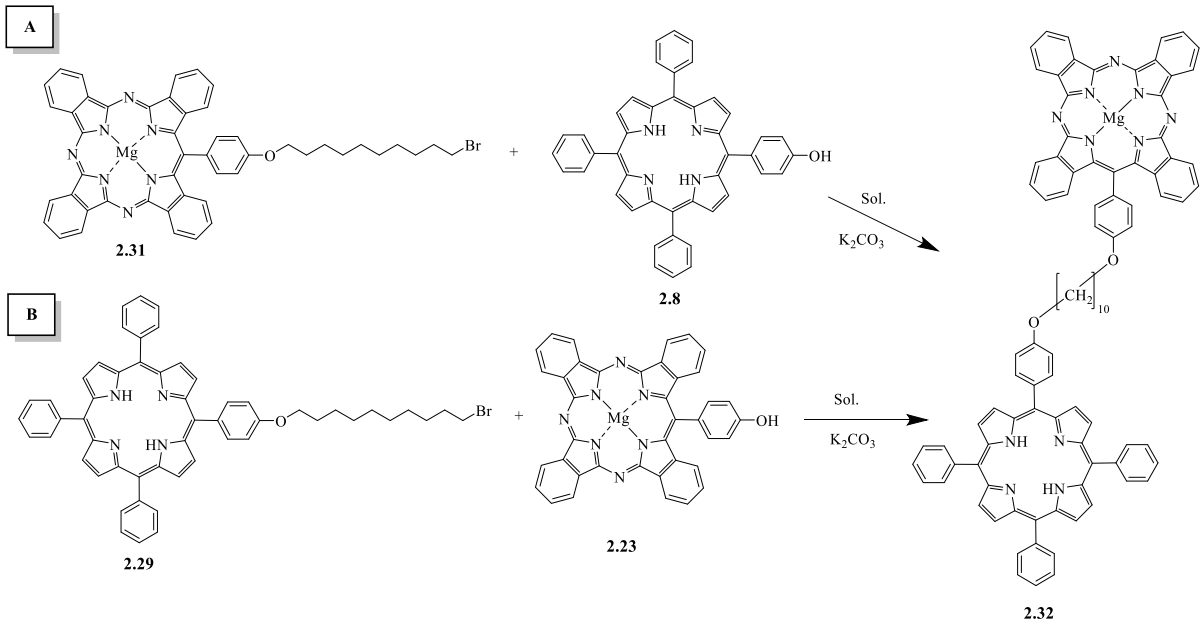

Scheme 2.19: Two proposed synthetic pathways to yield the unsymmetrical dyad **2.32**.

2.7.5 Synthesis of Mg-TBTAP-O-C_{10}-Br

In method A, the mono-alkylated Mg-TBTAP-O-C_{10}-Br **2.31** was first synthesised. Mg-TBTAP-OH **2.23** was added to an excess of 1,10 dibromodecane in the presence of K_2CO_3 (scheme 2.20). The reaction was first carried out in acetone and DMF at room temperature overnight (as in the case of synthesising TPP-O-C_{10}-Br **2.29**). TLC analysis revealed the absence of the product. Both reactions were heated to a temperature of 55 °C in sealed tubes. Analysis by TLC revealed that the reaction performed in acetone gave fewer undesirable products as compared to DMF. In an attempt to reduce the number of undesirable products, the reaction was out in using anhydrous acetone instead of the reagent grade acetone. This made no difference to the number of undesirable products. After 19 h, the reaction was stopped, and the product was isolated by column chromatography using DCM: THF as eluent. A recrystallisation from acetone: EtOH gave the title compound in a 48% yield.

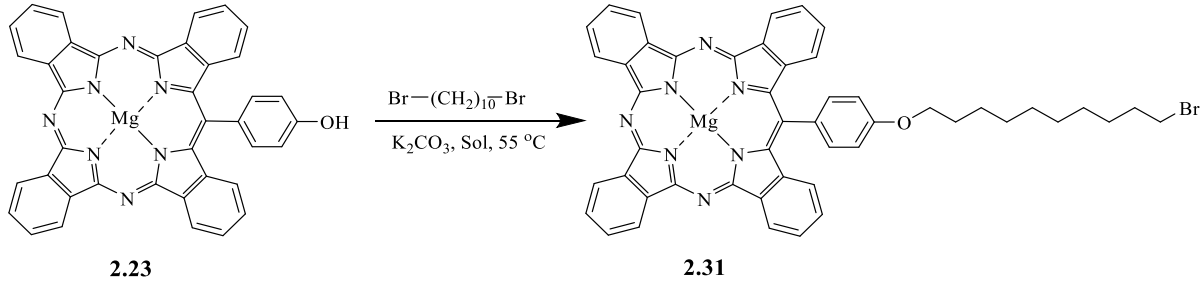

Scheme 2.20: Synthesis of Mg-TBTAP-O-C_{10}-Br **2.31**.

The ^{1}H-NMR spectrum is shown in figure 2.15. The 2 triplet peaks at around 4.41 ppm and 3.48 ppm correspond to the protons of the -OC*H*$_2$- and -C*H*$_2$-Br respectively. The aliphatic chain protons can be found at 2.08, 1.91 and 1.62 - 1.45 ppm. The positioning of the protons is shown in the figure 2.15. Analysis by MALDI-TOF MS showed a peak at 847 m/z corresponding to Mg-TBTAP-O-C$_{10}$-Br **2.31** (figure 2.14).

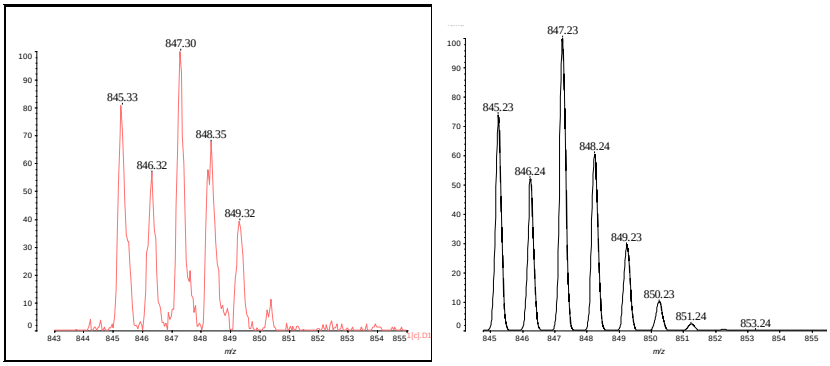

Figure 2.14: MALDI-TOF MS spectrum of Mg-TBTAP-O-C$_{10}$-Br **2.31** with its theoretical prediction.

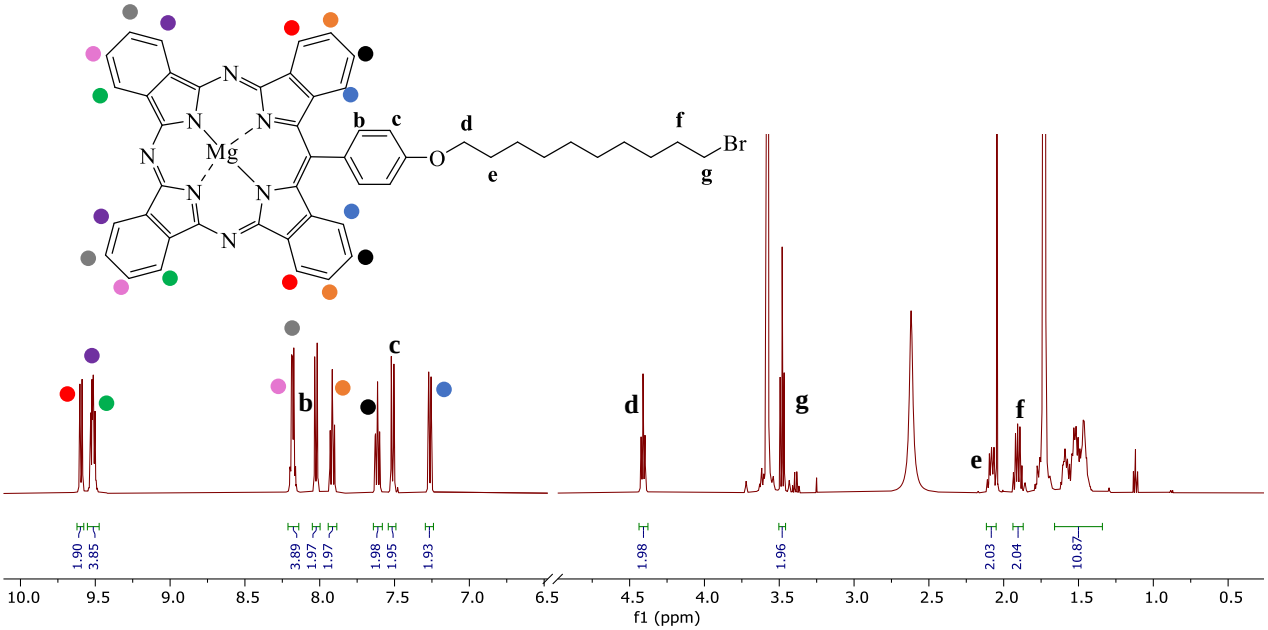

Figure 2.15: ^{1}H-NMR spectrum of Mg-TBTAP-O-C$_{10}$-Br **2.31** (500 MHz, THF-d_8, 25 °C).

Crystals of complex Mg-TBTAP-O-C$_{10}$-Br **2.31** suitable for X-ray diffraction were grown from methanol and THF solution at room temperature (figure 2.16). The magnesium is bonded to the four nitrogens inside the core and to the oxygen from methanol.

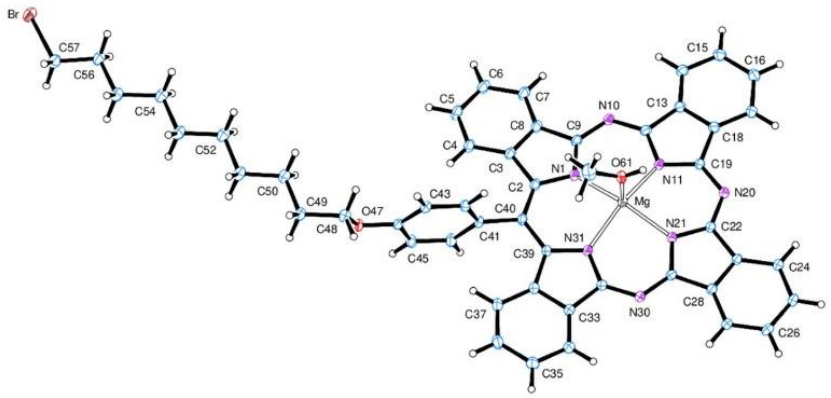

Figure 2.16: X-Ray analysis obtained for Mg-TBTAP-O-C_{10}-Br **2.31**.

Once the mono-alkylated Mg-TBTAP-O-C_{10}-Br **2.31** was produced, the next step was to react it with TPP-OH **2.8** in the presence of base (scheme 2.21). Different conditions were explored, and the results are summarised in the table 2.6.

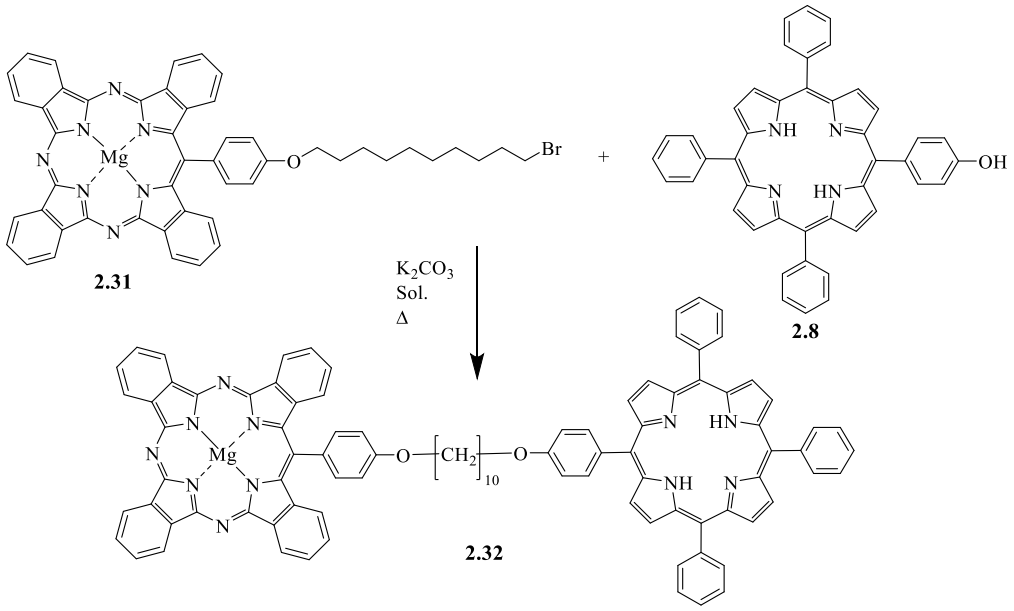

Scheme 2.21: Synthesis of unsymmetrical dyad **2.32** using Mg-TBTAP-O-C_{10}-Br **2.31**.

Table 2.6: Attempted conditions for the synthesis of unsymmetrical dyad **2.32**.

Entry	Solvent	Temperature (°C)	Volume (mL)	Time/days	Yield (%)[a]
1	Acetone	55	10	21	5
2	Acetone	55	2	10	4
3	DMF	55	10	21	10
4	DMF	70	2	14	15
5	DMF	80	2	14	18

6[b]	DMF	80	2	14	19
7[c]	DMF	80	2	14	23
8	DMF	80	2	7	21

[a]Isolated yield. [b]Potassium Iodide (KI) was added to reaction. [c]Reaction was carried out under nitrogen atmosphere. Mg-TBTAP-O-C_{10}-Br (0.11 mmol), TPP-OH (0.07 mmol), K_2CO_3 (0.9 mmol).

Caesium carbonate (Cs_2CO_3) as base was tried out and the yield did not improve. Varying changes in volume of solvents and temperatures did not significantly increase the yield (table 2.6). In an attempt to increase the yield small amount of potassium iodide (KI) was added (Table 2.6, entry 6). Analysis by TLC and MALDI-TOF MS of the reaction mixture, showed peaks at 766 m/z, 783 m/z and 1396 m/z corresponding to Mg-TBTAP-O- $C_{10}H_{20}$, Mg-TBTAP-O-$C_{10}H_{22}O$ and Mg-TBTAP-O-C_{10}-O-TPP **2.32** (the desired product) respectively.

Since the synthesis of the precursors, Mg-TBTAP-OH **2.23** and Mg-TBTAP-O-C_{10}-Br **2.31** required in the formation of the unsymmetrical dyad is time-consuming, a more straightforward alternative procedure (method B) was explored. This pathway was chosen as the synthesis of precursors involved, TPP-OH **2.8** and TPP-O-C_{10}-Br **2.8** were less time consuming (scheme 2.22). The results are summarised in the table 2.7.

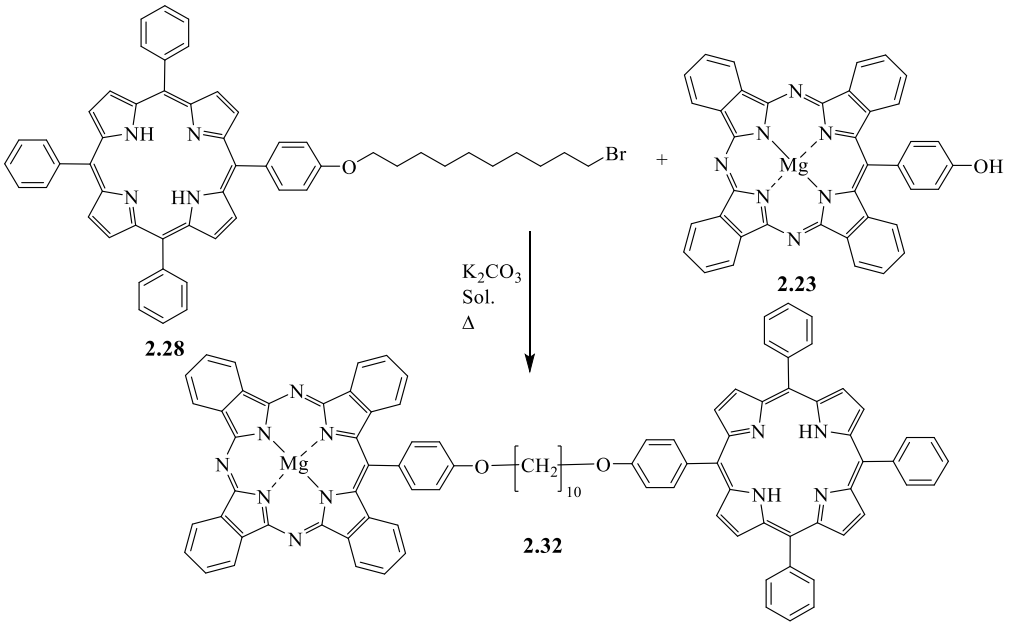

Scheme 2.22: Synthesis of unsymmetrical dyad **2.32** using TPP-O-C_{10}-Br **2.28**.

Table 2.7: Attempted conditions for the synthesis of unsymmetrical dyad **2.32**.

Entry	Solvent	Temperature (°C)	Volume (mL)	Time/days	Yield (%)[a]
1	Acetone	55	10	21	5
2	Acetone	55	2	12	5
3	DMF	55	10	15	6
4	DMF	70	5	10	10
5	DMF	70	2	8	10
6	DMF	80	5	12	34
7[b]	DMF	80	2	7	41
8	DMF	80	2	7	43
9[c]	DMF	80	2	7	40
10[c]	DMF	80	2	14	36

[a] Isolated yield. [b]Potassium Iodide (KI) was added to reaction. [c]Reaction was carried out under nitrogen atmosphere. TPP-O-C_{10}-Br (0.14 mmol), Mg-TBTAP-OH (0.08 mmol), K_2CO_3 (0.9 mmol).

Caesium carbonate as a base was chosen instead of potassium carbonate and the yield did not improve. As the temperature of the reaction was increased, the yield of the desired product was also increased (see above entries). In an attempt to increase the yield of the desired product, some potassium iodide (KI) was added (Table 2.7, entry 7) to the reaction mixture which clearly had a significant effect. The reaction was performed under an inert atmosphere and the yield did not improve (Table 2.7, entry 9). The reaction is dependent on temperature and concentration.

Analysis by MALDI-TOF MS from all of the reaction mixtures in the table above revealed the presence of the target dyad **2.32**, and side products TPP-O-$C_{10}H_{20}$ and TPP-O-$C_{10}H_{22}O$ with peaks at 1396 m/z, 769 m/z and 786 m/z respectively. As the reaction mixture is left to stir for a longer period of time, the presence of trace amount of water in the reaction mixture enhanced the production of the side product TPP-O-$C_{10}H_{22}O$ and thus the yield of the target dyad is reduced (Table 2.7, entry 10). After several days, TLC analysis revealed the presence of starting material, Mg-TBTAP-OH **2.23**. Thus, an excess of TPP-O-C_{10}-Br **2.28** was added and still not all the Mg-TBTAP-OH **2.23** was used up instead this favours the formation of the side products (Table 2.7, entry 10).

In both methods A and B the dyad was isolated by column chromatography using a solvent system of DCM: THF. A dark blue-purple fraction was collected, the solvent was removed and a recrystallisation performed using acetone and ethanol.

The ^{1}H-NMR spectrum of Mg-TBTAP-O-C_{10}-O-TPP **2.32** is more complex compared to the monomeric alkylated compounds. A comparison with the ^{1}H-NMR spectra of the Mg-TBTAP-O-C_{10}-Br **2.31** and TPP-O-C_{10}-Br **2.28** shows that the aromatic region for the dyad is essentially the sum of the two alkylated monomers (figure 2.17).

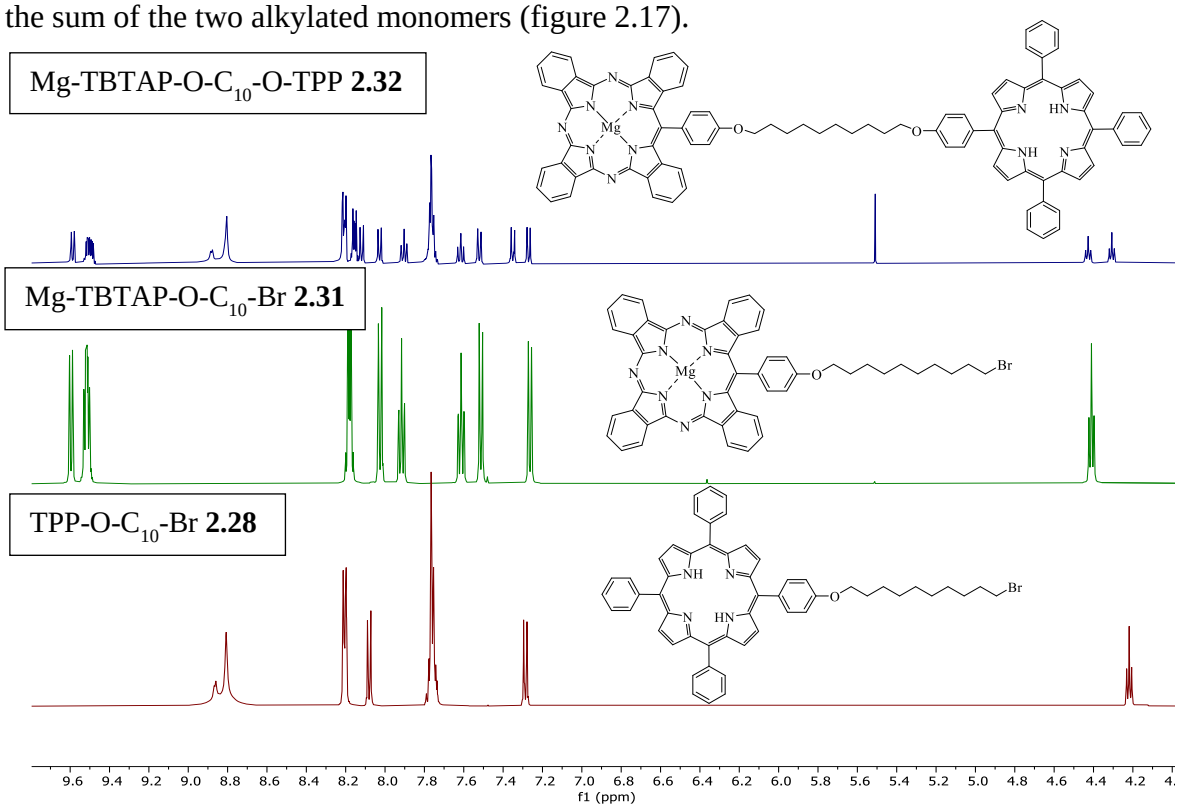

Figure 2.17: ^{1}H-NMR spectra of Mg-TBTAP-O-C_{10}-O-TPP **2.32**, Mg-TBTAP-O-C_{10}-Br **2.31** and TPP-O-C_{10}-Br **2.28** (500 MHz, THF-d_8, 25 °C).

The proton shifts for the TPP-O-C_{10}-Br **2.28** and Mg-TBTAP-O-C_{10}-Br **2.31** have already been discussed in previous sections. Therefore, the assignments of the protons in Mg-TBTAP-O-C_{10}-O-TPP **2.32** will be the same as its monomeric units. The only difference in the ^{1}H-NMR spectrum of the dyad **2.32** is that, since it is unsymmetrical, 2 triplets are observed at around 4.43 ppm and 4.31 ppm (figure 2.18). The assignment of the protons in the unsymmetrical dyad can be further confirmed by the COSY NMR (figure 2.19). Analysis from MALDI-TOF MS confirms the formation of Mg-TBTAP-O-C_{10}-TPP **2.32** (figure 2.20).

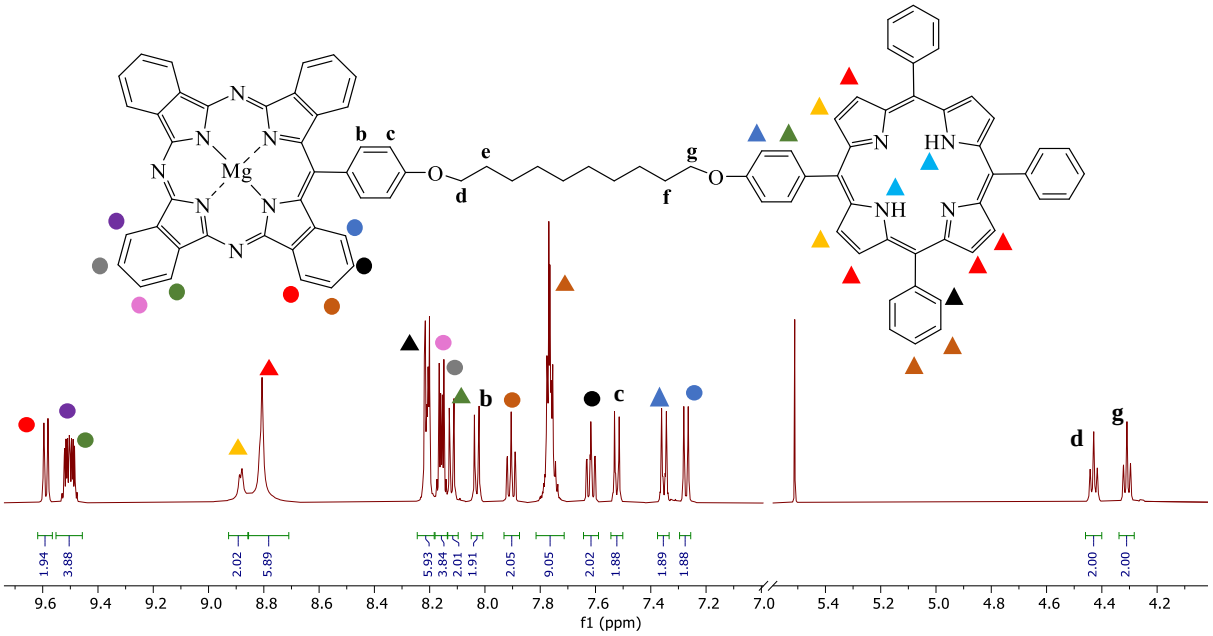

Figure 2.18: Assignment of peaks of ^{1}H-NMR spectrum of Mg-TBTAP-O-C$_{10}$-O-TPP **2.32** (500 MHz, THF-d_8, 25 °C).

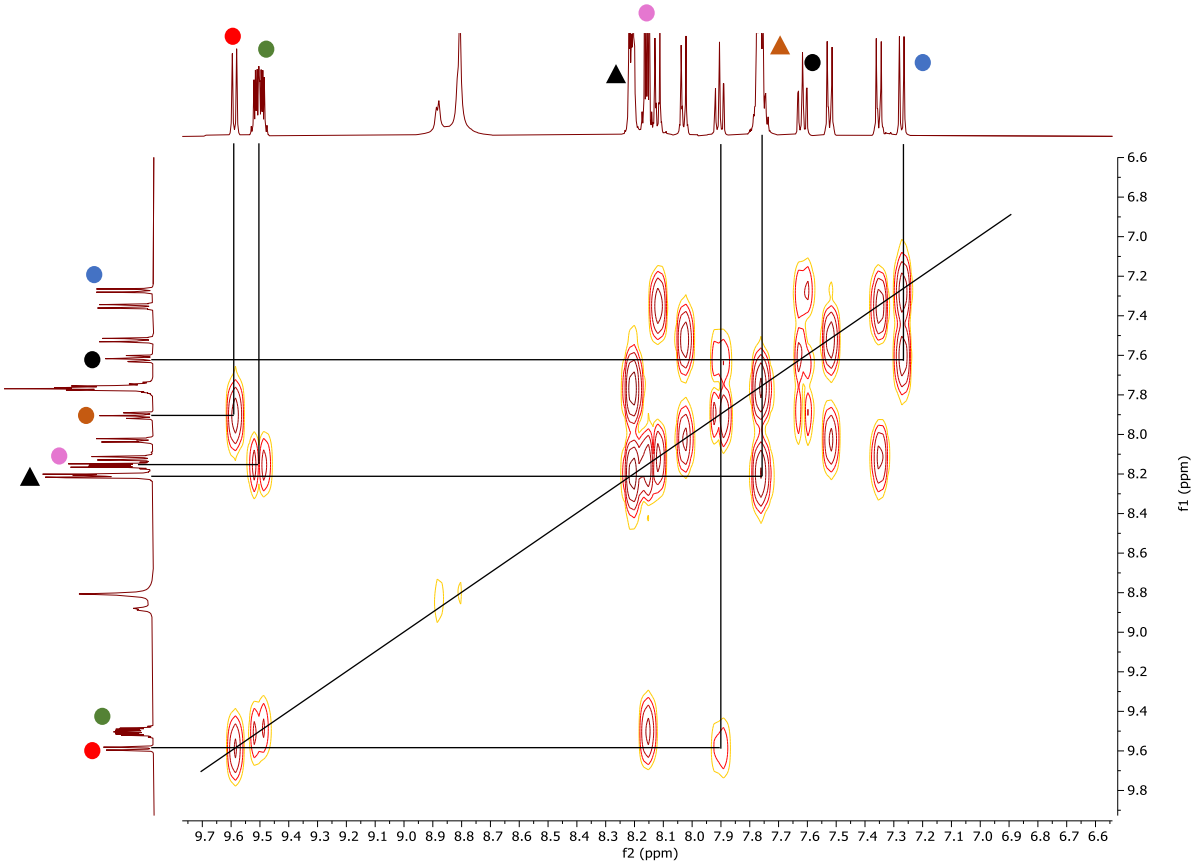

Figure 2.19: COSY NMR experiment showing cross peaks in Mg-TBTAP-O-C$_{10}$-O-TPP **2.32** (500 MHz, THF-d_8, 25 °C).

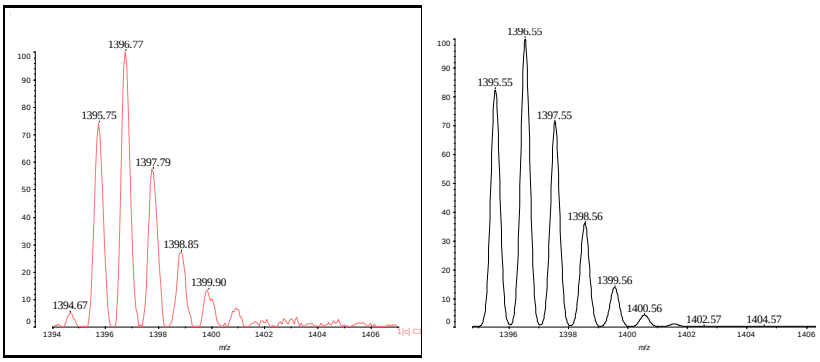

Figure 2.20: MALDI-TOF MS spectrum of dyad **2.32** with its theoretical prediction.

The UV-Vis spectrum of the unsymmetrical dyad **2.32** is shown in figure 2.21. The intense absorption in the B band at around 420 nm is characteristic of porphyrin. The characteristic Q bands of metallated-TBTAPs is split because of their decrease in molecular symmetry at around 670 and 650 nm.[13,14]

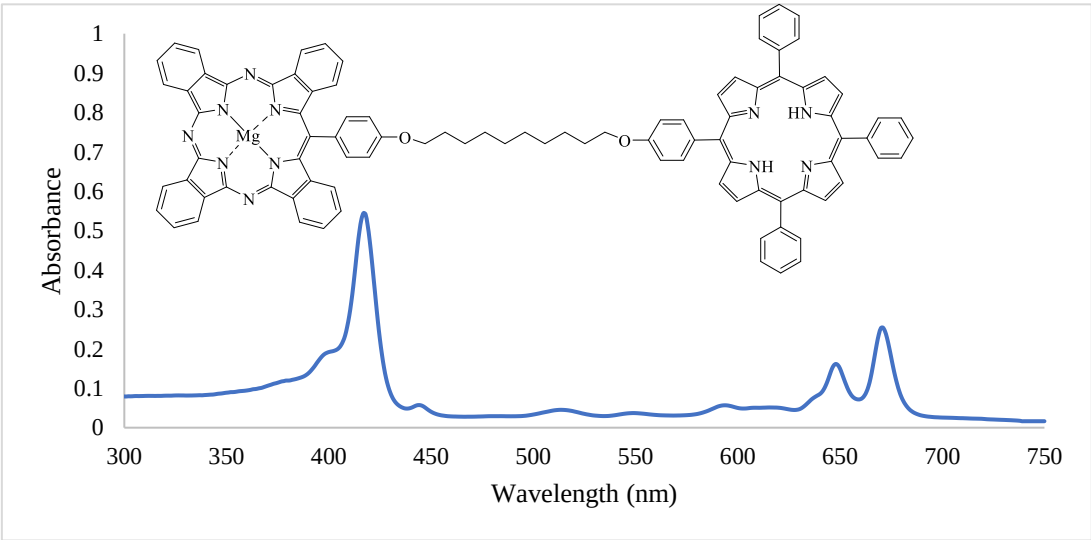

Figure 2.21: UV-Vis spectrum of unsymmetrical dyad **2.32** (in distilled THF).

2.8 Synthesis of unsymmetrical TPP-TBTAP dyad 2.35

After the successful synthesis of the unsymmetrical C_{10} dyad **2.32**, the synthesis of the unsymmetrical C_{12} dyad was then attempted following methods A and B previously described for the synthesis of unsymmetrical C_{10} dyad. Therefore, the preparation of Mg-TBTAP-O-C_{12}-Br **2.33** and TPP-O-C_{12}-Br **2.34** was carried out as starting materials (scheme 2.23).

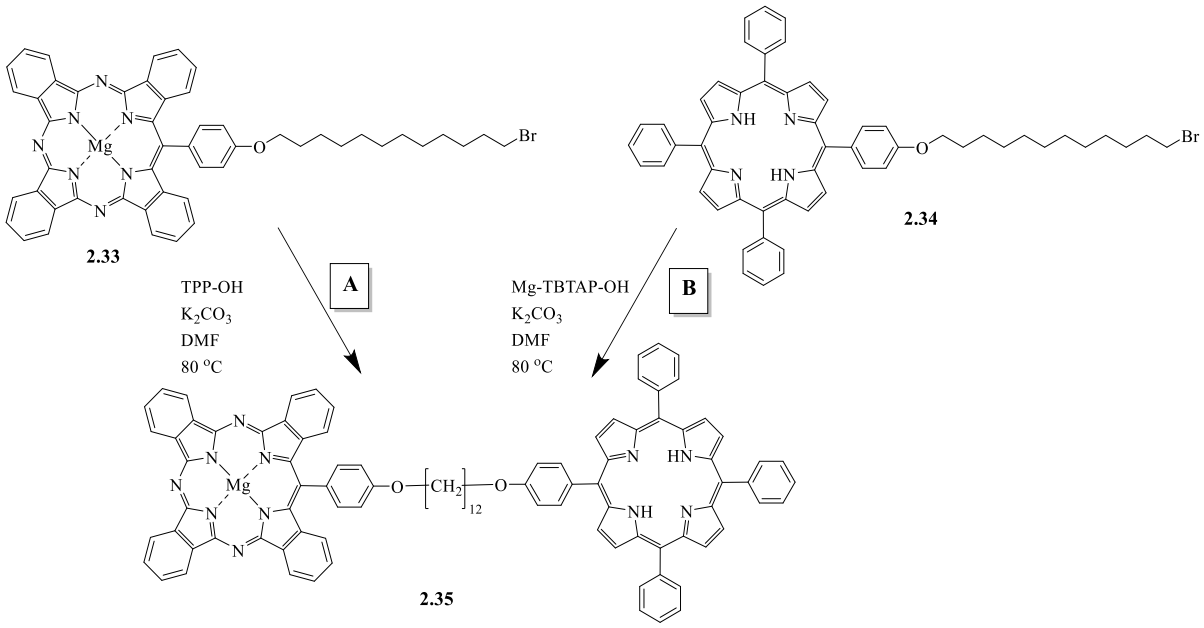

Scheme 2.23: Two synthetic pathways to yield the unsymmetrical dyad **2.35**.

MALDI-TOF MS analysis of the crude product from both pathways A and B showed a peak at 1424 m/z which corresponds to the unsymmetrical dyad. In pathway A, peaks at 794 m/z and 812 m/z corresponding to the side products, Mg-TBTAP-O-$C_{12}H_{26}O$ and Mg-TBTAP-O-$C_{12}H_{24}$ respectively. In pathway B the side products were TPP-O-$C_{12}H_{26}O$ and TPP-O-$C_{12}H_{24}$ with m/z of 814 and 796 respectively. Isolation and purification of the unsymmetrical dyad was achieved by following the procedure previously described, 25% and 51% yields were obtained from pathways A and B respectively. The peak from the MALDI-TOF MS at 1423 m/z further confirms the formation of Mg-TBTAP-O-C_{12}-O-TPP **2.35** (figure 2.22).

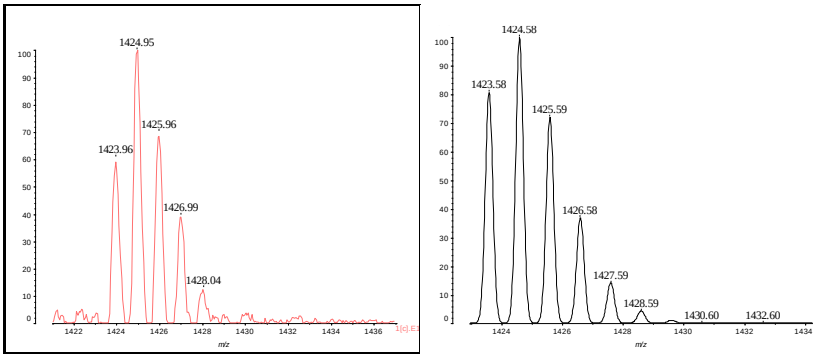

Figure 2.22: MALDI-TOF MS spectrum of dyad **2.35** with its theoretical prediction.

The ^{1}H-NMR spectrum of Mg-TBTAP-O-C_{12}-O-TPP **2.35** is essentially indistinguishable from that of Mg-TBTAP-O-C_{10}-O-TPP **2.32** as shown in the figure 2.23.

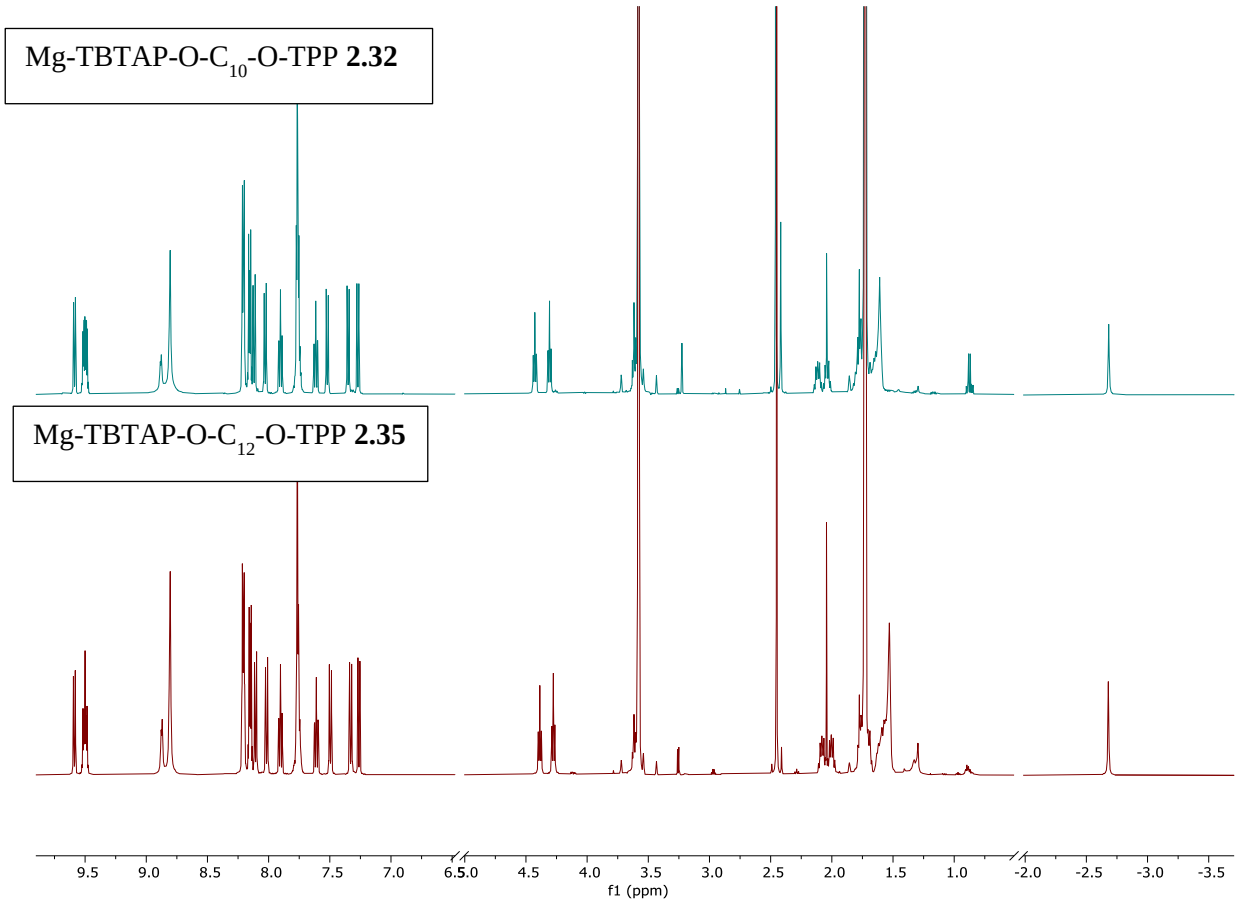

Figure 2.23: ^{1}H-NMR spectra of Mg-TBTAP-O-C_{10}-O-TPP **2.32** (top) and Mg-TBTAP-O-C_{12}-O-TPP **2.35** (bottom) (500 MHz, THF-d_8, 25 °C).

The expected number of peaks in the Mg-TBTAP-O-C_{12}-O-TPP dyad **2.35** remained unchanged when compared to Mg-TBTAP-O-C_{10}-O-TPP dyad **2.32**. The assignments of the protons in the unsymmetrical C_{12} dyad are similar to the previously described unsymmetrical C_{10} dyad. The only difference is that the total number of protons in the alkyl region of the ^{1}H-NMR spectrum of the C_{12} dyad from 2.15–1.47 ppm that integrates to 24.

2.9 Demetallation of the unsymmetrical dyad C_{10}

In a trial reaction, Mg-TBTAP-OMe **2.13** was dissolved in a minimum amount of concentrated H_2SO_4, stirred and sonicated for a few minutes and the resulting solution was added to ice. The precipitate formed was filtered off and washed with cold water followed by methanol. The resulting peak from the MALDI-TOF MS showed 619 m/z for TBTAP-OMe **2.24** (figure 2.24). A 90% yield of the product was obtained which required no further purification (scheme 2.24).

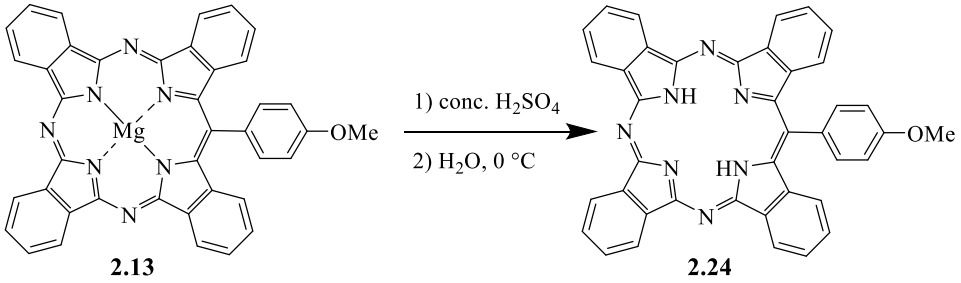

Scheme 2.24: Demetallation of Mg-TBTAP-OMe **2.13**.

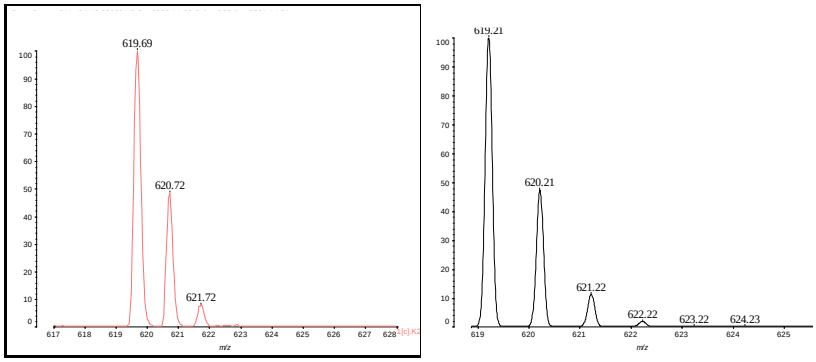

Figure 2.24: MALDI-TOF MS spectrum of TBTAP-OMe **2.24** with its theoretical prediction.

Following the successful outcome of the demetallation of Mg-TBTAP-OMe **2.13** by concentrated acid, the same procedure to demetallate the unsymmetrical compound, Mg-TBTAP-O-C_{10}-O-TPP **2.32** was attempted (scheme 2.25). Although the demetallation was fast (Table 2.8, entry 1), when the mixture was analysed by MALDI-TOF MS, a peak at 1374 m/z was obtained indicating the presence of the desired compound **2.36** with a yield of only 15%. The demetallation is a straightforward process in which the acid is reacting with the magnesium. Therefore, a higher yield of the desired compound **2.36** would have been expected with no side products. Such an outcome is probably due to the compound **2.32** being broken down by the strong acid (Table 2.8, entry 1-3).

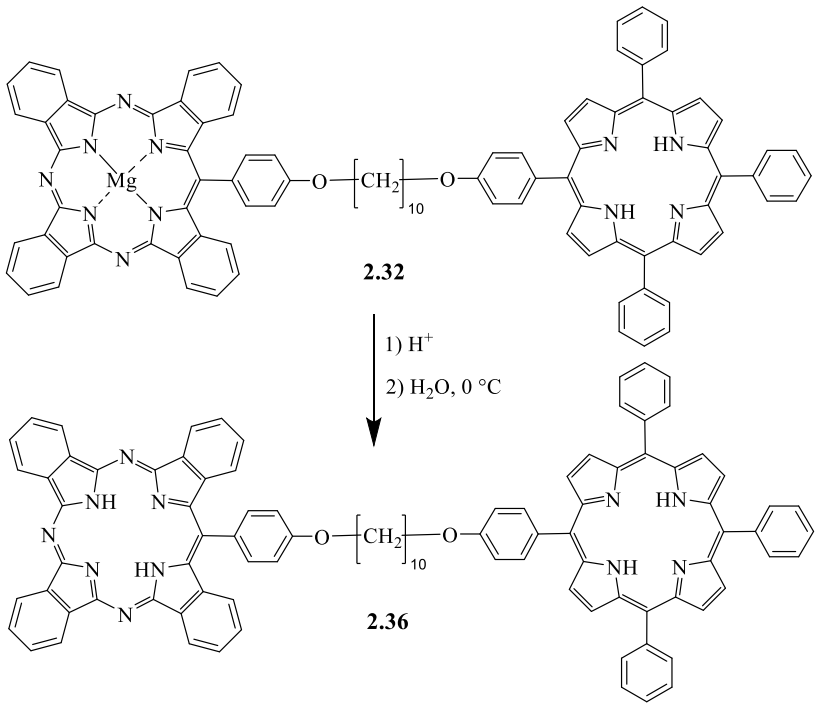

Scheme 2.25: Demetallation of unsymmetrical dyad **2.32**.

Table 2.8: Other acids used for the demetallation of unsymmetrical dyad **2.32**.

Entry	Acid	Pka	Time (h)	Yield (%)[a]
1	H_2SO_4	-3	0.04	15
2	H_2SO_4 (6M)	-3	0.04	20
3	Acetic acid	4.75	72	40
4	Trifluoroacetic acid	0.00	18	56
5	Glacial Formic acid	3.75	18	66

[a] Isolated yield.

Therefore, the demetallation process was repeated using a weaker acetic acid. Acetic acid was added to the unsymmetrical dyad and was left to stir overnight at room temperature.[9] Analysis by MALDI-TOF MS revealed that there was no conversion to the demetallated dyad. The reaction was then heated to a temperature of 80 °C for 72 h with continuous monitoring. MALDI-TOF MS analysis showed the presence of the demetallated unsymmetrical dyad **2.36** (Table 2.8, entry 3). After work-up by following the procedure mentioned above, a 40% yield was obtained. Other acids such as trifluoroacetic acid (TFA) and glacial formic acid were also used. The results are summarised in the table below (Table 2.8, entry 4, 5). Clearly, glacial formic acid is the best demetallating agent.

The demetallation of Mg-TBTAP-O-C_{12}-O-TPP **2.35** was then carried out under the same conditions as above using glacial formic acid. The isolation and purification were performed by using the same approach as in the synthetic route already described. A 75% yield of the unsymmetrical C_{12} dyad **2.37** was obtained. The peak from the MALDI-TOF MS at 1402 m/z further confirms the formation of TBTAP-O-C_{12}-O-TPP **2.37** (figure 2.26).

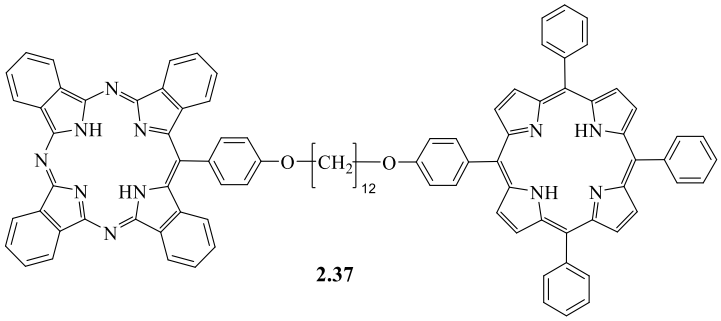

Figure 2.25: Structure of TBTAP-O-C_{12}-O-TPP **2.37**.

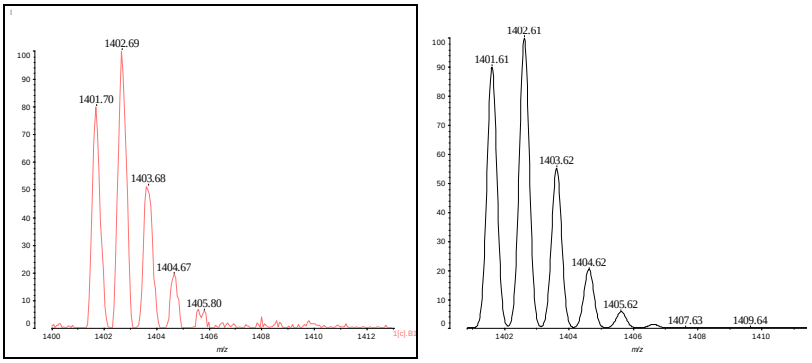

Figure 2.26: MALDI-TOF MS spectrum of TBTAP-O-C_{12}-O-TPP **2.37** with its theoretical prediction.

2.10 Synthesis of symmetrical TBTAP-TBTAP dyad 2.38

The synthesis of the unsymmetrical dyads (**2.32** and **2.35**) was successful, the next step was to synthesise the symmetrical dyad with TBTAP units using two different pathways. (Scheme 2.26).

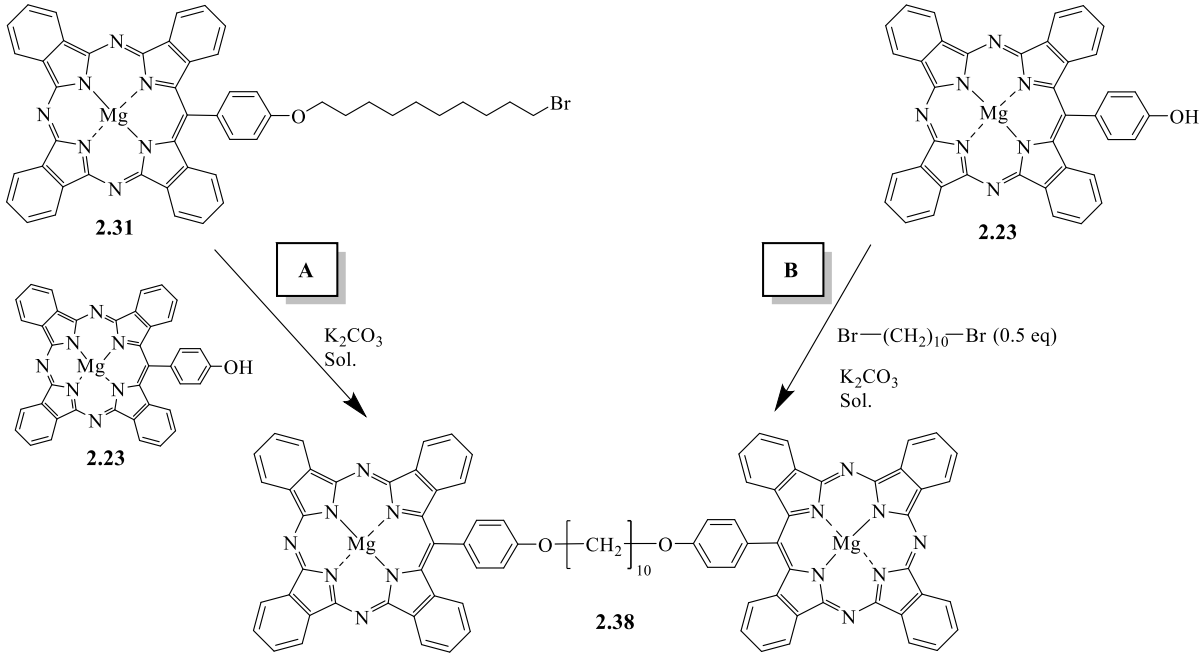

Scheme 2.26: Two synthetic pathways to yield the symmetrical dyad **2.38**.

In pathway A (scheme 2.26), the mono-alkylated Mg-TBTAP-O-C_{10}-Br **2.31** was added to Mg-TBTAP-OH **2.23** in the presence of a base, K_2CO_3. This reaction was investigated using solvents, acetone, DMF and methyl ethyl ketone (MEK) under different conditions as per table 2.8. When the crude mixture was analysed by MALDI-TOF MS, peaks at, 766 m/z, 783 m/z and 1394 m/z corresponding to Mg-TBTAP-O-$C_{10}H_{20}$, Mg-TBTAP-O-$C_{10}H_{22}O$ and Mg-TBTAP-O-C_{10}-O-Mg-TBTAP **2.38** respectively were obtained.

After the desired reaction time was achieved, the dyad was isolated by column chromatography using a solvent system of DCM: THF. A dark green fraction was collected, the solvent was removed, and the product was recrystallised using acetone and ethanol. A MALDI-TOF MS analysis of the product shows a peak at 1394 m/z which confirms the presence of Mg-TBTAP-O-C_{10}-O-Mg-TBTAP **2.38** (figure 2.28). The yields of the product **2.38** are recorded in table 2.8.

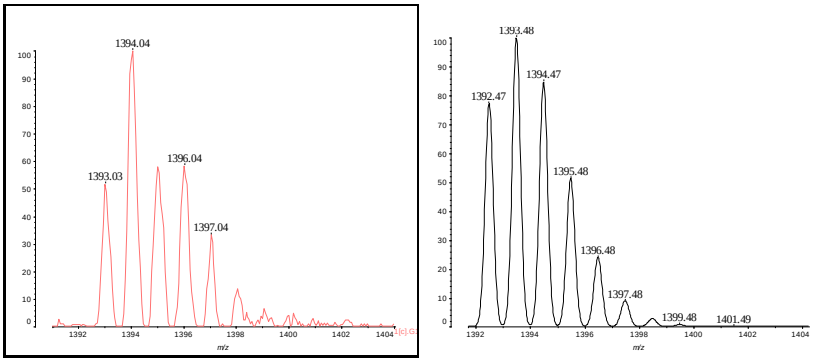

Figure 2.28: MALDI-TOF MS spectrum of dyad **2.38** with its theoretical prediction.

When the synthesis was carried out in acetone in a sealed tube, the yield was poor (Table 2.9, entry 1-2). Using DMF in a nitrogen atmosphere did not result in a significant change in the yield (Table 2.9, entry 6). When the reaction was performed at a higher concentration, a 30% yield was achievable (Table 2.9, entry 7). The results are tabulated below.

Table 2.9: Attempted conditions for the synthesis of symmetrical dyad **2.38** via pathway A.

Entry	Solvent	Volume (mL)	Temperature (°C)	Time (days)	Yield (%)[a]
1	Acetone	20	55	25	8
2	Acetone	10	65	14	10
3	DMF	10	55	14	20
4	DMF	5	80	12	24
5[b]	DMF	5	70	12	24
6[c]	DMF	5	70	12	25
7	DMF	2.5	70	12	30
8	MEK	2.5	70	12	24

[a] Isolated yield. [b]Potassium Iodide (KI) was added to reaction. [c]Reaction was carried out under nitrogen atmosphere. Mg-TBTAP-O-C_{10}-Br (0.09 mmol), Mg-TBTAP-OH (0.06 mmol), K_2CO_3 (0.9 mmol).

In pathway B (scheme 2.26), Mg-TBTAP-OH **2.22** and half equivalent of 1,10-dibromodecane were mixed in the presence of base, K_2CO_3. The results are tabulated below (table 2.10). When the reaction was performed in acetone, a 9% yield was achieved after 25 days with continuous monitoring (Table 2.10, entry 1). Although the reaction was heated at 70 °C in a sealed tube, this did not increase the yield of the symmetrical dyad.

Table 2.10: Attempted conditions for the synthesis of symmetrical dyad **2.38** via pathway B.

Entry	Solvent	Volume (mL)	Temperature (°C)	Time (days)	Yield (%)[a]
1	Acetone	10	55	30	9
2	DMF	10	55	14	12
3	DMF	5	70	15	15
4[b]	DMF	2.5	70	14	24
5[c]	DMF	2.5	70	14	25
6	DMF	2	70	14	27

[a] Isolated yield. [b]Reaction was carried out under nitrogen atmosphere. [c]Potassium Iodide (KI) was added to reaction Mg-TBTAP-OH (0.16 mmol), Dibromodecane (0.08 mmol), K_2CO_3 (1.6 mmol).

Clearly the reaction is dependent on concentration and temperature. When the reaction was carried out either under nitrogen or in the presence of KI the yield did not change (Table 2.10, entries 4, 5). When the reaction is performed in a more concentrated solution (Table 2.10, entry 6), a higher yield is obtained. Analysis by MALDI-TOF MS of the crude product gave similar results to pathway A.

The ^{1}H-NMR spectrum of Mg-TBTAP-O-C_{10}-O-Mg-TBTAP **2.38** is shown in figure 2.27. The proton signals in the aromatic region remain unchanged as compared to the Mg-TBTAP-OMe **2.13** previously described. Only 1 triplet at 4.45 ppm was observed which integrates to 4. This corresponds to the -OCH_2- as the molecule is symmetrical.

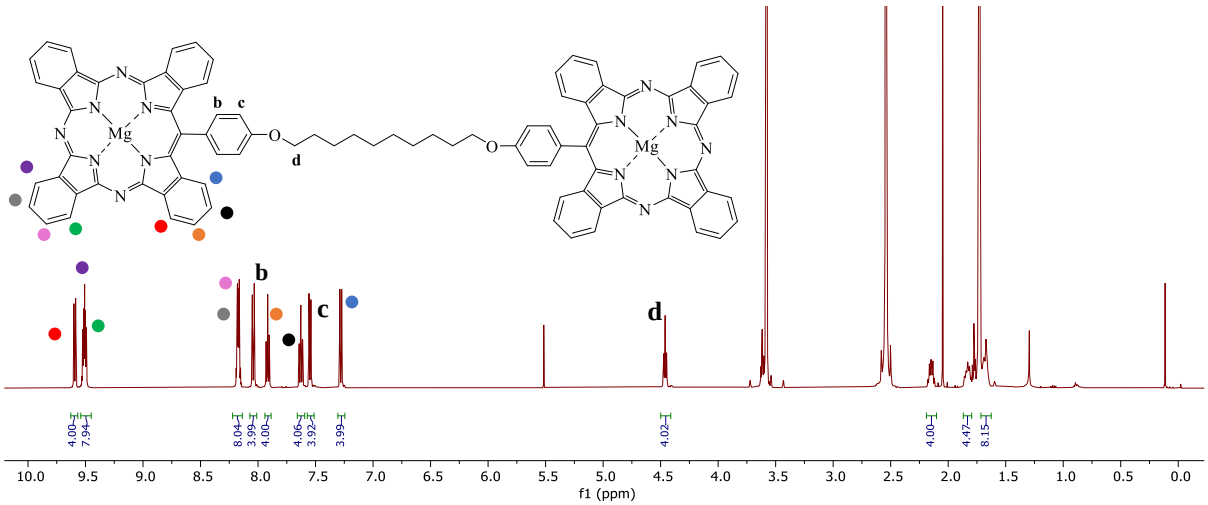

Figure 2.27: ^{1}H-NMR spectrum of the symmetrical dyad **2.38** (500 MHz, THF-d_8, 25 °C).

The product, Mg-TBTAP-O-C_{10}-O-Mg-TBTAP **2.38** was analysed by UV-Vis spectroscopy and showed the distinctive split Q-band at 672 and 649 nm as shown in the figure 2.29. A comparison of the shapes of the bands with those of Mg-TBTAP-OMe **2.13** from literature,[9] shows no significant differences.

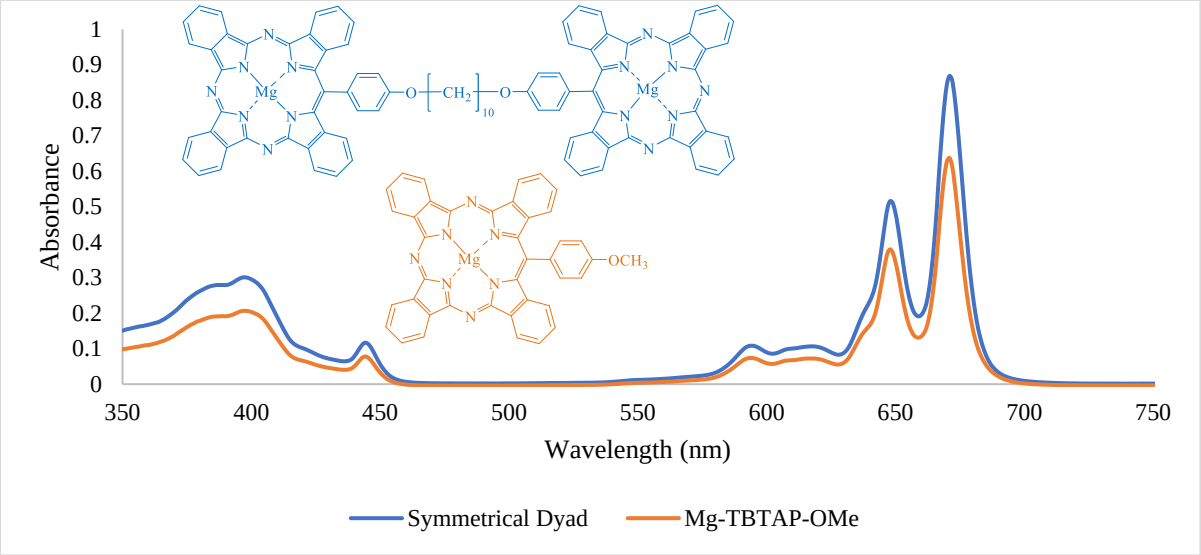

Figure 2.29: UV-Vis spectra of symmetrical dyad **2.38** and Mg-TBTAP-OMe **2.13** (in distilled THF).

2.11 Demetallation of the symmetrical dyad C_{10}

Following the successful demetallation of the unsymmetrical dyads using weaker acids such as TFA and formic acid, the same procedure (section 2.8) was used to demetallate the symmetrical dyad (scheme 2.27).

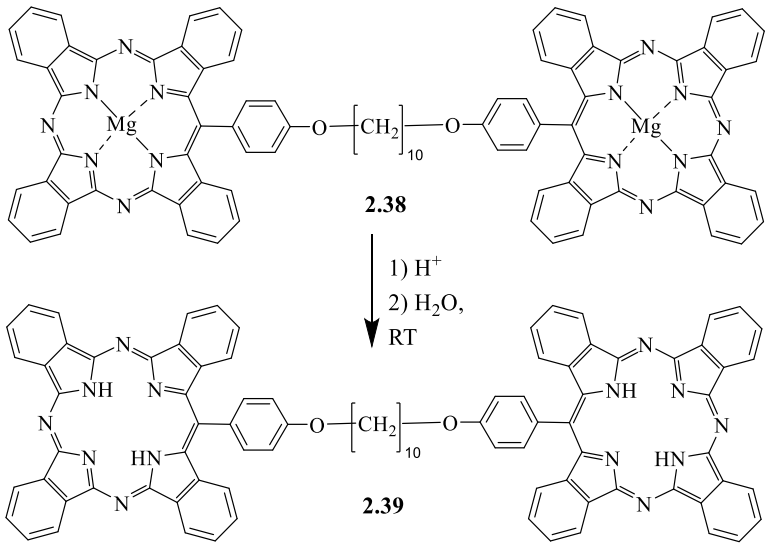

Scheme 2.27: Demetallation of symmetrical dyad.

The resulting compound was analysed by MALDI-TOF MS and a peak at 1349 m/z corresponding to TBTAP-O-C_{10}-O-TBTAP **2.39** (figure 2.30). No other peaks were present and therefore all the starting material has been used up. After isolation and purification, the yield obtained from TFA and glacial formic acid were 60% and 56% respectively.

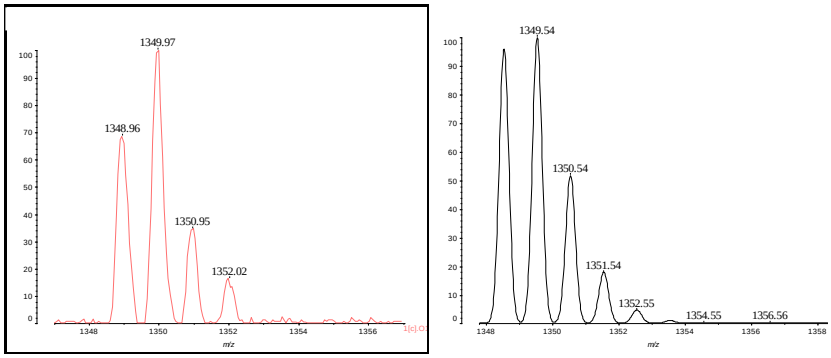

Figure 2.30: MALDI-TOF MS spectrum of TBTAP-O-C_{10}-O-TBTAP **2.39** with its theoretical prediction.

A UV-Vis spectrum of the TBTAP-O-C_{10}-O-TBTAP **2.39** run in distilled THF showed the two distinctive split Q-band at 685 and 647 nm respectively (figure 2.31). A feature between the metallated dyad and the demetallated dyad is that the splitting (ΔQ) is higher in the demetallated dyad and equals 41 nm. While in the metallated the symmetry of the macrocycle is increased and thus the ΔQ drops to 23 nm.[14] There are no distinguishable differences in the spectra from the demetallated TBTAP-OH **2.29** and the TBTAP-O-C_{10}-O-TBTAP **2.39**.

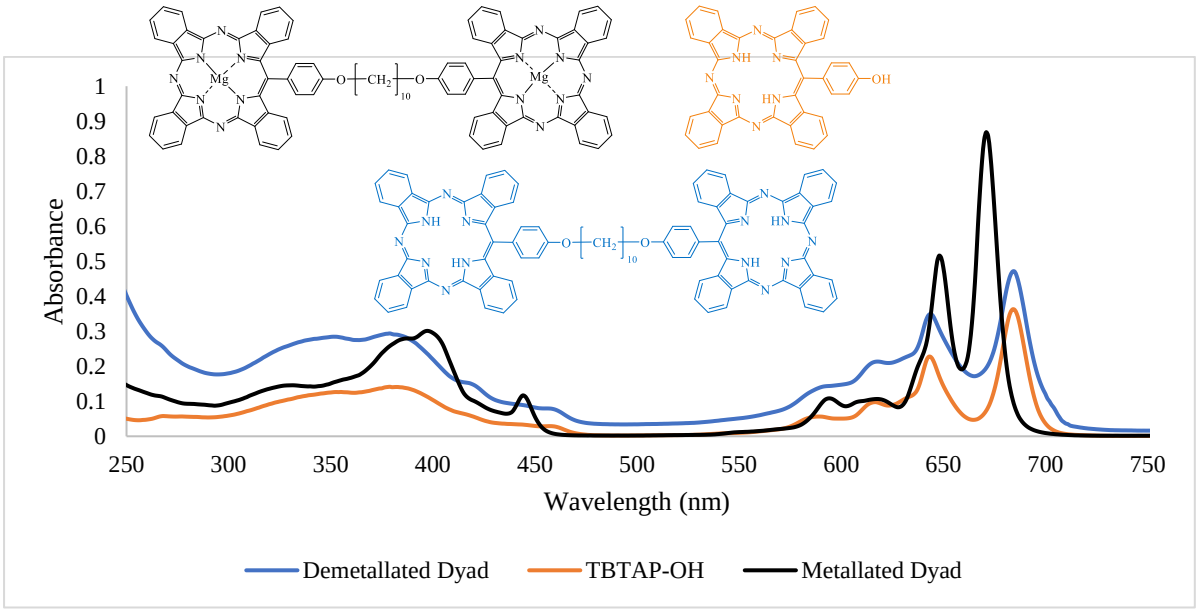

Figure 2.31: UV-Vis spectra of demetallated symmetrical dyad **2.39**, TBTAP-OH **2.29** and symmetrical dyad **2.38** (in distilled THF).

2.12 Synthesis of metal-free phthalocyanine

The metal-free phthalocyanine **2.40** is an important starting material for the synthesis of the lanthanide triple deckers.

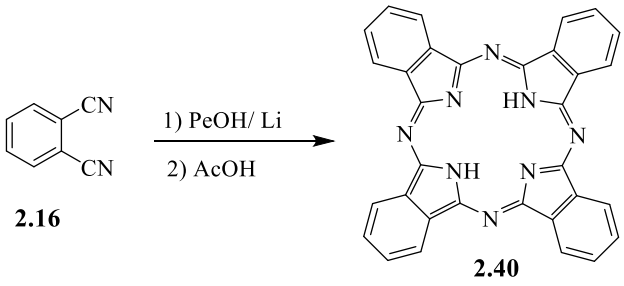

2.16 **2.40**

Scheme 2.28: Synthesis of metal-free phthalocyanine.

A solution of phthalonitrile in 1- pentanol was heated at a temperature of 120 °C and lithium metal was added to the reaction mixture. After 1 h, acetic acid was added to the reaction mixture which was allowed to cool to room temperature. Methanol was added to precipitate the product (scheme 2.28). Upon filtration, a dark blue solid was obtained. Analysis by MALDI-TOF MS showed a peak at 514 m/z confirming the formation of the phthalocyanine **2.40** (figure 2.32). The purity of the phthalocyanine was checked by TLC, no impurities were present. The yield of the phthalocyanine **2.40** was 50%. Further characterisation was not achieved due to the high insolubility in organic solvents.

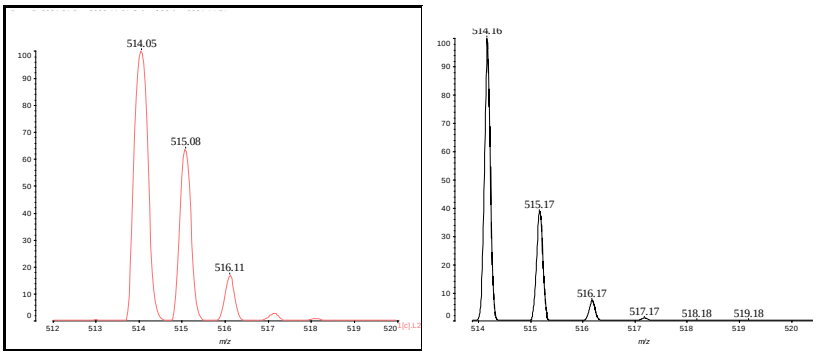

Figure 2.32: MALDI-TOF MS spectrum for metal-free phthalocyanine **2.40** with its theoretical prediction.

2.13 Alkylation of TPPOH

In the previous sections, symmetrical and unsymmetrical dyad were synthesised. These are the precursors to the synthesis of lanthanum triple decker. A comparative spectroscopic analysis of the newly synthesised TD with previously synthesised La-TPP TD[3] will be carried out. This

section describes the synthesis of a TPP dyad **2.1**, a precursor in the assembly of lanthanum triple decker (La-TPP TD).

The straightforward synthesis of the porphyrin dyad **2.1** was carried out by following a known alkylation procedure which has been developed for the synthesis of multiporphyrin arrays.[3,15,16]

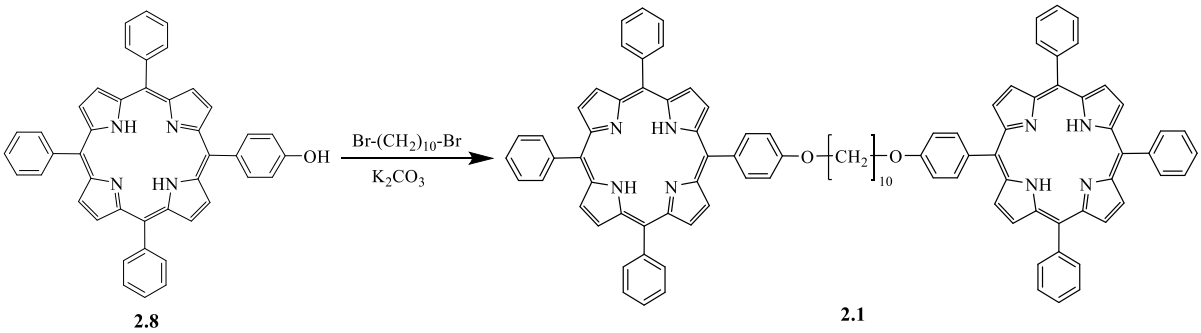

Scheme 2.29: Synthesis of the porphyrin dyad **2.1**.

The ^{1}H-NMR spectrum confirmed the formation of the porphyrin dyad and is shown in figure 2.33. The proton signals correspond to those of the porphyrin dyad from literature.[3]

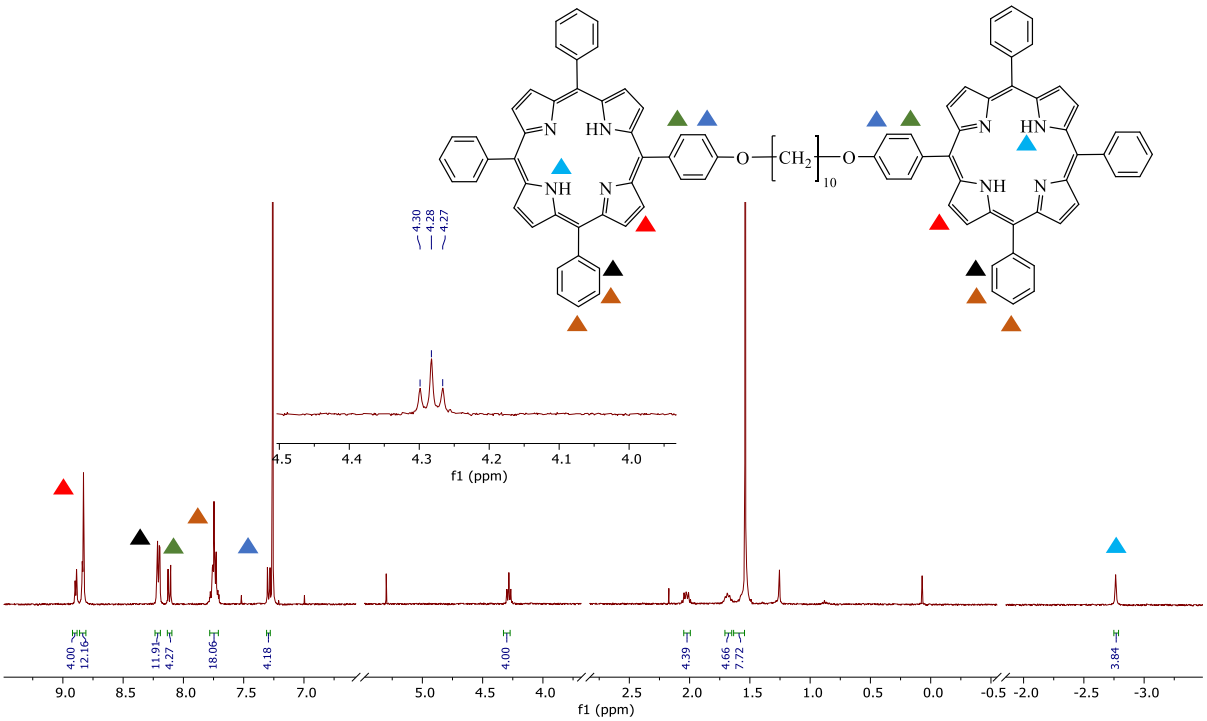

Figure 2.33: ^{1}H-NMR spectrum of porphyrin dyad **2.1** (500 MHz, $CDCl_3$, 25 °C).

2.14 Synthesis of bridged triple decker.

The synthesis of dyads with both decane and dodecane alkyl chain was successful. The next step was to investigate the controlled synthesis of heteroleptic triple deckers.

2.15 Synthesis of bridged La triple deckers

2.15.1 Synthesis of the La triple decker using TPP dyad 2.1

For spectroscopic comparison purposes, the synthesis of the triple decker La-TPP TD **2.2** was reproduced (scheme 2.30). The structure of La-TPP TD **2.2** consists of two porphyrin units which are linked together by a decane chain and a phthalocyanine molecule which is sandwiched between the two units.

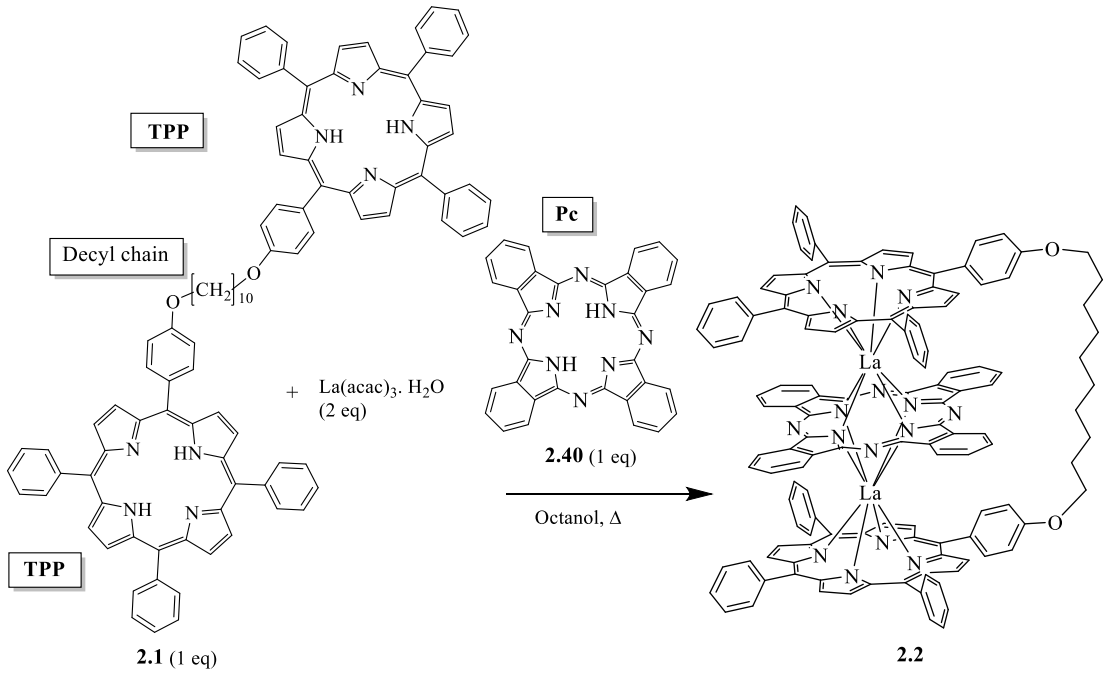

Scheme 2.30: Synthesis of La-TPP TD **2.2** using symmetrical TPP dyad **2.1**.[3]

In a two-step one pot reaction, the porphyrin dyad **2.1** (1 equivalent) and two equivalents of lanthanum (III) acetylacetonate were mixed in octanol and the resulting mixture was left to reflux at 200 °C. After 4 hours, one equivalent of Pc **2.40** was added to the reaction mixture and was left to further reflux. A TLC analysis after 19 hours showed the absence of starting materials. The solvent was distilled off and the resulting solids were recrystallised from a mixture of DCM: MeOH. Further purification by column chromatography and recrystallisation of the La-TPP TD **2.2** resulted in a 33% yield.

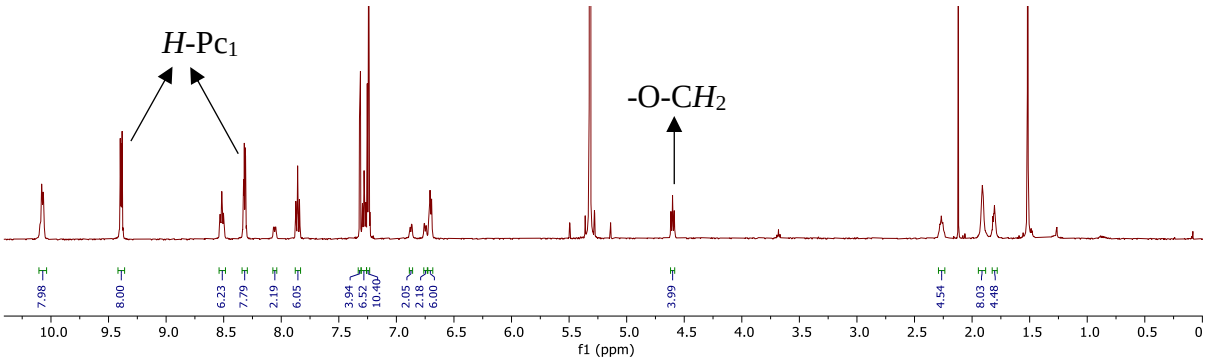

Figure 2.34: ^{1}H-NMR spectrum of heteroleptic triple decker **2.2** (500 MHz, CD_2Cl_2, 25 °C).

The ^{1}H-NMR spectrum confirmed the formation of the triple decker and was previously described by the Cammidge group.[3] It is observed that the characteristic signal at -2.7 ppm is not present, suggesting there is no metal-free porphyrin. The alkoxide peak (-O-C*H*$_2$) at around 4.6 ppm appears as a triplet which means that both ends of the aliphatic chain are in an identical environment (symmetrical molecule). Two signals for the protons on the phthalocyanine are observed at around 9.30 ppm and 8.30 ppm corresponding to *H*-Pc$_1$ and *H*-Pc$_2$ respectively.

2.15.2 Synthesis of the La triple decker using TPP-TBTAP dyad 2.36

In the above section, the synthesis of La-TPP TD **2.2** with Pc **2.40** in between the sandwich proves to be reproducible. Therefore, the next investigation in the synthesis of triple deckers was to use the phthalocyanine and the unsymmetrical porphyrin-TBTAP dyad.

Following the successful synthesis of La-TPP TD **2.2**, the same synthetic approach was adopted (scheme 2.31). After 19 hours, subsequent analysis by TLC of the reaction mixture showed 4 spots: a greenish-brown spot, a green spot, dark green spot and a spot on the baseline. This mixture was analysed by MALDI-TOF MS and m/z of 1509, 2160, 3018, 514 m/z were recorded corresponding to a bridged double decker, a TD, a bis double decker and unreacted Pc. The solvent was distilled off and a mixture of DCM/ MeOH was added to the dry residue which was left to precipitate overnight. The mixture was filtered and purified by column chromatography using a solvent system of DCM/PE. A final recrystallisation using a solvent system of DCM: MeOH was performed. The yield of the heteroleptic triple decker was 8%. Analysis by MALDI-TOF MS gave a m/z of 2160 corresponding to the desired triple decker, assumed to be **2.41** (figure 2.35).

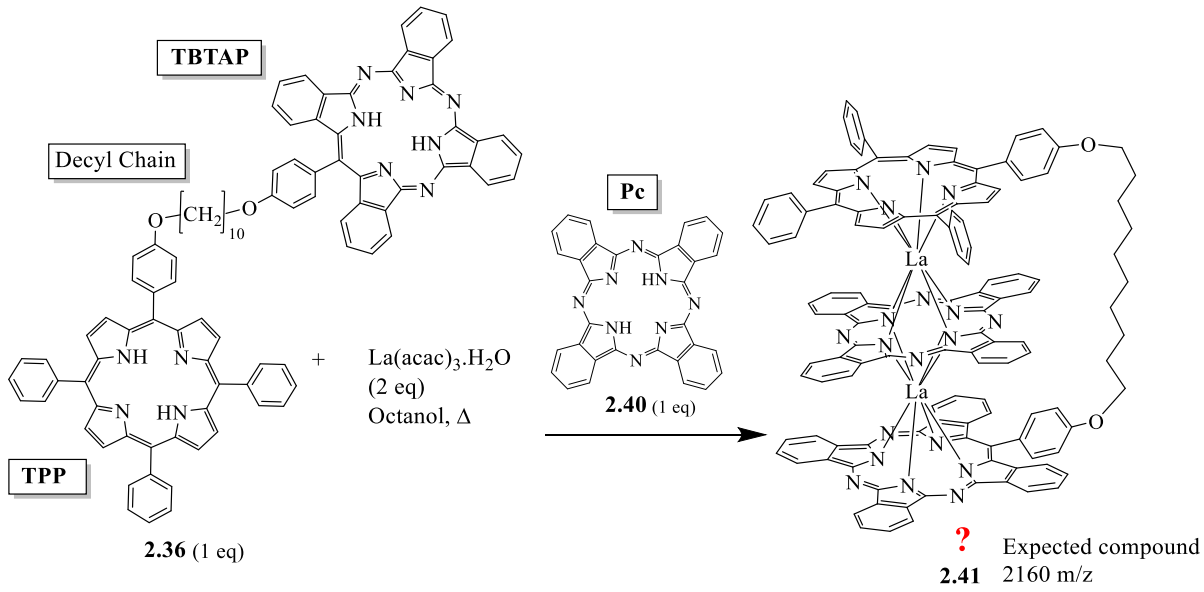

Scheme 2.31: Synthesis of La-TD, presumed to be **2.41**, using unsymmetrical dyad **2.36**.

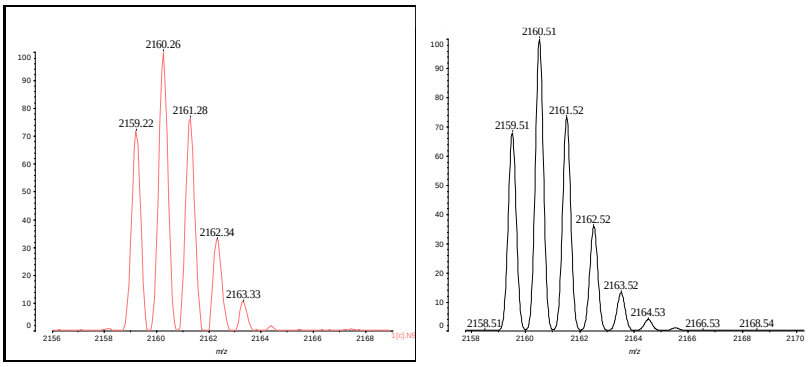

Figure 2.35: MALDI-TOF MS spectrum of the TD complex with theoretical prediction for triple decker (assumed to be **2.41**).

The ^{1}H-NMR spectrum in deuterated DCM was very different to the previous triple decker (La-TPP TD **2.2**) with poorly defined peaks especially in the aromatic region (figure 2.36).

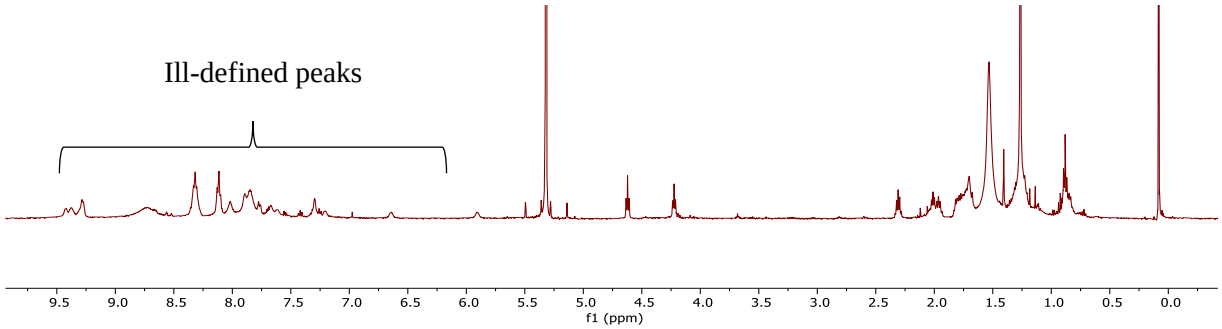

Figure 2.36: ^{1}H-NMR spectrum of heteroleptic triple decker (assumed to be **2.41**) (500 MHz, CD_2Cl_2, 25 °C).

The sample was then analysed again by more careful TLC and there were clearly at least two spots. Another column chromatography was performed on the impure sample, and this time

the desired fraction was collected and the solvent removed rapidly under reduced pressure. A recrystallisation using DCM: MeOH was then performed. This step was performed to avoid the slow decomposition of the desired triple decker. However, only a trace amount of the product was obtained. Further syntheses and isolation protocols were investigated to attempt to isolate the pure material, unfortunately, in all these cases repeated chromatography led to lower and lower recovery of the TD suggesting that the desired triple decker, is unstable and decomposes slowly on silica and possibly also in solution. The solution containing the TD was kept in the dark. Repeated analysis by TLC showed only 1 spot, indicating that isolation of pure TD was achieveable.

The reaction was repeated by using a 'one-pot technique. The unsymmetrical dyad **2.36** (1 equivalent), two equivalents of lanthanum (III) acetylacetonate and one equivalent of Pc **2.40** were refluxed in octanol in an argon atmosphere and monitored by TLC (scheme 2.30). After 4 hours no triple decker was detected, and the reaction was left to reflux overnight.

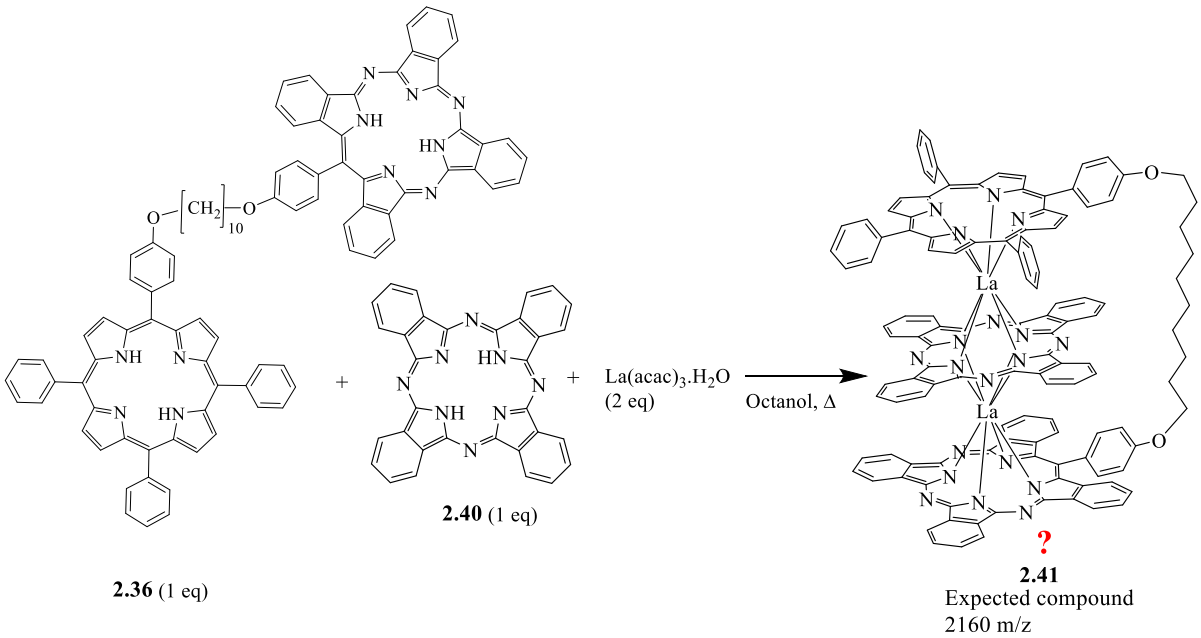

Scheme 2.32: Synthesis of heteroleptic triple decker (assumed to be **2.41**) using 'one-pot' method.

TLC analysis of the reaction mixture showed 4 spots, identical to the TLC from the previous approach. The triple decker was isolated and purified by column chromatography using the same solvent system as in the synthetic route previously described. However, the purification step was rapidly performed avoiding any source of light. The column was wrapped with aluminium foil and a fast separation technique was adopted so as to reduce contact time

between the triple decker and silica and also decomposition by light. All the fractions containing the desired product were evaporated immediately and combined. The sample was reprecipitated and a yield of 8% was recorded.

The ^{1}H-NMR spectrum of the La-TD (assumed to be **2.41**) is shown in figure 2.37. The peaks in the aromatic region are much clearer. It is observed that there are no peaks in the negative region of the spectrum. This indicates that there are no metal-free unsymmetrical dyad. Although complicated, as expected for such low symmetry TDs, the total number of peaks, their multiplicities and their integrations correlate with the total number of protons in the expected triple decker.

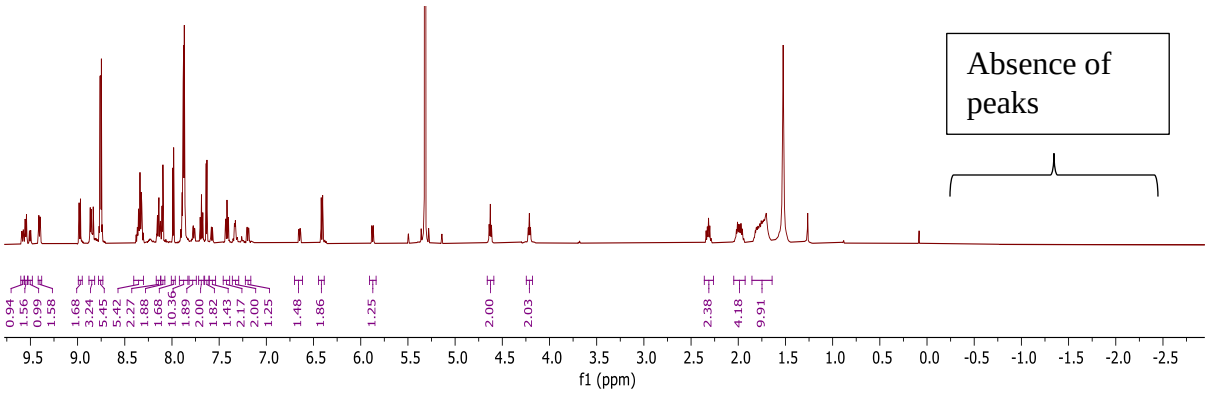

Figure 2.37: ^{1}H-NMR spectrum of heteroleptic triple decker (assumed to be **2.41**) (500 MHz, CD_2Cl_2, 25 °C).

2.15.3 Stability of the La-TD formed from 2.36+Pc

The stability of the heteroleptic triple decker (assumed to be **2.41**) in solution was investigated by monitoring an NMR solution (DCM) over 12 days (figure 2.38). Clearly, the aromatic proton signals did not alter after 12 days, indicating that the heteroleptic triple decker is stable when isolated.

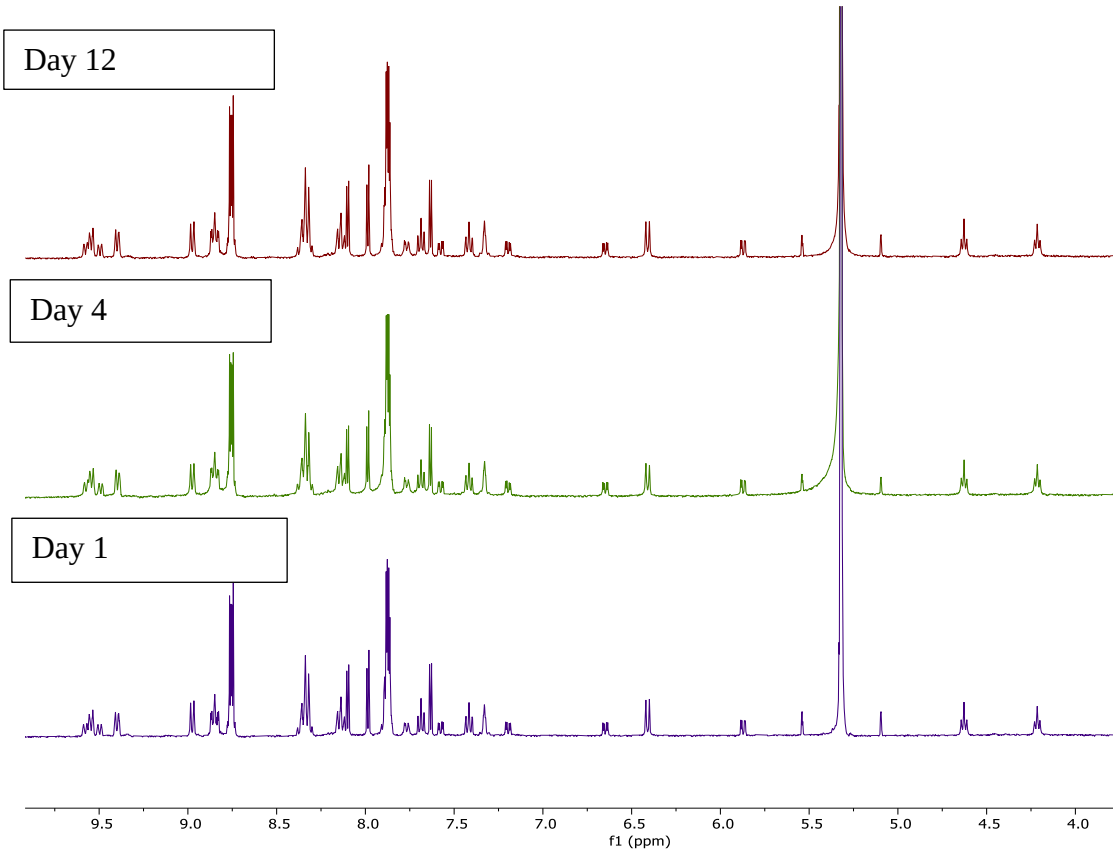

Figure 2.38: Stacked ^{1}H-NMR spectra of La-TD (assumed to be **2.41**) over 12 days (500 MHz, CD_2Cl_2, 25 °C), showing no discernable change.

2.15.4 Attempts to increase the yield of La-TD from 2.36+Pc

To determine whether the quality of the octanol affected the outcome of the reaction, a small-scale approach for the 'one pot' reaction was carried out with both normal octanol and freshly distilled octanol. The distilled octanol was obtained by drying over sodium metal. Both reactions were carefully monitored by TLC. After 24 hours, TLC analysis and MALDI-TOF MS of both reactions showed the presence of the triple decker. The reactions were stopped, and the solvent was distilled off. A mixture of DCM: MeOH was added to each of the reaction vessels and the mixtures left to precipitate overnight. The isolation and purification were carried out separately by using the same solvent system as mentioned in the previous section. The yields were identical in both reactions (8%). Clearly the nature of the octanol does not affect the outcome of the experiment.

To investigate the effect of temperature on the formation of the triple decker, the unsymmetrical dyad **2.36**, Pc **2.40** and the metal salt were all mixed (in the same ratio as above) in distilled

octanol at a temperature of 170 °C. After 24 hours, the mixture was analysed by TLC and MALDI-TOF MS indicated the presence of La-TD (assumed to be **2.41**), by-products and together with some starting material. The reaction was repeated at 195 °C and refluxed for 24 hours. Analysis by MALDI-TOF MS showed the presence of the triple decker and the various by-products as mentioned in the previous section. No starting material was detected. The La-TD (assumed to be **2.41**) was isolated and purified by column chromatography by using the solvent system as mentioned in the previous section. At 170 °C, only trace amount of the La-TD (assumed to be **2.41**) was obtained compared to 8% at 195 °C. This clearly shows that the formation of the heteroleptic triple decker is dependent on temperature of the reaction mixture.[10,17]

In an attempt to increase the yield of the product, a stepwise method was adopted. A mixture of the unsymmetrical dyad (1 equivalent) **2.36** and the phthalocyanine (1 equivalent) **2.40** in octanol was refluxed at 200 °C for 24 hours so as to increase the solubility of Pc **2.40**. This was followed by the addition of 2 equivalents of the lanthanum (III) acetylacetonate and the mixture was further refluxed for 18 hours (scheme 2.32).[18] The reaction was carried out using varying amounts of octanol (varying concentration) with no noticeable change in the yield (8%). The above method was repeated except that the starting materials were heated at 200°C for 48 hours with no significant change in the yield (7%).

2.15.5 Characterisation of the isolated La-TD from 2.36+Pc.

Assuming that the La-TD is structure **2.41**, the Pc **2.40** is sandwiched between the TPP and TPTAP units, part of the "sandwich" should structurally be similar to La-TPP TD **2.2** as shown in figure 2.39. The arrangement of the units in La-TPP TD **2.2** is as follows Por-Pc-Por,[3] therefore in La-TD **2.41** the arrangement of the units should be Por-Pc-TBTAP. It is of course expected that the overall ^{1}H-NMR spectra of La-TDs like **2.41** will be more complex than that of La-TPP TD **2.2** due to their lack of symmetry.

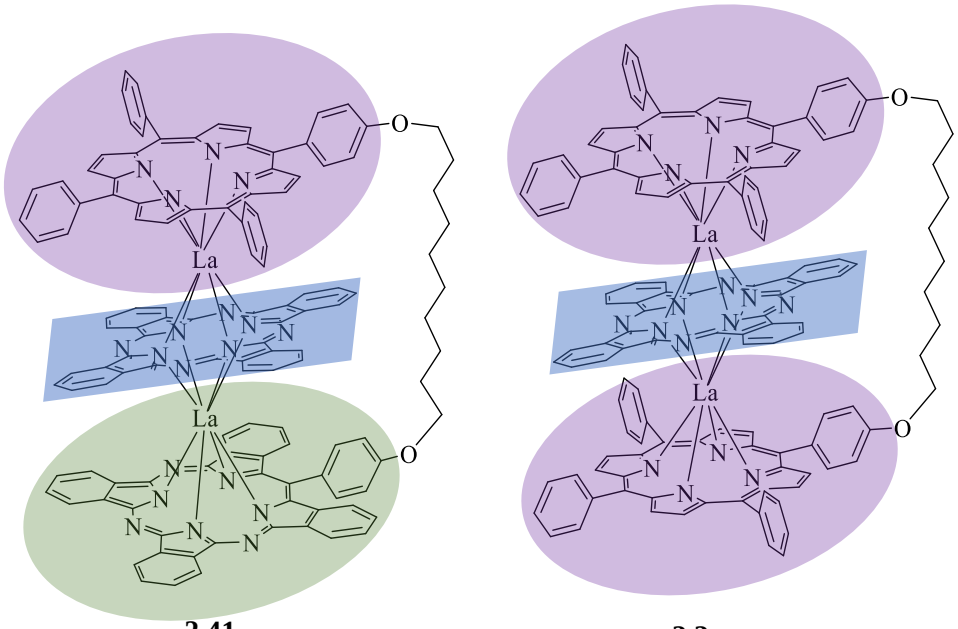

Figure 2.39: Comparaison between the structures of La-TD (assumed to be **2.41**) and La-TPP TD **2.2**.

The ^{1}H-NMR spectrum of the La-TD (assumed to be **2.41**) can therefore be compared to that of La-TPP TD **2.2**.

2.15.6 Comparison between the ^{1}H-NMR spectrum of La-TD (assumed to be 2.41) and La-TPP TD 2.2

Attempts to crystallise the La-TD (assumed to be **2.41**) were unfortunately unsuccessful, therefore the ^{1}H-NMR spectrum is the only reliable tool to confirm whether the orientation of the units in La-TD (assumed to be **2.41**) is similar to La-TPP TD **2.2**. Interpretation of the ^{1}H-NMR spectrum of La-TD (assumed to be **2.41**) proved to be challenging. The ^{1}H-NMR spectra of triple decker La-TD (assumed to be **2.41**) and La-TPP TD **2.2** were stacked together as shown in the figure 2.40. If the arrangements of the units are as in figure 2.39 (compound **2.41**), the Por unit 'sees' the Pc unit and therefore the proton signals on the Por unit should remain essentially unchanged compared to the proton signals of the Por unit in La-TPP TD **2.2**. Clearly there are huge differences in terms of the proton signals. In the ^{1}H-NMR spectrum of La-TPP TD **2.2**, the protons on the pyrrole unit (*H*-Pyrr) of Por unit are located at 7.31 ppm and 7.25 ppm. While the *H*-Pyrr in the La-TD (assumed to be **2.41**) are split and are more downfield compared to the latter and are positioned at 8.10, 7.97, 7.88 and 7.63 ppm. In the ^{1}H-NMR

spectrum of La-TD (assumed to be **2.41**), the protons signals corresponding to the Pc ring are shifted and resonate at 8.75 ppm and 7.87 ppm corresponding to *H*-Pc_1 and *H*-Pc_2 respectively. This indicates that the Pc in the La-TD (assumed to be **2.41**) is not sandwiched between Por and TBTAP units, therefore it exists as in a different isomeric form. The possible arrangement of the units is shown figure 2.41, (triple deckers **2.42** or **2.43**).

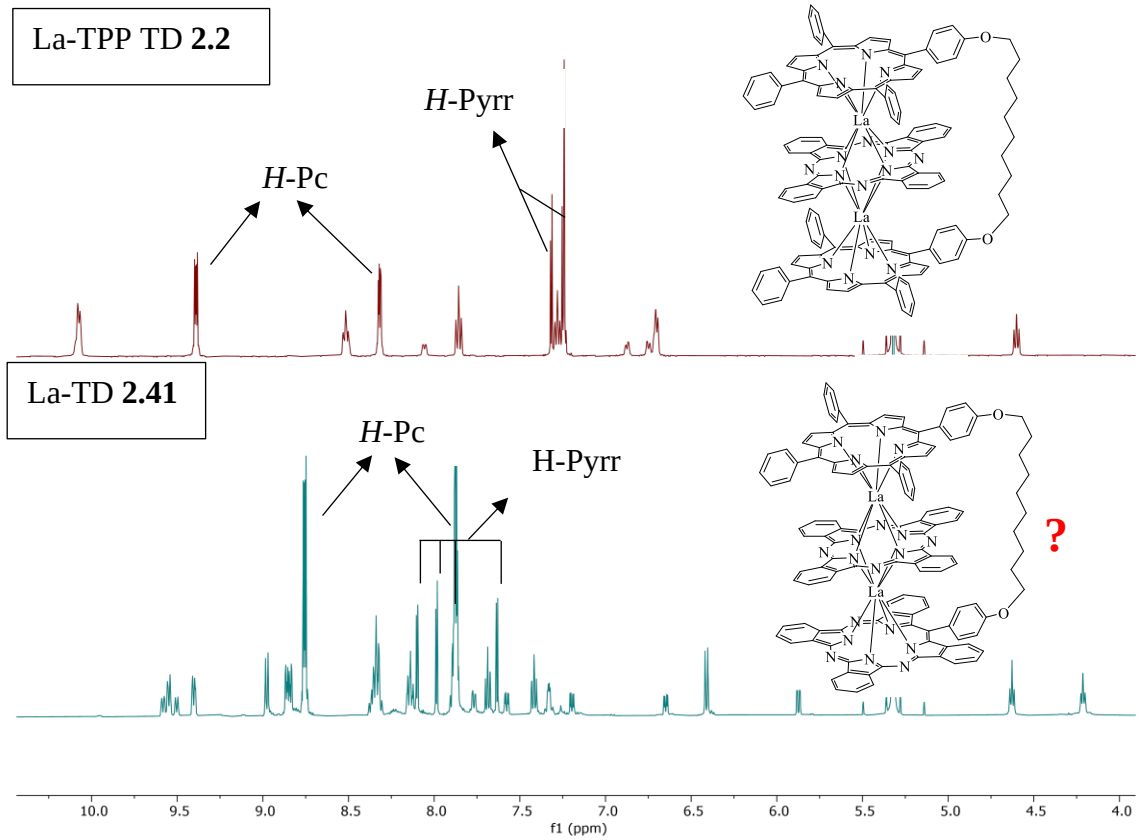

Figure 2.40: Stacked ^{1}H-NMR spectra of La-TD (assumed to be **2.41**) and La-TPP TD **2.2** (500 MHz, CD_2Cl_2, 25 °C).

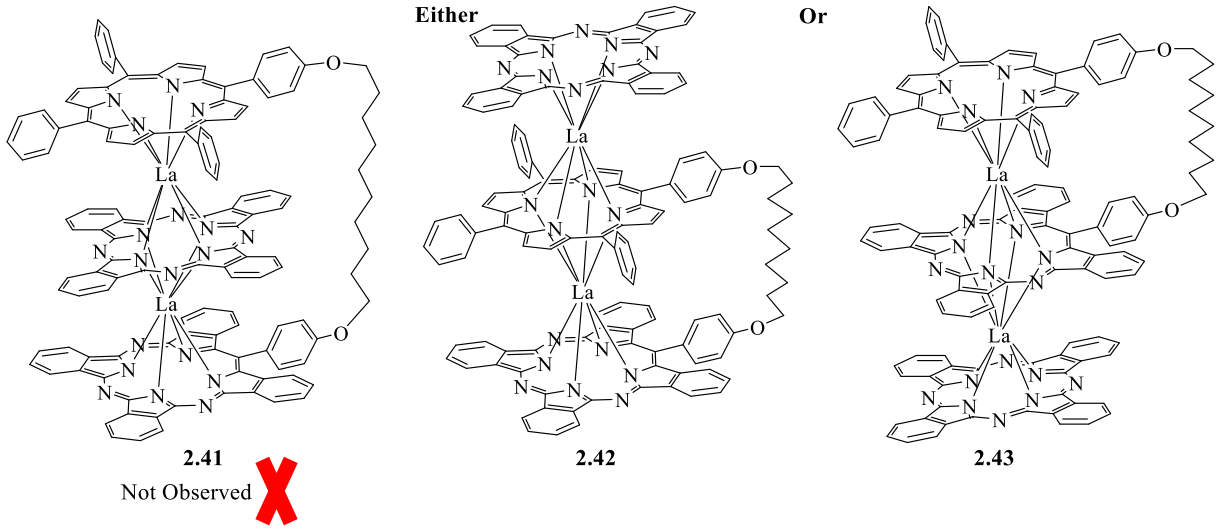

Figure 2.41: Plausible structures for the heteroleptic triple decker.

From the ^{1}H-NMR spectrum of the bis-triple decker **2.7** (figure 2.42) with lanthanum it was found that the Pc is situated above and below the Por unit.[3] The chemical shifts of the Pc protons in the bis-triple decker (8.82 ppm and 7.76 ppm) are closely related to the Pc protons expected in La-TD **2.42** (8.75 ppm and 7.87 ppm), suggesting La-TD **2.42** is the isomer isolated

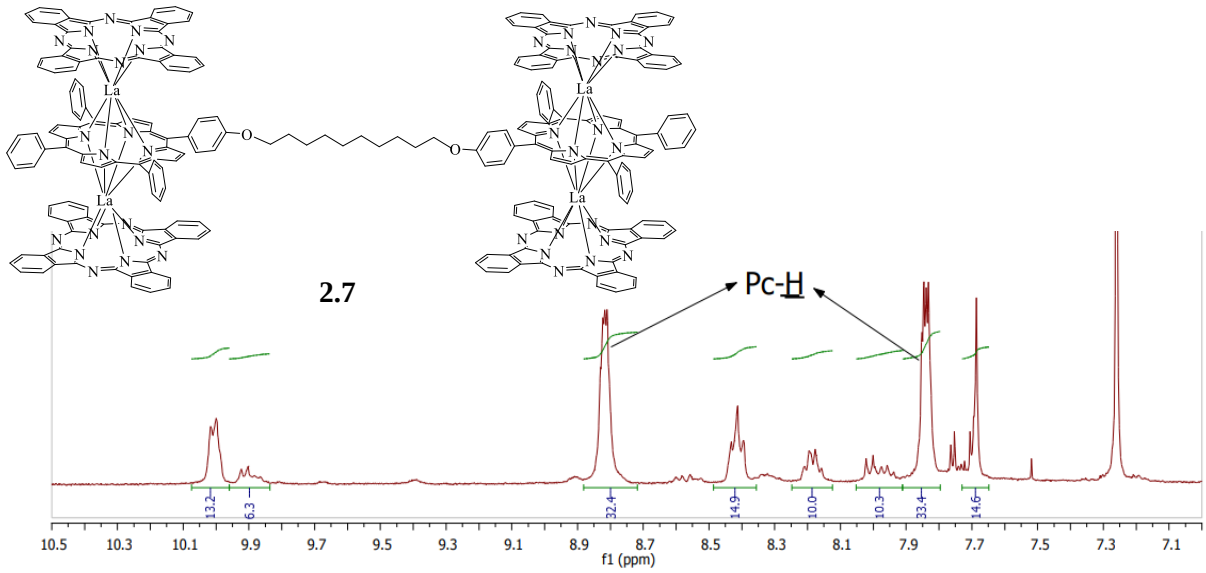

Figure 2.42: ^{1}H-NMR spectrum of bis-triple decker **2.7** (400 MHz, $CDCl_3$, 25 °C).[3]

2.15.7 Comparison between the UV-Vis spectrum of La-TD 2.42 and La-TPP TD 2.2

The UV-Vis spectra of the La-TD **2.42** and La-TPP TD **2.2** are reported in figure 2.43. There are some significant changes in the absorption bands. This can be an indication that the orientation of the units in La-TD **2.42** is not similar to La-TPP TD **2.2**. The La-TPP TD **2.2** shows a sharp absorption at the porphyrin region of 421 nm as well as a broad absorption at 300 nm typical of sandwich-like complexes in the UV-Vis spectroscopy and there was no absorption in the phthalocyanine region between 600 and 700 nm.[10] However, in the La-TD **2.42** the strong, sharp peak in the porphyrin region is not dominant, giving a further good indication that the porphyrin is not located on the outside of the sandwich complex. In addition, the UV-Vis spectral features of the TBTAP component, suggest that the TBTAP unit is on the outside of the TD, again consistent with structure **2.42**.

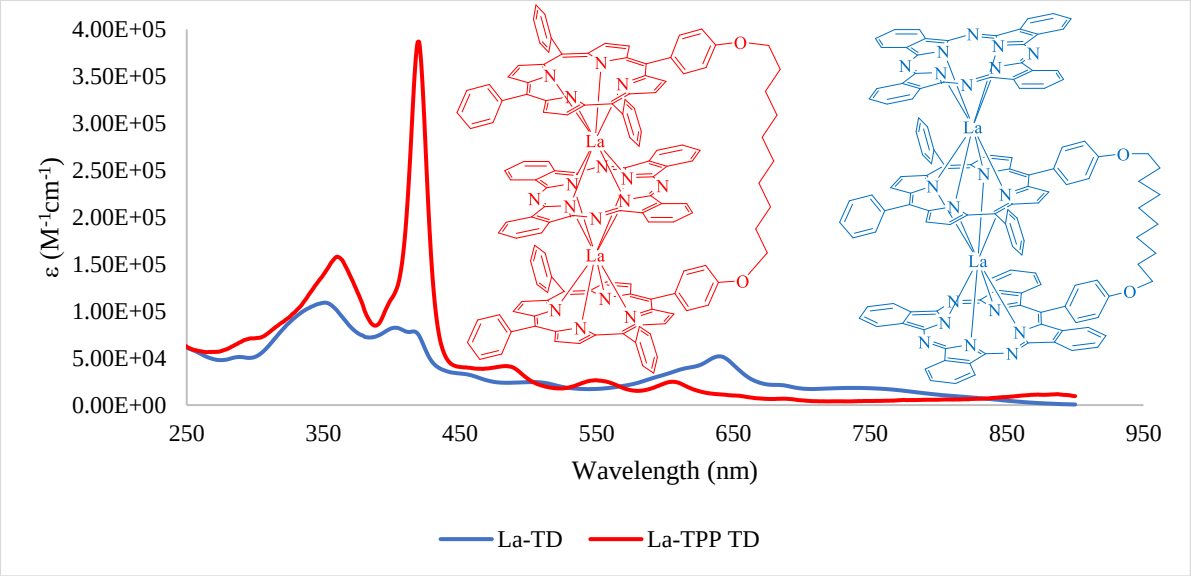

Figure 2.43: The UV-Vis spectra of the La-TD **2.42** and La-TPP TD **2.2** (in DCM).

2.15.8 Synthesis of La triple decker using TPP-TBTAP dyad 2.37

Before a full analysis of ^{1}H-NMR of La-TD **2.42** was conducted, the TD using the unsymmetrical C_{12} dyad **2.37** was synthesised (section 2.14.8) and its ^{1}H-NMR spectra compared to the ^{1}H-NMR spectra of La-TD **2.42**. The heteroleptic triple decker (La-TD **2.44**) using the unsymmetrical dyad **2.37** was successfully synthesised using the 'one-pot' fashion as shown in the scheme 2.33.

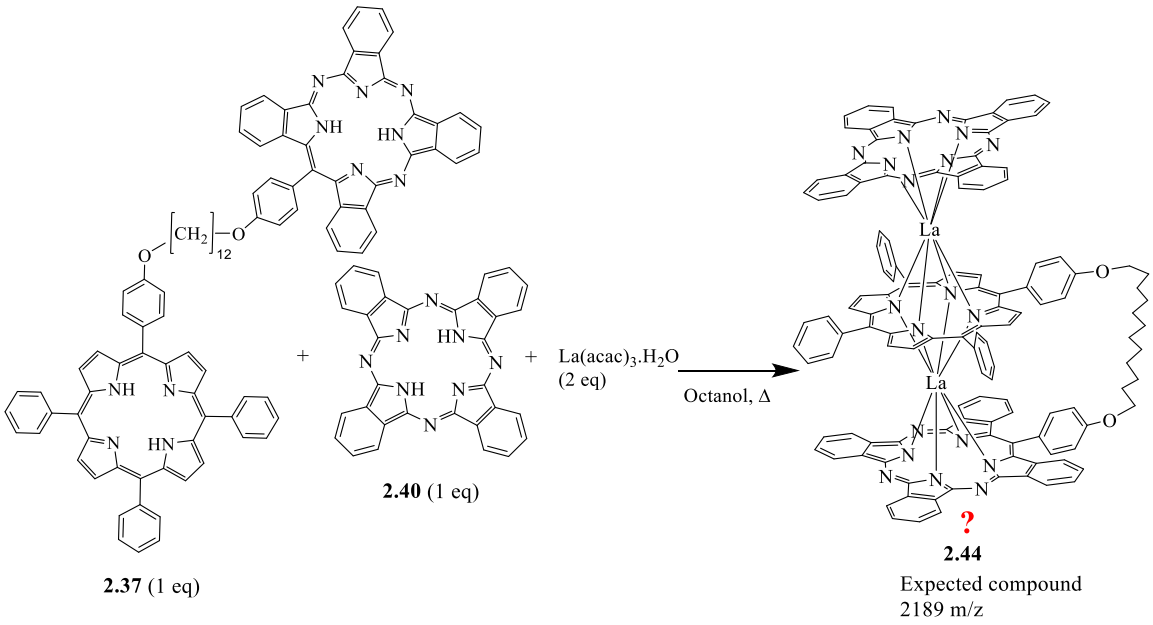

Scheme 2.33: Synthesis of heteroleptic La-TD **2.44** by using 'one-pot' method.

All the starting materials were mixed in octanol and refluxed overnight. Isolation and purification of the desired complex was achieved by following the same procedure as for the La-TD **2.42**. The crude mixture was analysed by MALDI-TOF MS (figure 2.44 **a**). The peaks at m/z 1538, 2189, 3077 and 515 correspond to a bridged double decker, a TD, a bis double decker and unreacted Pc.

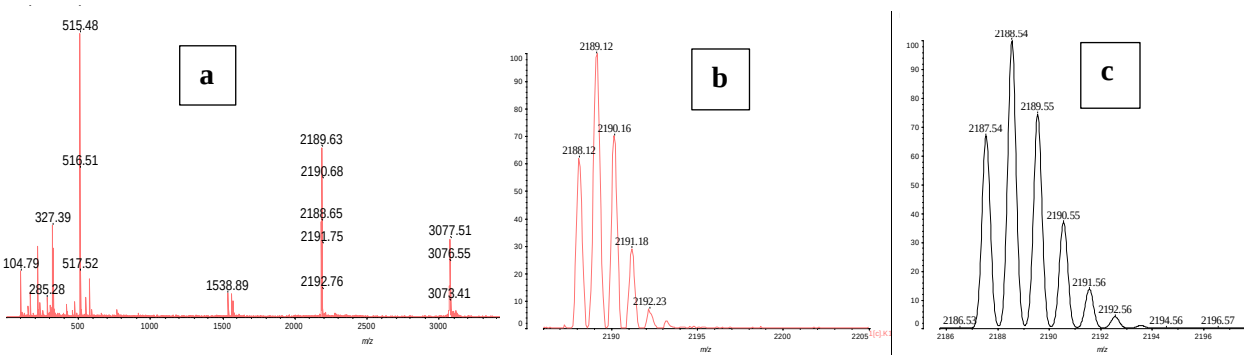

Figure 2.44: MALDI-TOF MS analysis of (**a**) reaction mixture, (**b**) pure La-TD **2.44** and (**c**) theoretical prediction.

2.15.9 The ^{1}H-NMR characterization of bridged triple decker 2.44 complex

The ^{1}H-NMR spectrum of the La-TD **2.44** is shown in figure 2.45 and again proved to be complex as expected. However, overall, it was considered a better spectrum in terms of clarity and peak separation.

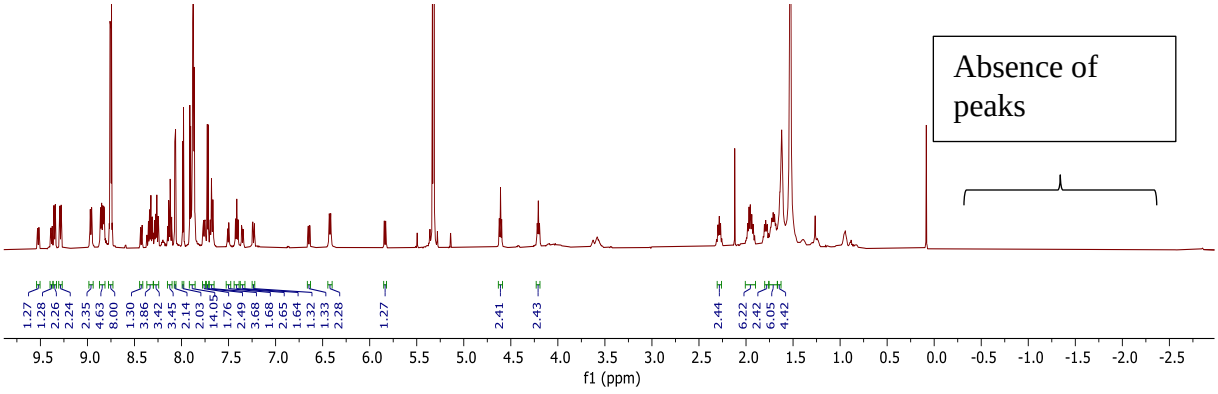

Figure 2.45: ^{1}H-NMR spectrum of La-TD **2.44** (500 MHz, CD_2Cl_2, 25 °C).

The ^{1}H-NMR spectra of both La-TD **2.42** and La-TD **2.44** were stacked together and the expansion of the aromatic region is reproduced in figure 2.46. The most noticeable differences between both spectra are as follows:

- The peak at 7.33 ppm in La-TD **2.42** which integrates to 2 protons is spread out in La-TD **2.44** at 7.34 ppm and 7.49 ppm with both having an integration of 1 proton each respectively.
- The set of peaks at 7.5 ppm- 7.8 ppm in La-TD **2.44** is separated and shifted in La-TD **2.42**.
- Both complexes show a peak at 7.86 ppm although in the case of the La-TD **2.44** the multiplet is clearly separated.
- Another stark difference is the multiplet peak at around 8.35 ppm is split into two sets of multiplets in the La-TD **2.44**.
- The set of peaks in the La-TD **2.42** from 9.59- 9.38 ppm which integrates as follows, 1: 2: 1: 2 is in contrast with the peaks at around 9.54- 9.27 ppm in La-TD **2.44** which integrates to 1: 1: 2: 1.
- The proton signals on the Pc units in both La-TD **2.42** and La-TD **2.44** are identical and resonate at 8.75 ppm and 7.86 ppm.

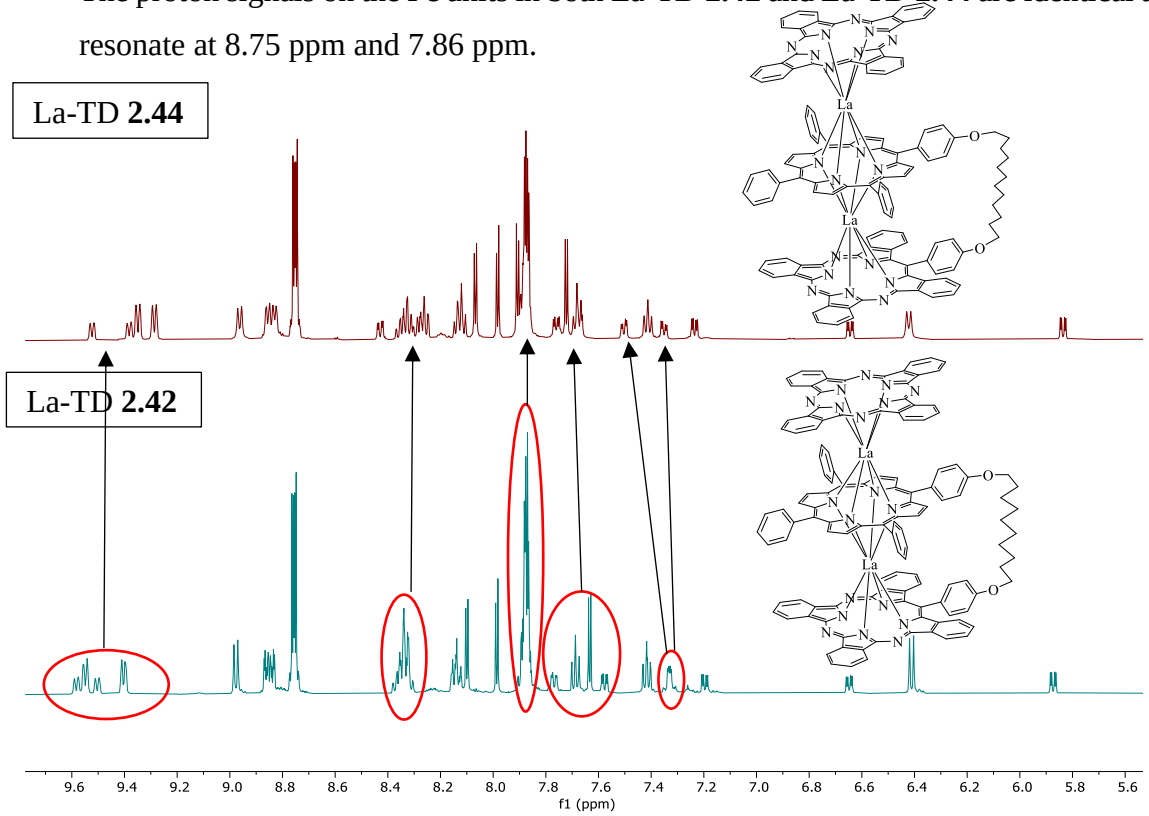

Figure 2.46: Stacked ^{1}H-NMR spectra of La-TD **2.42** and La-TD **2.44** (500 MHz, CD_2Cl_2, 25 °C).

The peaks in the ^{1}H-NMR spectrum of the La-TD **2.44** are more spread out compared to La-TD **2.42**, therefore further NMR analysis such as COSY (figure 2.48) and NOESY (figure 2.47) were conducted on this compound in order to try to identify key signals and interactions to

provide further evidence for the proposed structure. If the orientations of the units were as follows Por-Pc-TBTAP, i.e. the Pc in the middle of the TD, a correlation between the protons of the Pc unit and some on the bridging alkyl chain in the NOESY NMR spectrum would be expected. However, NOESY NMR could not detect such correlation, indicating that the Pc unit is not sandwiched between Por and TBTAP. From NOESY NMR spectrum (figure 2.47), there are correlations that can only correspond to the interactions between "inner" protons on each of the bridging *meso*-phenyl units of the Por unit and the TBTAP unit. This observation confirms our earlier assumption that the Por and TBTAP units are next to each other in the TD.

Based on the integration, the two peaks at 8.74 and 7.86 ppm correspond to the protons on the phthalocyanine ring. The porphyrin β-protons appear as doublet at around 8.06, 7.98, 7.90 and 7.72 ppm with coupling constant (J = 4.0 Hz) integrating 8. The highly deshielded proton at 8.96 ppm coupled with the proton at around 7.67 ppm, which both integrate to 2 protons, and are present on the TBTAP unit. The proton at around 6.41 ppm which face towards the methoxy phenyl ring of the TBTAP moiety and the proton at 7.41 ppm coupled with each other, both integrating to 2. The two protons on the methoxy phenyl ring of the TBTAP molecule which are closer to the oxygen both integrate to 1 and are positioned at 7.75 ppm and 5.81 ppm respectively. The interpretation is further confirmed by COSY NMR as depicted in figure 2.49. It is most likely that units are as follows Pc-Por-TBTAP. However, X-ray analysis would be the most conclusive.

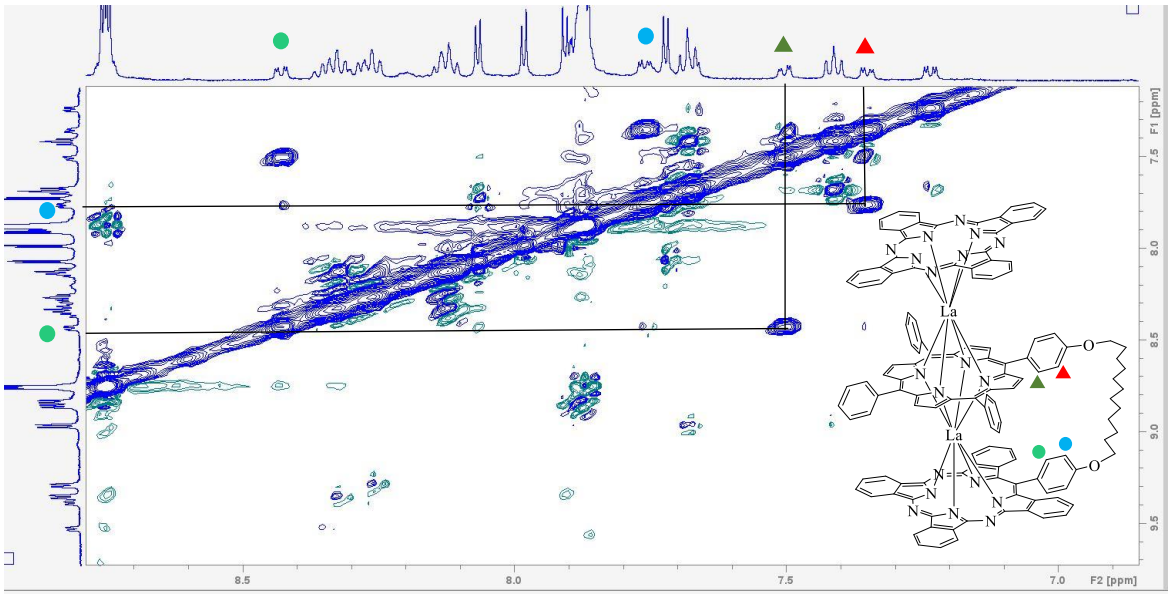

Figure 2.47: NOESY experiment showing cross peaks in La-TD **2.44** (500 MHz, CD_2Cl_2, 25 °C).

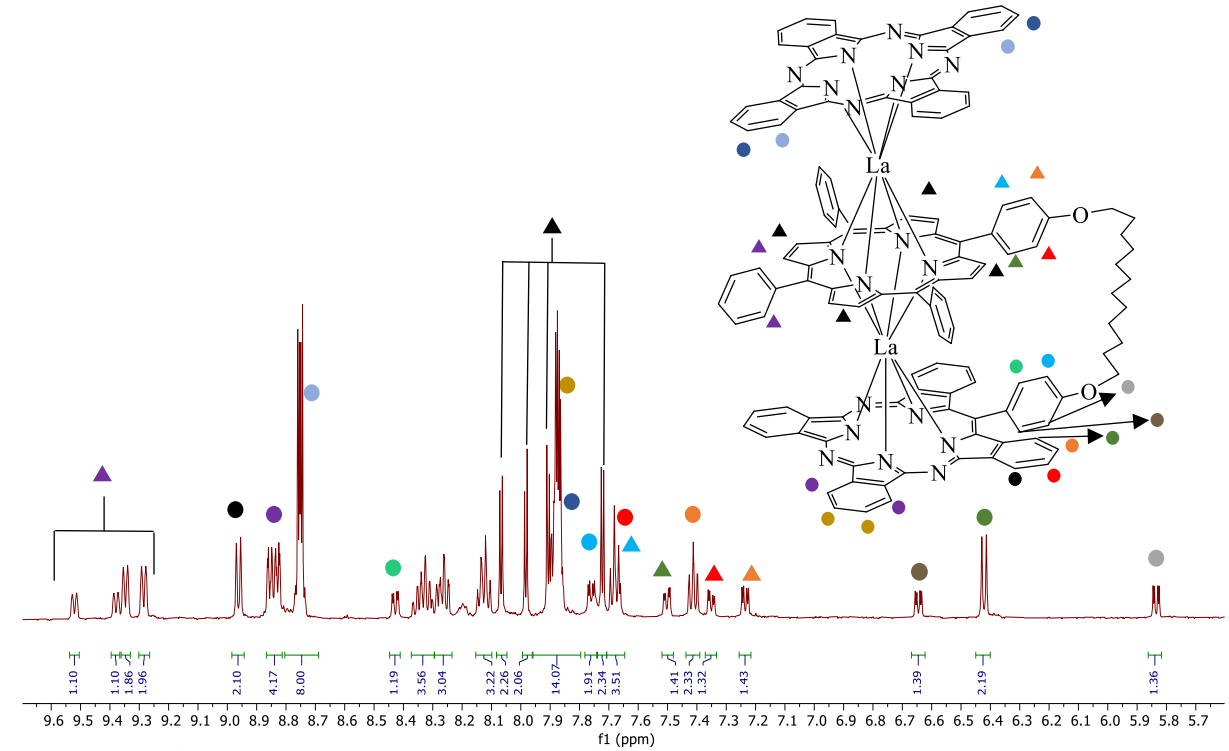

Figure 2.48: ^{1}H-NMR spectrum of heteroleptic La-TD **2.44** (500 MHz, CD_2Cl_2, 25 °C).

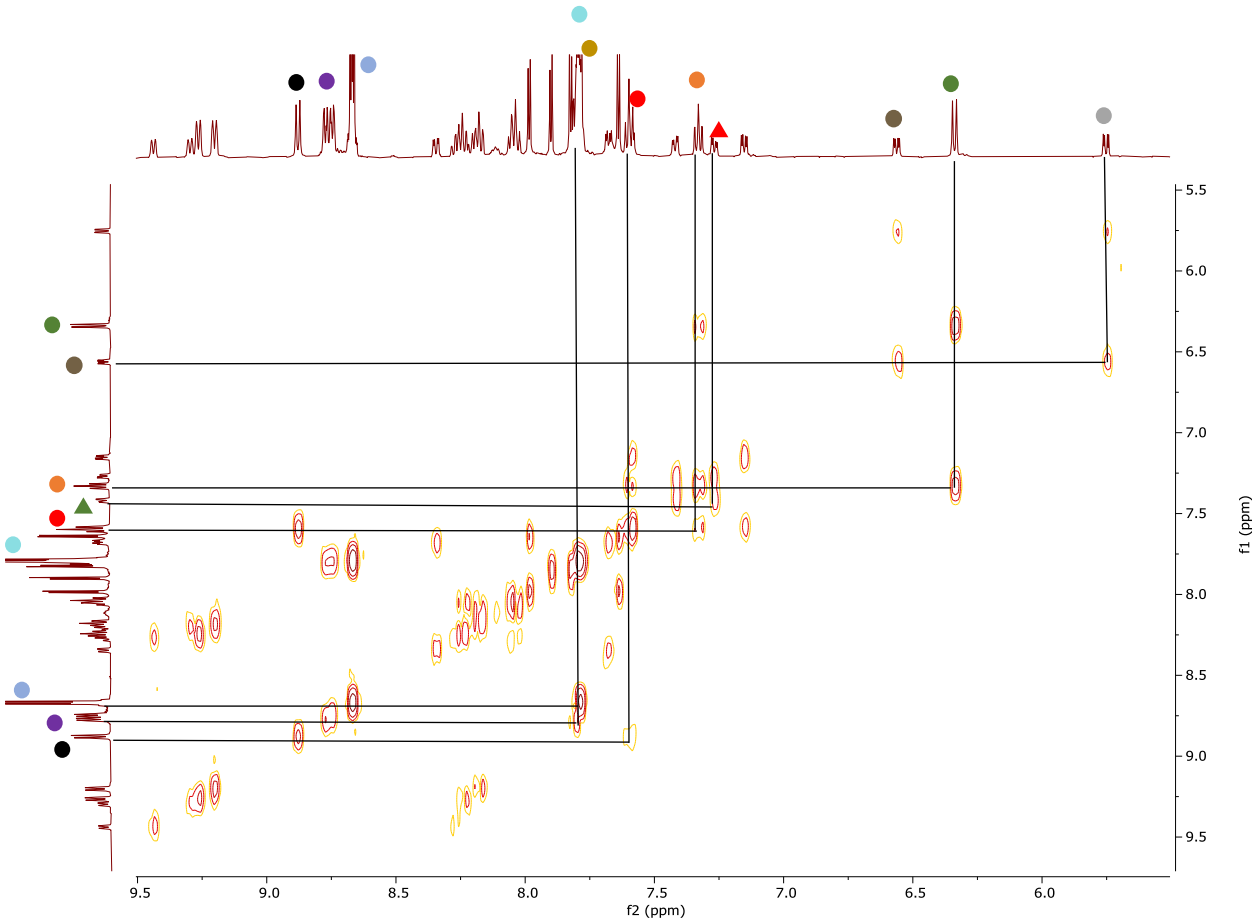

Figure 2.49: COSY NMR experiment showing cross peaks in La-TD **2.44** (500 MHz, CD_2Cl_2, 25 °C).

In the following sections, other TDs using different lanthanide metals such as Nd and Eu will be synthesised. Metals with very small ionic radii (from Tb to Lu) will not be used. Previous attempts to synthesise TD using the TPP dyad, and small ions such as Tb (92 pm), Dy (91 pm) and Yb (87 pm) were unsuccessful. The smaller the size of M^{3+} ions, the greater is the strain introduced into the chain making the macrocycles more unstable.[3] The chain prevents rotation, so *meso*-phenyls on adjacent macrocycles are forced closer together.

2.16 Synthesis of bridged Neodymium triple decker

2.16.1 Synthesis of the Nd triple decker using TPP-TBTAP dyad 2.36

The sandwich complex of neodymium (Nd) was synthesised and investigated. The heteroleptic triple decker Nd-TD, presumed to be **2.45**, was synthesised using the 'one-pot' procedure as shown in scheme 2.34. All the starting materials are mixed in refluxing octanol.

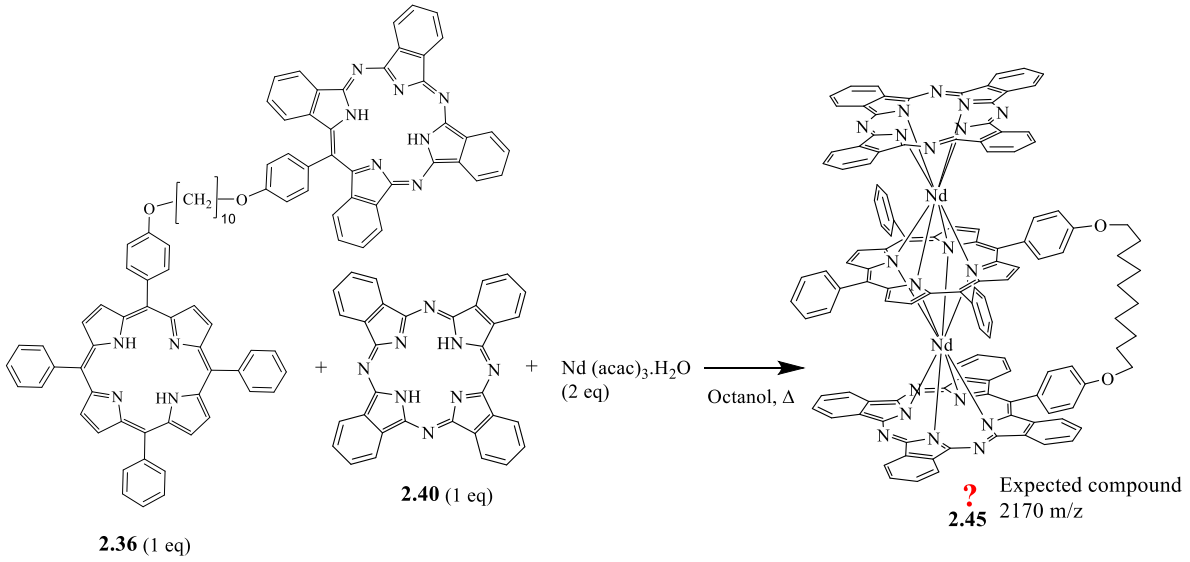

Scheme 2.34: Synthesis of Nd-TD presumed to be **2.45** using unsymmetrical dyad **2.36**.

After 24 hours TLC analysis resulted in 5 spots, a reddish-brown spot, a green spot, a grey green spot, a dark green spot and a spot on the baseline (whereas the La-TD **2.42** reaction only gave four spots). The reaction was continuously monitored using MALDI-TOF MS and peaks at 3034, 2170, 1512, 514 m/z were recorded corresponding to a bis double decker, a TD, a bridged double decker and unreacted Pc. At the end of the reaction, the solvent was distilled off, the crude compound was washed thoroughly with methanol and purified as described for La-TD **2.42**. Column chromatography of the compound was performed, and the different fractions were analysed by MALDI-TOF MS. It was found that two of the fractions had the

same m/z of 2170 corresponding to Nd triple decker (figure 2.50), one of which was green and the other one was grey green in colour, clearly indicating the presence of isomers which was not expected. After recrystallisation, the yield for the grey green (Nd-TD-G.G) **2.45** and green (Nd-TD-G) **2.46** fractions were 10% and 12% respectively.

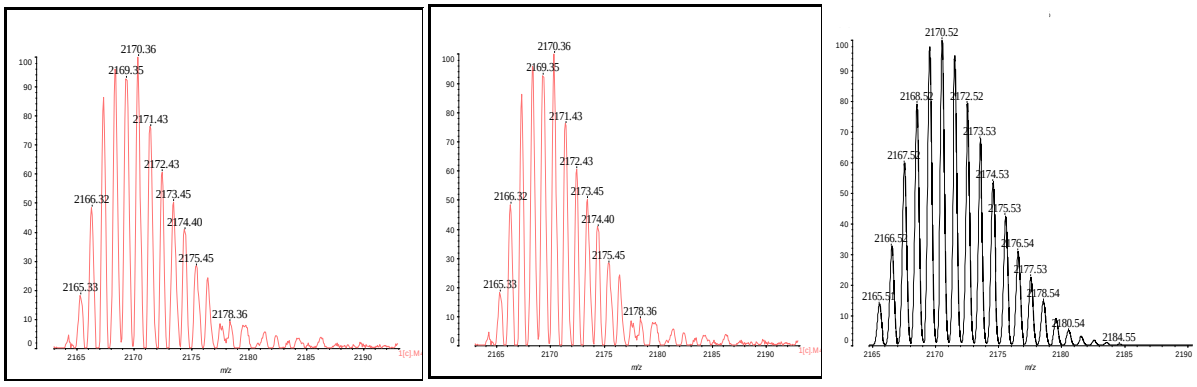

Green (Nd-TD-G.G) **2.45** Grey-green (Nd-TD-G) **2.46** Theoretical prediction.

Figure 2.50: MALDI-TOF MS spectra of complex **2.45** and **2.46** with its theoretical prediction.

The Nd-TD was then synthesised by the stepwise procedure and the reaction was constantly monitored. The starting materials, the unsymmetrical dyad **2.36** and Pc **2.40** were pre-mixed followed by the addition of metal salt, Nd $(acac)_3.H_2O$. The synthesis was repeated using different volumes of octanol (varying concentration) and reactions times. After 6 h, a TLC analysis of the reaction mixture confirmed the presence of the isomers however, the starting materials were still present and therefore the reaction was left to stir for longer. After isolation and purification, the results were identical to the ones from the 'one-pot' preparation.

2.16.2 Comparison between the UV-Vis spectra of Nd-TD-G.G 2.45, Nd-TPP TD 2.4 and Nd-TD-G 2.46

In the previous section, the UV-Vis spectrum of La-TD **2.42** indicates that the units are not in the orientation of Por-Pc-TBTAP. Therefore, the UV-Vis spectra of the Nd-TD-G.G **2.45**, Nd-TD-G **2.46** and with the known Nd-TPP TD **2.4** were compared as shown in figure 2.51. By comparing the three spectra, Nd-TD-G **2.46** has absorption bands that are related to the Nd-TPP TD **2.4** (from 250–450 nm). Clearly, this shows that the orientation of the units in the Nd-TD-G **2.46** are similar to the Nd-TPP TD **2.4**, that is Por-Pc-TBTAP. In addition, the shape of the bands are consistent with the results obtained by Birin and co-workers for a Por-Pc-Por complex.[17] In Nd-TD-G.G **2.45** the absorption bands are comparable to the La-TD **2.42**, clearly indicating that the orientation of the units in Nd-TD-G.G **2.45** is also Pc-Por-TBTAP. The Pc Soret bands for the Nd-TD-G.G **2.45** and Nd-TD-G **2.46** are at 348 and 351 nm respectively.[18]

They are shifted slightly to the blue as compared to the Nd-TPP TD **2.4** which is at 359 nm. The Q bands (600 – 700 nm) in all the three complexes are all red-shifted.

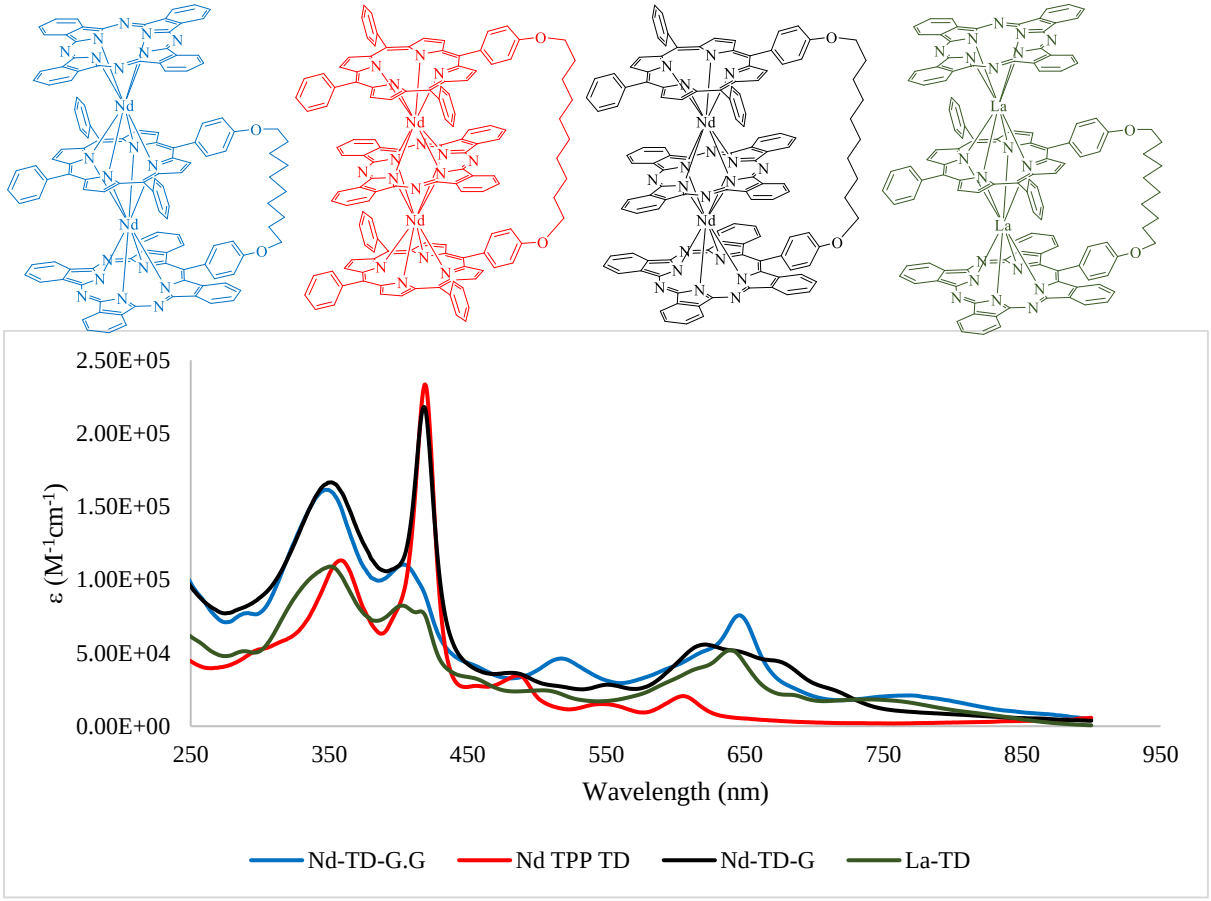

Figure 2.51: The UV-Vis spectra of the Nd-TD-G.G **2.45**, Nd-TPP TD **2.4**, Nd-TD-G **2.46** and La-TD **2.42** (in DCM).

2.16.3 ^{1}H-NMR comparison between Nd-TD-G.G 2.45, Nd-TD-G 2.46 and Nd-TPP TD 2.4

The ^{1}H-NMR spectra of Nd-TD-G.G **2.45** and Nd-TD-G **2.46** were compared with previously reported spectra of heteroleptic complex of Nd-TPP TD[3] **2.4** as shown in the figure 2.52, and give some further indications as to the location of the phthalocyanine unit in the two isomeric complexes. The phthalocyanine peaks in the symmetrical Nd-TPP TD **2.4** appear more upfield at 5.28 ppm and 4.26 ppm compared to the phthalocyanine peaks in Nd-TD-G.G **2.45** (7.32 ppm and 7.13 ppm). As expected, however, the phthalocyanine peaks in complex Nd-TD-G **2.46** resonate at similar frequencies (5.15 ppm and 3.63 ppm) giving further confidence that the Pc is in the middle of the sandwich.

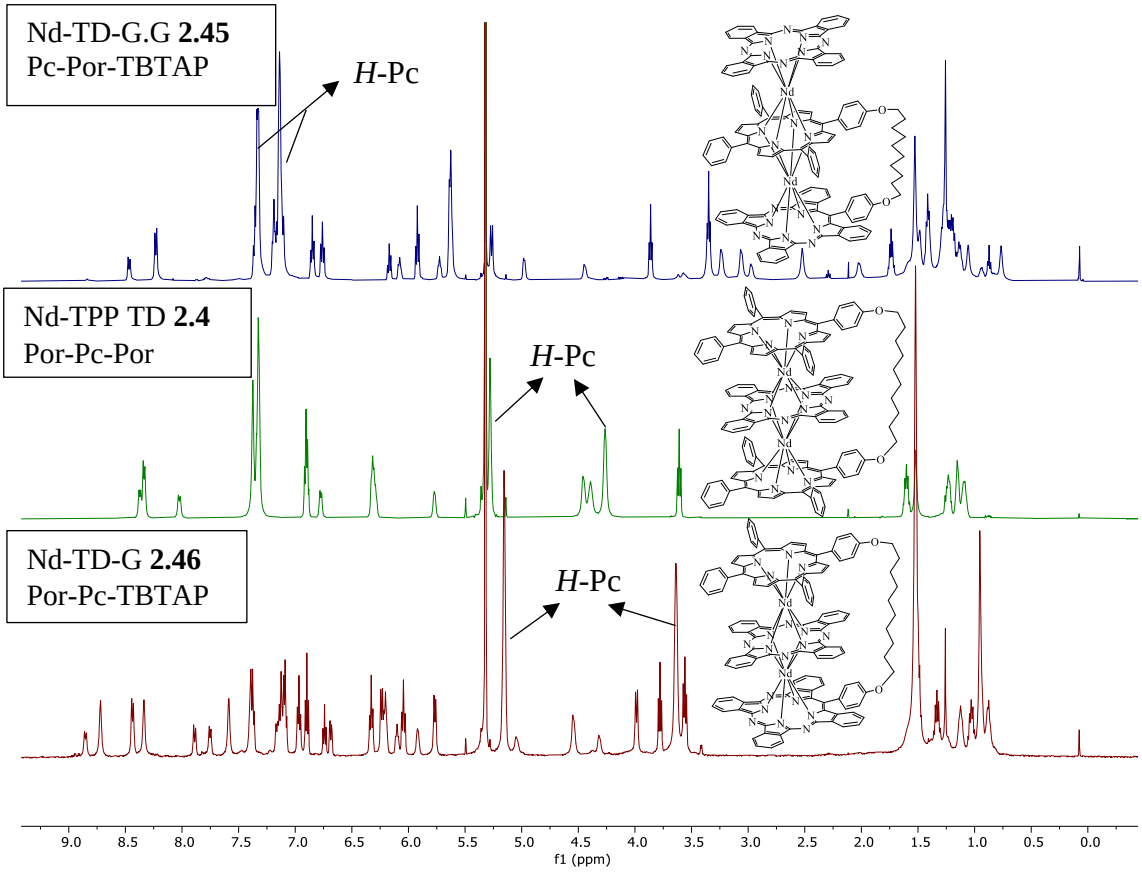

Figure 2.52: Stacked ^{1}H-NMR spectra of Nd-TD-G.G **2.45**, Nd-TPP TD **2.4** and Nd-TD-G **2.46** (500 MHz, CD_2Cl_2, 25 °C).

2.16.4 ^{1}H-NMR characterization of Nd-TD-G 2.46 complex

To further confirm the hypothesis that the Pc unit is sandwiched between the unsymmetrical dyad, a literature search was conducted. Analysis of the ^{1}H-NMR spectrum of the complex shown in figure 2.53, as reported by Birin and co-workers,[17] shows almost identical positioning of the proton on the Pc ring as in the ^{1}H-NMR spectrum of Nd-TD-G **2.46**. The authors reported that the proton on the Pc ring is upfield at around 3.61 ppm. In the Nd-TD-G **2.46**, one of the protons on the Pc ring resonate at around 3.63 ppm.

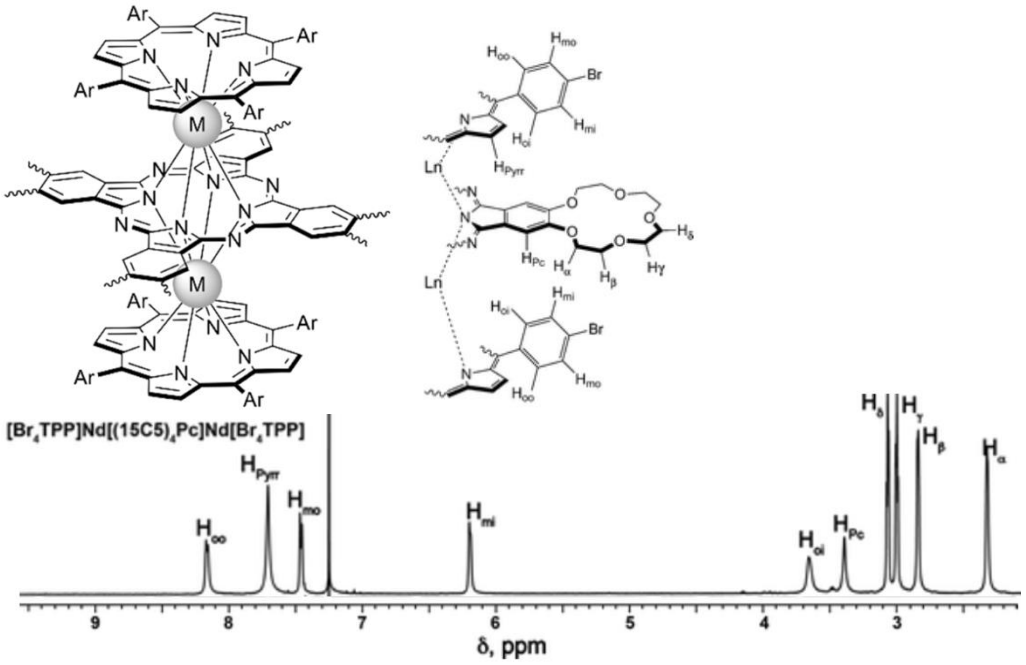

Figure 2.53: The ^{1}H-NMR spectrum of the heteroleptic triple decker in $CDCl_3$ reported by Birin and co-workers.[17]

The interpretation of the ^{1}H-NMR spectrum of Nd-TD-G **2.46** is shown in the figure 2.54. In order to fully interpret the ^{1}H-NMR spectrum, other NMR experiment such as COSY was run.

From the integration, the two singlets at 5.14 and 3.64 ppm corresponds to the protons on the phthalocyanine unit and each integrating to 8. The porphyrin β-protons appear as broad signals at around 8.72, 8.32, 7.58 and 7.38 ppm, integrating to 8. The proton at around 3.96 ppm which is on TBTAP moiety and the proton at 6.03 ppm coupled with each other, both integrating to 2. On the TBTAP molecule, the proton which faces the methoxy phenyl ring resonates at 5.76 ppm. The proton on the methoxy phenyl ring of the TPP unit at 5.90 ppm couples with the proton at 5.04 ppm. The two protons on the methoxy phenyl ring of the TBTAP molecule which are closer to the oxygen both integrate to 1 and are positioned at 7.07 ppm and 6.68 ppm respectively. The proton at 7.88 ppm couples with proton at 6.68 ppm while the proton at 7.74 ppm couples with the proton at 7.07 ppm. The COSY NMR (figure 2.55) experiment further confirmed the positioning of the assigned protons to the molecule.

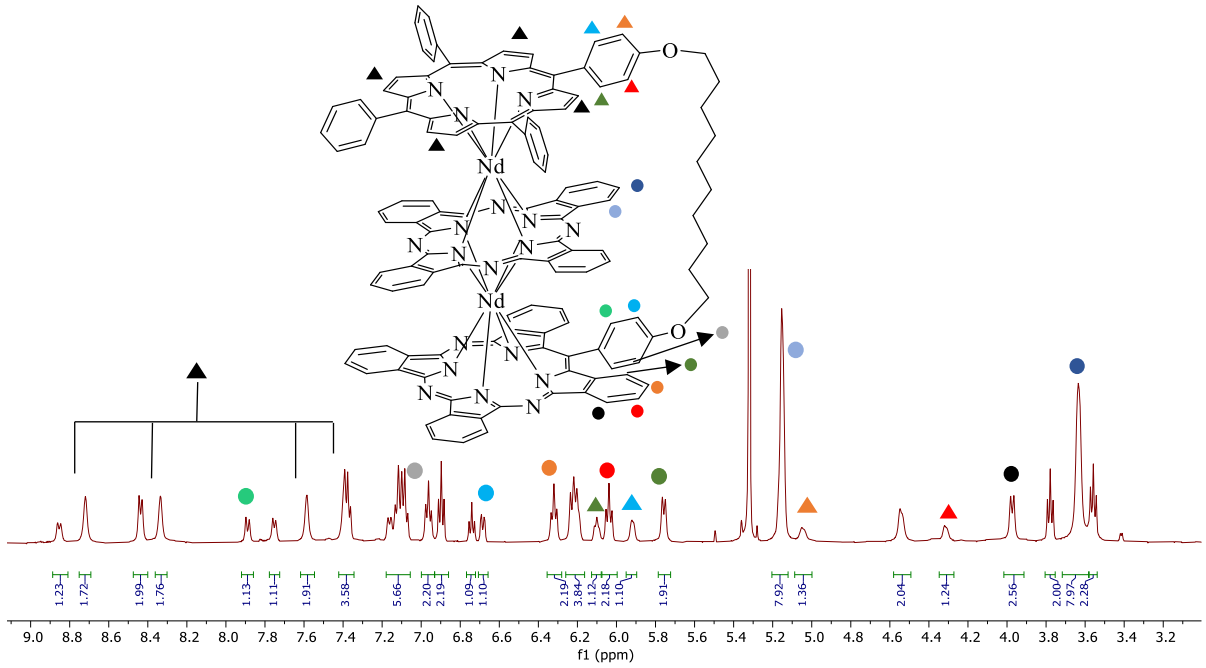

Figure 2.54: ^{1}H-NMR spectrum of Nd-TD-G **2.46** (500 MHz, CD_2Cl_2, 25 °C).

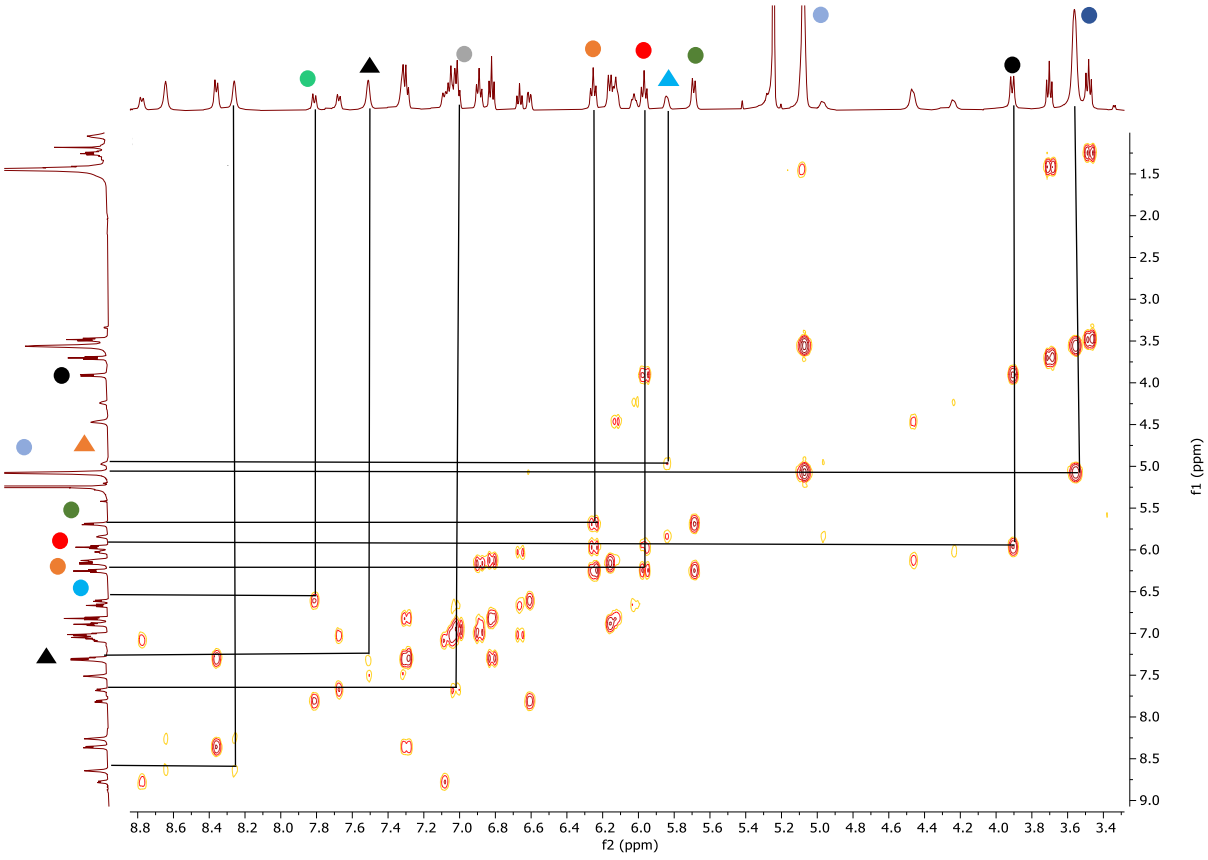

Figure 2.55: COSY NMR experiment showing cross peaks in Nd-TD-G **2.46** (500 MHz, CD_2Cl_2, 25 °C).

2.16.5 ^{1}H-NMR characterization of Nd-TD-G.G 2.45 complex

The ^{1}H-NMR spectrum of Nd-TD-G.G **2.45** is shown in the figure 2.56. Other NMR experiments such as COSY were also run so as to facilitate the analysis.

The two triplets at 3.86 ppm and 3.34 corresponds to the protons on the chain which are next to the oxygen. The proton at around 5.26 ppm appears as a doublet which faced towards the methoxy phenyl ring of the TBTAP moiety and the proton at 6.75 ppm as a triplet coupled with each other, both integrating to 2. This proton further couples to another triplet peak at 6.84 ppm. The latter peak couples to the overlapping peak at 7.12 ppm. The peaks corresponding to the phthalocyanine units couples at 7.32 ppm and 7.13 ppm respectively. The COSY NMR experiment shown in figure 2.57 further confirms the assignments of the peaks.

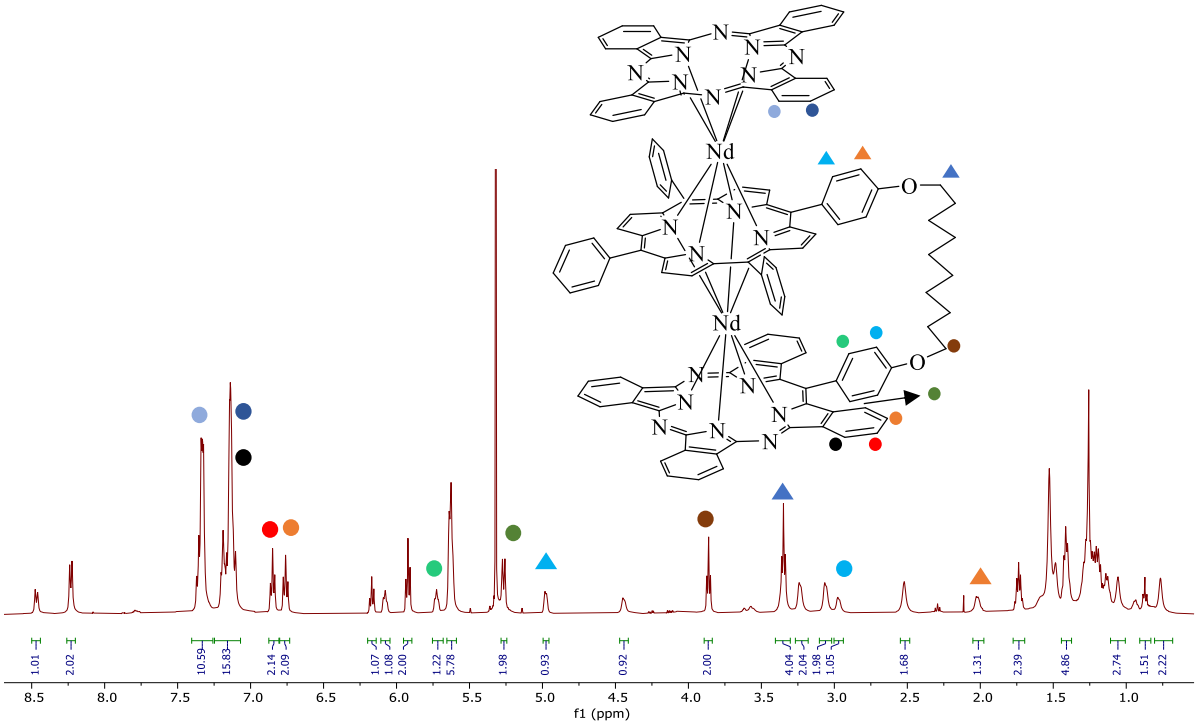

Figure 2.56: ^{1}H-NMR spectrum of Nd-TD-G.G **2.45** (500 MHz, CD_2Cl_2, 25 °C).

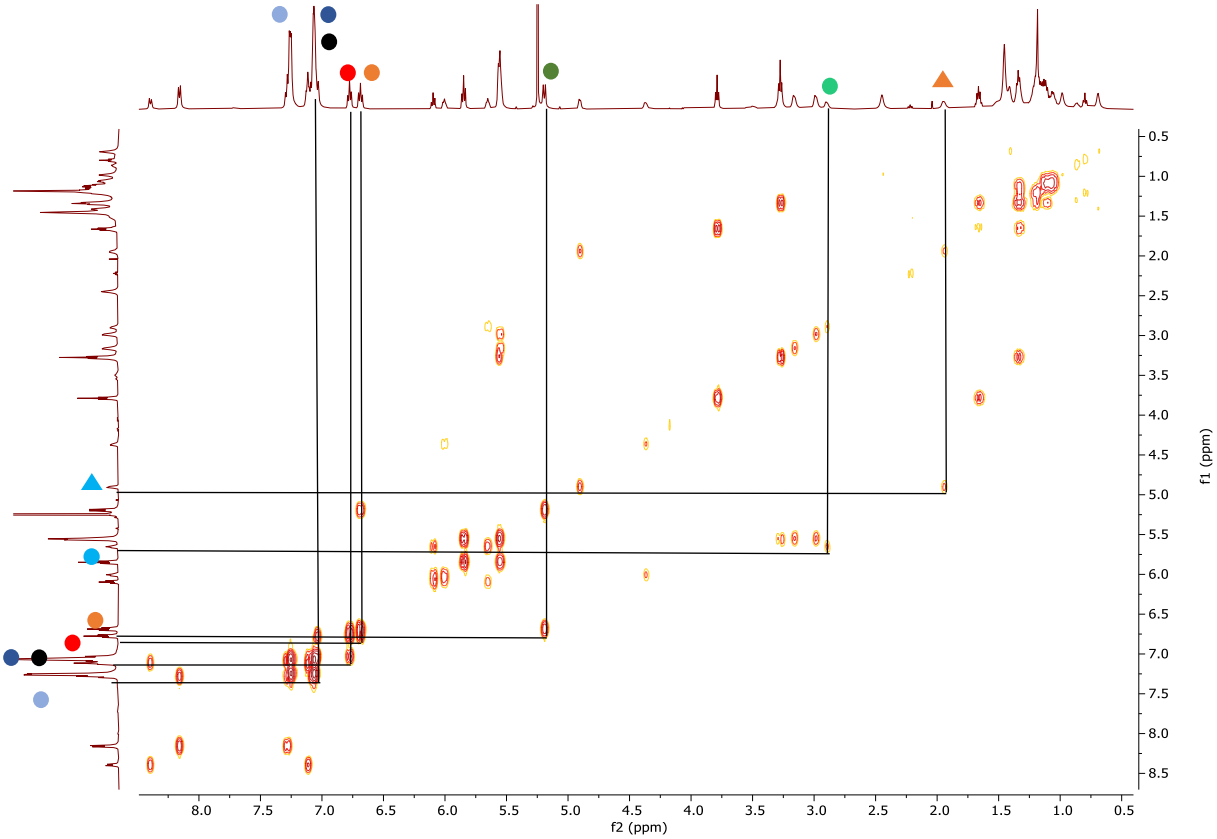

Figure 2.57: COSY NMR experiment showing cross peaks in Nd-TD-G.G **2.45** (500 MHz, CD_2Cl_2, 25 °C).

2.17 Synthesis of bridged Europium triple decker

2.17.1 Synthesis of Eu triple decker using TPP-TBTAP dyad 2.36

Following the unexpected formation of isomers in the synthesis of the TD using neodymium, the next step was to investigate the effect of the europium on the orientation of phthalocyanine unit in the complex. Following the logic that La exclusively produced the TD with the Pc located on the outside of the complex (Pc-Por-TBTAP) but Nd produced a mixture with the Pc in the middle of the sandwich, the Eu complex was expected to favour this latter arrangement (Por-Pc-TBTAP). Eu-TD **2.47** was synthesised by a 'one-pot' reaction under nitrogen. The reaction was carried out in octanol and the mixture was refluxed overnight (scheme 2.35).

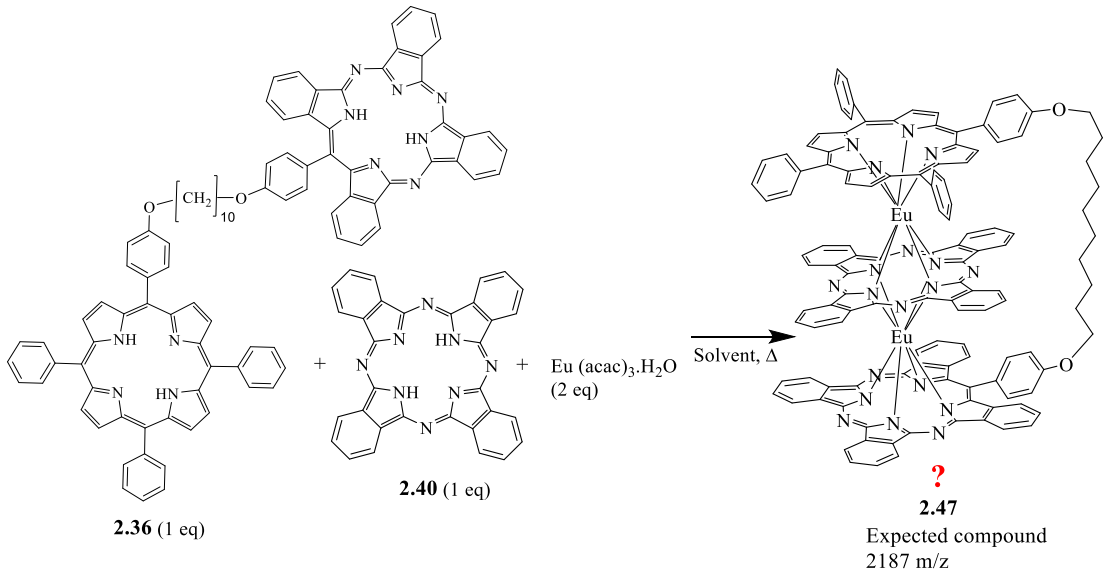

Scheme 2.35: Synthesis of triple decker (assumed to be) **2.47** using the 'one-pot' method.

TLC analysis indicated a red-brown spot, a green spot, dark green spot and a baseline spot. The reaction mixture was continuously monitored by MALDI-TOF MS. Peaks at 2897, 2188, 1522 and 514 m/z were recorded corresponding to a bis double decker, a TD, a bridged double decker and unreacted Pc. After 24 h the products were separated by column chromatography as in the case of La-TD **2.42** (discussed previously). Only a single TD compound was obtained. Analysis by MALDI-TOF MS confirmed the green fraction to correspond to Eu-TD, presumed to be **2.47**, where phthalocyanine is sandwiched between Por and TBTAP. Recrystallisation of the green fraction from a mixture of DCM: MeOH, resulted in a yield of 3%. The MALDI-TOF MS of the Eu-TD, presumed to be **2.47** with its theoretical prediction is shown in figure 2.58.

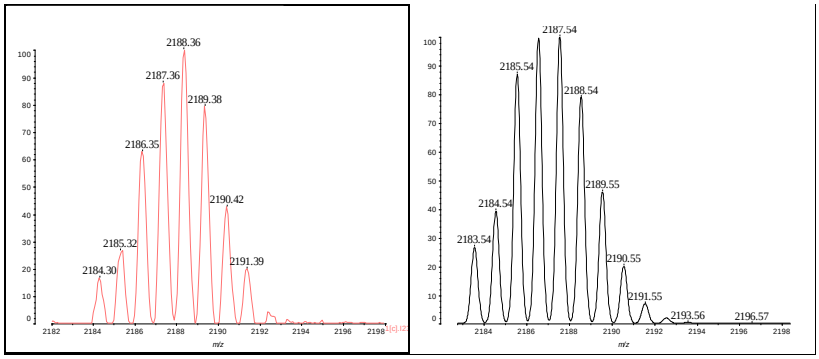

Figure 2.58: MALDI-TOF MS spectrum of the Eu-TD **2.47** with its theoretical prediction.

The stepwise method was then used to synthesise the Eu-TD **2.47**, but this did not significantly increase the yield. Increasing the equivalents of the metal salt and the reaction time did not make any difference to the yield of the triple decker. Other solvents such as 1,2,4-

trichlorobenzene (TCB) was investigated as the reaction mixture could be heated to a higher temperature of 215 °C, but with no significant increase in the yield.

The starting materials were mixed in a 'one-pot' fashion followed by a mixture of TCB and octanol as per the synthetic method developed by Martynov and co-workers.[19] The mixture was heated at 205 °C under nitrogen atmosphere for 8 h. Continuous monitoring by MALDI-TOF MS shows the presence of Eu-TD **2.47** and no starting materials. After the isolation and purification procedure was followed, an improved 20% yield of the triple decker was obtained. Increasing the reaction time to 24 h made no significant difference to the yield of the TD.

2.17.2 Comparison between the UV-Vis spectra of Eu-TPP TD 2.6 and Eu-TD 2.47

The UV-Vis spectra of the Eu-TPP TD **2.6** and Eu-TD (presumed to be **2.47**) is shown in figure 2.59. By comparing the spectra, the absorption bands of the triple decker of Eu-TD **2.47** are similar to the Eu-TPP TD **2.6**. This indicates that the orientation of the units in the Eu-TD **2.47** corresponds to the Eu-TPP TD **2.6** that is Por-Pc-TBTAP. The Pc Soret bands for the Eu-TD **2.47** and Eu-TPP TD **2.6** are at 346 and 356 nm respectively.[20] Both spectra show a sharp absorption band at the porphyrin region at around 418 nm. The TBTAP bands (600–700 nm) in Eu-TD **2.47** are consistent with the proposed structure with TBTAP on the outside of the complex.[20] Most notable is the observation that the spectrum is almost identical to the corresponding Nd-TD-G **2.46**.

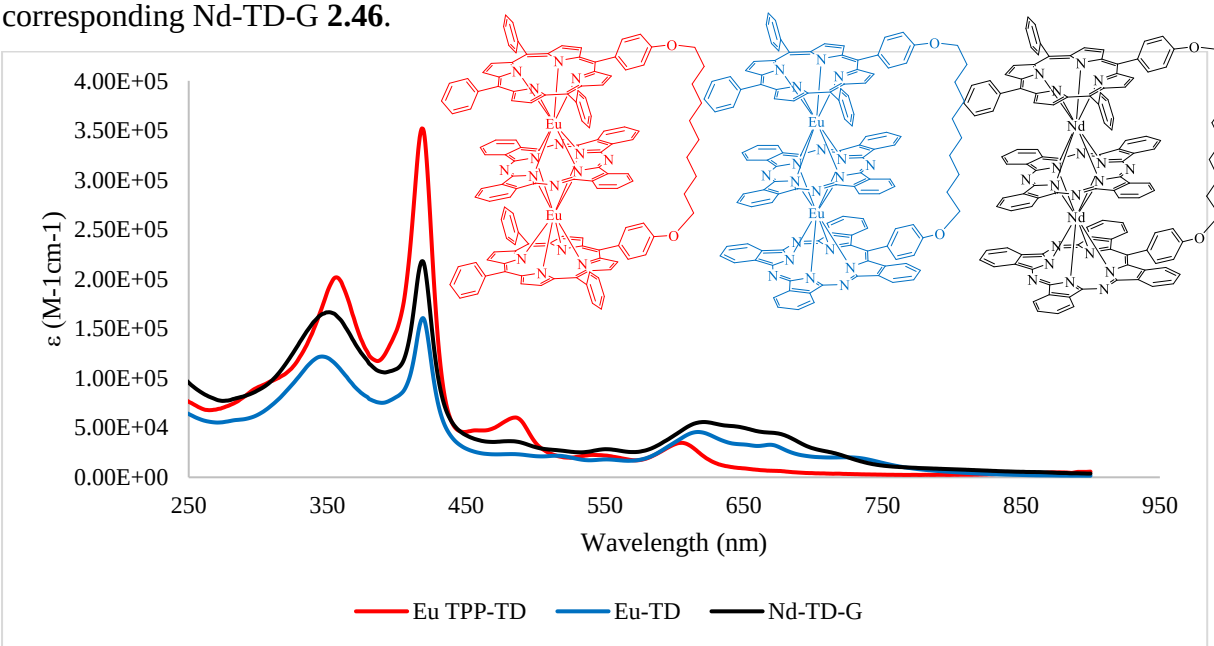

Figure 2.59: The UV-Vis spectra of the Eu-TPP TD **2.6**, Eu-TD **2.47** and Nd-TD-G **2.46** (in DCM).

2.17.3 The ^{1}H-NMR spectrum of Eu-TD 2.47 complex

The ^{1}H-NMR spectrum of Eu-TD **2.47** is shown in the figure 2.60. There are no peaks at –2.27 ppm and –0.29 ppm indicating that there is no metal-free unsymmetrical dyad.

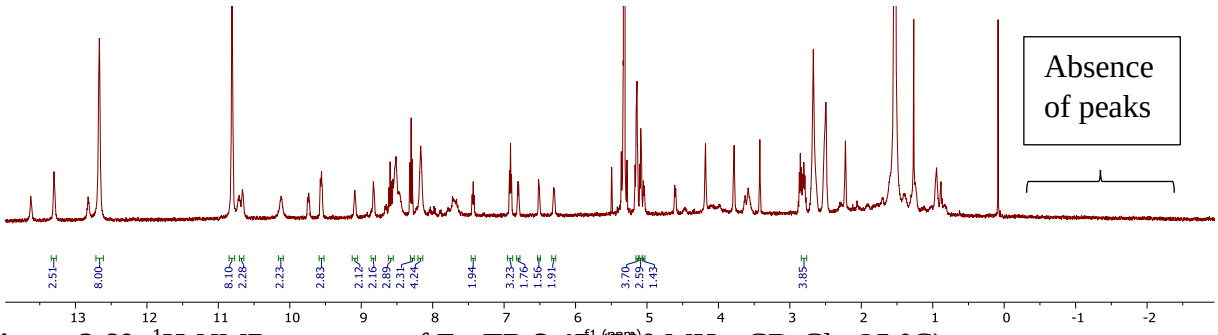

Figure 2.60: ^{1}H-NMR spectrum of Eu-TD **2.47** (500 MHz, CD_2Cl_2, 25 °C).

2.17.4 ^{1}H-NMR comparison between Eu-TD 2.47 and Eu-TPP TD 2.6

The ^{1}H-NMR spectra of Eu-TD **2.47** and the previously reported heteroleptic complex of Eu-TPP TD **2.6** were compared and stacked in the figure 2.61. In the ^{1}H-NMR spectrum of Eu-TD **2.47** complex the proton signals for the Pc ring are at 12.6 ppm and 10.76 ppm closely coincides with the Pc protons of Eu-TPP TD **2.6** at 12.91 ppm and 10.70 ppm. This indicates that the Pc ring is sandwiched between the porphyrin and TBTAP unit.

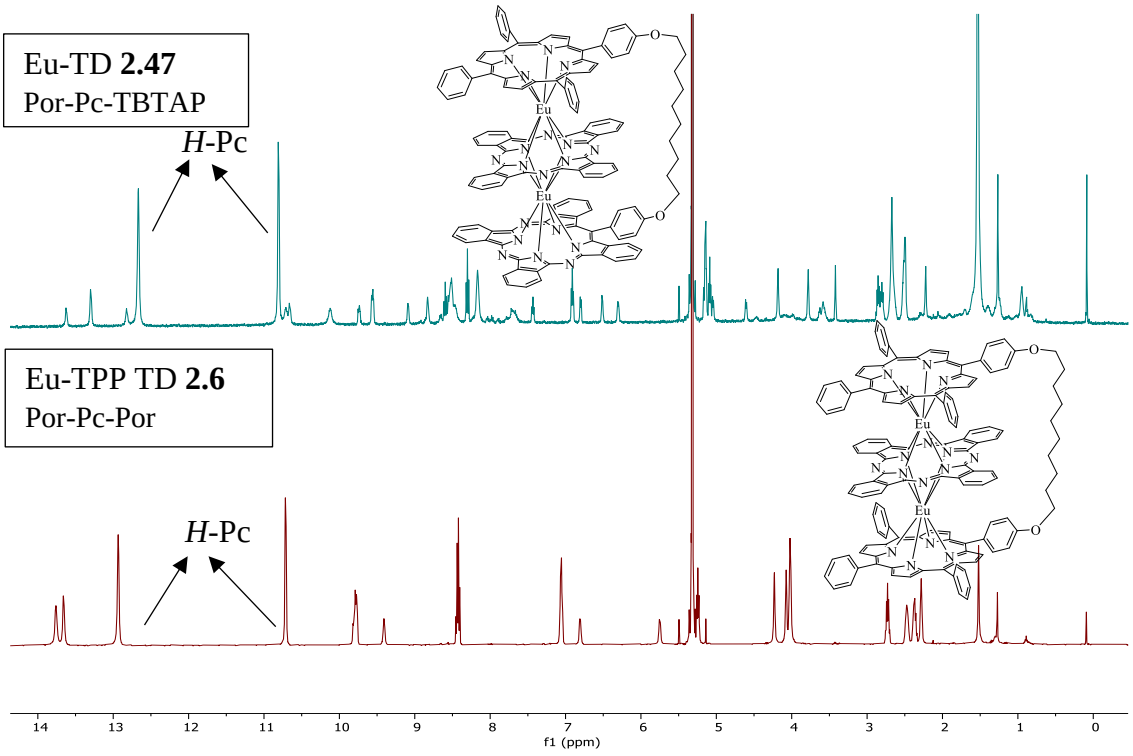

Figure 2.61: Stacked ^{1}H-NMR spectra of Eu-TPP TD **2.6** and Eu-TD **2.47** (500 MHz, CD_2Cl_2, 25 °C).

2.17.5 ^{1}H-NMR characterization of Eu-TD 2.47 complex

The ^{1}H-NMR spectrum of Eu-TD **2.47** is shown in figure 2.62. Further NMR experiments such as COSY were also conducted. However, the spectra are complicated and reveal phenomena/ artefacts that are impossible to explain with conventional analysis and are potentially instrumental features.

The two triplets at 5.18 ppm and 5.08 ppm corresponds to the protons on the chain which is next to the oxygen. These protons couples with the neigbouring proton at 2.82 ppm as a multiplet. The two protons on the Pc units resonates at 12.67 ppm and 10.78 ppm. Four of the porphyrin *β*-protons were identified and appear at 10.69 ppm and 8.81 ppm. The proton which faces the methoxyphenyl TBTAP ring resonate at 6.52 ppm which couples to the proton at 7.44 ppm as a triplet. Another triplet at 8.61 ppm couples with the deshielded proton at 9.73 ppm.

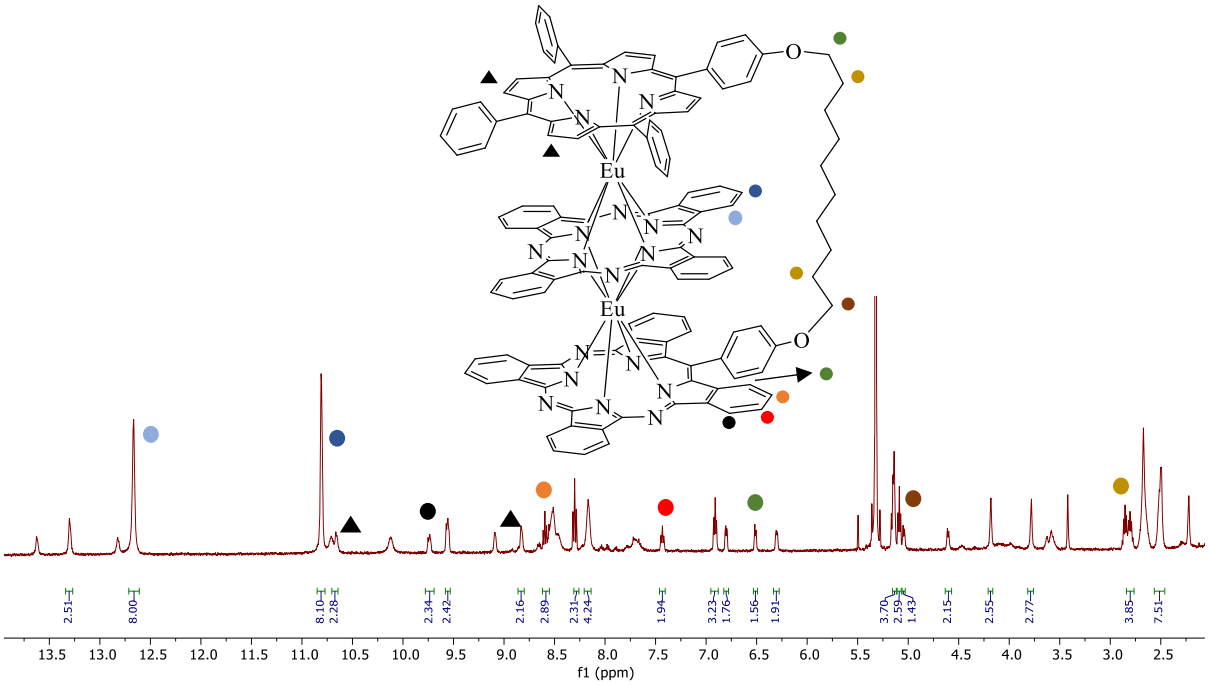

Figure 2.62: ^{1}H-NMR spectrum of Eu-TD **2.47** (500 MHz, CD_2Cl_2, 25 °C).

In the following sections, the synthesis of triple deckers using TBTAP-OMe and using the symmetrical dyad (TBTAP-O-C_{10}-O-TBTAP) will be explored.

2.18 Attempted synthesis of triple decker using TBTAP-OMe

The synthesis of TBTAP-OMe double and triple deckers using a modified version of Pushkarev and co-workers procedure was attempted.[14] A mixture of 3 equivalents of the *meso*-4-methoxyphenyl TBTAP **2.24** and two equivalents of $La(acac)_3.H_2O$ in the presence of lithium methoxide and *n*-hexadecanol was heated at 220 °C under inert atmosphere for 30 minutes (scheme 2.36). After a small-scale purification, the MALDI-TOF MS of the residue obtained showed no presence of the double or triple decker, instead, a peak at 619 m/z was present indicating the presence of the metal-free ligand **2.24** (starting material).

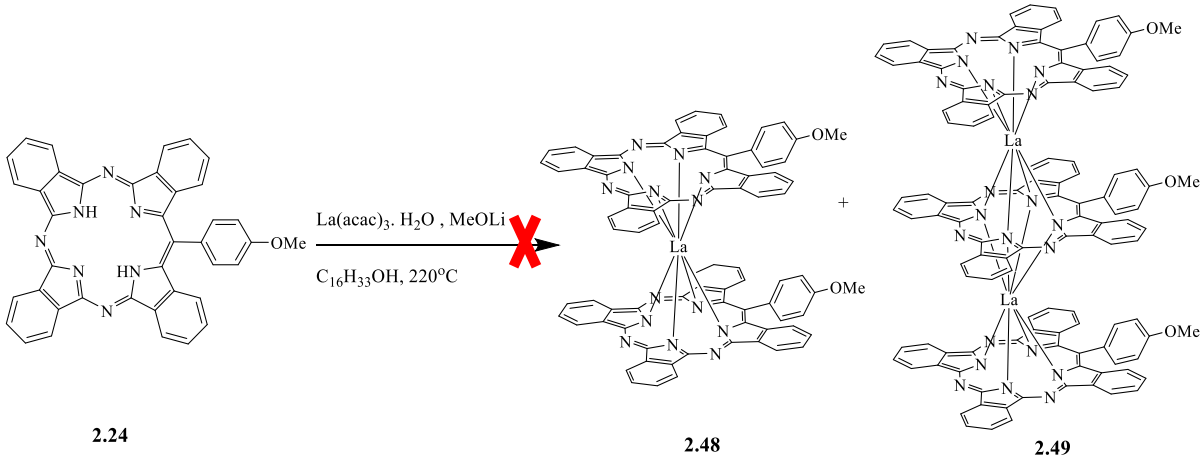

Scheme 2.36: Attempted synthesis of deckers using TBTAP-OMe.

In another attempt to synthesise the double **2.48** and triple **2.49** deckers, TBTAP-OMe **2.24** and lithium metal in octanol were heated to a temperature of 195 °C for 1 hour followed by the addition of $La(acac)_3.H_2O$. The reaction was monitored by MALDI-TOF MS and TLC hourly. No peaks above 1300 m/z were present indicating that no double and triple deckers were formed. After 24 h, $MgBr_2$ was added to the above reaction and both MALDI-TOF MS and TLC confirmed the formation of the metallated TBTAP-OMe (Mg-TBTAP-OMe **2.13**). This step was performed so as to retrieve the starting material **2.13**.

A different synthetic pathway was carried out in which a mixture of the same equivalences of starting materials, a 1: 1 volume ratio of octanol and TCB were heated at a temperature of 205 °C in an inert atmosphere (scheme 2.37). The reaction was continuously monitored by TLC and MALDI-TOF MS. After 9 hours, peaks at 1374 and 2130 m/z corresponding to the double (DD) **2.48** and triple decker (TD) **2.49** were observed (figure 2.63). The solvent was removed under reduced pressure and the crude product was purified by using column chromatography,

eluting the product with 100% DCM followed by a mixture of DCM: Et_2O (10:1). The yield of La-DD **2.48** was 60% while trace amount of the La-TD **2.49** was obtained.

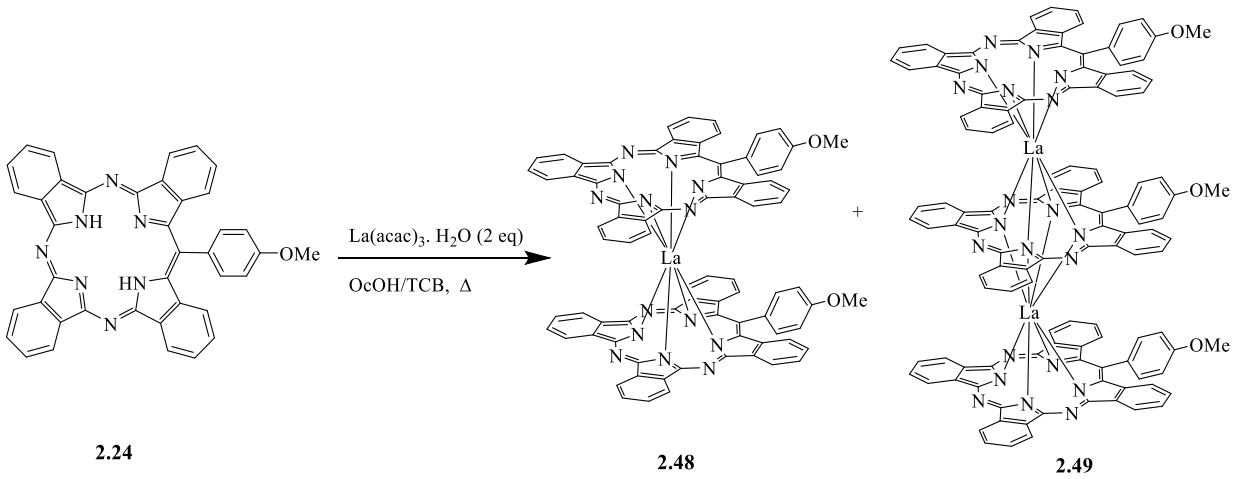

Scheme 2.37: Synthesis of deckers using TBTAP-OMe **2.24**.

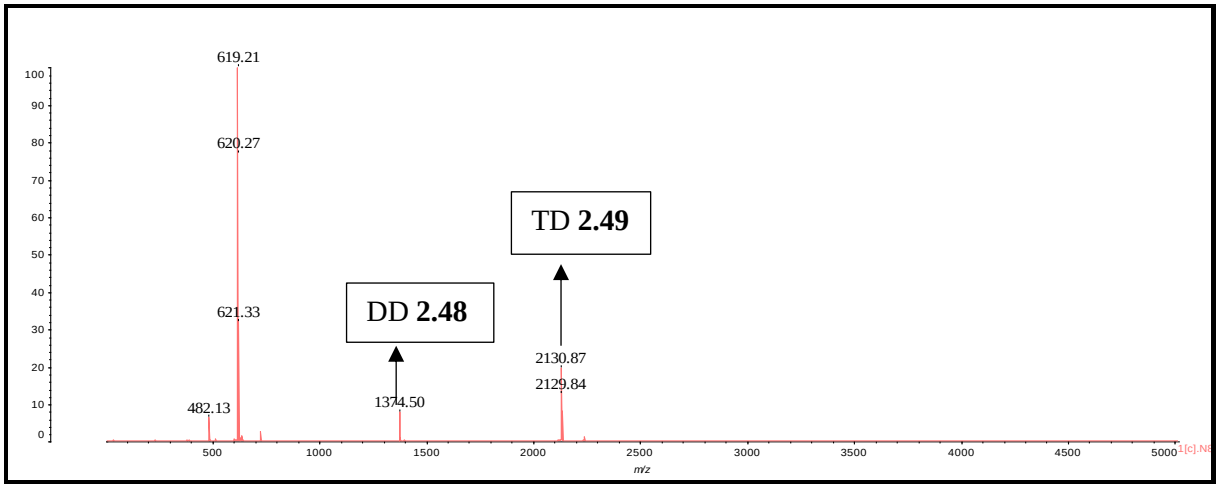

Figure 2.63: MALDI-TOF MS spectrum of the reaction mixture.

Attempts to increase the yield of the homoleptic triple decker **2.49** by increasing the amount of lanthanum salt and increasing the temperature of the reaction did not have any significant effect on the yield. All these variations failed to produce a significant yield of the triple decker **2.49**.

The UV-Vis spectrum of the double decker **2.48** is shown in figure 2.64 and is concordant with the data reported by Pushkarev and co-workers.[14]

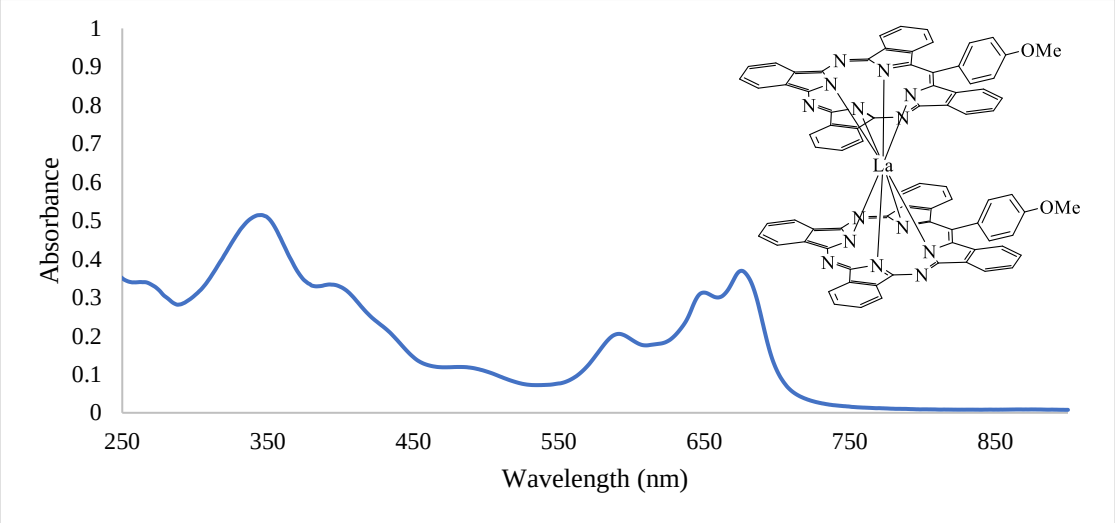

Figure 2.64: UV-Vis spectrum of La-DD **2.48** (in distilled THF).

2.19 Attempted synthesis of bridged triple decker using TBTAP-TBTAP dyad 2.39

The synthesis of the triple decker using the symmetrical dyad **2.39** and phthalocyanine **2.40** (as shown in scheme 2.38) involves two units of TBTAPs linked by an alkyl chain and a Pc unit. A mixture of one equivalent dyad **2.39**, one equivalent Pc **2.40**, and two equivalents of the lanthanum salt were mixed together in octanol (a 'one-pot' synthesis) and heated under reflux (scheme 2.38).

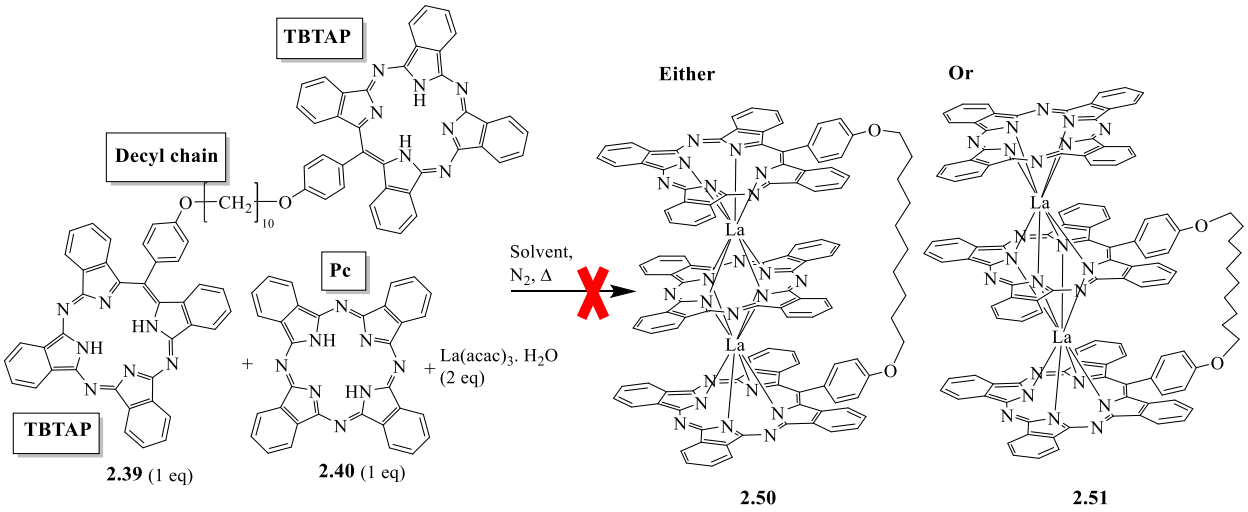

Scheme 2.38: Attempted synthesis of TD using symmetrical dyad **2.39**.

The reaction was continuously monitored by both TLC and MALDI-TOF MS. After 8 hours there was no peak at 2134 m/z indicating the absence of triple decker. However, a peak at 1349 m/z showed the presence of unreacted symmetrical dyad **2.39**. The mixture was therefore

refluxed overnight and subsequent MALDI-TOF MS analysis still showed no evidence for the target TD. The reaction mixture was left to reflux for 5 days with no appreciable change. Addition of more lanthanum salt followed by further refluxing for 48 hours failed to produce any target triple decker. Synthesis of the symmetrical dyad is time consuming and complicated, therefore any unreacted dyad should be retrieved. This was carried out by re-metallating the symmetrical dyad by the addition of $MgBr_2$ in the above reaction mixture and refluxing overnight. MALDI-TOF MS analysis gave a peak at 1395 m/z confirming the formation of the metallated form of the dyad which was reisolated.

The above synthesis was repeated using chlorobenzene as solvent instead of octanol and the resulting mixture was heated at a temperature of 150 °C in a sealed tube. A dark green solution was obtained. However, MALDI-TOF MS analysis showed no presence of triple decker. The temperature was increased to 180 °C and after 7 days no triple decker could be detected.

In another attempt to synthesise the triple decker, a mixture of the symmetrical dyad **2.39** (1eq) and Pc **2.40** (1eq) was heated to reflux in 1,2 dichlorobenzene overnight followed by the addition of the lanthanum salt (2 eq). MALDI-TOF MS once again did not show the presence of the target triple decker compound.

The reaction was then repeated using other solvents such as 1,2 dichlorobenzene and 1,3,5 trichlorobenzene (TCB) and a 1:1 of octanol and TCB and the reaction mixture was heated at a mantle temperature of 190 °C, 215 °C and 220 °C respectively for 7 days. MALDI-TOF MS analysis showed no peak at 2134 m/z, hence absence of the triple decker. However, from the MALDI-TOF MS (figure 2.66), a peak at 1484 m/z showed the presence of the double decker, La-DD **2.52** shown in figure 2.65.

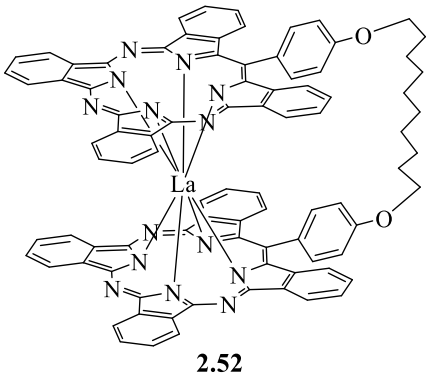

2.52

Figure 2.65: Double decker **2.52**.

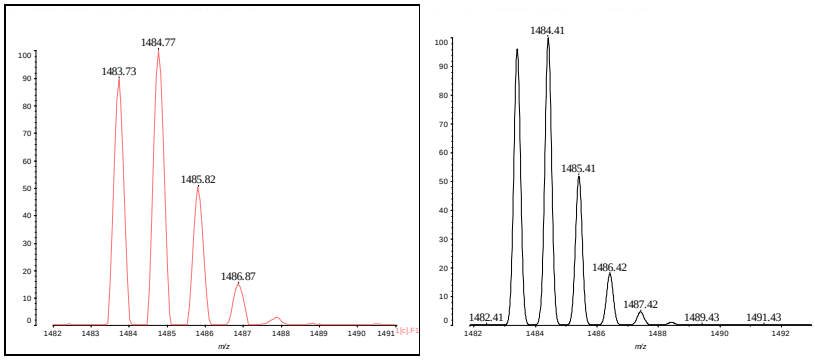

Figure 2.66: MALDI-TOF MS spectrum of the La-DD **2.52** with its theoretical prediction.

Crystals of the double decker **2.52** were grown from a saturated solution of DCM: MeOH and subjected to X-ray analysis. The resulting structure is shown in the figure below.

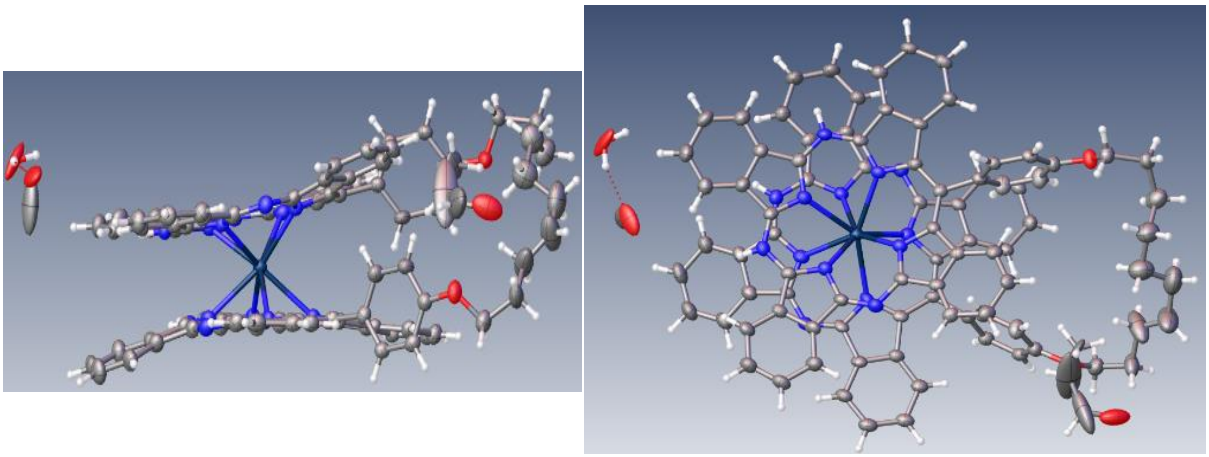

Figure 2.67: Preliminary X-Ray analysis obtained for double decker complex **2.52**.

The picture on the right-hand side, a top-view of the double decker complex shows the TBTAP ligands to be in staggered conformation giving rise to a square-antiprismatic environment.

The UV-Vis spectrum of the La-DD **2.52** is reported in figure 2.68. The splitting (ΔQ) of the main absorption maxima is 23 nm which correlates with the study performed by Pushkarev and co-workers.[14]

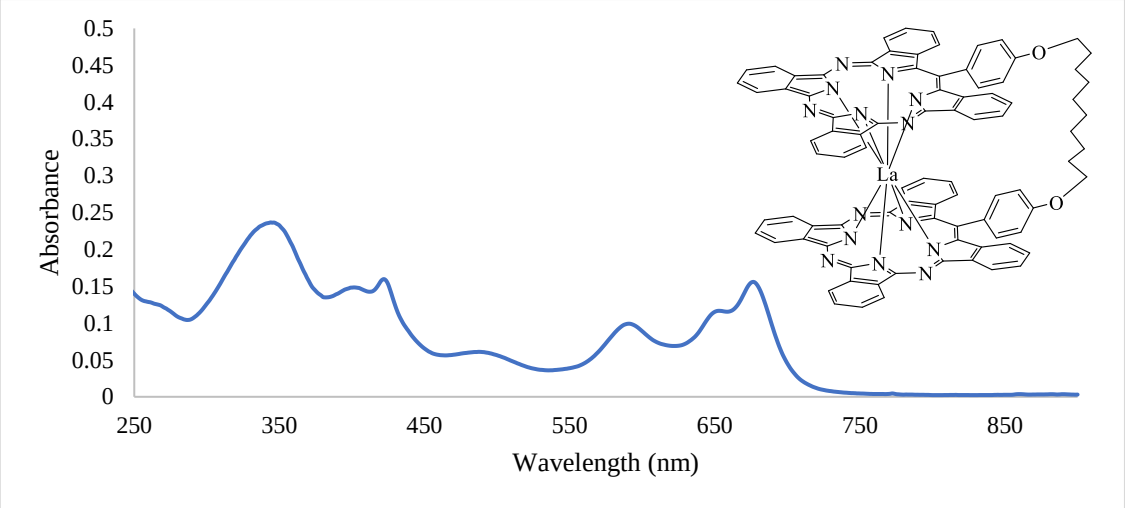

Figure 2.68: UV-Vis spectrum of La-DD **2.52** (in distilled THF).

2.20 Attempted synthesis of TD from Pc 2.40 and TBTAP-OMe 2.24

After the failure to synthesise bridged triple decker, the synthesis of heteropletic triple decker of TBTAP-OMe-Pc-TBTAP-OMe using a 'one-pot' procedure was attempted. A mixture of two equivalents of TBTAP-OMe **2.24**, one equivalent of Pc **2.40** and two equivalents $La(acac)_3.H_2O$ was refluxed in octanol. The reaction was constantly monitored by TLC and MALDI-TOF MS and after 3 days no target triple decker was formed (scheme 2.39).

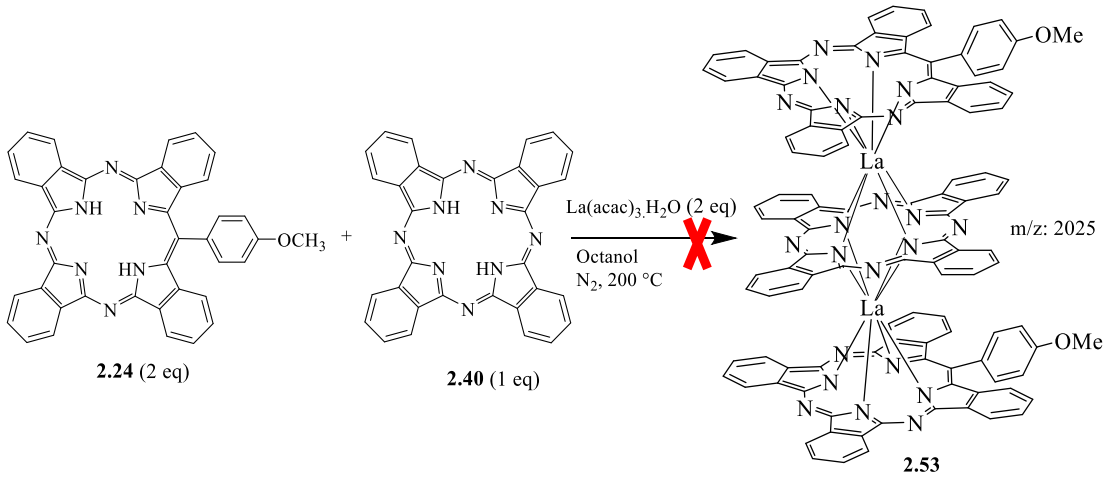

Scheme 2.39: Attempted synthesis of TD **2.53** using Pc and TBTAP-OMe.

A modified version of the above synthesis was carried out using TBTAP-OMe metallated with lithium methoxide, which could possibly increase its solubility in octanol and the mixture was again refluxed. After 1 hour, the lanthanum salt and the Pc **2.40** were added to the reaction mixture. After 24 h, the reaction mixture was analysed by TLC and MALDI-TOF MS and there

was no formation of the target triple decker but only peaks at 1374 m/z and 2132 m/z corresponding to the La-DD **2.48** and La-TD **2.49**. After 5 days, this pathway also failed to produce any heteroleptic triple decker. Using the same method, other solvents such as 1,2 dichlorobenzene and 1,3,5 trichlorobenzene and a solvent mixture of octanol and TCB in a volume ratio of 1:1 was employed, and no target compound was observed as confirmed by MALDI-TOF MS.

In summary, all attempts to synthesise La triple deckers using Pc and TBTAP-OMe precursors failed to produce the desired product as confirmed by MALDI-TOF MS. Double **2.48** and triple **2.49** deckers of TBTAP-OMe were only produced. The observation is consistent with the conclusions from the TD synthesis using Por-TBTAP dimers where TBTAP and Pc were not adjacent in TDs. In all cases TBTAP and porphyrin are adjacent and therefore, in the following section, the synthesis of triple deckers using TBTAP-OMe and porphyrins will be discussed.

2.21 Synthesis of triple decker complex from TBTAP-OMe 2.24 and TPP 2.28

The synthesis of triple decker shown in scheme 2.40 was carried out by using a mixture of 2 equivalents of TPP **2.28**, 1 equivalent of TBTAP-OMe **2.24** and 2 equivalents of the lanthanum salt and refluxing in octanol for 24 h.

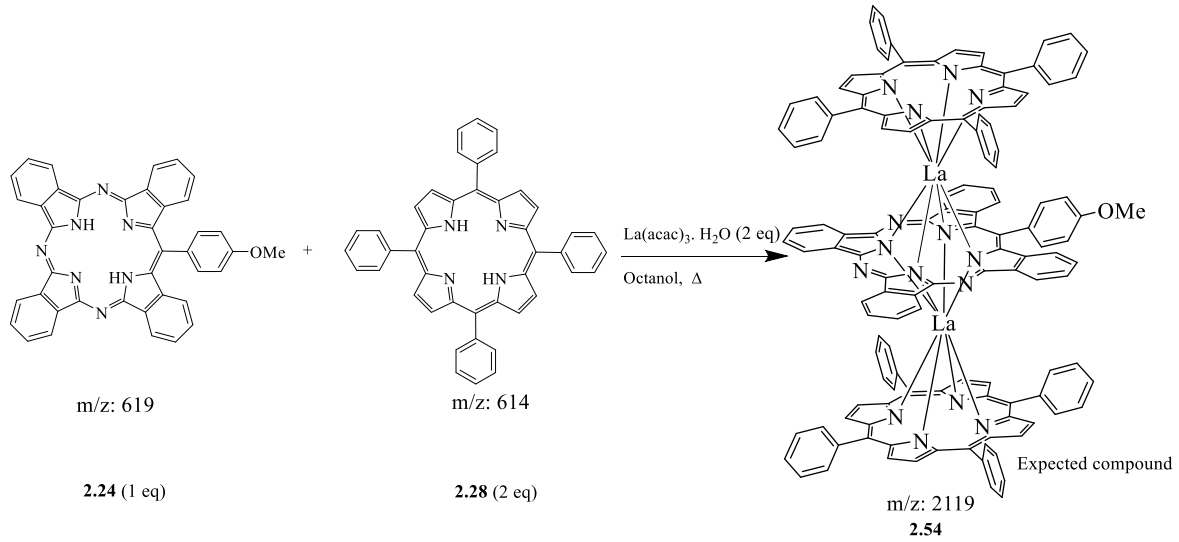

Scheme 2.40: Synthesis of TD using TPP and TBTAP-OMe.

The reaction mixture was subjected to MALDI-TOF MS analysis, and the result is shown in figure 2.69.

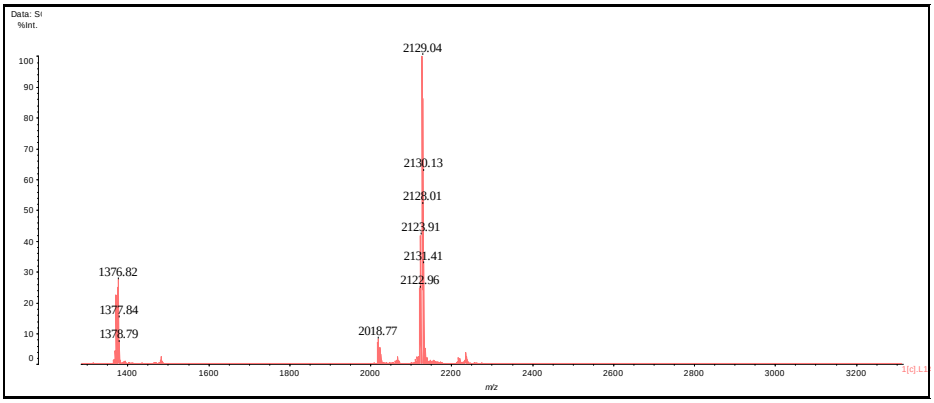

Figure 2.69: MALDI-TOF MS spectrum of the reaction mixture

MALDI-TOF MS analysis showed a cluster of peaks which corresponds to the presence of triple deckers. However, at this stage it was obvious that the selection of TPP as co-reactant was flawed due to the similarity of the molecular weights of TPP and TBTAP-OMe. The similarity meant that MALDI-TOF MS could not confidently work out the combination (or mixture of combinations) of TPP and TBTAP-OMe in the formed TD. This combination was therefore immediately abandoned, and a different TPP derivative was selected.

2.22 Synthesis of triple decker from TBTAP-OMe and TPP(OMe)$_4$

To facilitate the identification of the triple decker, the above synthesis was repeated using TPP(OMe)$_4$ (733 m/z) and demetallated TBTAP-OMe (619 m/z). These significantly different molecular weights made it easier to identify which triple decker (combination) was formed.

2.22.1 Synthesis of TPP(OMe)$_4$ 2.56

The TPP(OMe)$_4$ **2.56** was synthesised according to the Adler-Longo procedure.[11] A mixture of *p*-methoxy benzaldehyde and pyrrole was refluxed in propionic acid for 30 minutes. The mixture was then cooled to room temperature and methanol was added. The mixture was left to precipitate overnight in the fridge. After filtration, a purple solid of the title compound was obtained in a 32% yield (scheme 2.41).

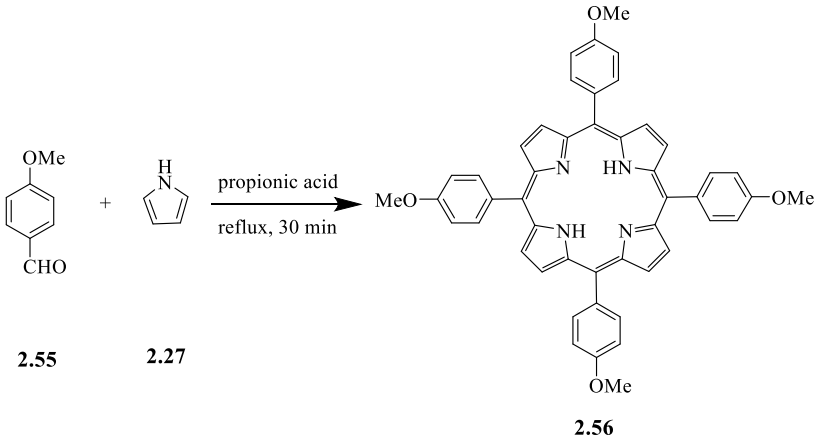

Scheme 2.41: Synthesis of TPP(OMe)$_4$ **2.56**.

2.22.2 Triple decker from TBTAP-OMe 2.24 and TPP(OMe)$_4$ 2.56

A mixture of two equivalents of La(acac)$_3$.H$_2$O, one equivalent of TBTAP-OMe **2.24** and two equivalents of TPP(OMe)$_4$ **2.56** in octanol was heated under reflux (scheme 2.42). The reaction was monitored by both TLC and MALDI-TOF MS. It was found that a triple decker was formed within 24 h.

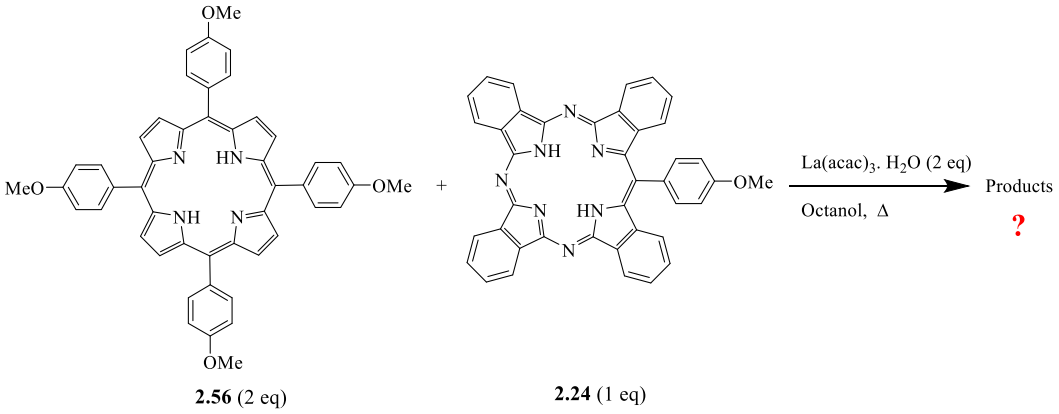

Scheme 2.42: Synthesis of TD using TPP(OMe)$_4$ **2.56** and TBTAP-OMe **2.24**.

Based on the number of equivalences of starting materials used in the synthesis, the dominated molecular weight of 2356 m/z was expected and should correspond to one of the structures in figure 2.70.

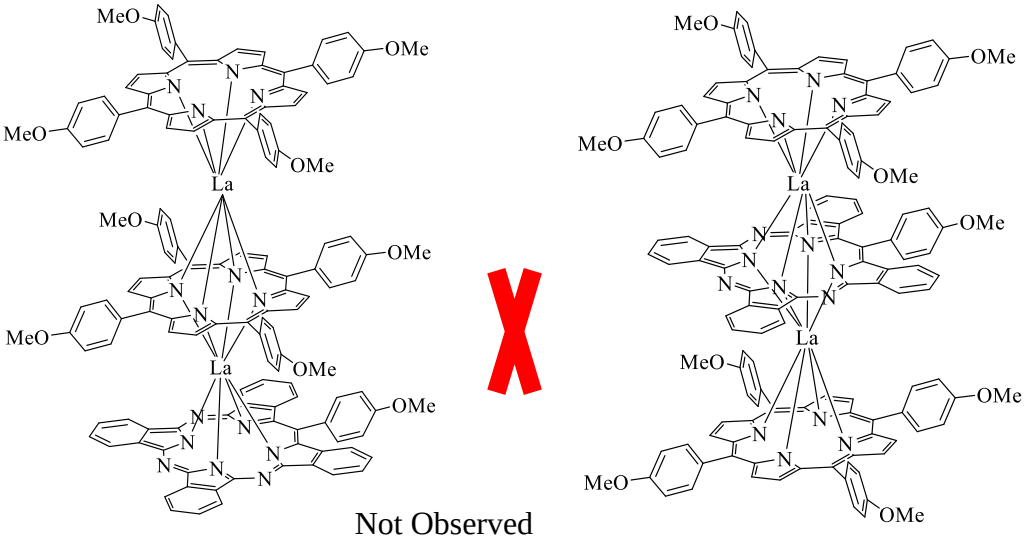

Figure 2.70: Plausible triple decker structures from above synthesis.

However, unexpectedly only a high mass peak at 2245 m/z was obtained which corresponds to a triple decker of TBTAP-OMe **2.24** and $TPP(OMe)_4$ **2.56** in a ratio of 2:1. Figure 2.71 shows the possible structures for such a triple decker.

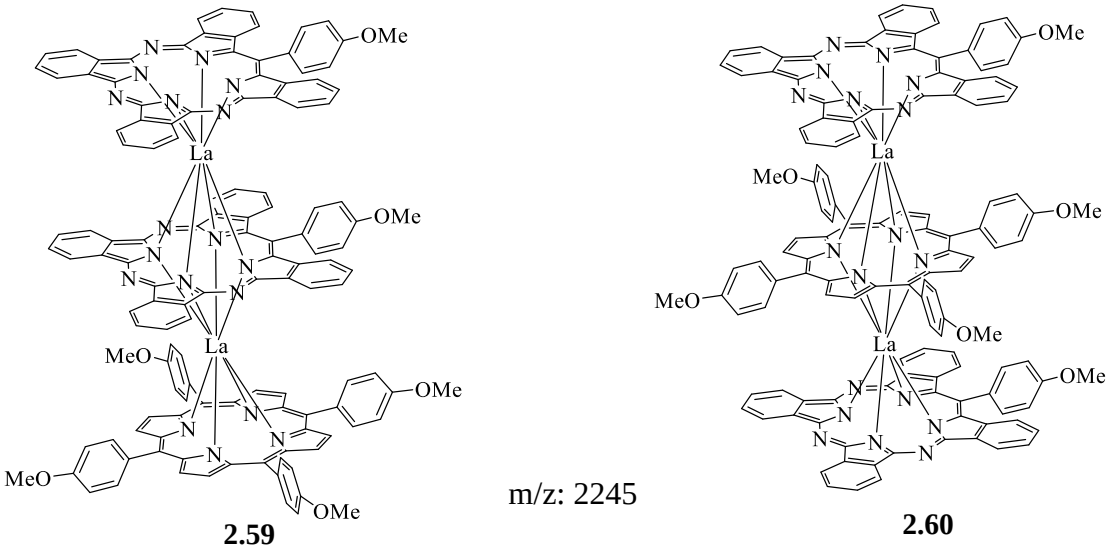

Figure 2.71: Plausible triple decker structures from above synthesis.

After the reaction was completed, the solvent was distilled off and DCM was added followed by MeOH so as to precipitate the product. After filtration the residue was separated by column chromatography using DCM/Hexane (3:2) followed by 100% DCM. The first fraction was purple and contained the unreacted porphyrin. The TD of unknown structure (figure 2.71) was

isolated as the second dark green fraction and a yield of 23% was obtained. Analysis of the green fraction by MALDI-TOF MS (figure 2.72) confirmed the formation of a TD.

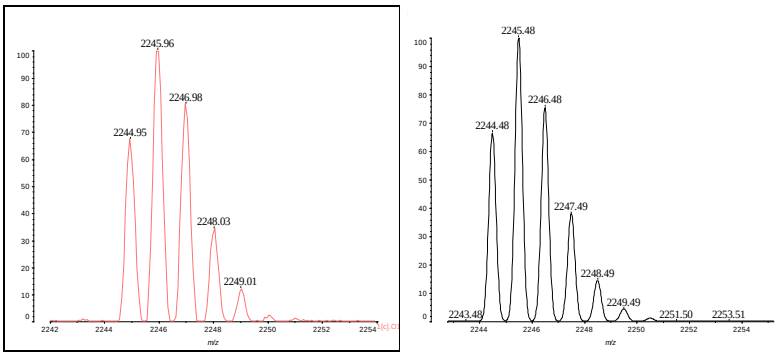

Figure 2.72: MALDI-TOF MS spectrum of a TD with its theoretical prediction.

2.22.3 The ^{1}H-NMR characterization of triple decker complex 2.60

The dark green fraction was analysed by ^{1}H-NMR spectroscopy which allowed identification of the triple decker as **2.60** (figure 2.73), with the Por molecule sandwiched between two TBTAP-OMe molecules. The protons were assigned from studying the ^{1}H-NMR and COSY NMR spectra (figure 2.74).

Based on the integration, the two singlets at 4.45 ppm and 4.03 ppm corresponds to the methyl group (-OCH_3) on the porphyrin and TBTAP-OMe molecule respectively. The porphyrin β-protons appear as a singlet at around 7.96 ppm, integrating to 8. This confirms that there is a symmetry in the complex and that the porphyrin unit is sandwiched between the two TBTAP-OMe units. The highly deshielded proton at 8.95 ppm couples with the proton at around 7.67 ppm, which both integrate to 4 protons, and are present on the TBTAP unit. The proton at around 6.36 ppm which faces towards the methoxy phenyl ring of the TBTAP moiety, and the proton at 7.40 ppm couple with each other, both integrating to 4. The two inner protons on the methoxy phenyl ring of the TBTAP molecule both integrate to 2 and are positioned at 7.52 ppm and 7.20 ppm respectively. The two outer protons which coupled to each other are more shielded and are located at 6.63 ppm and 5.83 ppm respectively. The protons on the methoxy phenyl ring of the porphyrin molecules are at 8.59 ppm and 7.69 ppm respectively.

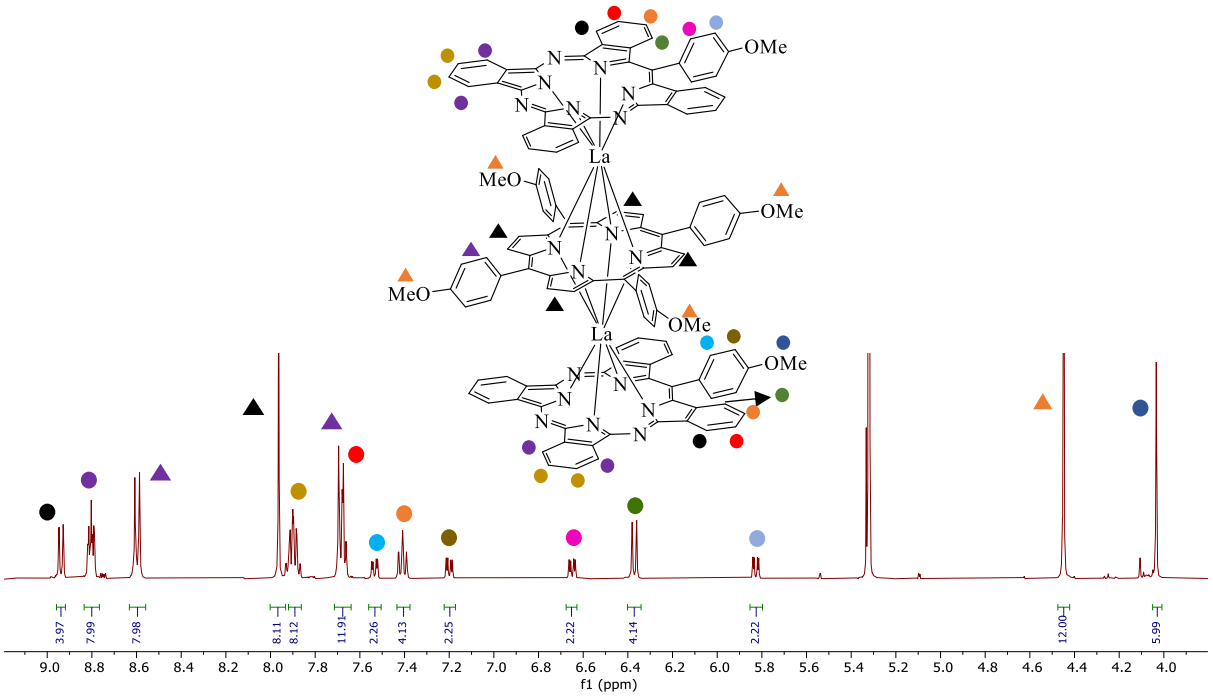

Figure 2.73: ^{1}H-NMR spectrum obtained for triple decker **2.60** (500 MHz, CD_2Cl_2, 25 °C).

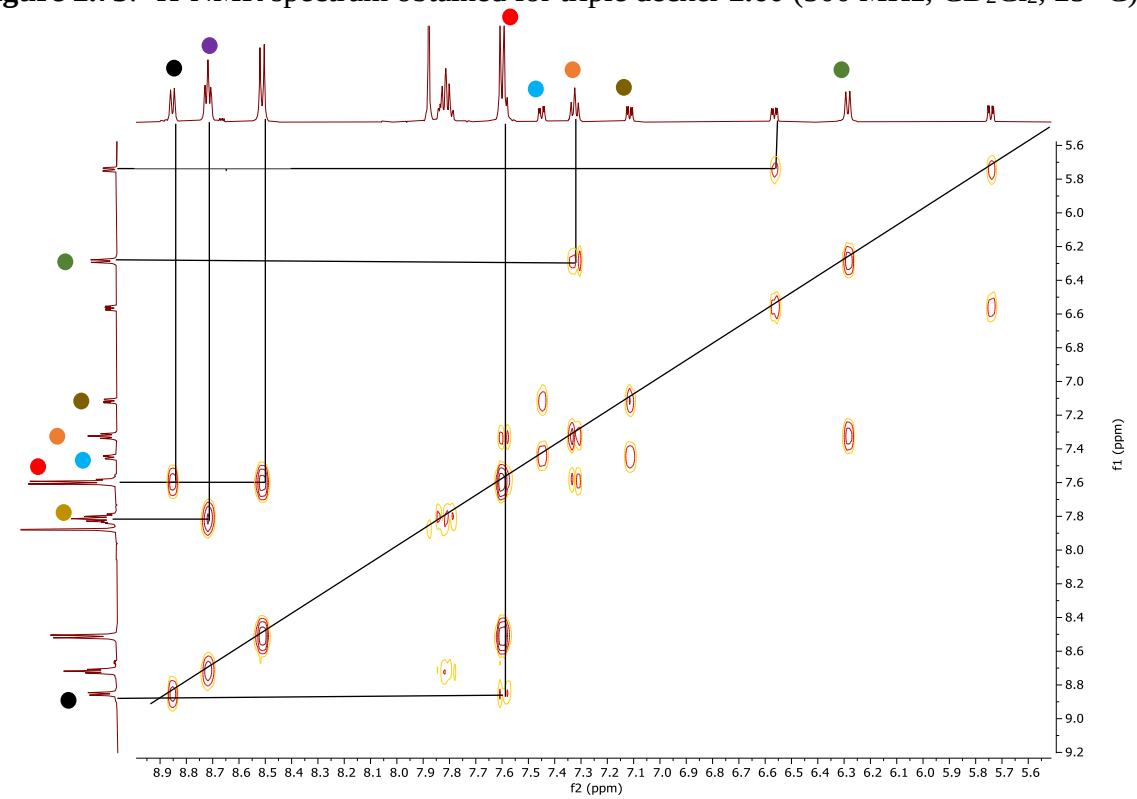

Figure 2.74: COSY NMR experiment showing cross peaks of triple decker **2.60** (500 MHz, CD_2Cl_2, 25 °C).

To fully confirm that the desired triple decker complex **2.60** in which the TPP(OMe)$_4$ unit is sandwiched between the two TBTAP-OMe unit, crystals of the triple decker complex suitable

for X-ray diffraction were grown from a saturated methanol and DCM solution at room temperature (figure 2.75).

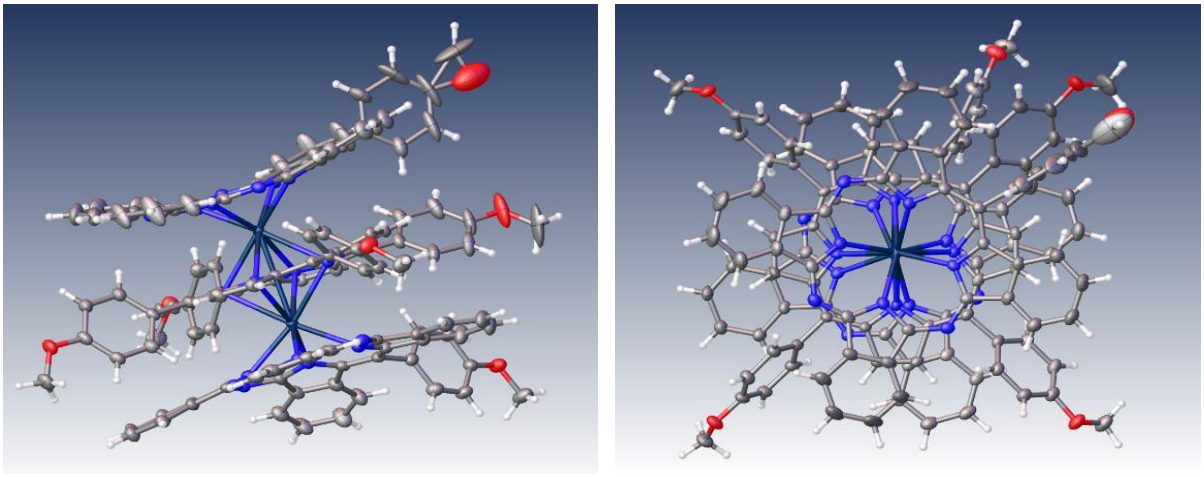

Figure 2.75: Preliminary X-Ray analysis obtained for triple decker complex **2.60**.

2.23 Synthesis of triple decker from TBTAP-OMe 2.40 and TPP-TBTAP dyad 2.36

In order to establish whether the porphyrin unit of the unsymmetrical dyad **2.36** can be sandwiched between two TBTAP units in a triple decker, following the unexpected outcome from the above reaction, a 'one-pot' synthesis was carried out using two equivalents of $La(acac)_3.H_2O$, one equivalent of TBTAP-OMe **2.40** and one equivalent of the unsymmetrical dyad **2.36**. The mixture was heated at a temperature of 200 °C in octanol for 24 h (scheme 2.43). MALDI-TOF MS analysis gave a peak at 2265 m/z showing the presence of the TD.

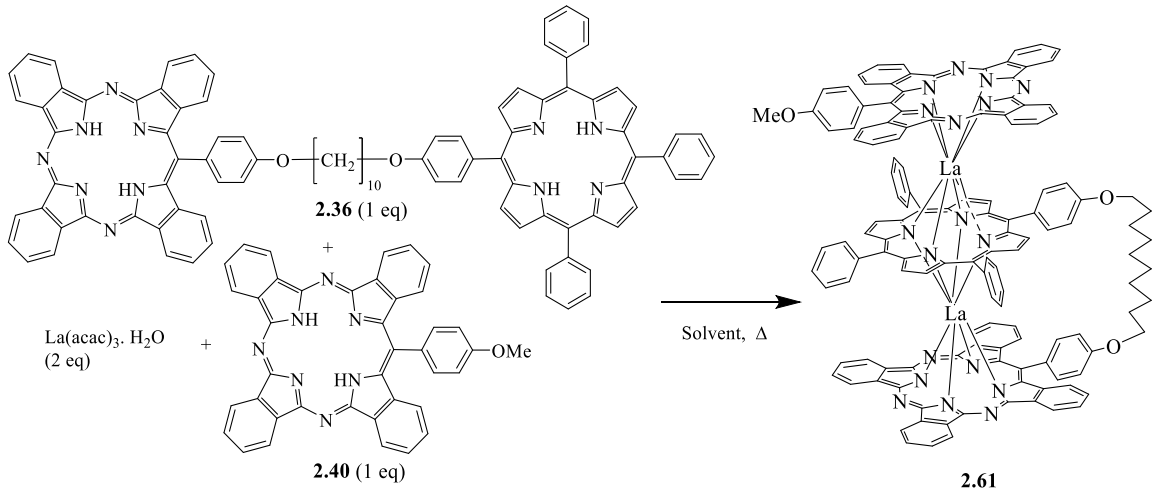

Scheme 2.43: Synthesis of TD **2.61** using unsymmetrical dyad and TBTAP-OMe.

The solvent was removed under high vacuum and a mixture of DCM: MeOH was added to the flask and was left to precipitate overnight. The residue was filtered off and was separated by

column chromatography using DCM/Hexane (3:2) followed by 100% DCM. After recrystallisation from DCM: MeOH, the TD was isolated as a dark green fraction with yield of 10%. In an attempt to increase the yield, the above reaction was repeated using a 1:1 ratio of octanol and TCB instead of 100% octanol, and the mixture was heated at 205 °C. It was found that a triple decker was formed within 6 h as confirmed by MALDI-TOF MS (figure 2.76). After the isolation and purification using the same solvent system for the column chromatography as above, a 25% yield was achieved. The same synthetic procedure was carried out for a period of 24 h and there was no increase in the yield.

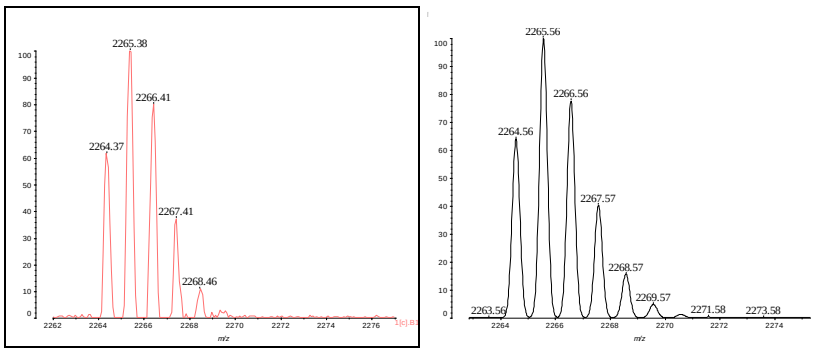

Figure 2.76: MALDI-TOF MS spectrum of the TD **2.61** with its theoretical prediction.

2.23.1 The ^{1}H-NMR characterization of triple decker complex 2.61

The ^{1}H-NMR spectra of heteroleptic triple deckers **2.60** and **2.61** were stacked together as shown in the figure 2.77.

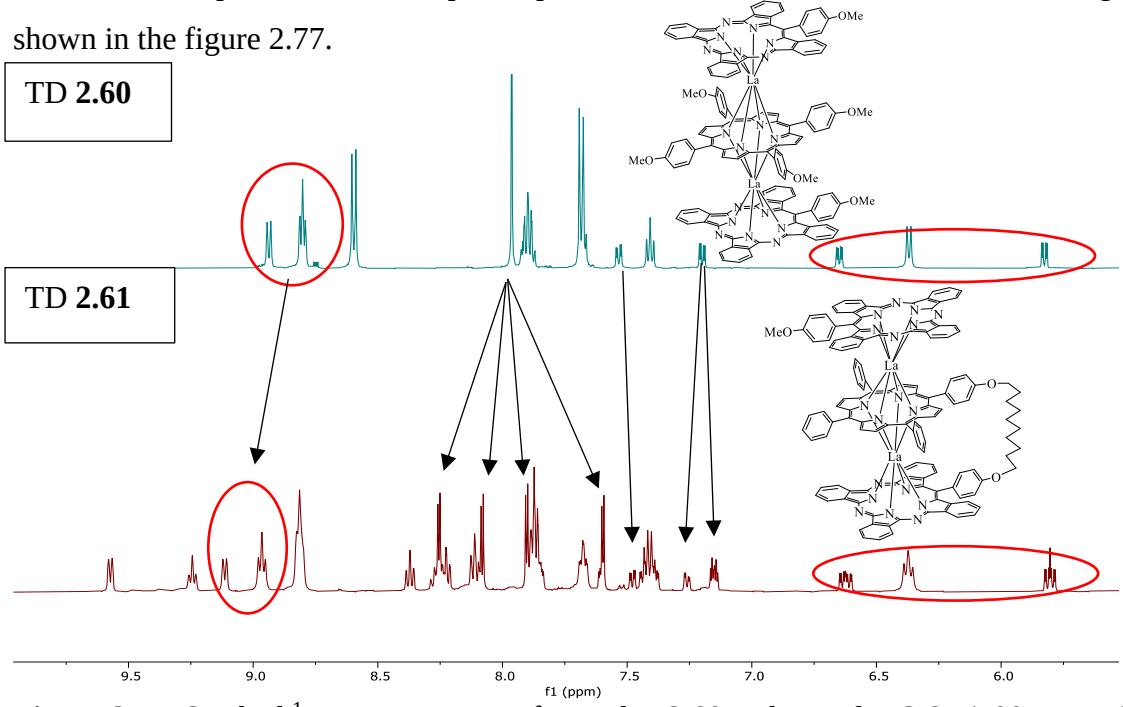

Figure 2.77: Stacked ^{1}H-NMR spectra of complex **2.60** and complex **2.61** (500 MHz, CD_2Cl_2, 25 °C).

While the heteroleptic triple decker **2.61** is different from complex **2.60**, there are some noticeable similarities (and differences) between both spectra:

- Both complexes **2.60** and **2.61** have peaks at 6.64 ppm, 6.37 ppm and 5.81 ppm, however in complex **2.61** the multiplicity of the peaks is increased.
- The peak at 7.20 ppm in complex **2.60** is split in complex **2.61** at 7.25 ppm and 7.15 ppm.
- The peak at 7.52 ppm in complex **2.60** is shifted in complex **2.61** at 7.47 ppm.
- The singlet at 7.95 ppm in complex **2.60** corresponds to the porphyrin *β*-protons and is separated in complex **2.61** at 8.25 ppm, 8.08 ppm, 7.90 ppm and 7.59 ppm.
- The two set of peaks in complex **2.60** at 8.94 ppm and 8.80 ppm is shifted in the complex **2.61**.

The TBTAP-OMe unit is on the porphyrin unit in complex **2.61**. The ^{1}H-NMR spectrum of heteroleptic triple decker **2.61** is shown in figure 2.78. The porphyrin *β*-protons appear as doublets at around 8.25 ppm, 8.08 ppm, 7.90 ppm and 7.60 ppm with coupling constant (J = 4.0 Hz) integrating to 2 each. The methoxy methyl proton on the TBTAP unit appears as a singlet and resonates at 4.01 ppm. The protons which are on the TBTAP units resonate at 8.80 ppm couples with the proton next to it at 7.86 ppm. COSY NMR was also conducted in order to determine the positioning of the peaks to which the protons are associated. There is a strong influence of the bridging chain which hinders the rotation of the TPP and the TBTAP and therefore the peaks are not averaging.

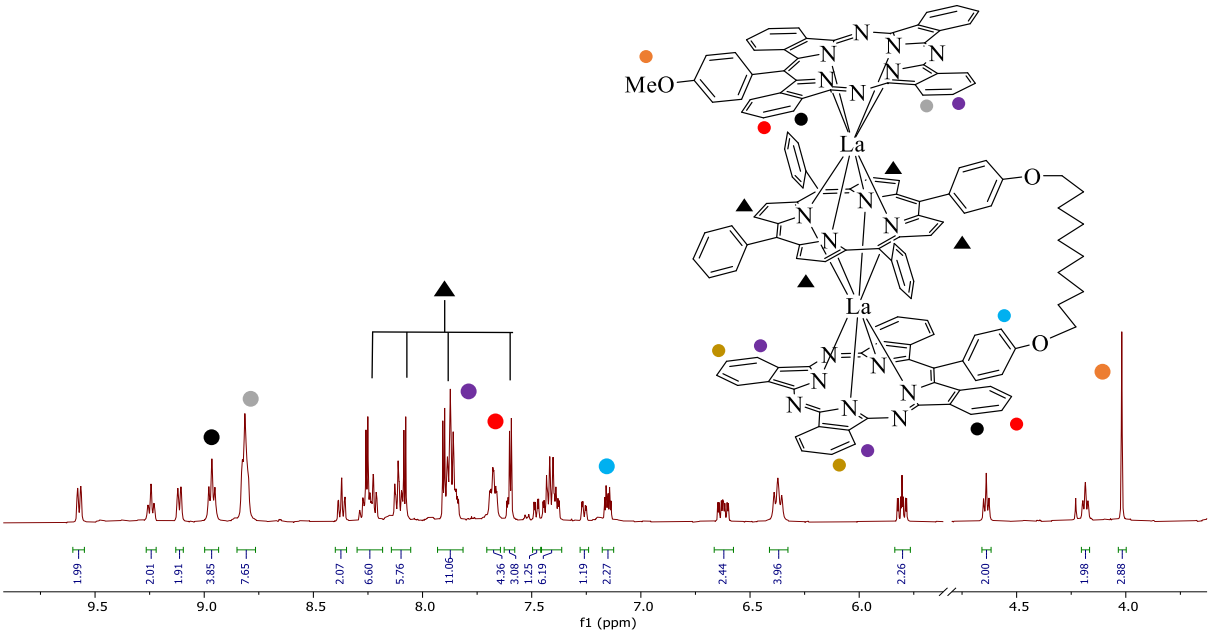

Figure 2.78: ^{1}H-NMR spectrum of heteroleptic TD **2.61** (500 MHz, CD_2Cl_2, 25 °C).

2.24 Conclusions and future works

Heteroleptic TDs containing a Por, Pc and TBTAP units have been synthesised and fully characterised for the first time. Controlled synthesis was achieved by linking TBTAP and Por with a flexible C_{10} and C_{12} chain. The synthesis of starting materials whereby a large part of this project's time was committed, proved to be somewhat challenging to scale up. However, spectroscopic analysis such as MALDI-TOF MS, NMR and UV-Vis determined the structure of the synthesised triple deckers to be significantly different to the arrangement previously obtained from the known triple decker Por-Pc-Por. Our new work revealed that the Pc unit is not in the middle of the sandwich and lies on the outside next to the Por unit rather than the TBTAP unit such that the orientation of the units are as follows Pc-Por-TBTAP when La salt was used in the synthesis. X-Ray crystallography analysis would give a conclusive result, however so far suitable crystals were not grown successfully. An unexpected result was obtained from the Nd triple decker synthesis where one of the fractions has its units orientated as follows Por-Pc-TBTAP, while the UV-Vis of the other fraction was similar to the newly synthesised La-TD. The Eu triple decker has its units oriented similar to one of the fractions of Nd triple decker that is exclusively Por-Pc-TBTAP. Many attempts to synthesise the La triple decker using the symmetrical TBTAP dyad and Pc proved to be unsuccessful. Instead, a double decker only is formed. Based on this result, this further proved that the Pc is less likely to be on the TBTAP unit and that the TBTAP is preferred to be on the Por unit.

Results have provided some surprising selectivities that were not predicted originally. The observations, particularly the switch between TD arrangements simply triggered by change in lanthanide, merit further investigation. In particular, future work could investigate whether selectivity is possible with mixed metals, investigating related strategies that could potentially deliver controlled synthesis of heteroleptic, heterometallic TDs with three different macrocycles and two different lanthanides, all in defined locations. This has always been the long-term goal of this and the group's parallel projects, and the surprising results from this study bring us much closer to this ambitious target.

References

(1) Birin, K. P.; Gorbunova, Y. G.; Tsivadze, A. Y. Efficient Scrambling-Free Synthesis of Heteroleptic Terbium Triple-Decker (Porphyrinato)(Crown-Phthalocyaninates). *Dalton Transactions* **2012**, *41* (32), 9672–9681.

(2) González Lucas Daniel. Molecular Machines Constructed from Multichromophore Arrays, University of East Anglia, 2014.

(3) González-Lucas, D.; Soobrattee, S. C.; Hughes, D. L.; Tizzard, G. J.; Coles, S. J.; Cammidge, A. N. Straightforward and Controlled Synthesis of Porphyrin–Phthalocyanine–Porphyrin Heteroleptic Triple-Decker Assemblies. *Chemistry - A European Journal* **2020**, *26* (47), 10724–10728.

(4) Dalai, S.; Belov, V. N.; Nizamov, S.; Rauch, K.; Finsinger, D.; De Meijere, A. Access to Variously Substituted 5,6,7,8-Tetrahydro-3H-Quinazolin-4-Ones via Diels-Alder Adducts of Phenyl Vinyl Sulfone to Cyclobutene-Annelated Pyrimidinones. *European J Org Chem* **2006**, No. 12, 2753–2765.

(5) Hellal, M.; Cuny, G. D. Microwave Assisted Copper-Free Sonogashira Coupling/5-Exo-Dig Cycloisomerization Domino Reaction: Access to 3-(Phenylmethylene)Isoindolin-1-Ones and Related Heterocycles. *Tetrahedron Lett* **2011**, *52* (42), 5508–5511.

(6) Jacob Gretton. Phthalocyanine and Subphthalocyanine Hybrid Macrocycles: Improved Accessibility and Synthetic Control via New Intermediates, University of East Anglia, 2022.

(7) Chambrier I; Cook M J. Reaction of Phthalonitrile with Alkoxide Ions. *J Chem Res Synop* **1990**, 322–323.

(8) Díaz-Moscoso, A.; Tizzard, G. J.; Coles, S. J.; Cammidge, A. N. Synthesis of Meso-Substituted Tetrabenzotriazaporphyrins: Easy Access to Hybrid Macrocycles. *Angewandte Chemie* **2013**, *125* (41), 10984–10987.

(9) Díaz-Moscoso, A.; Tizzard, G. J.; Coles, S. J.; Cammidge, A. N. Synthesis of Meso-Substituted Tetrabenzotriazaporphyrins: Easy Access to Hybrid Macrocycles. *Angewandte Chemie - International Edition* **2013**, *52* (41), 10784–10787.

(10) Alsaiari Norah. Multidecker Assemblies from Porphyrin and Phthalocyanine Derivatives, University of East Anglia, 2022.

(11) Lindsey, J. S.; Schreiman, I. C.; Hsu, H. C.; Kearney, P. C.; Marguerettaz, A. M. Rothemund and Adler-Longo Reactions Revisited: Synthesis of Tetraphenylporphyrins under Equilibrium Conditions. *J Org Chem* **1987**, *52* (5), 827–836.

(12) Kalashnikov, V. V; Pushkarev, V. E.; Tomilova, L. G. Tetrabenzotriazaporphyrins: Synthesis, Properties and Application. *Russian Chemical Reviews* **2014**, *83* (7), 657–675.

(13) Kalashnikov, V. V; Pushkarev, V. E.; Tomilova, L. G. A Novel Synthetic Approach to 27-Aryltetrabenzo [5, 10, 15] Triazaporphyrins. *Mendeleev Communications* **2011**, *21* (2), 92–93.

(14) Pushkarev, V. E.; Kalashnikov, V. V.; Tolbin, A. Y.; Trashin, S. A.; Borisova, N. E.; Simonov, S. V.; Rybakov, V. B.; Tomilova, L. G.; Zefirov, N. S. Meso-Phenyltetrabenzotriazaporphyrin Based Double-Decker Lanthanide(III) Complexes: Synthesis, Structure, Spectral Properties and Electrochemistry. *Dalton Transactions* **2015**, *44* (37), 16553–16564.

(15) Dolušicdolušic´, E.; Toppet, S.; Smeets, S.; Meervelt, L. Van; Tinant, B.; Dehaen, W. *Porphotetramethenes with 1,3-Alternate Conformation of Pyrrole Rings from Oxidative N-Alkylation of Porphyrin Tetraphenols*.

(16) Sibrian-Vazquez, M.; Hao, E.; Jensen, T. J.; Vicente, M. G. H. Enhanced Cellular Uptake with a Cobaltacarborane-Porphyrin-HIV-1 Tat 48-60 Conjugate. *Bioconjug Chem* **2006**, *17* (4), 928–934.

(17) Birin, K. P.; Gorbunova, Y. G.; Tsivadze, A. Y. Selective One-Step Synthesis of Triple-Decker (Porphyrinato) (Phthalocyaninato) Early Lanthanides: The Balance of Concurrent Processes. *Dalton Transactions* **2011**, *40* (43), 11539–11549.

(18) Martynov, A. G.; Birin, K. P.; Kirakosyan, G. A.; Gorbunova, Y. G.; Tsivadze, A. Y. Site-Selective Solvation-Induced Conformational Switching of Heteroleptic Heteronuclear Tb(III) and Y(III) Trisphthalocyaninates for the Control of Their Magnetic Anisotropy. *Molecules* **2023**, *28* (11).

(19) Martynov, A. G.; Polovkova, M. A.; Gorbunova, Y. G.; Tsivadze, A. Y. Redox-Triggered Switching of Conformational State in Triple-Decker Lanthanide Phthalocyaninates. *Molecules* **2022**, *27* (19), 6498.

(20) Sun, X.; Li, R.; Wang, D.; Dou, J.; Zhu, P.; Lu, F.; Ma, C.; Choi, C. F.; Cheng, D. Y. Y.; Ng, D. K. P.; Kobayashi, N.; Jiang, J. Synthesis and Characterization of Mixed Phthalocyaninato and Meso-Tetrakis(4-Chlorophenyl)Porphyrinato Triple-Decker Complexes - Revealing the Origin of Their Electronic Absorptions. *Eur J Inorg Chem* **2004**, No. 19, 3806–3813.

Chapter 3
Experimental

3.0 Experimental section
3.1 General methods
3.1.1 Physical measurement

The ^{1}H-NMR spectra were recorded either at 400 MHz MHz on Ultrashield Plus™ 400 spectrometer or 500 MHz using a Bruker Ascend™ 500 spectrometer in 5 mm diameter tubes. Signals are recorded in ppm as δ using residual solvent as reference. The coupling constant *J* are given in Hertz (Hz).^{13}C-NMR spectra were recorded at 101 MHz or 126 MHz using the above spectrometers. NMR spectra were performed in solution using deuterated chloroform, methanol, dichloromethane or tetrahydrofuran at room temperature unless otherwise stated.

UV- Vis spectra were taken on a Perkin-Elmer UV-Vis spectrometer Lamda XLS in solvent as stated.

Mass spectra were recorded on a Shimadzu Biotech Axima MALDI- TOF spectrometer by direct sample deposition. Characterisation of hybrids by MALDI-ToF-MS mass spectrometry was achieved by comparison of isotopic distribution to theory.

Thin layer chromatography (TLC) was carried out on a Merck aluminium backed silica gel 60 F254 coated plates and the and the compounds were visualised under short wavelength UV-light at 254 nm or long wavelength at 366 nm.

Column chromatography was achieved at ambient temperature and pressure or occasionally at moderate pressure by using Silica Gel Davisil LC 60 Å, 40–63 micron of 70–230 mesh (Grace GM BH & Co). Solvent ratios are given as v:v.

Melting points were measured and recorded using a Reichert Thermovar microscope with a thermopar based temperature control.

3.1.2 Reagents, solvents and reaction conditions

All reagents and solvents used were of analytical grade and were purchased from commercial sources and hence used without further purification, unless otherwise stated.

Petroleum ether is light petroleum of boiling point 40–60 °C. Other solvents were SLR- grade and used without drying, unless otherwise stated.

Reactions were carried out under an inert atmosphere (argon or nitrogen gas), in most air-sensitive reactions, argon was preferred.

Brine is a saturated aqueous solution of sodium chloride. Organic layers were dried over magnesium sulfate or sodium sulfate. Evaporation of solvent was carried out on a Büchi rotator evaporator at reduced pressure.

3.2 2-Bromobenzamidine hydrochloride (2.11)

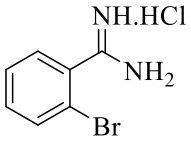

For the synthesis of 2-Bromobenzamidine hydrochloride, the procedure developed by Dalai *et al*. was followed.[1]

A solution of 2-bromobenzonitrile (4.29 g, 23 mmol) in THF (3 mL) was added to a solution of $LiN(SiMe_3)_2$ in anhydrous THF (1 M, 25 mL, 25 mmol). The reaction mixture was stirred at room temperature for 4 h. A 5M HCl solution in isopropanol (15 mL) was added to the cooled mixture. The crude reaction mixture was left overnight at 0 °C. The precipitate was filtered off and washed with diethyl ether to give the title compound as colourless crystals (5.16 g, 92%).

Mp > 250 °C

^{1}H-NMR (500 MHz, CD_3OD-d_4) δ 7.82 – 7.79 (m, 1H), 7.62 – 7.53 (m, 3H).

^{13}C-NMR (126 MHz, CD_3OD-d_4) δ 168.14, 134.76, 134.50, 133.04, 130.69, 129.25, 120.82.

3.3 (Z)-1-[(4-methoxy)benzylidene]-1H-isoindol-3-amine (2.12)

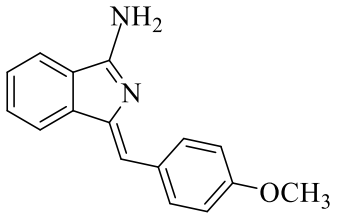

The procedure as reported by Hellal and Cuny was adopted.[2] A mixture of 2-bromobenzamidine hydrochloride (1.01 g, 4.3 mmol), BINAP (0.13 g, 0.2 mmol) and $PdCl_2(MeCN)_2$ (0.05 g, 0.02 mmol) was sealed in a microwave vessel and was then purged and refilled with N_2 three times. DBU (1.62 g, 1.60 mL, 10.6 mmol), 4-methoxyphenylacetylene (0.67 g, 0.66 mL, 5.1 mmol) and dry DMF (12 mL) were then added. The resultant reaction mixture was heated to 120 °C for 1 h by microwave irradiation. The reaction mixture was allowed to cool to room temperature and was subsequently diluted with ethyl acetate (50 mL) washed several times with saturated solution of $NaHCO_3$. The organic layer was dried over $MgSO_4$ and concentrated in vacuo. The residue collected was recrystallised twice from a mixture of DCM:PE (1:1) to afford the title compound. Other method involves purification by column chromatography using PE:AcOEt (1:1) then AcOEt as solvent gradient to yield the title compound as yellow needles (520 mg, 50%).

Mp 155–157 °C (lit. 156–157 °C)[3]

^{1}H-NMR (500 MHz, $CDCl_3$) δ 8.07 (d, *J* = 8.6 Hz, 2H), 7.78 (dt, *J* = 7.6 Hz, 1H), 7.48 (td, J = 7.5, 1.0 Hz, 1H), 7.45 (td, J = 7.5, 1.0 Hz, 1H), 7.35 (td, *J* = 7.4, 0.9 Hz, 1H), 6.94 (d, *J* = 8.2 Hz, 2H), 6.75 (s, 1H), 3.84 (s, 3H).

^{13}C-NMR (126 MHz, $CDCl_3$) δ 164.05, 159.56, 142.60, 142.07, 132.00, 130.11, 129.51, 128.77, 127.43, 120.26, 119.78, 115.60, 114.36, 55.46.

MS (MALDI-TOF): m/z = 250.67 $[M]^+$

Chemical Formula: $C_{16}H_{14}N_2O$; **Exact Mass**: 250.11 g·mol^{-1}

UV-vis (DCM): λ max (nm) (ε (dm^3.mol^{-1}.cm^{-1})) = 371 ($3.23\cdot10^4$)

3.4 1,1-dimethoxy-isoindol-3-amine (2.15)

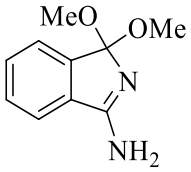

Phthalonitrile (1.01 g, 7.80 mmol) was added to a solution of freshly prepared sodium methoxide (0.42 g, 7.80 mmol) in MeOH (8 mL).[4] The mixture was allowed to stir for 2 h at room temperature. The crude was filtered and washed with ice-cold MeOH, and the white product was dried under vacuum (170 mg, 57%).

^{1}H-NMR (500 MHz, CD_3OD-d_4) δ 7.68 (dt, J = 6.9, 1.2 Hz, 1H), 7.53 – 7.46 (m, 3H), 3.28 (s, 6H).

^{13}C-NMR (126 MHz, CD_3OD-d_4) δ 166.27, 146.75, 134.78, 131.77, 130.83, 123.55, 121.91, 118.77, 51.35, 49.85.

3.5 (*Z*)-1-((1-((*Z*)-4-methoxybenzylidene)-1*H*-isoindol-3-yl)imino)-1*H*-isoindol-3-amine/ Intermediate (2.16)

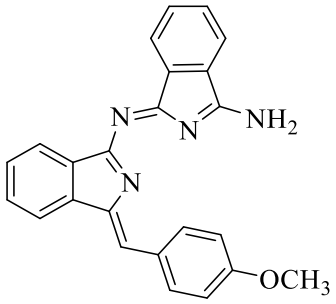

Aminoisoindoline **2.12** (0.10 g, 0.40 mmol), phthalonitrile (0.05 g, 0.40 mmol) and NaOMe (0.03 g, 0.61 mmol) was dissolved in dry MeOH (4 mL), and the reaction was refluxed.[5] After 2 h another equivalent of phthalonitrile and NaOMe was added to the reaction and was further refluxed for 1 h. The precipitate was filtered and washed with cold MeOH. The residue collected was purified by a flash column chromatography using DCM → DCM: AcOEt (1:1) → AcOEt as solvent gradient to collect an orange brown solid (73 mg, 47%).

Mp 169–172 °C

^{1}H-NMR (500 MHz, DMSO-d_6) δ 8.28 – 8.23 (m, 2H), 8.00 – 7.90 (m, 3H), 7.72 – 7.66 (m, 2H), 7.45 (td, *J* = 7.4, 1.2 Hz, 1H), 7.39 (d, *J* = 7.6 Hz, 1H), 7.32 (td, *J* = 7.3, 1.0 Hz, 1H), 7.26 (s, 1H), 7.03 – 6.98 (m, 2H), 3.81 (s, 3H).

^{13}C-NMR (126 MHz, DMSO-d_6) δ 159.63, 146.19, 141.95, 133.91, 133.01, 131.62, 131.26, 128.85, 128.34, 127.05, 122.18, 121.50, 121.37, 119.36, 114.11, 55.23.

MS (MALDI-TOF): m/z = 378.69 $[M]^+$

Chemical Formula: $C_{24}H_{18}N_4O$; **Exact Mass**: 378.15 g·mol^{-1}

UV-vis (DCM): λ max (nm) (ε ($dm^3.mol^{-1}.cm^{-1}$)) = 449 ($3.07\cdot10^4$), 324 ($3.79\cdot10^4$), 261 ($4.32\cdot10^4$).

3.6 Isolated by-product Trimer (2.18)

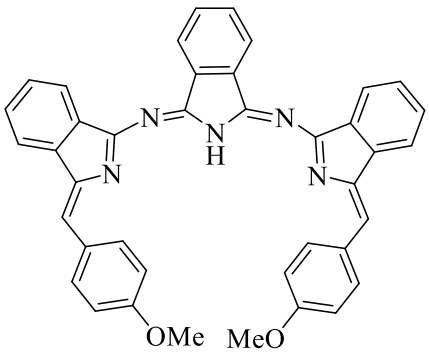

This compound was isolated as a by-product from the previous reaction as a side product and was obtained as brown solids (25 mg, 20%).

Mp 201–204 °C

^{1}H-NMR (500 MHz, $CDCl_3$) δ 8.19 (m, 2H), 7.99 (m, 2H), 7.95 (m, 4H), 7.72 (m, 4H), 7.46 (m, 4H), 6.62 (s, 2H), 6.40 (d, *J* = 8.4 Hz, 4H), 3.43 (s, 6H).

MS (MALDI-TOF): m/z = 612.59 $[M+1]^+$

Chemical Formula: $C_{40}H_{29}N_5O_2$; **Exact Mass**: 611.23 g·mol^{-1}

UV-vis (DCM): λ max (nm) (ε ($dm^3.mol^{-1}.cm^{-1}$)) = 477 ($1.59\cdot10^4$), 404 ($2.84\cdot10^4$), 332 ($5.34\cdot10^4$), 265 ($5.07\cdot10^4$).

3.7 Mg-TBTAP-OMe (2.13)[3]

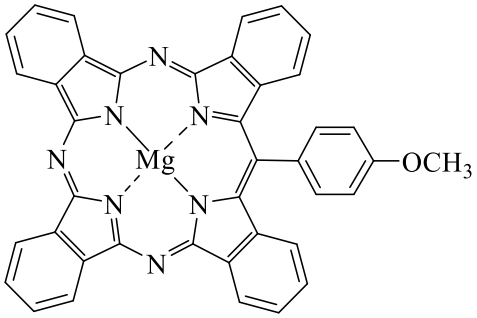

3.7.1 From One pot method

A mixture of aminoisoindoline **2.12** (0.17 g, 0.70 mmol), phthalonitrile (0.26 g, 2.03 mmol) and $MgBr_2$ (0.19 g, 1.02 mmol) was mixed in a 25 mL round bottom flask under a nitrogen atmosphere. Diglyme (2.0 mL) was then added, and the reaction was heated at a mantle temperature of 215 °C for 6 h. The solvent was removed under a nitrogen stream while cooling. A 1:1 mixture of DCM:PE (20 ml) was added, and the mixture sonicated and was left in the fridge overnight. The solid was collected by vacuum filtration and washed with cold MeOH. The crude compound was purified by flash chromatography. Using DCM→DCM: Et_3N (20:1)→DCM:THF:Et_3N (10:3:1) as eluent, the fractions were collected according to their colours. The second column purified only the green fraction using PE:THF:MeOH (10:3:1) as eluent. Recrystallisation from acetone and EtOH gave the title compound as purple crystals (160 mg, 37%).

3.7.2 From Stepwise method

Phthalonitrile (154 mg, 1.2 mmol) and $MgBr_2$ (110 mg, 0.6mmol) were mixed and stirred in dry diglyme (0.5 mL) for 10 min at a mantle temperature of 220 °C under a nitrogen atmosphere.[3] A solution of aminoisoindoline (100 mg, 0.4 mmol) and phthalonitrile (51 mg, 0.4 mmol) in dry diglyme (1 mL) was added dropwise over 1 h using a syringe pump. Finally, a solution of DABCO (67.5 mg, 0.6 mmol) and phthalonitrile (51 mg, 0.4 mmol) in dry diglyme (0.5 mL) was added dropwise over 1 h. The reaction was heated at 220 °C for a further 0.5 h under a nitrogen atmosphere. The solvent was removed under a nitrogen stream while cooling.

The purification and isolation of the compound is similar to the above procedure. Recrystallisation from acetone and EtOH gave the title compound as purple crystals (35 mg, 13%).

3.7.3 From Intermediate method

$MgBr_2$ (60 mg, 0.32 mmol) and dimer **2.16** (80 mg, 0.21 mmol) were mixed and stirred in dry xylene (3 mL) for 9 h at a mantle temperature of 170 °C under a nitrogen atmosphere. The solvent was removed under a nitrogen stream while cooling. DCM was added and the mixture sonicated and was left in the fridge overnight. The purification and isolation of the compound is similar to the above procedure. Recrystallisation from acetone and EtOH gave the title compound as purple crystals (22 mg, 33%).

Mp > 300 °C

^{1}H-NMR (500 MHz, THF-d_8) δ 9.60 (dt, *J* = 7.6, 1.0 Hz, 2H), 9.53 (m, 4H), 8.22 (m, 4H), 8.05 (br d, *J* = 8.5 Hz), 7.92 (ddd, *J* = 7.5, 6.9, 0.7 Hz, 2H), 7.62 (ddd, *J* = 8.0, 6.8, 1.2 Hz, 2H), 7.52 (br d, *J* = 8.4 Hz, 2H), 7.25 (br dt, *J* = 8.0, 0.7 Hz, 2H), 4.20 (s, 3H).

^{13}C-NMR (126 MHz, THF-d_8) δ 161.88, 156.47, 156.24, 154.14, 152.79, 143.45, 141.19, 141.09, 140.86, 140.12, 138.21, 135.87, 134.05, 129.94, 129.66, 128.89, 128.11, 127.25, 126.62, 125.96, 125.75, 123.77, 123.56, 123.50, 115.18, 68.27, 67.98, 67.80, 67.69, 67.63, 67.45, 67.28, 67.10, 56.02.

MS (MALDI-TOF): m/z = 641.77 $[M]^+$

Chemical Formula: $C_{40}H_{23}MgN_7O$; **Exact Mass**: 641.18 $g \cdot mol^{-1}$

UV-vis (dist. THF): λ max (nm) (ε ($dm^3.mol^{-1}.cm^{-1}$)) = 671 ($2.05 \cdot 10^6$), 648 ($1.22 \cdot 10^6$), 594 ($2.37 \cdot 10^5$), 444 ($2.50 \cdot 10^5$), 396 ($6.59 \cdot 10^5$).

3.8 Condensation product (2.19)

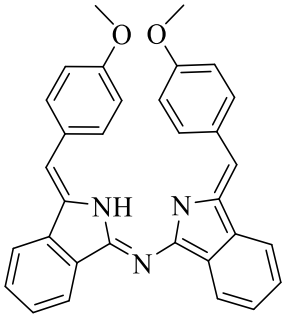

The red fraction isolated as a by-product from the one-pot procedure reaction (94 mg, 56%).[3]

Mp 203–205 °C (lit. 203–204 °C).

^{1}H-NMR (500 MHz, $CDCl_3$) δ 13.09 (s, 1H), 8.09 (dt, *J* = 7.4, 1.1 Hz, 2H), 7.88 – 7.84 (m, 4H), 7.80 (dt, *J* = 7.6, 0.9 Hz, 2H), 7.51 (dtd, *J* = 24.6, 7.3, 1.1 Hz, 4H), 6.78 (s, 2H), 6.64 – 6.57 (m, 4H), 3.70 (s, 6H).

^{13}C-NMR (101 MHz, $CDCl_3$) δ 165.86, 159.18, 140.34, 139.84, 134.70, 131.29, 130.06, 128.59, 128.04, 122.43, 119.33, 114.76, 114.14, 55.14.

MS (MADLI-TOF): m/z = 484.44 $[M+1]^+$

Chemical Formula: $C_{32}H_{25}N_3O_2$; **Exact Mass**: 483.19 g·mol^{-1}

3.9 Zn-TBTAP-OMe (2.21)

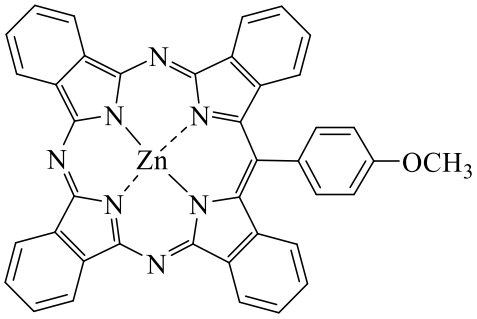

A mixture of aminoisoindoline **2.12** (50 mg, 0.20 mmol), phthalonitrile (80 mg, 0.60 mmol) and $ZnCl_2$ (54 mg, 0.40 mmol) was added in a 25 mL round bottom flask under a nitrogen atmosphere. Diglyme (2.0 mL) was then added, and the reaction was heated at 215 °C for 6 h.[3] The solvent was removed under a nitrogen stream while cooling. A 1:1 mixture of DCM:PE

(20 ml) was added, and the mixture sonicated and was left in the fridge overnight. The solid was collected by vacuum filtration and washed with cold MeOH. The crude compound was purified by flash chromatography column. Using DCM→DCM: Et_3N (20:1)→DCM:THF:Et_3N (10:3:1) as eluent, the fractions were collected according to their colours. The second column purified only the green fraction using PE:THF:MeOH (10:3:1) as eluent. Recrystallisation from acetone and EtOH gave the title compound as purple crystals (6.80 mg, 5%).

Mp >300 °C

^{1}H-NMR (500 MHz, THF-d_8) δ 9.60 (d, *J* = 7.5 Hz, 2H), 9.54 – 9.47 (m, 4H), 8.20 – 8.14 (m, 4H), 8.03 (d, *J* = 7.8 Hz, 2H), 7.90 (t, *J* = 7.2 Hz, 2H), 7.60 (td, *J* = 7.4, 6.7, 1.2 Hz, 2H), 7.54 – 7.49 (m, 2H), 7.23 (d, *J* = 8.0 Hz, 2H), 4.19 (s, 3H).

MS (MADLI-TOF): m/z = 681.63 $[M]^+$

Chemical Formula: $C_{40}H_{23}N_7OZn$; **Exact Mass**: 681.13 g·mol^{-1}

UV-vis (dist. THF): λ max (nm) (ε (dm^3.mol^{-1}.cm^{-1})) = 671 ($4.46\cdot10^4$), 647 ($2.40\cdot10^4$), 595 ($4.93\cdot10^3$), 443 ($4.03\cdot10^3$), 385 ($1.27\cdot10^3$).

3.10 Mg-TBTAP-(4-OH-Ph) (2.23)

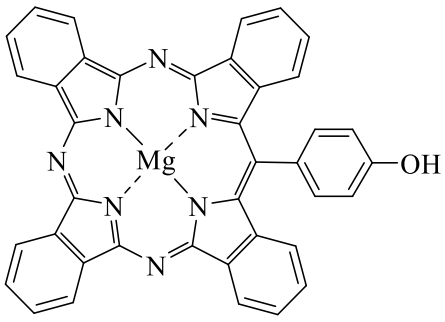

Mg-TBTAP-OMe **2.13** (195 mg, 0.30 mmol) and MgI_2 (422 mg, 1.51 mmol) was dissolved in toluene (6 mL) and the mixture was refluxed for 48 h.[3] After cooling, MeOH (50 ml) was added, and the mixture stirred for 30 minutes. The solvents were removed under vacuum and the crude was purified by column chromatography using PE: THF: MeOH (10:3:1) as eluent. Recrystallisation from acetone and MeOH gave purple crystals (128 mg, 68%).

Mp 244 °C (dec.)

^{1}H-NMR (500 MHz, THF-d_8) δ 9.58 (dt, *J* = 7.6, 1.0 Hz, 2H), 9.51 (m, 4H) 8.94 (s, 1H), 8.17 (m, 4H), 7.92 (br d, *J* = 8.4 Hz, 2H), 7.91 (br ddd, *J* = 7.5, 6.9, 0.7 Hz, 2H), 7.63 (ddd, *J* = 8.0, 6.9, 1.0 Hz, 2H), 7.35 (br d, *J* = 8.4 Hz, 2H), 7.34 (br dt, *J* = 8.0, 0.7 Hz, 2H).

^{13}C-NMR (125.7 MHz, THF-d_8) δ 159.8, 156.3, 153.2, 152.6, 143.2, 141.6, 141.2, 140.9, 140.3, 134.5, 133.9, 130.1, 129.6, 128.1, 127.4, 127.0, 125.7, 123.4, 123.2, 123.5, 116.4.

MS (MADLI-TOF): m/z = 627.78 $[M]^+$

Chemical Formula: $C_{39}H_{21}MgN_7O$; **Exact Mass**: 627.17 g·mol^{-1}

UV-vis (dist. THF): λ max (nm) (ε (dm^3.mol^{-1}.cm^{-1})) = 671 ($2.40\cdot10^5$), 648 ($2.00\cdot10^5$), 594 ($3.91\cdot10^4$), 444 ($4.41\cdot10^4$), 398 ($1.09\cdot10^5$).

3.11 5-(*p*-Hydroxyphenyl)- 10, 15, 20 triphenylporphyrin (TPP-OH) (2.8)

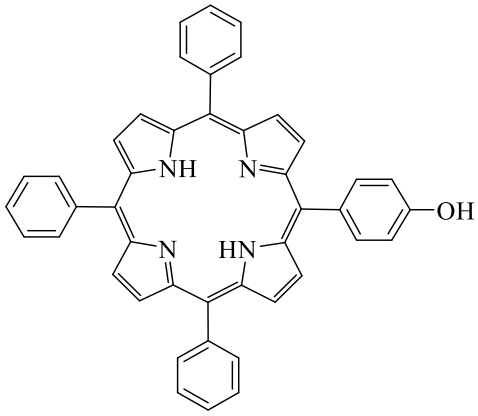

For the synthesis of the porphyrin derivative TPP-OH, a modified version of the procedure as reported by Adler was followed.[6]

Benzaldehyde (3.82 mL, 3.97 g, 37.4 mmol) and *p*-hydroxybenzaldehyde (1.52 g, 12.5 mmol) were dissolved in propionic acid and the mixture was allowed to reflux. Freshly distilled pyrrole (3.25 mL, 3.14 g, 50 mmol) was then added dropwise. Once the addition was completed, the resulting mixture was refluxed (at a temperature of 145 °C) for a further 30 min. The reaction mixture was allowed to cool to room temperature, MeOH (200 mL) was added, and the mixture was left to precipitate overnight. The resulting purple solid was collected by vacuum filtration and washed with MeOH. The crude compound was chromatographed on a

silica gel column using DCM: Pet Ether (1:1 v/v) mixture as eluent. The first pink band collected was the symmetrical porphyrin TPP. Finally, DCM (100%) was used and TPP-OH separated out as a dark purple fraction. The title compound was recrystallised from a mixture of DCM:MeOH as a purple solid (275 mg, 3.6%).

Mp > 300 °C

^{1}H-NMR (400 MHz, $CDCl_3$) δ 8.88 (d, *J* = 4.5 Hz, 2H), 8.84 (d, *J* = 4.5 Hz, 6H), 8.23 – 8.19 (m, 6H), 8.08 (d, *J* = 8.5 Hz, 2H), 7.80 – 7.71 (m, 9H), 7.22 (d, *J* = 8.5 Hz, 2H), 5.18 (s, 1H), -2.77 (s, 2H).

^{13}C-NMR (126 MHz, $CDCl_3$) δ 155.6, 142.4, 135.6, 134.8, 134.7 127.7, 126.6, 120.2, 120.1, 120.0 113.8.

MS (MALDI-TOF): m/z = 630.55 $[M]^+$

Chemical Formula: $C_{44}H_{30}N_4O$; **Exact Mass**: 630.24 $g \cdot mol^{-1}$

UV-vis (DCM): λ max (nm) (ε ($dm^3.mol^{-1}.cm^{-1}$)) = 648 ($5.18 \cdot 10^4$), 591 ($5.17 \cdot 10^4$), 550 ($6.06 \cdot 10^4$), 515 ($8.58 \cdot 10^4$), 418 ($1.2 \cdot 10^6$).

3.12 Tetraphenylporphyrin (2.28)

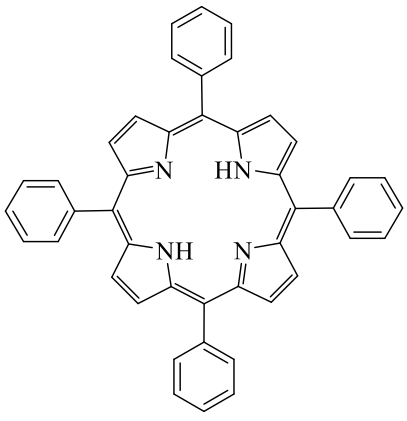

This compound was isolated from the previous reaction as side product and was obtained as a purple solid (0.93 g, 16%).

Mp > 350 ˚C.

^{1}H-NMR (400 MHz, $CDCl_3$) δ 8.85 (s, 8H), 8.22 (d, *J* = 7.8 Hz, 8H), 7.80 – 7.72 (m, 12H), -2.77 (s, 2H).

^{13}C-NMR (126 MHz, CDCl3) δ 142.20, 134.59, 127.73, 126.71, 120.16.

MS (MALDI-TOF): m/z = 614.94 $[M]^+$

Chemical Formula: $C_{44}H_{30}N_4$; **Exact Mass**: 614.25 $g \cdot mol^{-1}$

UV-vis (DCM): λ max (nm) (ε ($dm^3.mol^{-1}.cm^{-1}$)) = 648 ($5.42 \cdot 10^4$), 590 ($5.46 \cdot 10^4$), 549 ($6.13 \cdot 10^4$), 514 ($8.60 \cdot 10^4$), 417 ($1.10 \cdot 10^6$).

3.13 5,10,15-Tris-[*p*-(methoxy)phenyl]-20-(4-hydroxyphenyl) porphyrin (2.56)

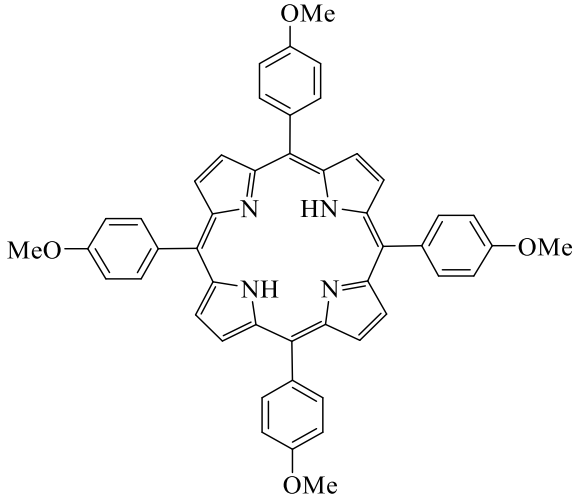

Following a modified version of Adler's general procedure,[6] freshly distilled pyrrole (3.35 g, 50 mmol) was added dropwise to *p*-methoxybenzaldehyde (6.81 g, 50 mmol) in refluxing propionic acid (150 mL). After 30 min, the mixture was cooled down to room temperature and MeOH (200 mL) added. The mixture was filtered and washed several times by MeOH. A purple solid of title compound was obtained (3.0 g, 32.6%).

Mp > 300 °C

^{1}H-NMR (500 MHz, $CDCl_3$) δ 8.86 (s, 8H), 8.15 – 8.10 (m, 8H), 7.31 – 7.27 (m, 8H), 4.10 (s, 12H), -2.75 (s, 2H).

^{13}C-NMR (101 MHz, $CDCl_3$) δ 159.53, 135.74, 134.81, 119.88, 112.34, 55.73.

MS (MALDI-TOF): m/z = 735.39 $[M+1]^+$

Chemical Formula: $C_{48}H_{38}N_4O_4$; **Exact Mass**: 734.29 $g \cdot mol^{-1}$

UV-vis (DCM) λ max (nm) (ε ($dm^3.mol^{-1}.cm^{-1}$)) = 651 ($4.78 \cdot 10^4$), 592 ($4.77 \cdot 10^4$), 556 ($5.27 \cdot 10^4$), 520 ($5.72 \cdot 10^4$), 422 ($3.43 \cdot 10^5$).

3.14 Porphyrin C_{10} dyad (TPP-O-$(CH_2)_{10}$-O-TPP) (2.1)

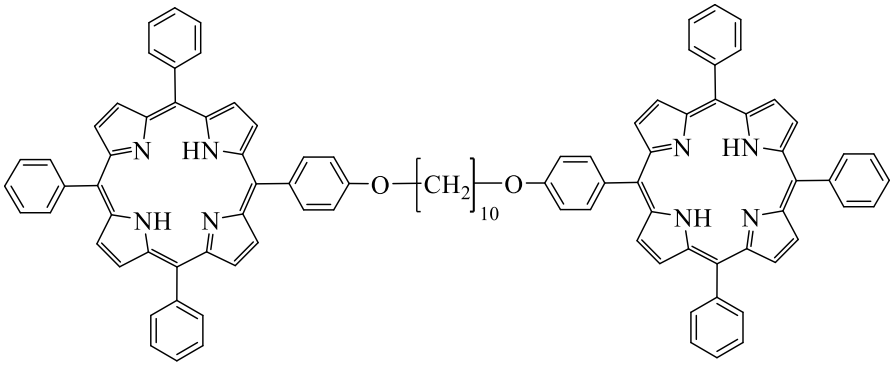

A mixture of TPP-OH **2.28** (200 mg, 0.32 mmol) and 1,10- dibromodecane (47.6 mg, 0.16 mmol), acetone (20 mL) and K_2CO_3 (220 mg, 1.5 mmol) was placed in a sealed tube and heated at 70 °C for 7 days.[7] The solvent was removed, and the residue dissolved in DCM and washed with water. The organic layer was evaporated and was finally purified by two slow and careful recrystallisations from a mixture of DCM: MeOH, to yield the pure product as a purple solid (112 mg, 50%).

Mp > 300 °C

^{1}H-NMR (500 MHz, $CDCl_3$) δ 8.89 (d, *J* = 4.5 Hz, 4H), 8.83 (m, 12H), 8.21 (dd, *J* = 7.6, 1.5 Hz, 12H), 8.12(dd, *J* = 7.6, 1.5 Hz, 4H), 7.77 – 7.70 (m, 18H), 7.29 (dd, *J* = 7.6, 1.5 Hz, 4H), 4.28 (t, *J* = 6.5 Hz, 4H), 2.06 – 1.98 (m, 4H), 1.72 – 1.64 (m, 4H), 1.54 (s, 8H), -2.76 (s, 4H);

^{13}C-NMR (126 MHz, $CDCl_3$) δ 159.2, 142.4, 135.8, 134.7, 134.5, 127.8, 126.8, 125.8, 120.3, 120.2, 120.1, 112.9, 68.51, 31.01, 29.86, 29.75, 26.50.

MS (MALDI-tof): m/z = 1400.80 $[M+1]^+$

Chemical Formula: $C_{98}H_{78}N_8O_2$; **Exact Mass**: 1399.63 $g \cdot mol^{-1}$

UV-vis (DCM) λ max (nm) (ε ($dm^3.mol^{-1}.cm^{-1}$)) = 648 ($1.06 \cdot 10^4$), 591 ($1.14 \cdot 10^4$), 551 ($1.86 \cdot 10^4$), 516 ($3.84 \cdot 10^4$), 419 ($9.51 \cdot 10^5$).

3.15 Metal free phthalocyanine (2.40)

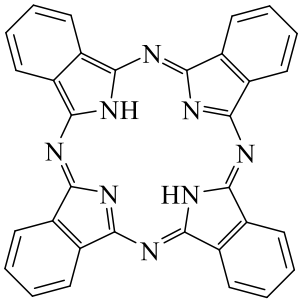

Phthalonitrile (0.5 g, 4 mmol) was dissolved in 1-pentanol (6 mL) and the mixture was stirred and heated at a temperature of 120 °C. An excess of lithium (50 mg, 7.2 mmol) was added to the reaction mixture which was refluxed for another hour. Acetic acid (10 mL) was then added, and the mixture was refluxed for another hour. The resulting reaction mixture was allowed to cool to room temperature and methanol (100 mL) was added to precipitate the product, a dark blue solid of pure phthalocyanine which was collected by vacuum filtration (255 mg, 50%).

Mp > 300 °C

MS (MALDI-tof): m/z = 514.75 $[M]^+$

Chemical Formula: $C_{32}H_{18}N_8$; **Exact Mass**: 514.17 $g \cdot mol^{-1}$

UV-vis (THF)/nm (log ε): 689 (0.68), 654 (0.72), 339 (0.56).

3.16 5-(*p*-bromodecanoxyphenyl) -10,15,20-triphenylporphyrin (TPP-O-C_{10}-Br) (2.29)

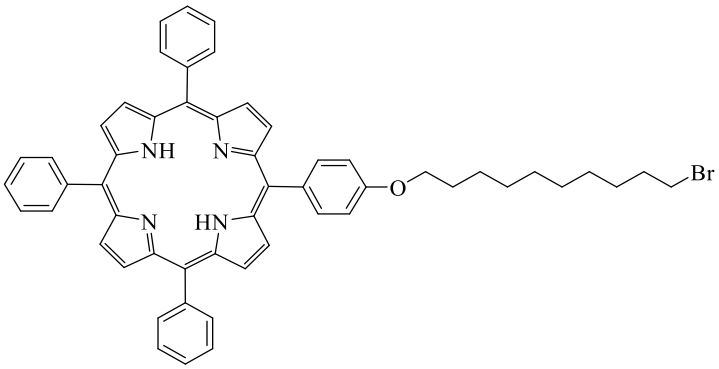

TPP-OH **2.28** (0.20 g, 0.32 mmol), 1,10-dibromohexane (0.95 g, 3.17 mmol) and potassium carbonate (0.44 g, 3.17 mmol) were added to dry DMF (40 mL), and the mixture stirred at room temp overnight. The crude mixture was then precipitated with distilled water (100 mL) and was extracted with DCM (3 x 50 mL). The combined organic extracts were dried ($MgSO_4$) and the solvent removed in vacuo. The product was purified by column chromatography (eluting with DCM: petroleum ether, 1:1). Recrystallisation from DCM: MeOH gave bromoalkoxyporphyrin as a purple solid. (0.12 g, 47%).

Mp > 300 °C

^{1}H-NMR (500 MHz, $CDCl_3$) δ 8.89 (d, *J* = 4.5 Hz, 2H), 8.84 (s, 6H), 8.22 (m, 6H), 8.12 (dd, *J* = 2.0, 6.5 Hz, 2H), 7.77 (m, 9H), 7.28 (dd, *J* = 2.0, 6.5 Hz, 2H), 4.25 (t, *J* = 7 Hz, 2H), 3.44 (t, *J* = 7 Hz, 2H), 2.01 – 1.96 (m, 2H), 1.90 (m, 2H), 1.63 (m, 2H), 1.39 (m, 10H), -2.75 (s, 2H).

^{13}C-NMR (126 MHz, $CDCl_3$) δ 159.02, 142.26, 135.63, 134.58, 134.35, 127.70, 126.69, 120.07, 112.76, 68.33, 34.09, 32.88, 29.56, 29.53, 29.50, 29.46, 28.83, 28.23, 26.25.

MS (MALDI-tof): m/z = 851.69 $[M+1]^+$

Chemical Formula: $C_{54}H_{49}BrN_4O$; **Exact Mass**: 850.31 g·mol^{-1}

UV-vis (DCM): λ max (nm) (ε ($dm^3.mol^{-1}.cm^{-1}$)) = 651 ($5.59\cdot10^4$), 592 ($5.67\cdot10^4$), 551 ($6.37\cdot10^4$), 516 ($8.17\cdot10^4$), 418 ($9.06\cdot10^5$).

3.17 5-(*p*-bromododecanoxyphenyl)-10,15,20-triphenylporphyrin (TPP-O-C_{12}-Br) (2.34)

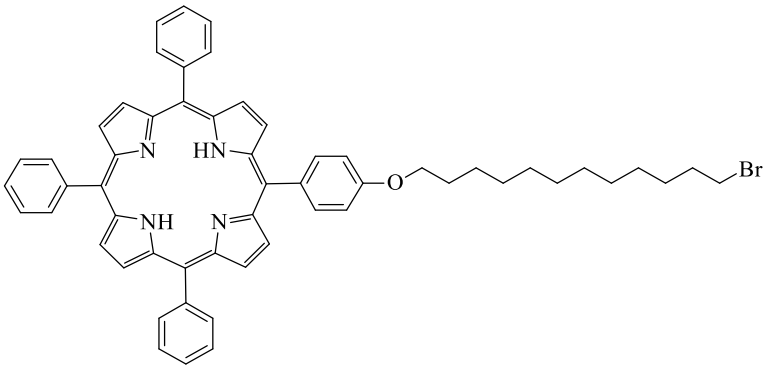

TPP-OH **2.28** (0.40 g, 0.63 mmol), 1,12-dibromododecane (2.08 g, 6.34 mmol) and potassium carbonate (0.88 g, 6.34 mmol) were added to dry DMF (80 mL), and the mixture stirred at room temp overnight. The crude mixture was then precipitated with distilled water (100 mL) and was extracted with DCM (3 x 50 mL). The combined organic extracts were dried ($MgSO_4$) and the solvent removed in vacuo. The product was purified by column chromatography (eluting with DCM: PE, v/v 1:1). Recrystallisation from DCM: MeOH gave bromoalkoxyporphyrin as a purple solid. (0.51 g, 92%).

Mp > 300 °C

^{1}H-NMR (400 MHz, $CDCl_3$) δ 8.89 (d, *J* = 4.8 Hz, 2H), 8.84 (s, 6H), 8.25 (m, 6H), 8.14 (dd, *J* = 2.0, 6.5 Hz, 2H), 7.80 (m, 9H), 7.29 (dd, *J* = 2.0, 6.5 Hz, 2H), 4.25 (t, *J* = 6.5 Hz, 2H), 3.41 (d, *J* = 6.9 Hz, 2H), 2.02 (m, 2H), 1.91(m, 2H), 1.70 (m, 4H), 1.45 (m, 12H), -2.77 (s, 2H).

^{13}C-NMR (126 MHz, $CDCl_3$) δ 159.15, 142.38, 142.35, 135.76, 134.71, 134.46, 127.83, 126.82, 120.35, 120.20, 120.08, 112.87, 68.46, 34.23, 33.00, 29.79, 29.76, 29.72, 29.67, 29.65, 29.62, 28.95, 28.35, 26.38.

MS (MALDI-tof): m/z = 879.84 $[M+1]^+$

Chemical Formula: $C_{56}H_{53}BrN_4O$; **Exact Mass:** 878.34 g·mol^{-1}

UV-vis (DCM): λ max (nm) (ε (dm^3.mol^{-1}.cm^{-1})) = 647 ($5.38\cdot10^4$), 592 ($5.60\cdot10^4$), 550 ($6.49\cdot10^4$), 517 ($8.78\cdot10^4$), 419 ($1.19\cdot10^6$).

3.18 Mg-TBTAP-O-C_{10}-Br (2.31)

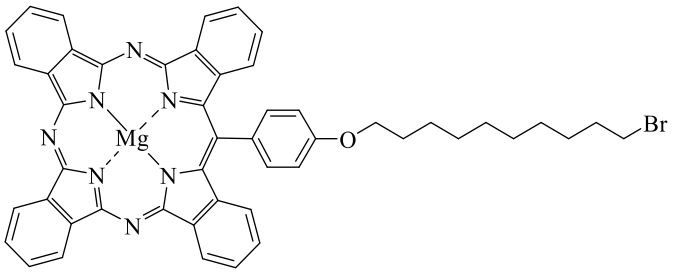

Mg-TBTAP-OH **2.23** (0.12 g, 0.19 mmol), 1,10-dibromohexane (0.57 g, 1.91 mmol) and potassium carbonate (0.26 g, 1.91 mmol) were dissolved in acetone (20 mL) and the mixture was left to stir at 70 °C overnight. The crude mixture was then precipitated with distilled water (100 mL) and was extracted with DCM (3 x 50 mL). The combined organic extracts were dried ($MgSO_4$) and the solvent removed in vacuo. The product was purified by column chromatography eluting with DCM: THF (20:1). Recrystallisation from acetone/EtOH gave the title product as a green solid (78 mg, 48%).

Mp > 300 °C

^{1}H-NMR (500 MHz, THF-d_8) δ 9.60 (d, *J* = 7.5 Hz, 2H), 9.55 – 9.47 (m, 4H), 8.21 – 8.15 (m, 4H), 8.06 – 8.01 (m, 2H), 7.92 (t, *J* = 7.2 Hz, 2H), 7.64 – 7.59 (m, 2H), 7.53 – 7.48 (m, 2H), 7.26 (d, *J* = 8.0 Hz, 2H), 4.41 (t, *J* = 6.5 Hz, 2H), 3.48 (t, *J* = 6.8 Hz, 2H), 2.12 – 2.05 (m, 2H), 1.94 – 1.86 (m, 2H), 1.79 – 1.74 (m, 2H), 1.63 – 1.41 (m, 10H).

^{13}C-NMR (126 MHz, THF-d_8) δ 161.43, 156.61, 153.57, 152.66, 143.60, 141.32, 141.21, 140.99, 140.25, 135.88, 134.14, 130.08, 129.79, 128.23, 127.37, 126.80, 125.90, 123.90, 123.69, 123.62, 115.88, 69.37, 68.39, 30.79, 30.73, 30.68, 29.98, 29.32, 27.42, 26.56, 25.98.

MS (MALDI-tof): m/z = 847.30 $[M]^+$

Chemical Formula: $C_{49}H_{40}BrMgN_7O$; **Exact Mass**: 847.23 g·mol^{-1}

UV-vis (dist. THF): λ max (nm) (ε (dm^3.mol^{-1}.cm^{-1})) = 671 ($3.37\cdot10^5$), 648 ($1.95\cdot10^5$), 594 ($3.84\cdot10^4$), 444 ($4.15\cdot10^4$), 398 ($1.06\cdot10^5$).

3.19 Mg-TBTAP-O-C_{12}-Br (2.33)

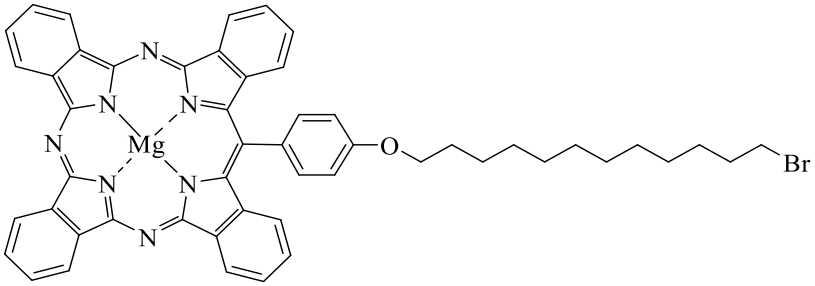

Mg-TBTAP-OH **2.23** (0.11 g, 0.18 mmol), 1,12-dibromododecane (0.57 g, 1.80 mmol) and potassium carbonate (0.26 g, 1.91 mmol) were dissolved in acetone (20 mL) and the mixture was left to stir at 70 °C overnight. The crude mixture was then precipitated with distilled water (100 mL) and was extracted with DCM (3 x 50 mL). The combined organic extracts were dried ($MgSO_4$) and the solvent removed in vacuo. The product was purified by column chromatography (eluting with DCM: THF (20:1). Recrystallisation from acetone/EtOH gave the title product as a green solid (80 mg, 52%).

Mp > 300 °C

^{1}H-NMR (500 MHz, THF-d_8) δ 9.59 (dt, *J* = 7.6, 1.0 Hz, 2H), 9.54 – 9.48 (m, 4H), 8.21 – 8.15 (m, 4H), 8.04 – 8.00 (m, 2H), 7.92 (t, *J* = 7.2 Hz, 2H), 7.64 – 7.59 (m, 2H), 7.53 – 7.49 (m, 2H), 7.26 (d, *J* = 8.0 Hz, 2H), 4.41 (t, *J* = 6.5 Hz, 2H), 3.46 (t, *J* = 6.8 Hz, 2H), 2.12 – 2.03 (m, 2H), 1.91 – 1.84 (m, 2H), 1.61 – 1.55 (m, 2H), 1.54 – 1.32 (m, 14H).

^{13}C-NMR (126 MHz, THF-d_8) δ 161.44, 156.56, 153.52, 152.60, 143.55, 141.33, 141.22, 140.99, 140.25, 135.86, 134.14, 130.08, 129.79, 128.23, 127.38, 126.82, 125.91, 123.91, 123.70, 123.63, 115.86, 69.38, 68.10, 34.51, 34.07, 30.90, 30.84, 30.79, 30.74, 30.70, 29.97, 29.29, 27.43, 25.98, 25.81.

MS (MALDI-tof): m/z = 875.45 $[M]^+$

Chemical Formula: $C_{51}H_{44}BrMgN_7O$; **Exact Mass**: 875.26 g·mol^{-1}

UV-vis (dist. THF): λ max (nm) (ε (dm^3.mol^{-1}.cm^{-1})) = 671 ($6.90\cdot10^5$), 648 ($4.03\cdot10^5$), 594 ($7.96\cdot10^4$), 444 ($8.51\cdot10^4$), 398 ($2.22\cdot10^5$).

3.20 Unsymmetrical C_{10} dyad (Mg-TBTAP-O-C_{10}-O-TPP) (2.32)

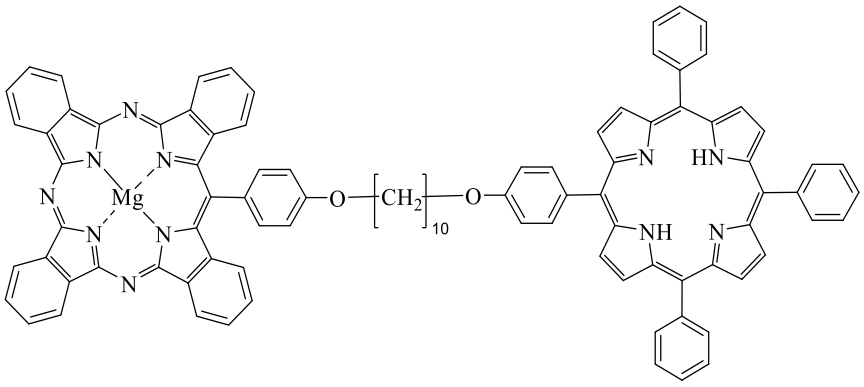

3.20.1 Dyad 2.31 from Mg-TBTAP-O-C_{10}-Br 2.31

A mixture of Mg-TBTAP-O-C_{10}-Br **2.31** (0.1 g, 0.11 mmol) and TPP-OH **2.8** (0.04 g, 0.07 mmol) was dissolved in DMF (2 mL), then an excess of potassium carbonate (0.2 g, 1.4 mmol) was added, and the mixture was heated to 80 °C for 14 days. The crude mixture was then precipitated with 50 mL of distilled water and was extracted with DCM (3 x 50 mL). The organic layer was finally washed with brine solution. The combined organic extracts were dried ($MgSO_4$) and the solvent removed in vacuo. The product was purified by column chromatography (eluting with DCM: THF 20:1). Recrystallisation from Acetone/EtOH gave the title product as a green-purple solid (35 mg, 23%).

3.20.2 Dyad 2.31 from TPP-O-C_{10}-Br 2.29

A mixture of TPP-O-C_{10}-Br **2.29** (0.12 g, 0.14 mmol) and Mg-TBTAP-OH **2.23** (0.05 g, 0.08 mmol) was dissolved in DMF (2 mL), then an excess of potassium carbonate (0.2 g, 1.4 mmol) was added, and the mixture was heated to 80 °C for 7 days. The crude mixture was then precipitated with 50 ml of distilled water and was extracted with DCM (3 x 50 mL). The organic layer was finally washed with brine solution. The combined organic extracts were dried ($MgSO_4$) and the solvent removed in vacuo. The product was purified by column chromatography (eluting with DCM: THF 20:1). Recrystallisation from Acetone/EtOH gave the title product as a green-purple solid (80 mg, 43%).

Mp > 300 °C

^{1}H-NMR (500 MHz, THF-d_8) δ 9.59 (dt, *J* = 7.5, 1.0 Hz, 2H), 9.52 – 9.47 (m, 4H), 8. 81 (d, *J* = 4.7 Hz, 2H), 8.23 – 8.18 (d, *J* = 4.8 Hz, 6H), 8.23 – 8.18 (m, 6H), 8.14 – 8.09 (m,, 4H), 8.05 – 8.00 (m, 2H), 7.93 – 7.88 (m, 2H), 7.79 – 7.73 (m, 9H), 7.62 (ddd, *J* = 8.1, 6.8, 1.2 Hz, 2H), 7.54 – 7.50 (m, 2H), 7.37 – 7.33 (m, 2H), 7.27 (d, *J* = 8.0 Hz, 2H), 4.42 (t, *J* = 6.5 Hz, 2H), 4.30 (t, *J* = 6.3 Hz, 2H), 2.14 – 2.07(m, 2H), 2.06 – 2.00 (m, 2H), 1.80 – 1.76 (m, 4H), 1.68 – 1.57 (m, 8H), -2.80 (s, 2H).

^{13}C-NMR (126 MHz, THF-d_8) δ 161.44, 160.50, 156.57, 153.53, 152.63, 143.57, 143.50, 143.46, 141.33, 141.20, 140.98, 140.25, 136.54, 135.87, 135.50, 135.32, 134.14, 130.06, 129.77, 128.75, 128.24, 127.73, 127.38, 126.82, 125.91, 123.89, 123.68, 123.63, 121.35, 121.07, 120.94, 115.88, 113.75, 69.38, 69.08, 68.10, 30.92, 30.88, 30.78, 30.75, 30.74, 27.49, 27.47, 25.98, 25.81, 25.65.

MS (MALDI-tof): m/z = 1396.77 $[M]^+$

Chemical Formula: $C_{93}H_{69}MgN_{11}O_2$; **Exact Mass**: 1396.55 g·mol^{-1}

UV-vis (dist. THF): λ max (nm) (ε (dm^3.mol^{-1}.cm^{-1})) = 671 ($5.86\cdot10^5$), 648 ($3.52\cdot10^5$), 616 ($7.17\cdot10^4$), 594 ($8.61\cdot10^4$), 549 ($3.54\cdot10^4$), 514 ($5.56\cdot10^4$), 444 ($8.34\cdot10^4$), 417 ($1.32\cdot10^6$).

3.21 Isolated compound from above reaction (2.62)

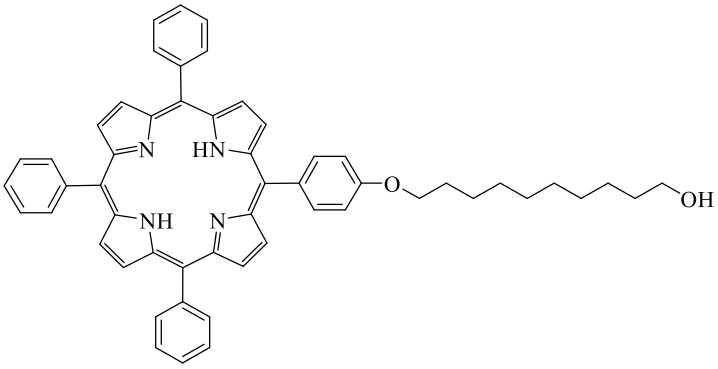

This compound was isolated from the previous reaction as side product and was obtained as a purple solid (20 mg, 18%).

Mp > 300 °C

^{1}H-NMR (500 MHz, $CDCl_3$) δ 8.89 (d, *J* = 4.8 Hz, 2H), 8.84 (d, *J* = 3.0 Hz, 6H), 8.22 (dt, *J* = 7.7, 1.3 Hz, 6H), 8.14 – 8.10 (m, 2H), 7.81 – 7.72 (m, 9H), 7.30 – 7.27 (m, 2H), 4.25 (t, *J* = 6.5 Hz, 2H), 3.67 (t, *J* = 6.4 Hz, 2H), 1.98 – 1.92 (m, 2H), 1.61 – 1.58 (m, 2H), 1.52 – 1.45 (m, 2H), 1.35 (m, 10H), -2.76 (s, 2H).

^{13}C-NMR (126 MHz, $CDCl_3$) δ 159.15, 142.38, 142.35, 135.76, 134.71, 134.46, 127.83, 126.82, 120.35, 120.20, 120.08, 112.88, 68.46, 63.25, 32.97, 29.75, 29.73, 29.65, 29.61, 26.38, 25.92.

MS (MALDI-tof): m/z = 786.63 $[M]^+$

Chemical Formula: $C_{54}H_{50}N_4O_2$; **Exact Mass**: 786.39 g·mol^{-1}

UV-vis (DCM): λ max (nm) (ε (dm^3.mol^{-1}.cm^{-1})) = 646 (4.58·10^4), 591 (4.72·10^4), 551 (5.24·10^4), 517 (6.49·10^4), 418 (6.73·10^5).

3.22 Unsymmetrical C_{12} dyad (Mg-TBTAP-O-C_{12}-O-TPP) (2.35)

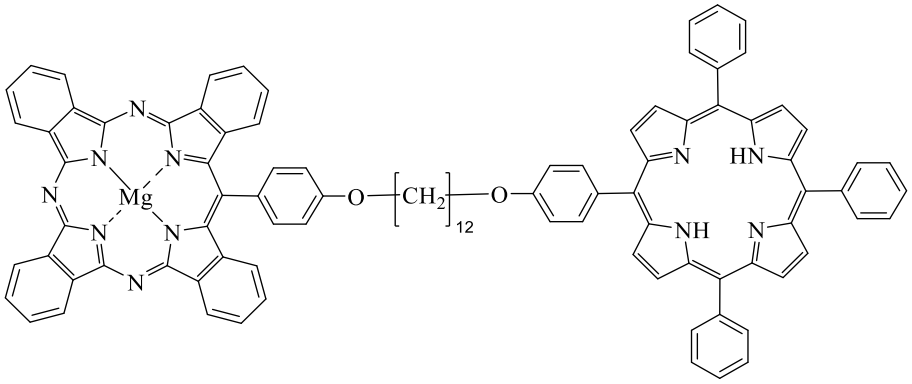

3.22.1 From Mg-TBTAP-O-C_{12}-Br 2.33

A mixture of Mg-TBTAP-O-C_{12}-Br **2.33** (0.10 g, 0.11 mmol) and TPP-OH **2.8** (0.05 g, 0.08 mmol) was dissolved in DMF (2 mL), then an excess of potassium carbonate (0.2 g, 1.4 mmol) was added, and the mixture was heated to 80 °C for 10 days. The crude mixture was then precipitated with 50 mL of distilled water and was extracted with DCM (3 x 50 mL). The combined organic extracts were dried ($MgSO_4$) and the solvent removed in vacuo. The product was purified by column chromatography (eluting with DCM: THF 20:1). Recrystallisation from acetone/EtOH gave the title product as a green-purple solid (39 mg, 25%).

3.22.2 From TPP-O-C_{12}-Br

A mixture of TPP-O-C_{12}-Br **2.34** (0.12 g, 0.14 mmol) and Mg-TBTAP-OH **2.23** (0.08 g, 0.10 mmol) was dissolved in DMF (2.5 mL), then an excess of potassium carbonate (0.2 g, 1.4 mmol) was added, and the mixture was heated to 80 °C for 10 days. The crude mixture was then precipitated with 50 mL of distilled water and was extracted with DCM (3 x 50 mL). The combined organic extracts were dried ($MgSO_4$), and the solvent removed in vacuo. The product was purified by column chromatography (eluting with DCM: THF 20:1). Recrystallisation from acetone/EtOH gave the title product as a green-purple solid (100 mg, 51%).

Mp > 300 °C

^{1}H-NMR (500 MHz, THF-d_8) δ 9.59 (d, *J* = 7.5 Hz, 2H), 9.53 – 9.47 (m, 4H), 8.87 (d, *J* = 4.7 Hz, 2H), 8.81 (d, *J* = 4.3 Hz, 6H), 8.21 (dt, *J* = 7.6, 1.8 Hz, 6H), 8.17 – 8.13 (m, 4H), 8.12 – 8.09 (m, 2H), 8.03 – 8.00 (m, 2H), 7.90 (t, *J* = 7.2 Hz, 2H), 7.79 – 7.74 (m, 9H), 7.61 (ddd, *J* = 8.1, 6.8, 1.2 Hz, 2H), 7.51 – 7.48 (m, 2H), 7.35 – 7.32 (m, 2H), 7.26 (d, *J* = 8.0 Hz, 2H), 4.39 (t, *J* = 6.4 Hz, 2H), 4.28 (t, *J* = 6.4 Hz, 2H), 2.10 – 2.05 (m, 2H), 2.03 – 1.95 (m, 2H), 1.68 – 1.46 (m, 14H), 1.31 (d, *J* = 14.8 Hz, 2H).

^{13}C-NMR (126 MHz, THF-d_8) δ 161.43, 160.49, 156.57, 153.53, 152.62, 143.57, 143.50, 143.46, 141.33, 141.20, 140.97, 140.25, 136.53, 135.85, 135.50, 135.31, 134.13, 130.05, 129.77, 128.75, 128.24, 127.73, 127.38, 126.82, 125.91, 123.89, 123.68, 123.63, 121.35, 121.07, 120.94, 115.86, 113.74, 69.35, 69.06, 68.39, 68.10, 30.94, 30.87, 30.76, 30.73, 27.46, 26.55, 25.98, 25.81.

MS (MALDI-tof): m/z = 1424.45 $[M]^+$

Chemical Formula: $C_{95}H_{73}MgN_{11}O_2$; **Exact Mass**: 1424.58 g·mol^{-1}

UV-vis (dist. THF): λ max (nm) (ε (dm^3.mol^{-1}.cm^{-1})) = 671 ($6.26\cdot10^5$), 648 ($3.71\cdot10^5$), 616 ($6.87\cdot10^4$), 594 ($8.41\cdot10^4$), 549 ($2.92\cdot10^4$), 514 ($4.92\cdot10^4$), 444 ($8.27\cdot10^4$), 417 ($1.34\cdot10^6$).

3.23 Isolated compound from above reaction (2.63)

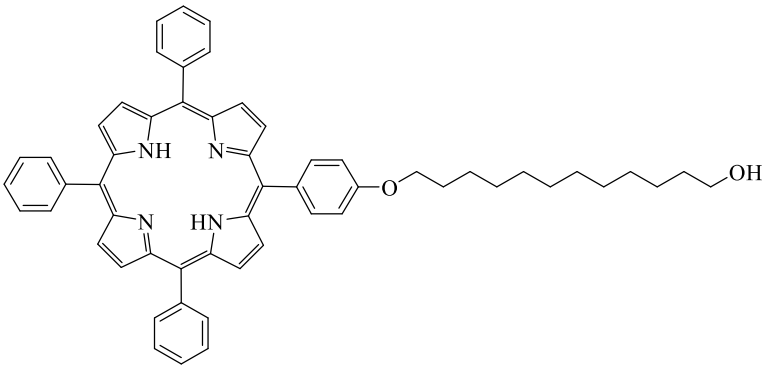

This compound was isolated from the previous reaction as side product and was obtained as a purple solid (18 mg, 16%).

Mp > 300 °C

^{1}H-NMR (500 MHz, $CDCl_3$) δ 8.89 (d, *J* = 4.8 Hz, 2H), 8.84 (d, *J* = 3.0 Hz, 6H), 8.22 (dt, *J* = 7.5, 1.3 Hz, 6H), 8.14 – 8.09 (m, 2H), 7.80 – 7.72 (m, 9H), 7.28 (d, *J* = 6.9 Hz, 2H), 4.25 (t, *J* = 6.5 Hz, 2H), 3.64 (t, *J* = 6.4 Hz, 2H), 1.98 – 1.85 (m, 2H), 1.64 – 1.56 (m, 4H), 1.52 – 1.45 (m, 2H), 1.35 (s, 12H), -2.76 (s, 2H).

^{13}C-NMR (126 MHz, $CDCl_3$) δ 159.14, 142.38, 142.35, 135.76, 134.71, 134.45, 127.83, 126.82, 120.38, 120.22, 120.21, 120.09, 112.87, 68.44, 63.21, 32.95, 29.79, 29.78, 29.67, 29.63, 29.60, 26.37, 25.90.

MS (MALDI-tof): m/z = 814.99 $[M]^+$

Chemical Formula: $C_{56}H_{54}N_4O_2$; **Exact Mass**: 814.42 $g \cdot mol^{-1}$

UV-vis (DCM): λ max (nm) (ε ($dm^3.mol^{-1}.cm^{-1}$)) = 647 ($4.38 \cdot 10^4$), 590 ($4.61 \cdot 10^4$), 550 ($5.36 \cdot 10^4$), 516 ($7.37 \cdot 10^4$), 418 ($1.01 \cdot 10^6$).

3.24 Isolated compound from above reaction (2.64)

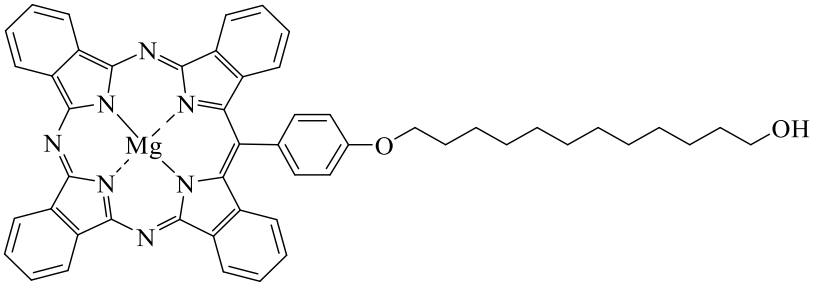

This compound was isolated from the unsymmetrical dyad as side product and was obtained as a purple solid (9 mg, 10%).

Mp > 300 °C

^{1}H-NMR (500 MHz, THF-d_8) δ 9.60 (d, *J* = 7.5 Hz, 2H), 9.52 (ddd, *J* = 8.7, 4.5, 1.6 Hz, 4H), 8.21 – 8.15 (m, 4H), 8.04 – 8.00 (m, 2H), 7.92 (t, *J* = 7.2 Hz, 2H), 7.64 – 7.59 (m, 2H), 7.54 – 7.49 (m, 2H), 7.26 (d, *J* = 8.0 Hz, 2H), 4.41 (t, *J* = 6.5 Hz, 2H), 3.47 (td, *J* = 6.4, 4.8 Hz, 2H), 2.12 – 2.04 (m, 2H), 1.62 – 1.54 (m, 2H), 1.54 – 1.33 (m, 16H).

^{13}C-NMR (126 MHz, THF-d_8) δ 161.43, 156.63, 153.59, 152.70, 143.64, 141.31, 141.19, 140.97, 140.24, 135.88, 134.13, 130.06, 129.77, 128.22, 127.36, 126.78, 125.89, 123.88, 123.67, 123.60, 115.90, 69.38, 68.10, 62.72, 34.29, 30.96, 30.92, 30.89, 30.84, 30.80, 30.73, 27.43, 27.16.

MS (MALDI-tof): m/z = 811.84 $[M]^+$

Chemical Formula: $C_{51}H_{45}MgN_7O_2$; **Exact Mass:** 811.35 g·mol^{-1}

UV-vis (dist. THF): λ max (nm) (ε (dm^3.mol^{-1}.cm^{-1})) = 671 ($4.09\cdot10^5$), 648 ($2.39\cdot10^5$), 594 ($4.72\cdot10^4$), 444 ($5.04\cdot10^4$), 398 ($1.32\cdot10^5$).

3.25 Symmetrical C_{10} dyad (Mg-TBTAP-O-C_{10}-O-Mg-TBTAP) (2.38)

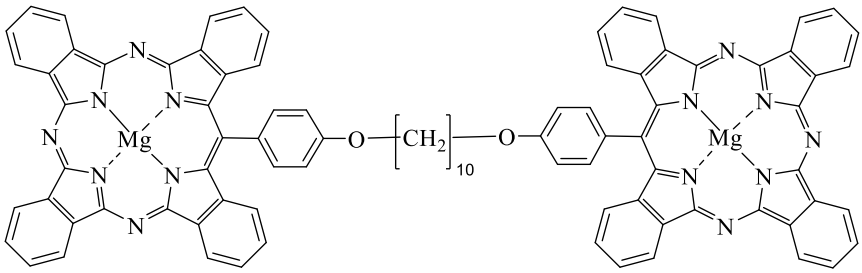

3.25.1 From Mg-TBTAP-O-C_{10}-Br (2.31)

A mixture of Mg-TBTAP-O-C_{10}-Br **2.31** (76.1 mg, 0.09 mmol) and Mg-TBTAP-OH **2.23** (37.6 mg, 0.06 mmol) was dissolved in DMF (2.5 mL), then an excess of potassium carbonate (0.2 g, 1.4 mmol) was added, and the mixture was heated to 70 °C for 12 days. The crude mixture was then precipitated with 50 mL of distilled water and was extracted with DCM (3 x 50 mL). The combined organic extracts were dried ($MgSO_4$) and the solvent removed in vacuo. The product was purified by column chromatography (eluting with DCM: THF (20:1). Recrystallisation from Acetone/EtOH gave the title product as a green solid. (25 mg, 30%).

3.25.2 From Mg-TBTAP-OH (2.23)

A mixture of 1,10-dibromodecane (23.8 mg, 0.08 mmol) and Mg-TBTAP-OH **2.23** (100 mg, 0.16 mmol) was dissolved in DMF (2 mL), then an excess of K_2CO_3 (240 mg, 1.6 mmol) was added and the mixture heated at 70 °C for 14 days. The crude mixture was then precipitated with 50 ml of distilled water and was extracted with DCM (3 x 50 mL). The combined organic extracts were dried ($MgSO_4$) and the solvent removed in vacuo. The product was purified by column chromatography (eluting with DCM: THF 20:1). Recrystallisation from Acetone/EtOH gave the title product as a green solid. (30 mg, 27%).

Mp > 300 °C

^{1}H-NMR (500 MHz, THF-d_8) δ 9.59 (br dt, *J* = 7.6, 1.1 Hz, 4H), 9.54 (m, 8H), 8.19 (m, 8H), 8.06 (br d, *J* = 8.5 Hz, 4H), 7.94 (ddd, *J* = 7.5, 6.9, 0.7, 4H), 7.63 (ddd, *J* = 8.0, 6.8, 1.2 Hz, 4H), 7.57 (br d, *J* = 8.4 Hz, 4H), 7.28 (br dt, *J* = 8.0, 0.7 Hz, 4H), 4.46 (t, *J* = 6.5 Hz, 4H), 2.15 (dt, *J* = 14.9, 6.6 Hz, 4H), 1.86 (m, 4H), 1.70 (m, 8H).

^{13}C-NMR (126 MHz, THF-d_8) δ 161.24, 156.68, 153.60, 152.70, 143.70, 141.29, 141.17, 140.95, 140.23, 134.07, 133.92, 130.05, 129.76, 129.34, 128.20, 127.34, 126.71, 125.87, 123.85, 123.64, 115.93, 68.10, 30.97, 30.91, 30.79, 30.53, 26.55.

MS (MALDI-tof): m/z = 1394.04 $[M]^+$

Chemical Formula: $C_{88}H_{60}Mg_2N_{14}O_2$; **Exact Mass**: 1393.48 g·mol^{-1}

UV-vis (dist. THF): λ max (nm) (ε (dm^3.mol^{-1}.cm^{-1})) = 671 ($8.90\cdot10^4$), 648 ($5.29\cdot10^4$), 594 ($1.11\cdot10^4$), 444 ($1.20\cdot10^4$), 397 ($3.09\cdot10^4$).

3.26 By-product from above reaction and from unsymmetrical dyad (2.65)

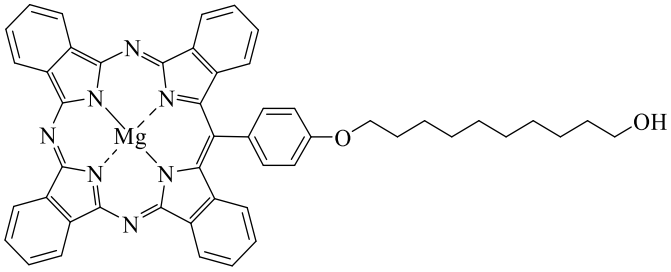

This compound was isolated from the previous reaction, from symmetrical and unsymmetrical dyad as side product and was obtained as a purple solid (8 mg, 11%).

Mp > 300 °C

^{1}H-NMR (500 MHz, THF-d_8) δ 9.59 (dd, J = 7.5, 1.1 Hz, 2H), 9.55 – 9.46 (m, 4H), 8.18 (m, 4H), 8.01 (br d, , J = 8.5Hz, 2H), 7.91 (ddd, , J = 7.5, 6.9, 0.7, 2H), 7.61 (ddd, J = 8.1, 6.8, 1.2 Hz, 2H), 7.51 (br d, 2H), 7.26 (d, J = 8.0 Hz, 2H), 4.41 (t, J = 6.5 Hz, 2H), 3.54 (t, J = 6.4 Hz, 2H), 2.12 (m, 2H), 1.60 (m, 2H), 1.56 (m, 4H), 1.48 (m, 8H).

^{13}C-NMR (126 MHz, THF-d_8) δ 161.42, 156.65, 153.62, 152.73, 143.67, 141.30, 141.19, 140.96, 140.24, 134.12, 130.05, 129.77, 128.21, 127.35, 125.88, 123.87, 123.65, 123.59, 115.90, 69.38, 62.74, 34.32, 30.93, 30.89, 30.84, 30.82, 30.73, 27.43, 27.19.

MS (MALDI-tof): m/z = 783.85 $[M]^+$

Chemical Formula: $C_{49}H_{41}MgN_7O_2$; **Exact Mass**: 783.32 g·mol^{-1}

UV-vis (dist. THF): λ max (nm) (ε ($dm^3.mol^{-1}.cm^{-1}$)) = 671 ($3.11\cdot10^5$), 648 ($1.82\cdot10^5$), 594 ($3.62\cdot10^4$), 444 ($3.90\cdot10^4$), 397 ($1.01\cdot10^5$).

3.27 TBTAP-(4-OMe-Ph) (2.24)

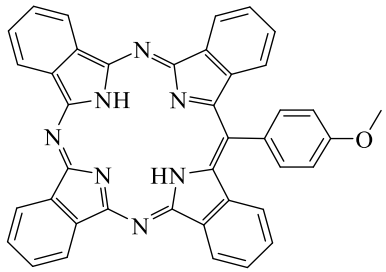

Mg-TBTAP-OMe **2.13** (0.07 g, 0.11 mmol) was dissolved in a 1.5 mL of concentrated H_2SO_4. The solution turned to a brown colour and was then sonicated in ultrasonic bath for 5 min and the resulting solution was added to into ice. A green precipitate was formed. The precipitate was filtered and washed with cold water followed by methanol and dried. A green solid was obtained with no further purification (60 mg, 90%).

Mp > 300 °C

MS (MALDI-tof): m/z = 619.69 $[M]^+$

Chemical Formula: $C_{40}H_{25}N_7O$; **Exact Mass**: 619.21 $g\cdot mol^{-1}$

UV-vis (dist. THF): λ max (nm) (ε ($dm^3.mol^{-1}.cm^{-1}$)) = 684 ($1.86\cdot10^4$), 643 ($1.13\cdot10^4$), 617 ($4.80\cdot10^3$), 589 ($2.69\cdot10^3$), 383 ($7.23\cdot10^3$).

3.28 TBTAP-(4-OH-Ph) (2.9)

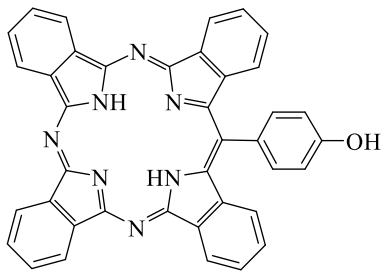

Mg-TBTAP-OH **2.23** (0.06 g, 0.10 mmol) was dissolved in a 1.5 mL of concentrated H_2SO_4. The solution turned to a brown colour and was then sonicated in ultrasonic bath for 5 min and

the resulting solution was added to into ice. A green precipitate was formed. The precipitate filtered and washed with cold water followed by methanol and dried. A green solid was obtained with no further purification (46 mg, 79%).

Mp > 300 °C

MS (MALDI-tof): m/z = 605.21 $[M]^+$

Chemical Formula: $C_{39}H_{23}N_7O$; **Exact Mass**: 605.19 $g \cdot mol^{-1}$

UV-vis (dist. THF): λ max (nm) (ε ($dm^3.mol^{-1}.cm^{-1}$)) = 684 ($1.66 \cdot 10^4$), 643 ($1.04 \cdot 10^4$), 617 ($4.47 \cdot 10^3$), 589 ($2.59 \cdot 10^3$), 382 ($6.46 \cdot 10^3$).

3.29 Demetallated Unsymmetrical dyad C_{10} (2.36)

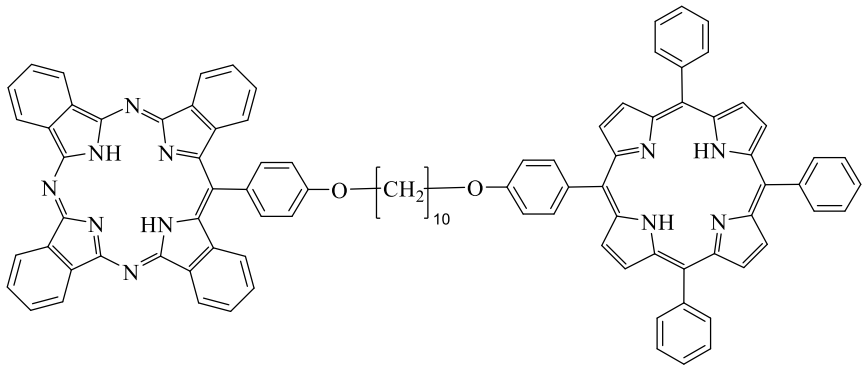

Mg-TBTAP-O-C_{10}-O-TPP **2.32** (0.02 g, 0.012 mmol) was dissolved in 2 mL of glacial HCOOH and was stirred overnight at room temperature. Distilled water (30 mL) and the precipitate was washed several times with water and finally with methanol. A purple-green solid was obtained with no further purification (0.013 g, 66%).

Mp > 300 °C

MS (MALDI-tof): m/z = 1375.25 $[M]^+$

Chemical Formula: $C_{93}H_{71}N_{11}O_2$; **Exact Mass**: 1374.58 $g \cdot mol^{-1}$

UV-vis (dist. THF): λ max (nm) (ε ($dm^3.mol^{-1}.cm^{-1}$)) = 685 ($2.29\cdot10^5$), 644 ($1.43\cdot10^5$), 617 ($6.04\cdot10^4$), 591 ($4.10\cdot10^4$), 549 ($1.75\cdot10^4$), 514 ($2.69\cdot10^4$), 45 ($1.70\cdot10^4$), 418 ($6.93\cdot10^5$).

3.30 Demetallated Unsymmetrical dyad C_{12} (2.37)

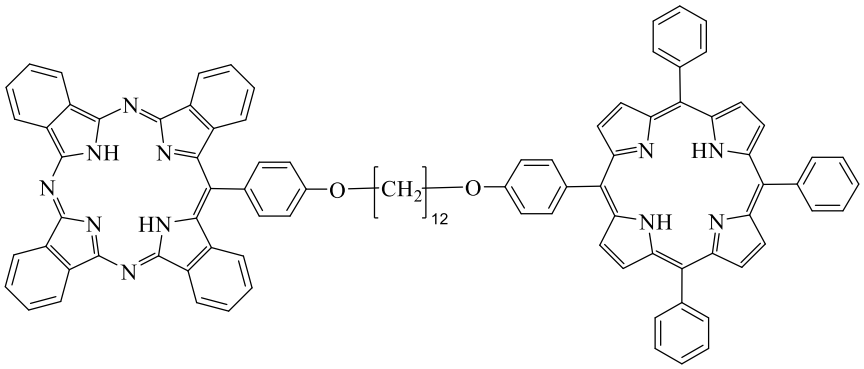

Mg-TBTAP-O-C_{12}-O-TPP **2.35** (0.023 g, 0.016 mmol) was dissolved in 4 mL of glacial HCOOH and was stirred overnight at room temperature. Distilled water (30 mL) and the precipitate was washed several times with water and finally with methanol. A purple-green solid was obtained with no further purification (0.017 g, 75%).

Mp > 300 °C

MS (MALDI-tof): m/z = 1401.53 $[M]^+$

Chemical Formula: $C_{95}H_{75}N_{11}O_2$; **Exact Mass**: 1402.62 $g\cdot mol^{-1}$

UV-vis (dist. THF): λ max (nm) (ε ($dm^3.mol^{-1}.cm^{-1}$)) = 685 ($2.46\cdot10^5$), 644 ($1.56\cdot10^5$), 617 ($6.50\cdot10^4$), 590 ($4.49\cdot10^4$), 551 ($1.93\cdot10^4$), 515 ($2.99\cdot10^4$), 457 ($1.69\cdot10^4$), 418 ($7.90\cdot10^5$).

3.31 Demetallated Symmetrical dyad (2.39)

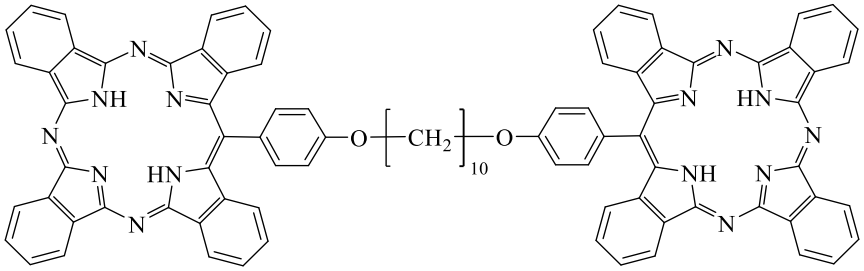

Mg-TBTAP-O-C_{10}-O-Mg-TBTAP **2.38** (0.039 g, 0.03 mmol) was dissolved in 3 mL of TFA and was stirred at room temperature. The demetallation was monitored by TLC and MALDI-

TOF-MS until no starting material was left. After 24 h, distilled water (30 mL) was added. The precipitate was filtered, washed with cold MeOH followed by Et_2O to yield a green solid (0.024 g, 60%).

Mp > 300 °C

MS (MALDI-tof): m/z = 1349.97 $[M]^+$

Chemical Formula: $C_{88}H_{64}N_{14}O_2$; **Exact Mass**: 1349.54 $g \cdot mol^{-1}$

UV-vis (dist. THF): λ max (nm) (ε ($dm^3.mol^{-1}.cm^{-1}$)) = 685 ($7.05 \cdot 10^5$), 644 ($5.23 \cdot 10^5$), 618 ($3.20 \cdot 10^5$), 590 ($2.10 \cdot 10^5$), 379 ($4.40 \cdot 10^5$).

Due to high insolubility in organic solvents further characterisation was not possible.

3.32 La-TD (2.42)

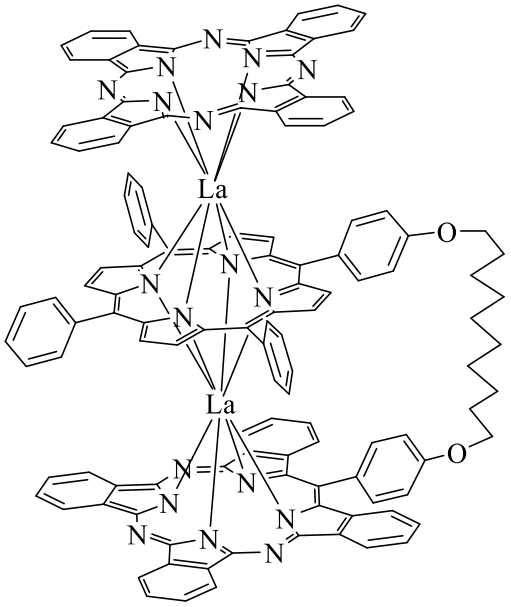

The demetallated unsymmetrical dyad **2.36** (30 mg, 0.021 mmol), La (III) acetylacetonate (21 mg, 0.045 mmol) and metal-free phthalocyanine **2.40** (12 mg, 0.021 mmol) were dissolved in octanol (4 mL) and was refluxed under a nitrogen atmosphere. The reaction was monitored by MALDI- TOF MS until all the starting materials have been consumed. After 16 h, the octanol was distilled under reduced pressure and to the resulting solid a mixture of DCM: MeOH (1:1 v/v) was added and left to precipitate overnight. The precipitate was filtered off and was

chromatographed on a silica gel column using PE: DCM (2:3 v/v) mixture as eluent. A green fraction containing the desired compound was collected and recrystallised from a mixture of DCM: MeOH to yield the product (3.7 mg, 8%).

Mp > 300 °C

^{1}H-NMR (500 MHz, CD_2Cl_2-d_2) δ 9.58 (d, *J* = 7.2 Hz, 1H), 9.55 (dq, *J* = 7.0, 1.2 Hz, 2H), 9.50 (d, *J* = 7.2 Hz, 1H), 9.40 (dt, *J* = 7.6, 1.7 Hz, 2H), 8.98 (dt, *J* = 7.3, 1.0 Hz, 2H), 8.88 – 8.82 (m, 3H), 8.78 – 8.73 (m, 8H), 8.40 – 8.30 (m, 6H), 8.17 – 8.12 (m, 2H), 8.10 (d, *J* = 4.2 Hz, 2H), 7.99 (d, *J* = 4.3 Hz, 2H), 7.92 – 7.83 (m, 10H), 7.77 (dd, *J* = 8.4, 2.4 Hz, 2H), 7.69 (ddd, *J* = 7.3, 6.5, 0.8 Hz, 2H), 7.63 (d, *J* = 4.2 Hz, 2H), 7.58 (dd, *J* = 8.0, 2.4 Hz, 1H), 7.42 (ddd, *J* = 7.7, 6.5, 1.1 Hz, 2H), 7.36 – 7.29 (m, 2H), 7.20 (dd, *J* = 8.0, 2.9 Hz, 1H), 6.65 (dd, *J* = 8.1, 2.9 Hz, 1H), 6.45 – 6.39 (m, 2H), 5.87 (dd, *J* = 8.1, 2.4 Hz, 1H), 4.63 (t, *J* = 6.2 Hz, 2H), 4.21 (t, *J* = 6.1 Hz, 2H), 2.35 – 2.28 (m, 2H), 2.05 – 1.93 (m, 4H), 1.85 – 1.64 (m, 16H).

^{13}C-NMR (126 MHz, CD_2Cl_2-d_2) δ 173.88, 173.71, 168.59, 166.95, 165.73, 164.95, 163.18, 162.43, 162.37, 162.04, 155.88, 155.14, 155.00, 154.72, 153.79, 151.55, 151.31, 151.20, 151.16, 151.04, 150.60, 150.52, 149.95, 146.53, 146.19, 143.25, 143.00, 142.88, 141.84, 141.51, 141.08, 140.93, 140.64, 138.30, 136.69, 136.43, 136.27, 136.20, 135.01, 134.24, 133.39, 128.75, 128.28, 128.11, 126.67, 82.49, 68.00, 43.82, 43.39, 42.45, 42.35, 42.27, 41.89, 40.07, 39.64.

MS (MALDI-tof): m/z = 2160.26 $[M]^+$

Chemical Formula: $C_{125}H_{83}La_2N_{19}O_2$; **Exact Mass**: 2160.51 $g \cdot mol^{-1}$

UV-vis (DCM): λ max (nm) (ε ($dm^3.mol^{-1}.cm^{-1}$)) = 750 ($1.80 \cdot 10^4$), 683 ($2.15 \cdot 10^4$), 640 ($5.19 \cdot 10^4$), 506 ($2.45 \cdot 10^4$), 416 ($7.84 \cdot 10^4$), 403 ($8.24 \cdot 10^4$), 353 ($1.09 \cdot 10^5$).

3.32.1 By-product (double decker) (2.66)

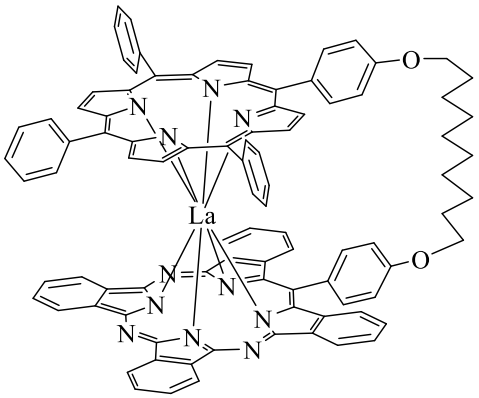

This compound was isolated from the previous reaction as side product and was obtained as a purple solid (0.38 mg, 1.2%).

MS (MALDI-tof): m/z = 1509.42 $[M]^+$

Chemical Formula: $C_{93}H_{67}LaN_{11}O_2$**; Exact Mass:** 1509.46 $g \cdot mol^{-1}$

UV-vis (DCM): λ max (nm) (ε ($dm^3.mol^{-1}.cm^{-1}$)) = 687 ($7.39 \cdot 10^3$), 646 ($6.96 \cdot 10^3$), 553 ($1.19 \cdot 10^4$), 417 ($1.03 \cdot 10^5$), 336 ($4.21 \cdot 10^4$).

3.33 La-TPP TD (2.2)

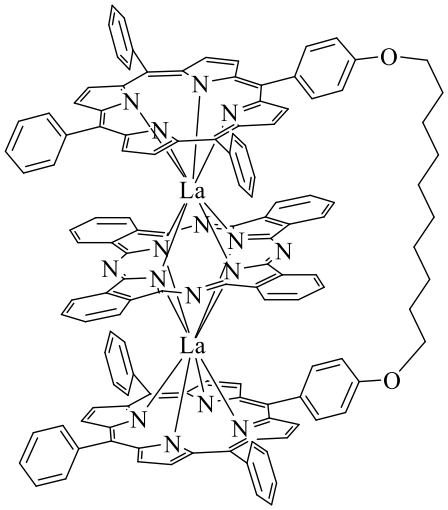

In a 25 ml round bottom flask, C_{10} porphyrin dyad **2.1** (20 mg, 0.0143 mmol) and La (III) acetylacetonate (12.5 mg, 0.0287 mmol)) were dissolved in octanol (6 mL). The resulting mixture was heated to reflux under a stream of argon for 4 h. Metal-free phthalocyanine **2.40** (7.35 mg, 0.0143 mmol) was then added to the above mixture and was left to reflux overnight.

The octanol was distilled off under reduced pressure and the crude was recrystallised with DCM/MeOH. The resulting solid was chromatographed on a silica gel column using DCM: Hexane (3:2 v/v) mixture as eluent. A dark green fraction containing the desired compound was collected and was recrystallised from a mixture of DCM: MeOH to yield the product (10.4 mg, 33%).

^{1}H-NMR (500 MHz, CD_2Cl_2-d_2) δ 10.07 (d, *J* = 7.2 Hz, 8H), 9.39 (dd, *J* = 5.3, 2.9 Hz, 8H), 8.52 (t, *J* = 7.5 Hz, 6H), 8.34 – 8.29 (m, 8H), 8.06 (d, *J* = 7.5 Hz, 2H), 7.88 – 7.83 (m, 6H), 7.32 (d, *J* = 4.2 Hz, 4H), 7.31 – 7.26 (m, 7H), 7.26 – 7.23 (m, 10H), 6.87 (d, *J* = 7.2 Hz, 2H), 6.75 (d, *J* = 7.8 Hz, 2H), 6.70 (d, *J* = 6.8 Hz, 6H), 4.60 (t, *J* = 7.3 Hz, 4H), 2.31 – 2.20 (s, 4H), 1.94 – 1.85 (m, 8H), 1.83 –1.76 (m, 4H).

UV-vis (DCM): λ max (nm) (ε ($dm^3.mol^{-1}.cm^{-1}$)) = 605 ($2.84\cdot10^4$), 550 ($2.64\cdot10^4$), 484 ($4.15\cdot10^4$), 420 ($3.87\cdot10^5$), 361 ($1.58\cdot10^5$).

3.34.1 Nd-TD-G (2.46)

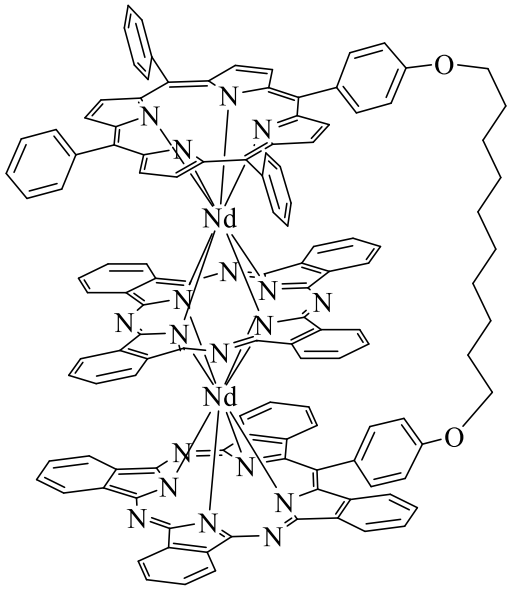

The demetallated compound **2.36** (40 mg, 0.030 mmol) and metal-free phthalocyanine **2.40** (14 mg, 0.030 mmol) were mixed in octanol and was allowed to reflux under a nitrogen atmosphere overnight. Then Nd (III) acetylacetonate (26 mg, 0.064 mmol) was added and the reaction was further refluxed. The reaction was monitored by MALDI-TOF MS until all the starting materials have been consumed. After 16 hours, the octanol was distilled under reduced pressure and the resulting solid were washed in MeOH. The residue was chromatographed on a silica gel column using PE: DCM (2:3 v/v) mixture as eluent. A dark green fraction containing the

desired compound was collected and recrystallised from a mixture of DCM: MeOH to give the product (6.5 mg, 10%).

Mp > 300 °C

^{1}H-NMR (500 MHz, CD_2Cl_2-d_2) δ 8.85 (d, *J* = 8.4 Hz, 1H), 8.72 (s, 2H), 8.44 (d, *J* = 7.6 Hz, 2H), 8.34 (s, 2H), 7.89 (d, *J* = 8.6 Hz, 1H), 7.75 (d, *J* = 7.8 Hz, 1H), 7.59 (s, 2H), 7.42 – 7.34 (m, 4H), 7.17 – 7.05 (m, 4H), 6.96 (t, *J* = 7.4 Hz, 2H), 6.90 (t, *J* = 7.1 Hz, 2H), 6.74 (t, *J* = 7.1 Hz, 1H), 6.68 (d, *J* = 7.9 Hz, 1H), 6.32 (t, *J* = 7.5 Hz, 2H), 6.26 – 6.16 (m, 2H), 6.10 (s, 1H), 6.04 (t, *J* = 7.8 Hz, 2H), 5.92 (s, 1H), 5.76 (d, *J* = 7.8 Hz, 2H), 5.15 (d, *J* = 5.5 Hz, 8H), 5.05 (s, 1H), 4.55 (s, 2H), 4.32 (s, 1H), 3.97 (d, *J* = 8.4 Hz, 2H), 3.78 (t, *J* = 7.3 Hz, 2H), 3.63 (d, *J* = 5.9 Hz, 8H), 3.56 (t, *J* = 7.5 Hz, 2H), 1.64 – 1.51 (m, 10H) 1.36 – 1.29 (m, 2H), 1.08 – 1.00 (m, 2H), 0.98 – 0.85 (m, 8H).

^{13}C-NMR (126 MHz, CD_2Cl_2-d_2) δ 160.89, 159.15, 158.35, 158.06, 158.02, 155.99, 155.37, 154.97, 153.84, 153.77, 140.53, 138.14, 138.03, 136.88, 136.55, 136.44, 135.65, 135.10, 134.81, 133.65, 132.59, 129.31, 129.10, 128.74, 128.16, 127.51, 126.82, 126.63, 126.41, 126.05, 125.72, 125.39, 125.16, 124.96, 122.70, 122.30, 121.32, 121.28, 117.08, 116.73, 115.06, 111.38, 110.17, 68.31, 30.08, 29.88, 29.70, 29.06, 28.69, 28.66, 28.07, 25.98, 25.84.

MS (MALDI-tof): m/z = 2170.36 $[M]^+$

Chemical Formula: $C_{125}H_{83}N_{19}Nd_2O_2$; **Exact Mass**: 2170.52 g·mol^{-1}

UV-vis (DCM): λ max (nm) (ε ($dm^3.mol^{-1}.cm^{-1}$)) = 670 ($4.50\cdot10^4$), 622 ($5.58\cdot10^4$), 552 ($2.83\cdot10^4$), 483 ($3.64\cdot10^4$), 419 ($2.18\cdot10^5$), 351 ($1.67\cdot10^5$).

3.34.2 Nd-TD-G.G (2.45)

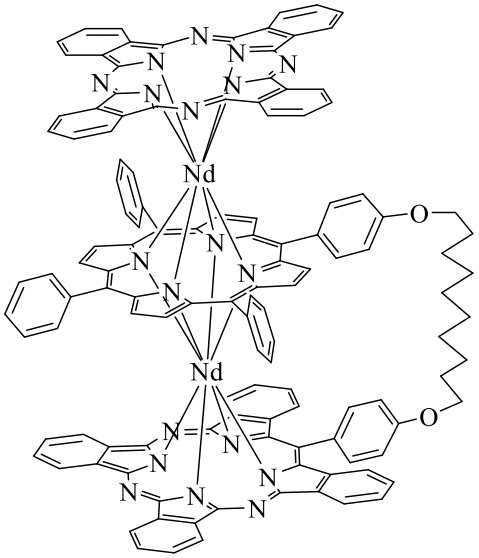

The other grey green fraction collected from above synthesis is recrystallised from a mixture of DCM and MeOH to yield the product (7.8 mg, 12%).

Mp > 300 °C

^{1}H-NMR (500 MHz, CD_2Cl_2-d_2) δ 8.47 (d, *J* = 8.4 Hz, 1H), 8.23 (d, *J* = 8.0 Hz, 2H), 7.40 – 7.26 (m, 10H), 7.25 – 7.07 (m, 16H), 6.85 (t, *J* = 7.4 Hz, 2H), 6.76 (t, *J* = 7.9 Hz, 2H), 6.17 (t, *J* = 7.2 Hz, 1H), 6.08 (d, *J* = 6.9 Hz, 1H), 5.92 (t, *J* = 7.2 Hz, 2H), 5.73 (d, *J* = 7.1 Hz, 1H), 5.63 (d, *J* = 7.0 Hz, 6H), 5.28 – 5.24 (m, 2H), 4.98 (d, *J* = 6.4 Hz, 1H), 4.44 (s, 1H), 3.86 (t, *J* = 6.3 Hz, 2H), 3.35 (t, *J* = 6.4 Hz, 4H), 3.24 (s, 2H), 3.06 (s, 2H), 2.97 (s, 1H), 2.52 (s, 2H), 2.02 (d, *J* = 8.0 Hz, 1H), 1.77 – 1.69 (m, 2H), 1.41 (d, *J* = 7.0 Hz, 4H), 1.24 – 1.10 (m, 10H), 1.06 (s, 2H), 0.91 – 0.83 (m, 2H), 0.77 (s, 2H).

^{13}C-NMR (126 MHz, CD_2Cl_2-d_2) δ 162.50, 159.07, 158.79, 158.42, 157.11, 141.82, 140.65, 139.05, 138.87, 136.67, 135.01, 133.95, 131.98, 131.70, 131.52, 129.26, 128.65, 127.86, 127.38, 125.86, 124.60, 124.47, 123.87, 123.58, 123.36, 123.24, 122.40, 122.13, 114.83, 112.93, 111.24, 109.58, 68.01, 67.04, 29.67, 28.35, 27.88, 27.76, 27.66, 27.53, 27.33, 25.16, 25.11.

MS (MALDI-tof): m/z = 2170.84 $[M]^+$

Chemical Formula: $C_{125}H_{83}N_{19}Nd_2O_2$; **Exact Mass**: 2170.52 g·mol^{-1}

UV-vis (DCM): λ max (nm) (ε ($dm^3.mol^{-1}.cm^{-1}$)) = 756 ($9.53\cdot10^4$), 647 ($3.50\cdot10^5$), 518 ($2.13\cdot10^5$), 404 ($5.13\cdot10^5$), 348 ($7.41\cdot10^5$), 292 ($3.52\cdot10^5$).

3.34.3 By-product Nd (double decker) (2.67)

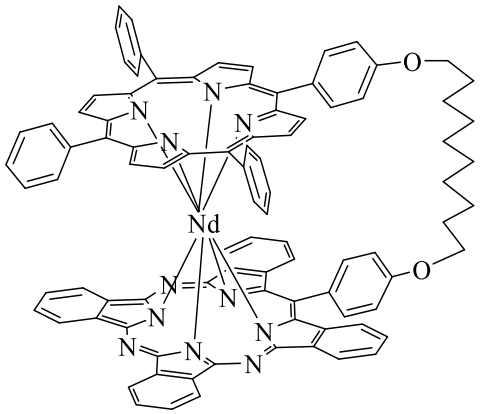

This compound was isolated from the previous reaction as side product and was obtained as a purple solid (0.75 mg, 1.6%).

MS (MALDI-tof): m/z = 1514.70 $[M+1]^+$

Chemical Formula: $C_{93}H_{67}N_{11}NdO_2$; **Exact Mass**: 1513.46 $g\cdot mol^{-1}$

UV-vis (DCM): λ max (nm) (ε ($dm^3.mol^{-1}.cm^{-1}$)) = 686 ($9.40\cdot10^3$), 645 ($9.14\cdot10^3$), 545 ($1.72\cdot10^4$), 418 ($1.32\cdot10^5$), 338 ($6.17\cdot10^4$).

3.35 Eu-TD (2.47)

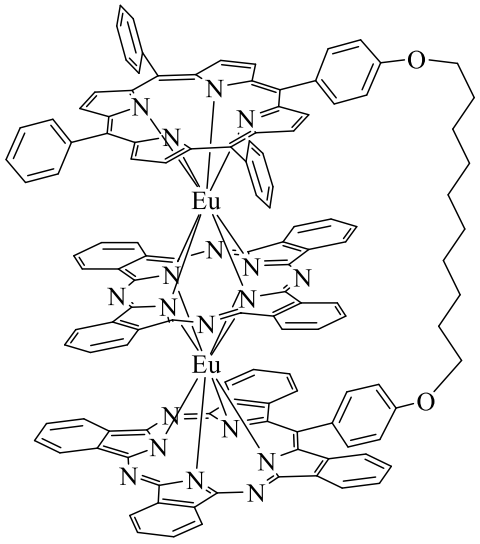

In a 25 mL round bottom flask, the demetallated dyad **2.36** (50 mg, 0.036 mmol), metal-free phthalocyanine **2.40** (19 mg, 0.036 mmol) and Eu (III) acetylacetonate (36 mg, 0.080 mmol)

were mixed in a solvent mixture of octanol: TCB (2:1 v/v) in a total volume of 4 mL and was allowed to reflux under a nitrogen atmosphere for 8 h. The reaction was monitored by MALDI-MS until all the starting materials have been consumed. The solvent was distilled under reduced pressure and the resulting solid was recrystallised in DDM and MEOH. The residue was filtered off and was chromatographed on a silica gel column using PE: DCM (2:3 v/v) mixture as eluent. A dark green fraction containing the desired compound was collected and recrystallised from a mixture of DCM: MeOH to yield the product (16 mg, 20%).

The same reaction was repeated by following the same procedure as above except octanol (4 mL) was used and the reaction was refluxed for overnight to yield the product (2.3 mg, 3%).

Mp > 300 °C

^{1}H-NMR (500 MHz, CD_2Cl_2-d_2) δ 13.30 (s, 2H), 12.67 (s, 8H), 10.81 (s, 8H), 10.66 (s, 2H), 9.74 (d, *J* = 8.8 Hz, 2H), 9.56 (d, *J* = 8.6 Hz, 2H), 8.83 (s, 2H), 8.62 – 8.55 (m, 3H), 8.29 (d, *J* = 8.6 Hz, 2H), 8.17 (s, 4H), 7.43 (t, *J* = 7.2 Hz, 2H), 6.91 (t, *J* = 7.2 Hz, 3H), 6.82 – 6.78 (m, 2H), 6.51 (d, *J* = 6.2 Hz, 2H), 6.30 (d, *J* = 6.8 Hz, 2H), 5.15 (d, *J* = 6.2 Hz, 4H), 5.09 (t, *J* = 6.9 Hz, 3H), 5.04 (d, *J* = 7.0 Hz, 1H), 4.61 (d, *J* = 6.9 Hz, 2H), 4.18 (s, 2H), 3.78 (s, 3H), 2.81 (dd, *J* = 16.2, 8.8 Hz, 4H), 2.72 – 2.60 (m, 10H) 2.50 (m, 8H).

^{13}C-NMR (126 MHz, CD_2Cl_2-d_2) δ 201.18, 160.20, 158.43, 153.80, 134.94, 133.39, 133.05, 132.66, 131.12, 129.51, 129.43, 128.53, 128.03, 127.10, 126.91, 126.58, 126.51, 126.47, 126.39, 125.81, 125.31, 121.66, 120.61, 120.26, 118.77, 118.48, 117.72, 114.74, 87.52, 71.50, 69.79, 69.47, 68.01, 67.33, 31.98, 31.86, 31.32, 31.07, 30.11, 29.78, 29.31, 27.34, 27.20.

MS (MALDI-tof): m/z = 2188.36 $[M]^+$

Chemical Formula: $C_{125}H_{83}Eu_2N_{19}O_2$; **Exact Mass**: 2187.54 $g \cdot mol^{-1}$

UV-vis (DCM): λ max (nm) (ε ($dm^3.mol^{-1}.cm^{-1}$)) = 728 ($2.01 \cdot 10^4$), 670 ($3.28 \cdot 10^4$), 618 ($4.57 \cdot 10^4$), 551 ($1.81 \cdot 10^4$), 515 ($2.18 \cdot 10^4$), 485 ($2.34 \cdot 10^4$), 419 ($1.61 \cdot 10^5$), 346 ($1.22 \cdot 10^5$).

3.35.1 By-product (double decker) (2.68)

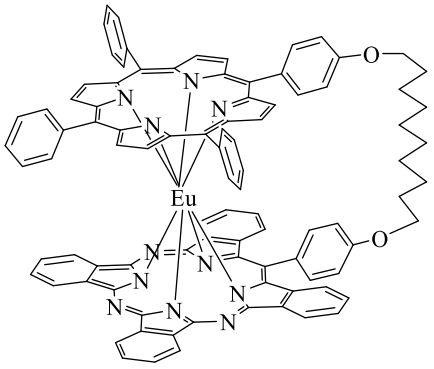

This compound was isolated from the previous reaction as side product and was obtained as a purple solid (0.93 mg, 1.7%).

MS (MALDI-tof): m/z = 1522.63 $[M]^+$

Chemical Formula: $C_{93}H_{67}EuN_{11}O_2$; **Exact Mass**: 1522.47 $g \cdot mol^{-1}$

UV-vis (DCM): λ max (nm) (ε ($dm^3.mol^{-1}.cm^{-1}$)) = 685 ($3.90 \cdot 10^3$), 643 ($4.68 \cdot 10^3$), 547 ($1.47 \cdot 10^4$), 407 ($9.84 \cdot 10^4$), 340 ($5.59 \cdot 10^4$).

3.36 La-TD (2.44)

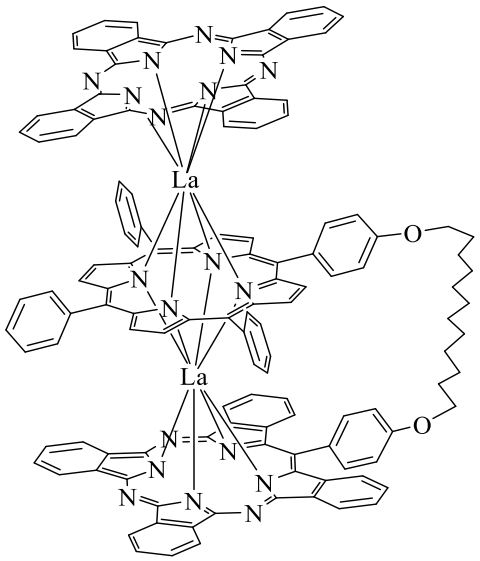

The demetallated unsymmetrical dyad **2.37** (30 mg, 0.021 mmol), La (III) acetylacetonate (21 mg, 0.045 mmol) and metal-free phthalocyanine **2.40** (12 mg, 0.021 mmol) were dissolved in octanol (4 mL) and was refluxed under a nitrogen atmosphere. After 18 h, the octanol was distilled under reduced pressure and to the resulting solid a mixture of DCM: MeOH (1:1 v/v) was added and left to precipitate overnight. The residue was filtered off and was

chromatographed on a silica gel column using PE: DCM (2:3 v/v) mixture as eluent. A green fraction containing the desired compound was collected and recrystallised from a mixture of DCM: MeOH to yield the product (4.1 mg, 9%).

The demetallated unsymmetrical dyad **2.37** (40 mg, 0.029 mmol), La (III) acetylacetonate (27 mg, 0.060 mmol) and metal-free phthalocyanine **2.40** (16 mg, 0.029 mmol) were dissolved in a solvent mixture of octanol: TCB (2:1 v/v) in a total volume of 5 mL and was allowed to reflux under an inert atmosphere for 18 h. The solvent was distilled under reduced pressure and the resulting solid was recrystallized in a mixture of DCM: MeOH (1:1 v/v). The above purification process was adopted. A green fraction containing the desired compound was collected and recrystallised from a mixture of DCM: MeOH to give the product (15.6 mg, 25%).

Mp > 300 °C

^{1}H-NMR (500 MHz, CD_2Cl_2-d_2) δ 9.52 (d, *J* = 7.3 Hz, 1H), 9.38 (d, *J* = 7.5 Hz, 1H), 9.36 – 9.33 (m, 2H), 9.28 (d, *J* = 7.3 Hz, 2H), 8.96 (d, *J* = 7.3 Hz, 2H), 8.87 – 8.81 (m, 4H), 8.75 (dd, *J* = 5.3, 2.9 Hz, 8H), 8.43 (dd, *J* = 8.0, 2.5 Hz, 1H), 8.37 – 8.29 (m, 4H), 8.29 – 8.23 (m, 3H), 8.13 (tdt, *J* = 7.9, 5.7, 1.2 Hz, 3H), 8.07 (d, *J* = 4.2 Hz, 2H), 7.98 (d, *J* = 4.3 Hz, 2H), 7.96 – 7.80 (m, 14H), 7.76 (dd, *J* = 8.0, 2.8 Hz, 2H), 7.72 (d, *J* = 4.2 Hz, 2H), 7.71 – 7.65 (m, 4H), 7.50 (dd, *J* = 7.9, 2.5 Hz, 1H), 7.41 (ddd, *J* = 7.7, 6.5, 1.2 Hz, 2H), 7.35 (dd, *J* = 7.9, 2.8 Hz, 1H), 7.24 (dd, *J* = 8.0, 2.9 Hz, 1H), 6.65 (dd, *J* = 8.1, 2.9 Hz, 1H), 6.42 (d, *J* = 7.8 Hz, 2H), 5.84 (dd, *J* = 8.0, 2.4 Hz, 1H), 4.61 (t, *J* = 6.4 Hz, 2H), 4.21 (t, *J* = 6.0 Hz, 2H), 2.33 – 2.26 (m, 4H), 1.99 – 1.89 (m, 6H), 1.84 – 1.65 (m, 10H).

^{13}C-NMR (126 MHz, CD_2Cl_2-d_2) δ 160.11, 159.85, 154.89, 153.23, 151.99, 151.22, 149.41, 148.74, 148.66, 148.41, 142.20, 141.16, 140.96, 140.72, 140.05, 137.80, 137.64, 137.52, 137.43, 136.82, 136.77, 136.22, 132.83, 132.55, 129.54, 129.27, 129.18, 128.06, 127.89, 127.80, 127.33, 127.22, 126.90, 124.58, 122.95, 122.71, 122.54, 122.46, 121.20, 120.53, 119.85, 115.22, 114.32, 112.96, 69.05, 68.57, 30.10, 29.98, 29.43, 29.17, 28.93, 28.70, 28.49, 28.29, 28.23, 26.07, 25.88.

MS (MALDI-tof): m/z = 2189.12 $[M]^+$

Chemical Formula: $C_{127}H_{87}La_2N_{19}O_2$; **Exact Mass**: 2188.55 g·mol^{-1}

UV-vis (DCM): λ max (nm) (ε ($dm^3.mol^{-1}.cm^{-1}$)) = 747 ($3.93\cdot10^3$), 686 ($7.60\cdot10^3$), 643 ($1.20\cdot10^4$), 506 ($1.81\cdot10^3$), 417 ($2.08\cdot10^4$), 407 ($2.01\cdot10^4$), 352 ($2.43\cdot10^4$), 292 ($1.22\cdot10^4$).

3.36.1 By-product (double decker) (2.69)

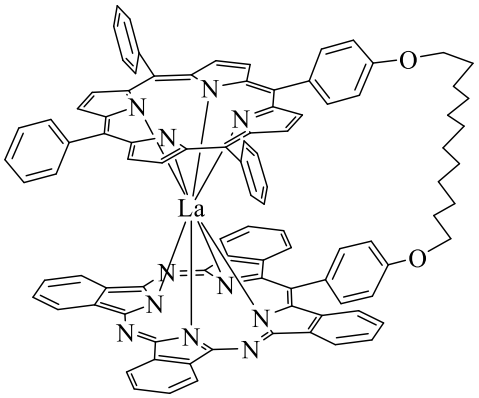

This compound was isolated from the previous reaction as side product and was obtained as a purple solid (0.45 mg, 1.4%).

MS (MALDI-tof): m/z = 1537.97 $[M]^+$

Chemical Formula: $C_{95}H_{71}LaN_{11}O_2$; **Exact Mass**: 1537.49 $g\cdot mol^{-1}$

UV-vis (DCM): λ max (nm) (ε ($dm^3.mol^{-1}.cm^{-1}$)) = 686 ($2.26\cdot10^5$), 646 ($1.59\cdot10^5$), 617 ($1.02\cdot10^5$), 590 ($1.08\cdot10^5$), 550 ($1.24\cdot10^5$), 420 ($1.37\cdot10^6$), 338 ($4.12\cdot10^5$).

3.37 Synthesis of La-DD (2.48)

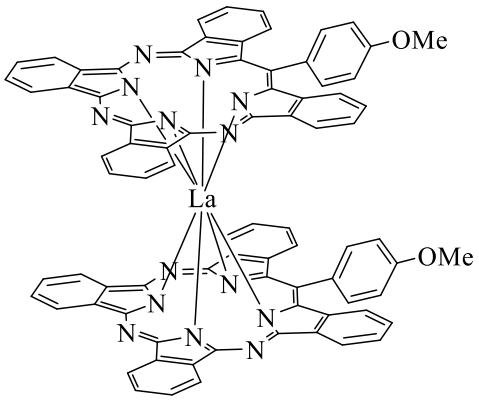

In a 25 mL round bottom flask, TBTAP-OMe **2.24** (25 mg, 0.040 mmol) and lanthanum (III) acetylacetonate hydrate (10 mg, 0.024 mmol) were mixed in a mixture of solvents octanol: TCB (1:1 v/v) and was allowed to reflux for 9 h. The solvent was removed under reduced pressure and the resulting solids was washed with methanol (50 mL) trice. The crude product

was then purified over silica gel column chromatography using eluting the product with DCM (100 %) followed by a mixture of DCM: Et_2O (10:1 v/v). The dark green fraction collected contained the title compound (16 mg, 57%).

Mp > 300 °C

MS (MALDI-tof): m/z = 1372.86 $[M]^+$

Chemical Formula: $C_{80}H_{46}LaN_{14}O_2$; **Exact Mass**: 1373.30 $g \cdot mol^{-1}$

UV-vis (dist. THF): λ max (nm) (ε ($dm^3.mol^{-1}.cm^{-1}$)) = 676 ($2.82 \cdot 10^4$), 650 ($2.39 \cdot 10^4$), 592 ($1.57 \cdot 10^4$), 483 ($9.10 \cdot 10^3$), 393 ($2.55 \cdot 10^4$), 346 ($3.93 \cdot 10^4$), 267 ($2.59 \cdot 10^4$).

3.38 Triple decker of TBTAP-OMe (2.49)

This compound was isolated in trace amount from the previous reaction.

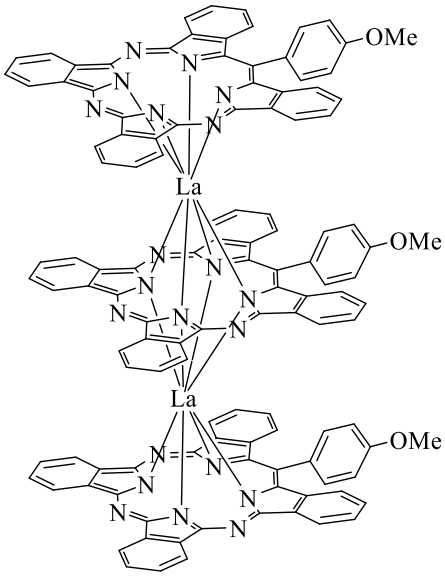

MS (MALDI-tof): m/z = 2130.36 $[M]^+$

Chemical Formula: $C_{120}H_{69}La_2N_{21}O_3$; **Exact Mass**: 2130.40 $g \cdot mol^{-1}$

3.39 Synthesis of La triple decker using symmetrical C_{10} dyad instead DD (2.52)

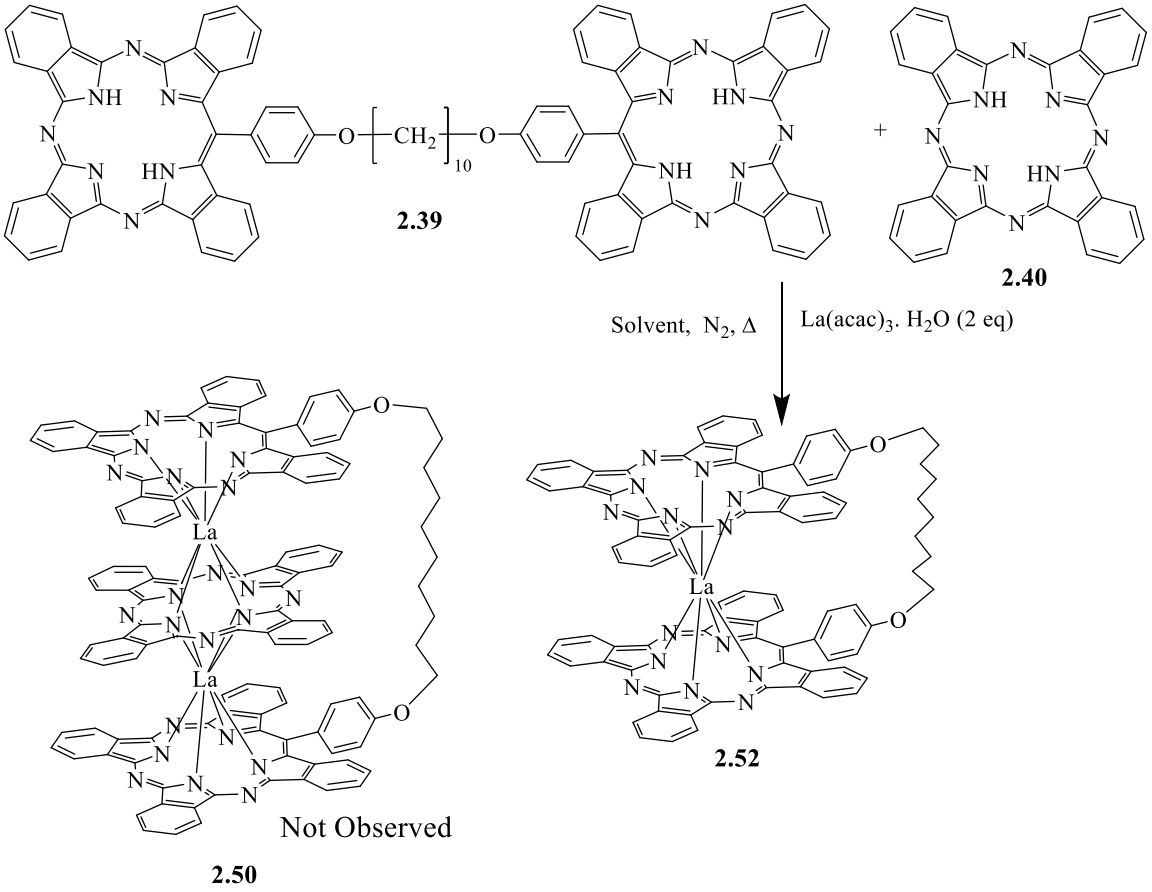

The La-DD **2.52** was isolated from the attempted synthesis of triple decker **2.50**. In a 25 mL round bottom flask, symmetrical dyad **2.39** (50 mg, 0.037 mmol), Pc **2.40** (30 mg, 0.040 mmol) and lanthanum (III) acetylacetonate hydrate (34 mg, 0.078 mmol) were mixed in a mixture of solvents octanol: TCB (1:1 v/v) in a total volume of 4 mL and was allowed to reflux for 24 h. The solvent was removed under reduced pressure. The crude was dissolved in DCM and methanol was added. The precipitate was filtered off and the crude product was then purified over silica gel column chromatography using eluting the product with DCM (100%) followed by a mixture of DCM: Et_2O (10:1 v/v). The dark green fraction was collected and a recrystallisation from DCM and methanol yielded the D.D (12.6 mg, 23%).

MS (MALDI-tof): m/z = 1484.77 $[M]^+$

Chemical Formula: $C_{88}H_{60}LaN_{14}O_2$; **Exact Mass**: 1484.41 $g \cdot mol^{-1}$

UV-vis (dist. THF): λ max (nm) (ε ($dm^3.mol^{-1}.cm^{-1}$)) = 677 ($2.51 \cdot 10^3$), 655 ($1.88 \cdot 10^3$), 592 ($1.60 \cdot 10^3$), 488 ($9.84 \cdot 10^2$), 421 ($2.56 \cdot 10^3$), 404 ($2.39 \cdot 10^3$), 347 ($2.81 \cdot 10^3$).

3.40 Synthesis of TD (2.60) using TBTAP-OMe and TPP(OMe)$_4$

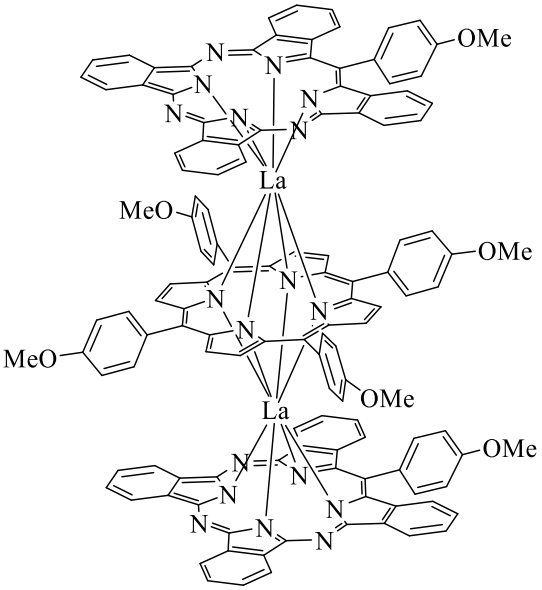

In a 25 mL round bottom flask, the porphyrin TPP(OMe)$_4$ **2.56** (50 mg, 0.068 mmol), TBTAP-OMe **2.24** (21 mg, 0.034 mmol) and lanthanum (III) acetylacetonate hydrate (29 mg, 0.068 mmol) were mixed in octanol (4 mL) and was heated to reflux for 18 h. The mixture was allowed to cool to room temperature, methanol was then added, and the mixture was left to precipitate overnight. The product was filtered off and the crude compound was purified over silica gel column chromatography using a mixture of DCM: Hexane (3:2 v/v) followed by DCM (100%). The dark green fraction collected contained the title compound (18 mg, 47%).

Mp > 300 °C

^{1}H-NMR (400 MHz, CD_2Cl_2-d_2) δ 8.94 (dt, *J* = 7.6, 1.0 Hz, 4H), 8.80 (t, *J* = 4.4 Hz, 8H), 8.63 – 8.56 (m, 8H), 7.96 (s, 8H), 7.92 – 7.86 (m, 8H), 7.71 – 7.64 (m, 12H), 7.53 (dd, *J* = 8.2, 2.4 Hz, 2H), 7.41 (ddd, *J* = 7.9, 6.8, 1.1 Hz, 4H), 7.20 (dd, *J* = 8.2, 2.8 Hz, 2H), 6.65 (dd, *J* = 8.3, 2.8 Hz, 2H), 6.40 – 6.34 (m, 4H), 5.83 (dd, *J* = 8.2, 2.3 Hz, 2H), 4.45 (s, 12H), 4.03 (s, 6H).

^{13}C-NMR (101 MHz, CD_2Cl_2-d_2) δ 160.48, 160.13, 154.95, 152.00, 151.26, 148.86, 142.19, 139.98, 137.89, 137.48, 136.91, 136.28, 133.57, 133.12, 132.90, 132.30, 129.47, 129.08, 127.69, 126.79, 124.59, 124.19, 122.89, 122.65, 122.45, 120.55, 114.35, 113.76, 113.07, 56.38, 55.87.

MS (MALDI-tof): m/z = 2245.96 $[M]^+$

Chemical Formula: $C_{128}H_{82}La_2N_{18}O_6$; **Exact Mass**: 2245.48 g·mol^{-1}

UV-vis (DCM): λ max (nm) (ε ($dm^3.mol^{-1}.cm^{-1}$)) = 737 ($2.99\cdot10^4$), 584 ($5.12\cdot10^4$), 643 ($1.04\cdot10^5$), 513 ($3.96\cdot10^4$), 395 ($2.09\cdot10^5$), 349 ($1.55\cdot10^5$).

3.41 Triple decker (2.61)

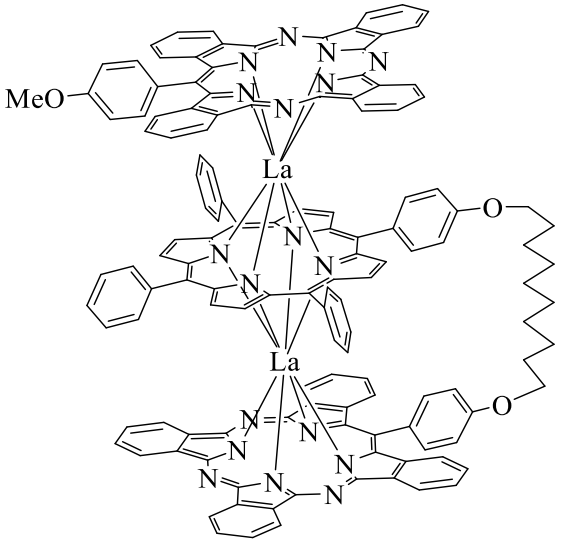

In a 25 mL round bottom flask, unsymmetrical dyad **2.36** (25 mg, 0.011 mmol), TBTAP-OMe **2.24** (13 mg, 0.011 mmol) and lanthanum (III) acetylacetonate hydrate (17 mg, 0.04 mmol) were mixed in a mixture of solvents octanol: TCB (1:1 v/v) in a total volume of 4 mL and was allowed to reflux for 6 h. The solvent was removed under reduced pressure. The crude product was then purified over silica gel column chromatography using eluting the product with DCM (100%) followed by a mixture of DCM: Et_2O (10:1 v/v). The dark green fraction collected contained the title compound (10 mg, 25%).

Mp > 300 °C

^{1}H-NMR (500 MHz, CD_2Cl_2-d_2) δ 9.57 (d, *J* = 7.3 Hz, 2H), 9.24 (t, *J* = 7.0 Hz, 2H), 9.11 (d, *J* = 7.2 Hz, 2H), 8.96 (t, *J* = 7.1 Hz, 4H), 8.81 (t, *J* = 5.5 Hz, 8H), 8.37 (td, *J* = 7.5, 1.5 Hz, 2H), 8.30 – 8.18 (m, 7H), 8.14 – 8.05 (m, 6H), 7.93 – 7.81 (m, 11H), 7.68 (td, *J* = 6.9, 2.7 Hz, 4H), 7.60 (dd, *J* = 6.8, 3.5 Hz, 3H), 7.48 (dd, *J* = 8.0, 2.4 Hz, 1H), 7.46 – 7.36 (m, 6H), 7.26 (dd, *J* = 8.0, 2.5 Hz, 1H), 7.15 (dt, *J* = 8.1, 3.3 Hz, 2H), 6.62 (ddd, *J* = 13.1, 8.1, 2.9 Hz, 2H), 6.37 (t, *J* = 8.8 Hz, 4H), 5.80 (ddd, *J* = 10.5, 8.0, 2.4 Hz, 2H), 4.64 (t, *J* = 6.2 Hz, 2H), 4.19 (t, *J* = 6.0 Hz, 2H), 4.02 (s, 3H), 2.36 – 2.27 (m, 4H), 2.03 – 1.93 (m, 4H), 1.85 – 1.65 (m, 12H).

^{13}C-NMR (126 MHz, CD_2Cl_2) δ 160.05, 159.75, 159.66, 154.46, 151.58, 150.89, 148.44, 148.05, 147.66, 140.76, 137.83, 137.56, 137.07, 136.50, 135.85, 132.69, 132.32, 132.15,

131.92, 131.82, 129.02, 128.65, 127.56, 127.29, 127.01, 126.83, 126.40, 124.18, 122.51, 122.28, 122.07, 120.47, 114.08, 68.47, 68.43, 68.37, 55.42, 29.36, 28.29, 28.20, 28.08 27.76, 25.99, 25.47.

MS (MALDI-tof): m/z = 2265.38 $[M]^+$

Chemical Formula: $C_{134}H_{94}La_2N_{18}O_3$; **Exact Mass**: 2265.56 $g \cdot mol^{-1}$

UV-vis (DCM): λ max (nm) (ε ($dm^3.mol^{-1}.cm^{-1}$)) = 740 ($8.30 \cdot 10^4$), 685 ($2.88 \cdot 10^5$), 644 ($3.99 \cdot 10^5$), 617 ($2.67 \cdot 10^5$), 589 ($1.69 \cdot 10^5$), 514 ($1.24 \cdot 10^5$), 417 ($5.70 \cdot 10^5$), 393 ($7.44 \cdot 10^5$).

References

(1) Dalai, S.; Belov, V. N.; Nizamov, S.; Rauch, K.; Finsinger, D.; De Meijere, A. Access to Variously Substituted 5,6,7,8-Tetrahydro-3H-Quinazolin-4-Ones via Diels-Alder Adducts of Phenyl Vinyl Sulfone to Cyclobutene-Annelated Pyrimidinones. *European J Org Chem* **2006**, No. 12, 2753–2765.

(2) Hellal, M.; Cuny, G. D. Microwave Assisted Copper-Free Sonogashira Coupling/5-Exo-Dig Cycloisomerization Domino Reaction: Access to 3-(Phenylmethylene)Isoindolin-1-Ones and Related Heterocycles. *Tetrahedron Lett* **2011**, *52* (42), 5508–5511.

(3) Díaz-Moscoso, A.; Tizzard, G. J.; Coles, S. J.; Cammidge, A. N. Synthesis of Meso-Substituted Tetrabenzotriazaporphyrins: Easy Access to Hybrid Macrocycles. *Angewandte Chemie - International Edition* **2013**, *52* (41), 10784–10787.

(4) Chambrier I; Cook M J. Reaction of Phthalonitrile with Alkoxide Ions. *J Chem Res Synop* **1990**, 322–323.

(5) Jacob Gretton. Phthalocyanine and Subphthalocyanine Hybrid Macrocycles: Improved Accessibility and Synthetic Control via New Intermediates, University of East Anglia, 2022.

(6) Adler, A. D.; Longo, F. R.; Shergalis, W. Mechanistic Investigations of Porphyrin Syntheses. I. Preliminary Studies on Ms-Tetraphenylporphin. *J Am Chem Soc* **1964**, *86* (15), 3145–3149.

(7) González-Lucas, D.; Soobrattee, S. C.; Hughes, D. L.; Tizzard, G. J.; Coles, S. J.; Cammidge, A. N. Straightforward and Controlled Synthesis of Porphyrin–Phthalocyanine–Porphyrin Heteroleptic Triple-Decker Assemblies. *Chemistry - A European Journal* **2020**, *26* (47), 10724–10728.

4. Appendix

Crystal data and structure refinement for Mg-TBTAP-O-C_{10}-Br (2.31)

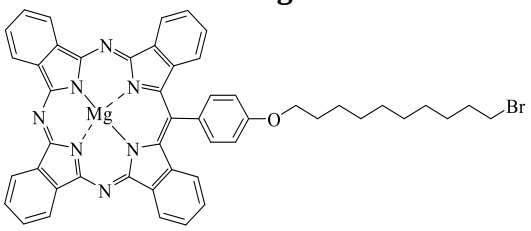

Identification code	isabf1232
Elemental formula	C50 H44 Br Mg N7 O2, *ca* C9.45
Formula weight	992.63
Crystal system, space group	Triclinic, P-1 (no. 2)
Unit cell dimensions	a = 13.3934(2) Å α = 108.1449(17) ° b = 13.4734(3) Å β = 101.9951(14) ° c = 14.5663(2) Å γ = 95.1688(15) °
Volume	2409.18(8) $Å^3$
Z, calculated density	2, 1.368 Mg/m^3
F(000)	1025
Absorption coefficient	1.710 mm^{-1}
Temperature	100.01(10) K
Wavelength	1.54184 Å
Crystal colour, shape	dark blue rhombus
Crystal size	0.46 x 0.22 x 0.06 mm
Crystal mounting:	on a small loop, in oil, fixed in cold N_2 stream
On the diffractometer:	
Theta range for data collection	7.654 to 69.985 °
Limiting indices	-16<=h<=16, -16<=k<=16, -17<=l<=17
Completeness to theta = 67.684	99.3 %

Absorption correction Semi-empirical from equivalents

Max. and min. transmission 1.00000 and 0.36517

Reflections collected (not including absences) 31099

No. of unique reflections 8979 [R(int) for equivalents = 0.057]

No. of 'observed' reflections ($I > 2\sigma_I$) 7881

Structure determined by: dual methods, in SHELXT

Refinement: Full-matrix least-squares on F^2, in SHELXL

Data / restraints / parameters 8979 / 1 / 690

Goodness-of-fit on F^2 1.053

Final R indices ('observed' data) $R_1 = 0.057$, $wR_2 = 0.161$

Final R indices (all data) $R_1 = 0.063$, $wR_2 = 0.165$

Reflections weighted:
$w = [\sigma^2(Fo^2)+(0.1014P)^2+1.8884P]^{-1}$ where $P=(Fo^2+2Fc^2)/3$

Extinction coefficient n/a

Largest diff. peak and hole 0.90 and -0.68 e.Å^{-3}

Location of largest difference peak near Mg

Table 1. Atomic coordinates (x 10^4) and equivalent isotropic displacement parameters (Å^2 x 10^4). U(eq) is defined as one third of the trace of the orthogonalized Uij tensor. E.s.ds are in parentheses.

	x	y	z	U(eq)	S.o.f.#
Mg	1462.7(7)	4015.1(7)	8568.4(7)	273(2)	
N(1)	2515.6(17)	4601.0(18)	7947.4(17)	254(5)	
C(2)	2718(2)	4088(2)	7043(2)	254(5)	
C(3)	3358(2)	4857(2)	6784(2)	267(5)	
C(4)	3784(2)	4826(2)	5971(2)	306(6)	
C(5)	4380(2)	5739(3)	6014(2)	362(7)	
C(6)	4578(2)	6676(3)	6826(2)	365(7)	
C(7)	4148(2)	6723(2)	7620(2)	328(6)	
C(8)	3534(2)	5811(2)	7580(2)	274(6)	
C(9)	2981(2)	5629(2)	8282(2)	255(5)	
N(10)	2948.5(17)	6418.8(17)	9109.1(17)	253(5)	

	N(11)	1898.7(16)	5397.7(17)	9781.6(16)	241(4)
	C(12)	2451(2)	6306(2)	9770(2)	250(5)
	C(13)	2434(2)	7190(2)	10651(2)	254(5)
	C(14)	2875(2)	8252(2)	10982(2)	297(6)
	C(15)	2721(2)	8913(2)	11865(2)	334(6)
	C(16)	2134(2)	8512(2)	12404(2)	343(6)
	C(17)	1703(2)	7447(2)	12078(2)	305(6)
	C(18)	1857(2)	6784(2)	11191(2)	257(5)
	C(19)	1541.9(19)	5642(2)	10621.3(19)	233(5)
	N(20	1014.3(17)	4966.4(17)	10932.0(16)	241(4)
	N(21)	959.9(17)	3385.9(17)	9539.1(16)	244(4)
	C(22)	766(2)	3916(2)	10427.8(19)	241(5)
	C(23)	229(2)	3164(2)	10784.1(19)	241(5)
	C(24)	-131(2)	3265(2)	11636(2)	278(5)
	C(25)	-618(2)	2356(2)	11726(2)	294(6)
	C(26)	-736(2)	1362(2)	10986(2)	303(6)
	C(27)	-378(2)	1262(2)	10146(2)	263(5)
	C(28)	113(2)	2168(2)	10057.0(19)	250(5)
	C(29)	584(2)	2323(2)	9290(2)	239(5)
	N(30)	631.0(17)	1526.8(17)	8498.1(16)	251(5)
	N(31)	1543.1(17)	2520.3(17)	7693.4(16)	247(5)
	C(32)	1065(2)	1626(2)	7771(2)	249(5)
	C(33)	1051(2)	724(2)	6909(2)	267(5)
	C(34)	651(2)	-344(2)	6658(2)	326(6)
	C(35)	728(3)	-1033(2)	5754(2)	402(7)
	C(36)	1177(3)	-658(2)	5118(2)	399(7)
	C(37)	1577(2)	401(2)	5362(2)	328(6)
	C(38)	1519(2)	1110(2)	6280(2)	270(5)
	C(39)	1841(2)	2259(2)	6807.2(19)	250(5)
	C(40)	2367(2)	3001(2)	6495.9(19)	251(5)
	C(41)	2522(2)	2612(2)	5463.3(19)	248(5)
	C(42)	1764(2)	2673(2)	4684(2)	267(5)
	C(43)	1848(2)	2327(2)	3706(2)	259(5)
	C(44)	2736(2)	1935(2)	3502.1(19)	248(5)
	C(45)	3503(2)	1856(2)	4276(2)	284(6)
	C(46)	3391(2)	2185(2)	5245(2)	292(6)
	O(47)	2931.2(14)	1628.1(15)	2581.8(13)	272(4)
	C(48)	2074(2)	1487(2)	1743(2)	308(6)
	C(49)	2491(2)	1278(2)	827(2)	322(6)
	C(50)	3090(2)	2283(2)	793(2)	341(6)
	C(51)	3511(2)	2090(3)	-130(2)	352(6)
	C(52)	4053(2)	3099(3)	-209(2)	373(7)
	C(53)	4473(2)	2890(3)	-1127(2)	365(7)
	C(54)	5061(2)	3873(3)	-1201(2)	352(6)
	C(55)	5471(2)	3631(2)	-2132(2)	350(6)
	C(56)	6101(2)	4590(3)	-2203(2)	343(6)
	C(57)	6521(3)	4262(3)	-3119(2)	388(7)
	Br	7321.5(2)	5472.4(3)	-3267.5(2)	394.3(13)
	O(61)	126.1(15)	4215.4(15)	7777.8(15)	299(4)
	C(62)	-198(3)	3970(3)	6757(3)	556(9)
	C(201)	4640(11)	-472(8)	4374(8)	910(4)
0.5					
	C(202)	5729(10)	497(11)	4942(10)	890(4)
0.5					
	C(203)	6191(7)	1525(9)	5246(8)	900(4)
0.6					
	C(204)	5470(30)	150(40)	4100(40)	1170(12)*
0.2					

	C(205)	5532(11)	-195(12)	3356(12)	900(4)*
0.45					
	C(206)	5429(9)	307(13)	2854(14)	1100(5)
0.55					
	C(207)	5259(8)	304(8)	2359(9)	590(2)*
0.55					
	C(208)	5238(8)	342(6)	1665(12)	800(3)
0.5					
	C(209)	5519(9)	555(8)	986(10)	910(4)
0.55					
	C(210)	6552(13)	842(12)	1223(12)	780(4)*
0.4					
	C(211)	7012(4)	879(4)	1736(6)	671(14)
0.9					
	C(212)	6930(20)	1040(20)	2470(20)	1010(8)*
0.25					
	C(213)	6429(13)	284(11)	2503(10)	940(4)
0.45					
	C(214)	6470(30)	840(40)	3270(30)	1190(12)*
0.2					
	C(215)	6495(17)	1796(17)	4805(16)	1090(7)*
0.4					
	C(216)	-2490(20)	2720(20)	4880(20)	810(7)*
0.2					
	C(217)	-1840(30)	3550(30)	4350(30)	1190(10)*
0.25					
	C(218)	-1357(6)	3921(8)	4096(6)	790(2)
0.65					
	C(219)	-471(7)	3689(6)	4335(5)	780(2)
0.7					
	C(220)	-1288(6)	4696(7)	4847(6)	750(2)
0.65					

- site occupancy, if different from 1.
* - U(iso) (Å^2 x 10^4)

Table 2. Molecular dimensions. Bond lengths are in Ångstroms, angles in degrees. E.s.ds are in parentheses.

Mg-O(61)	2.007(2)	Mg-N(21)	2.052(2)
Mg-N(31)	2.047(2)	Mg-N(11)	2.064(2)
Mg-N(1)	2.050(2)		
O(61)-Mg-N(31)	99.24(9)	N(1)-Mg-N(21)	156.87(10)
O(61)-Mg-N(1)	101.45(9)	O(61)-Mg-N(11)	103.61(9)
N(31)-Mg-N(1)	88.59(9)	N(31)-Mg-N(11)	157.08(10)
O(61)-Mg-N(21)	101.63(9)	N(1)-Mg-N(11)	88.66(9)
N(31)-Mg-N(21)	89.19(9)	N(21)-Mg-N(11)	84.50(9)
N(1)-C(9)	1.358(3)	C(6)-C(7)	1.382(4)
N(1)-C(2)	1.379(3)	C(7)-C(8)	1.394(4)
C(2)-C(40)	1.413(4)	C(8)-C(9)	1.446(4)
C(2)-C(3)	1.473(4)	C(9)-N(10)	1.347(4)
C(3)-C(8)	1.399(4)	N(10)-C(12)	1.317(4)
C(3)-C(4)	1.407(4)	N(11)-C(19)	1.361(3)
C(4)-C(5)	1.383(4)	N(11)-C(12)	1.379(3)
C(5)-C(6)	1.394(5)	C(12)-C(13)	1.459(4)

C(13)-C(14)	1.389(4)	C(35)-C(36)	1.395(5)
C(13)-C(18)	1.400(4)	C(36)-C(37)	1.384(4)
C(14)-C(15)	1.387(4)	C(37)-C(38)	1.402(4)
C(15)-C(16)	1.404(4)	C(38)-C(39)	1.474(4)
C(16)-C(17)	1.390(4)	C(39)-C(40)	1.410(4)
C(17)-C(18)	1.391(4)	C(40)-C(41)	1.496(4)
C(18)-C(19)	1.475(4)	C(41)-C(42)	1.385(4)
C(19)-N(20)	1.344(3)	C(41)-C(46)	1.395(4)
N(20)-C(22)	1.349(3)	C(42)-C(43)	1.387(4)
N(21)-C(22)	1.360(3)	C(43)-C(44)	1.394(4)
N(21)-C(29)	1.381(3)	C(44)-O(47)	1.363(3)
C(22)-C(23)	1.472(4)	C(44)-C(45)	1.397(4)
C(23)-C(24)	1.395(4)	C(45)-C(46)	1.386(4)
C(23)-C(28)	1.398(4)	O(47)-C(48)	1.443(3)
C(24)-C(25)	1.391(4)	C(48)-C(49)	1.508(4)
C(25)-C(26)	1.405(4)	C(49)-C(50)	1.532(4)
C(26)-C(27)	1.379(4)	C(50)-C(51)	1.522(4)
C(27)-C(28)	1.389(4)	C(51)-C(52)	1.531(4)
C(28)-C(29)	1.450(4)	C(52)-C(53)	1.513(4)
C(29)-N(30)	1.325(3)	C(53)-C(54)	1.524(4)
N(30)-C(32)	1.345(3)	C(54)-C(55)	1.521(4)
N(31)-C(32)	1.361(3)	C(55)-C(56)	1.521(4)
N(31)-C(39)	1.381(3)	C(56)-C(57)	1.511(4)
C(32)-C(33)	1.445(4)	C(57)-Br	1.964(3)
C(33)-C(34)	1.394(4)		
C(33)-C(38)	1.408(4)	O(61)-C(62)	1.382(4)
C(34)-C(35)	1.384(4)	O(61)-H(61)	0.791(18)

C(9)-N(1)-C(2)	109.0(2)	C(16)-C(17)-C(18)	118.2(3)
C(9)-N(1)-Mg	123.97(18)	C(17)-C(18)-C(13)	120.2(2)
C(2)-N(1)-Mg	126.03(18)	C(17)-C(18)-C(19)	134.1(3)
N(1)-C(2)-C(40)	123.8(2)	C(13)-C(18)-C(19)	105.7(2)
N(1)-C(2)-C(3)	108.4(2)	N(20)-C(19)-N(11)	126.9(2)
C(40)-C(2)-C(3)	127.7(2)	N(20)-C(19)-C(18)	123.3(2)
C(8)-C(3)-C(4)	118.8(3)	N(11)-C(19)-C(18)	109.7(2)
C(8)-C(3)-C(2)	105.8(2)	C(19)-N(20)-C(22)	123.0(2)
C(4)-C(3)-C(2)	135.3(3)	C(22)-N(21)-C(29)	108.3(2)
C(5)-C(4)-C(3)	118.0(3)	C(22)-N(21)-Mg	127.71(18)
C(4)-C(5)-C(6)	122.7(3)	C(29)-N(21)-Mg	123.07(17)
C(7)-C(6)-C(5)	119.9(3)	N(20)-C(22)-N(21)	127.0(2)
C(6)-C(7)-C(8)	118.0(3)	N(20)-C(22)-C(23)	123.4(2)
C(7)-C(8)-C(3)	122.5(3)	N(21)-C(22)-C(23)	109.6(2)
C(7)-C(8)-C(9)	130.3(3)	C(24)-C(23)-C(28)	120.2(2)
C(3)-C(8)-C(9)	107.2(2)	C(24)-C(23)-C(22)	134.0(2)
N(10)-C(9)-N(1)	128.8(2)	C(28)-C(23)-C(22)	105.8(2)
N(10)-C(9)-C(8)	121.6(2)	C(25)-C(24)-C(23)	118.2(2)
N(1)-C(9)-C(8)	109.5(2)	C(24)-C(25)-C(26)	121.0(3)
C(12)-N(10)-C(9)	124.5(2)	C(27)-C(26)-C(25)	120.8(3)
C(19)-N(11)-C(12)	108.5(2)	C(26)-C(27)-C(28)	118.2(3)
C(19)-N(11)-Mg	127.09(17)	C(27)-C(28)-C(23)	121.6(2)
C(12)-N(11)-Mg	123.26(18)	C(27)-C(28)-C(29)	131.5(2)
N(10)-C(12)-N(11)	128.5(2)	C(23)-C(28)-C(29)	106.9(2)
N(10)-C(12)-C(13)	122.3(2)	N(30)-C(29)-N(21)	128.2(2)
N(11)-C(12)-C(13)	109.2(2)	N(30)-C(29)-C(28)	122.5(2)
C(14)-C(13)-C(18)	121.6(3)	N(21)-C(29)-C(28)	109.3(2)
C(14)-C(13)-C(12)	131.5(3)	C(29)-N(30)-C(32)	124.9(2)
C(18)-C(13)-C(12)	106.9(2)	C(32)-N(31)-C(39)	108.8(2)
C(15)-C(14)-C(13)	118.1(3)	C(32)-N(31)-Mg	123.35(17)
C(14)-C(15)-C(16)	120.5(3)	C(39)-N(31)-Mg	125.94(17)
C(17)-C(16)-C(15)	121.3(3)	N(30)-C(32)-N(31)	128.5(2)

N(30)-C(32)-C(33)	121.7(2)	C(42)-C(43)-C(44)	119.1(2)
N(31)-C(32)-C(33)	109.8(2)	O(47)-C(44)-C(43)	124.4(2)
C(34)-C(33)-C(38)	122.3(3)	O(47)-C(44)-C(45)	115.9(2)
C(34)-C(33)-C(32)	130.7(3)	C(43)-C(44)-C(45)	119.7(2)
C(38)-C(33)-C(32)	107.0(2)	C(46)-C(45)-C(44)	120.1(2)
C(35)-C(34)-C(33)	117.7(3)	C(45)-C(46)-C(41)	120.7(2)
C(34)-C(35)-C(36)	120.6(3)	C(44)-O(47)-C(48)	116.9(2)
C(37)-C(36)-C(35)	122.1(3)	O(47)-C(48)-C(49)	107.7(2)
C(36)-C(37)-C(38)	118.3(3)	C(48)-C(49)-C(50)	112.2(2)
C(37)-C(38)-C(33)	119.1(2)	C(51)-C(50)-C(49)	113.0(3)
C(37)-C(38)-C(39)	135.2(3)	C(50)-C(51)-C(52)	113.7(3)
C(33)-C(38)-C(39)	105.7(2)	C(53)-C(52)-C(51)	112.9(3)
N(31)-C(39)-C(40)	123.7(2)	C(52)-C(53)-C(54)	114.1(3)
N(31)-C(39)-C(38)	108.6(2)	C(55)-C(54)-C(53)	112.6(3)
C(40)-C(39)-C(38)	127.8(2)	C(54)-C(55)-C(56)	113.6(3)
C(39)-C(40)-C(2)	126.5(2)	C(57)-C(56)-C(55)	109.8(3)
C(39)-C(40)-C(41)	116.8(2)	C(56)-C(57)-Br	111.8(2)
C(2)-C(40)-C(41)	116.6(2)		
C(42)-C(41)-C(46)	118.3(2)	C(62)-O(61)-Mg	128.0(2)
C(42)-C(41)-C(40)	118.5(2)	C(62)-O(61)-H(61)	119(2)
C(46)-C(41)-C(40)	123.2(2)	Mg-O(61)-H(61)	113(2)
C(41)-C(42)-C(43)	122.0(2)		

C(201)-C(202)#1	1.208(17)	C(207)-C(214)	1.79(4)
C(201)-C(204)	1.53(5)	C(208)-C(209)	1.230(18)
C(201)-C(202)	1.73(2)	C(209)-C(210)	1.344(19)
C(202)-C(204)	1.13(5)	C(210)-C(211)	0.848(14)
C(202)-C(203)	1.359(17)	C(210)-C(212)	1.71(3)
C(203)-C(215)	0.97(2)	C(211)-C(212)	1.06(3)
C(204)-C(205)	1.06(5)	C(212)-C(213)	1.18(3)
C(205)-C(206)	1.138(19)	C(212)-C(214)	1.50(5)
C(205)-C(207)	1.770(19)	C(213)-C(214)	1.12(4)
C(206)-C(207)	0.709(14)	C(215)-C(216)#2	1.72(4)
C(206)-C(214)	1.42(4)	C(217)-C(218)	0.98(4)
C(206)-C(213)	1.53(2)	C(217)-C(220)	1.52(4)
C(206)-C(208)	1.71(2)	C(218)-C(220)	1.235(11)
C(207)-C(208)	1.022(16)	C(218)-C(219)	1.260(11)
C(207)-C(213)	1.54(2)		

C(202)#1-C(201)-C(202)	103.6(11)	C(208)-C(207)-C(213)	88.0(11)
C(202)-C(201)-C(203)#1	136.9(9)	C(208)-C(207)-C(214)	115.9(18)
C(201)#1-C(201)-C(203)	101.1(11)	C(209)-C(208)-C(213)	104.8(10)
C(204)-C(202)-C(201)#1	136(3)	C(208)-C(209)-C(210)	110.8(11)
C(204)-C(202)-C(203)	111(3)	C(211)-C(210)-C(209)	131.0(18)
C(201)#1-C(202)-C(203)	102.5(13)	C(209)-C(210)-C(212)	104.4(15)
C(204)-C(202)-C(215)	89(3)	C(210)-C(211)-C(212)	127(2)
C(201)#1-C(202)-C(215)	126.6(13)	C(210)-C(211)-C(213)	109.3(13)
C(215)-C(203)-C(202)	120.7(18)	C(212)-C(211)-C(209)	100.0(17)
C(205)-C(204)-C(201)	114(4)	C(211)-C(212)-C(213)	108(3)
C(201)-C(204)-C(206)	127(3)	C(213)-C(212)-C(210)	100(2)
C(204)-C(205)-C(206)	118(3)	C(214)-C(212)-C(210)	138(3)
C(204)-C(205)-C(207)	129(3)	C(214)-C(213)-C(212)	81(3)
C(204)-C(205)-C(214)	101(3)	C(212)-C(213)-C(206)	124(2)
C(207)-C(206)-C(214)	110(3)	C(214)-C(213)-C(207)	83(2)
C(205)-C(206)-C(214)	92(2)	C(212)-C(213)-C(207)	115.6(19)
C(205)-C(206)-C(213)	102.5(13)	C(214)-C(213)-C(211)	114(2)
C(214)-C(206)-C(208)	100(2)	C(206)-C(213)-C(211)	136.2(12)
C(214)-C(206)-C(204)	87(2)	C(207)-C(213)-C(211)	113.6(10)
C(213)-C(206)-C(204)	117.6(16)	C(214)-C(213)-C(208)	108(3)

C(212)-C(213)-C(208)	96.6(17)	C(203)-C(215)-C(216)#2	139(2)
C(211)-C(213)-C(208)	82.2(8)	C(220)-C(217)-C(216)	129(2)
C(206)-C(214)-C(212)	110(3)	C(216)-C(217)-C(219)	127(2)
C(212)-C(214)-C(207)	89(2)	C(217)-C(218)-C(220)	86(2)
C(213)-C(214)-C(205)	86(3)	C(217)-C(218)-C(219)	109(2)
C(212)-C(214)-C(205)	137(3)	C(220)-C(218)-C(219)	98.5(7)

Symmetry transformations used to generate equivalent atoms:
#1 : 1-x, -y, 1-z #2 : x+1, y, z

Table 3. Anisotropic displacement parameters ($Å^2$ x 10^4) for the expression:

$$\exp\{-2\pi^2(h^2a^{*2}U_{11} + \ldots + 2hka^*b^*U_{12})\}$$

E.s.ds are in parentheses.

	U_{11}	U_{22}	U_{33}	U_{23}	U_{13}	U_{12}
Mg	347(5)	236(4)	298(5)	106(4)	187(4)	54(3)
N(1)	261(11)	275(11)	283(11)	121(9)	140(9)	66(9)
C(2)	239(12)	307(13)	279(13)	145(11)	121(10)	62(10)
C(3)	252(12)	322(14)	289(13)	153(11)	115(10)	62(10)
C(4)	308(14)	359(15)	314(14)	154(12)	156(11)	51(11)
C(5)	364(15)	434(16)	362(16)	188(13)	185(12)	25(13)
C(6)	387(16)	377(16)	391(16)	183(13)	176(13)	-8(13)
C(7)	339(14)	342(15)	335(15)	141(12)	138(12)	-1(12)
C(8)	246(12)	328(14)	297(14)	142(11)	115(11)	51(10)
C(9)	241(12)	267(13)	303(13)	130(11)	114(10)	37(10)
N(10)	253(11)	256(11)	305(12)	133(9)	123(9)	51(9)
N(11)	248(10)	249(11)	282(11)	126(9)	131(9)	42(8)
C(12)	244(12)	234(12)	311(13)	131(11)	92(10)	46(10)
C(13)	242(12)	262(13)	296(13)	123(11)	95(10)	64(10)
C(14)	300(13)	270(13)	364(15)	139(11)	128(11)	49(11)
C(15)	363(15)	262(13)	381(16)	88(12)	142(12)	37(11)
C(16)	386(15)	290(14)	349(15)	64(12)	161(12)	42(12)
C(17)	332(14)	283(13)	329(14)	99(11)	151(11)	45(11)
C(18)	247(12)	243(13)	301(14)	97(11)	99(10)	52(10)
C(19)	239(12)	233(12)	269(13)	102(10)	118(10)	52(10)
N(20)	262(11)	237(10)	259(11)	96(9)	117(9)	59(8)
N(21)	272(11)	229(10)	275(11)	102(9)	131(9)	55(8)
C(22)	259(12)	253(12)	264(13)	118(10)	120(10)	66(10)
C(23)	251(12)	257(12)	262(13)	123(10)	105(10)	45(10)
C(24)	334(14)	262(13)	286(13)	114(11)	141(11)	65(11)
C(25)	335(14)	319(14)	294(14)	147(11)	158(11)	49(11)
C(26)	331(14)	292(14)	337(14)	162(12)	125(11)	12(11)
C(27)	300(13)	256(12)	267(13)	121(10)	99(10)	34(10)
C(28)	263(13)	272(13)	266(13)	131(11)	104(10)	70(10)
C(29)	261(12)	224(12)	268(13)	114(10)	94(10)	42(10)
N(30)	295(11)	251(11)	251(11)	115(9)	110(9)	60(9)
N(31)	289(11)	252(11)	269(11)	125(9)	150(9)	74(9)
C(32)	282(13)	242(12)	270(13)	110(10)	122(10)	75(10)
C(33)	309(13)	258(13)	268(13)	108(11)	114(11)	50(10)
C(34)	406(15)	279(14)	331(15)	113(12)	168(12)	42(12)
C(35)	534(19)	264(14)	404(17)	65(12)	212(14)	-3(13)
C(36)	516(18)	336(15)	338(16)	38(12)	225(14)	27(13)
C(37)	396(15)	327(14)	299(14)	98(12)	179(12)	58(12)
C(38)	295(13)	270(13)	276(13)	97(11)	122(11)	63(10)
C(39)	280(13)	260(13)	260(13)	104(10)	138(10)	76(10)
C(40)	254(12)	309(13)	260(13)	135(11)	136(10)	92(10)

C(41)	269(12)	280(13)	242(13)	115(10)	126(10)	42(10)
C(42)	252(12)	280(13)	309(14)	125(11)	116(10)	57(10)
C(43)	263(12)	276(13)	263(13)	122(10)	73(10)	34(10)
C(44)	292(13)	229(12)	242(13)	92(10)	102(10)	12(10)
C(45)	252(13)	347(14)	293(14)	117(11)	122(11)	85(11)
C(46)	277(13)	380(15)	264(13)	136(11)	101(11)	101(11)
O(47)	318(10)	299(9)	221(9)	92(7)	109(7)	47(8)
C(48)	318(14)	346(14)	280(14)	126(11)	88(11)	49(11)
C(49)	365(15)	340(14)	293(14)	130(12)	121(12)	42(12)
C(50)	343(15)	388(16)	323(15)	150(12)	119(12)	23(12)
C(51)	358(15)	407(16)	341(15)	179(13)	128(12)	31(12)
C(52)	358(15)	436(17)	386(16)	208(14)	130(13)	45(13)
C(53)	331(15)	431(17)	403(16)	219(14)	132(13)	42(13)
C(54)	314(14)	426(16)	368(16)	202(13)	99(12)	42(12)
C(55)	318(14)	396(16)	371(16)	174(13)	103(12)	40(12)
C(56)	303(14)	427(16)	384(16)	226(13)	129(12)	65(12)
C(57)	434(17)	417(17)	412(17)	214(14)	187(14)	103(13)
Br	399(2)	431(2)	426(2)	212.4(15)	174.2(14)	23.1(14)
O(61)	343(10)	305(10)	310(10)	109(8)	192(8)	88(8)
C(62)	630(20)	590(20)	510(20)	193(18)	240(18)	176(19)
C(201)	1260(100)	600(60)	750(70)	190(50)	-140(70)	620(60)
C(202)	1060(900	1080(100)	870(80)	520(70)	410(70)	790(80)
C(203)	530(50)	930(70)	810(60)	-120(50)	-200(40)	320(50)
C(206)	640(60)	1570(130)	1410(120)	990(110)	180(70)	280(70)
C(208)	700(60)	240(40)	1230(110)	120(50)	30(60)	-90(30)
C(209)	850(70)	520(50)	1110(80)	170(50)	-190(60)	200(50)
C(211)	530(30)	540(30)	1040(50)	280(30)	340(30)	160(20)
C(213)	1300(120)	810(80)	730(80)	210(60)	430(80)	60(80)
C(218)	560(40)	930(60)	760(50)	170(50)	110(40)	160(40)
C(219)	1030(60)	700(40)	620(40)	250(30)	110(40)	270(40)
C(220)	560(40)	840(50)	750(50)	90(40)	220(30)	100(40)

Table 4. Hydrogen coordinates (x 10^4) and isotropic displacement parameters ($Å^2$ x 10^3). All hydrogen atoms were included in idealised positions with U(iso)'s set at 1.2*U(eq) or, for the methyl group hydrogen atoms, 1.5*U(eq) of the parent carbon atoms.

	x	y	z	U(iso)	S.o.f.#
H(4)	3665	4196	5411	37	
H(5)	4667	5728	5467	43	
H(6)	5007	7281	6834	44	
H(7)	4268	7357	8176	39	
H(14)	3271	8518	10613	36	
H(15)	3014	9643	12108	40	
H(16)	2030	8978	13005	41	
H(17)	1314	7179	12450	37	
H(24)	-45	3935	12141	33	
H(25)	-875	2408	12298	35	
H(26)	-1067	751	11066	36	
H(27)	-465	592	9641	32	
H(34)	336	-590	7091	39	
H(35)	474	-1768	5567	48	
H(36)	1209	-1144	4496	48	
H(37)	1883	641	4920	39	
H(42)	1168	2960	4825	32	

H(43)	1308	2358	3182	31
H(45)	4102	1575	4138	34
H(46)	3912	2120	5766	35
H(48A)	1749	2131	1850	37
H(48B)	1545	882	1661	37
H(49A)	1908	981	224	39
H(49B)	2954	744	819	39
H(50A)	2627	2818	808	41
H(50B)	3674	2577	1395	41
H(51A)	2932	1752	-730	42
H(51B)	4008	1590	-121	42
H(52A)	3556	3599	-226	45
H(52B)	4630	3442	392	45
H(53A)	3889	2577	-1727	44
H(53B)	4940	2361	-1126	44
H(54A)	4596	4403	-1206	42
H(54B)	5649	4187	-605	42
H(55A)	4879	3344	-2727	42
H(55B)	5909	3076	-2141	42
H(56A)	5658	5133	-2241	41
H(56B)	6680	4903	-1599	41
H(57A)	5938	3933	-3718	47
H(57B)	6969	3726	-3071	47
H(62A)	323	4318	6525	83
H(62B)	-857	4216	6592	83
H(62C)	-291	3201	6430	83
H(61)	-250(20)	4460(30)	8110(20)	30(8)

Table 5. Torsion angles, in degrees. E.s.ds are in parentheses.

C(9)-N(1)-C(2)-C(40)	178.6(2)	C(13)-C(18)-C(19)-N(11)	-1.2(3)
Mg-N(1)-C(2)-C(40)	-12.5(4)	N(11)-C(19)-N(20)-C(22)	0.2(4)
C(9)-N(1)-C(2)-C(3)	-0.4(3)	C(18)-C(19)-N(20)-C(22)	-177.2(2)
Mg-N(1)-C(2)-C(3)	168.51(17)	C(19)-N(20)-C(22)-N(21)	-2.7(4)
N(1)-C(2)-C(3)-C(8)	1.6(3)	C(19)-N(20)-C(22)-C(23)	177.2(2)
C(40)-C(2)-C(3)-C(8)	-177.4(3)	C(29)-N(21)-C(22)-N(20)	179.7(2)
N(1)-C(2)-C(3)-C(4)	-178.3(3)	Mg-N(21)-C(22)-N(20)	-11.1(4)
C(40)-C(2)-C(3)-C(4)	2.7(5)	C(29)-N(21)-C(22)-C(23)	-0.2(3)
C(8)-C(3)-C(4)-C(5)	1.6(4)	Mg-N(21)-C(22)-C(23)	168.94(17)
C(2)-C(3)-C(4)-C(5)	-178.5(3)	N(20)-C(22)-C(23)-C(24)	-1.2(5)
C(3)-C(4)-C(5)-C(6)	0.5(5)	N(21)-C(22)-C(23)-C(24)	178.7(3)
C(4)-C(5)-C(6)-C(7)	-1.7(5)	N(20)-C(22)-C(23)-C(28)	179.8(2)
C(5)-C(6)-C(7)-C(8)	0.8(5)	N(21)-C(22)-C(23)-C(28)	-0.3(3)
C(6)-C(7)-C(8)-C(3)	1.3(4)	C(28)-C(23)-C(24)-C(25)	-1.1(4)
C(6)-C(7)-C(8)-C(9)	-179.1(3)	C(22)-C(23)-C(24)-C(25)	179.9(3)
C(4)-C(3)-C(8)-C(7)	-2.5(4)	C(23)-C(24)-C(25)-C(26)	0.7(4)
C(2)-C(3)-C(8)-C(7)	177.6(3)	C(24)-C(25)-C(26)-C(27)	-0.5(4)
C(4)-C(3)-C(8)-C(9)	177.8(2)	C(25)-C(26)-C(27)-C(28)	0.8(4)
C(2)-C(3)-C(8)-C(9)	-2.1(3)	C(26)-C(27)-C(28)-C(23)	-1.3(4)
C(2)-N(1)-C(9)-N(10)	177.0(3)	C(26)-C(27)-C(28)-C(29)	178.7(3)
Mg-N(1)-C(9)-N(10)	7.8(4)	C(24)-C(23)-C(28)-C(27)	1.5(4)
C(2)-N(1)-C(9)-C(8)	-1.0(3)	C(22)-C(23)-C(28)-C(27)	-179.3(2)
Mg-N(1)-C(9)-C(8)	-170.13(17)	C(24)-C(23)-C(28)-C(29)	-178.5(2)
C(7)-C(8)-C(9)-N(10)	4.2(5)	C(22)-C(23)-C(28)-C(29)	0.7(3)
C(3)-C(8)-C(9)-N(10)	-176.1(2)	C(22)-N(21)-C(29)-N(30)	-178.4(3)
C(7)-C(8)-C(9)-N(1)	-177.7(3)	Mg-N(21)-C(29)-N(30)	11.9(4)
C(3)-C(8)-C(9)-N(1)	2.0(3)	C(22)-N(21)-C(29)-C(28)	0.7(3)
N(1)-C(9)-N(10)-C(12)	1.6(4)	Mg-N(21)-C(29)-C(28)	-169.11(17)
C(8)-C(9)-N(10)-C(12)	179.3(2)	C(27)-C(28)-C(29)-N(30)	-1.8(4)
C(9)-N(10)-C(12)-N(11)	1.8(4)	C(23)-C(28)-C(29)-N(30)	178.2(2)
C(9)-N(10)-C(12)-C(13)	-179.6(2)	C(27)-C(28)-C(29)-N(21)	179.1(3)
C(19)-N(11)-C(12)-N(10)	178.0(3)	C(23)-C(28)-C(29)-N(21)	-0.9(3)
Mg-N(11)-C(12)-N(10)	-13.6(4)	N(21)-C(29)-N(30)-C(32)	-0.5(4)
C(19)-N(11)-C(12)-C(13)	-0.8(3)	C(28)-C(29)-N(30)-C(32)	-179.5(2)
Mg-N(11)-C(12)-C(13)	167.66(17)	C(29)-N(30)-C(32)-N(31)	1.0(4)
N(10)-C(12)-C(13)-C(14)	0.6(4)	C(29)-N(30)-C(32)-C(33)	-177.5(2)
N(11)-C(12)-C(13)-C(14)	179.5(3)	C(39)-N(31)-C(32)-N(30)	-177.9(3)
N(10)-C(12)-C(13)-C(18)	-178.9(2)	Mg-N(31)-C(32)-N(30)	-12.7(4)
N(11)-C(12)-C(13)-C(18)	0.0(3)	C(39)-N(31)-C(32)-C(33)	0.7(3)
C(18)-C(13)-C(14)-C(15)	-0.6(4)	Mg-N(31)-C(32)-C(33)	165.95(18)
C(12)-C(13)-C(14)-C(15)	180.0(3)	N(30)-C(32)-C(33)-C(34)	-1.2(5)
C(13)-C(14)-C(15)-C(16)	0.0(4)	N(31)-C(32)-C(33)-C(34)	-180.0(3)
C(14)-C(15)-C(16)-C(17)	0.7(5)	N(30)-C(32)-C(33)-C(38)	177.1(2)
C(15)-C(16)-C(17)-C(18)	-0.7(4)	N(31)-C(32)-C(33)-C(38)	-1.6(3)
C(16)-C(17)-C(18)-C(13)	0.1(4)	C(38)-C(33)-C(34)-C(35)	0.1(4)
C(16)-C(17)-C(18)-C(19)	179.3(3)	C(32)-C(33)-C(34)-C(35)	178.3(3)
C(14)-C(13)-C(18)-C(17)	0.5(4)	C(33)-C(34)-C(35)-C(36)	-1.1(5)
C(12)-C(13)-C(18)-C(17)	-179.9(2)	C(34)-C(35)-C(36)-C(37)	1.2(5)
C(14)-C(13)-C(18)-C(19)	-178.9(2)	C(35)-C(36)-C(37)-C(38)	-0.3(5)
C(12)-C(13)-C(18)-C(19)	0.7(3)	C(36)-C(37)-C(38)-C(33)	-0.6(4)
C(12)-N(11)-C(19)-N(20)	-176.5(2)	C(36)-C(37)-C(38)-C(39)	180.0(3)
Mg-N(11)-C(19)-N(20)	15.6(4)	C(34)-C(33)-C(38)-C(37)	0.8(4)
C(12)-N(11)-C(19)-C(18)	1.2(3)	C(32)-C(33)-C(38)-C(37)	-177.8(3)
Mg-N(11)-C(19)-C(18)	-166.64(17)	C(34)-C(33)-C(38)-C(39)	-179.7(3)
C(17)-C(18)-C(19)-N(20)	-2.7(5)	C(32)-C(33)-C(38)-C(39)	1.8(3)
C(13)-C(18)-C(19)-N(20)	176.6(2)	C(32)-N(31)-C(39)-C(40)	-179.5(2)
C(17)-C(18)-C(19)-N(11)	179.5(3)	Mg-N(31)-C(39)-C(40)	15.8(4)

C(32)-N(31)-C(39)-C(38)	0.4(3)	C(41)-C(42)-C(43)-C(44)	-1.9(4)
Mg-N(31)-C(39)-C(38)	-164.32(18)	C(42)-C(43)-C(44)-O(47)	-176.2(2)
C(37)-C(38)-C(39)-N(31)	178.0(3)	C(42)-C(43)-C(44)-C(45)	2.6(4)
C(33)-C(38)-C(39)-N(31)	-1.4(3)	O(47)-C(44)-C(45)-C(46)	177.7(2)
C(37)-C(38)-C(39)-C(40)	-2.1(5)	C(43)-C(44)-C(45)-C(46)	-1.3(4)
C(33)-C(38)-C(39)-C(40)	178.5(3)	C(44)-C(45)-C(46)-C(41)	-0.8(4)
N(31)-C(39)-C(40)-C(2)	3.8(4)	C(42)-C(41)-C(46)-C(45)	1.6(4)
C(38)-C(39)-C(40)-C(2)	-176.1(3)	C(40)-C(41)-C(46)-C(45)	-178.8(3)
N(31)-C(39)-C(40)-C(41)	-172.9(2)	C(43)-C(44)-O(47)-C(48)	-13.9(4)
C(38)-C(39)-C(40)-C(41)	7.2(4)	C(45)-C(44)-O(47)-C(48)	167.2(2)
N(1)-C(2)-C(40)-C(39)	-5.5(4)	C(44)-O(47)-C(48)-C(49)	173.4(2)
C(3)-C(2)-C(40)-C(39)	173.3(3)	O(47)-C(48)-C(49)-C(50)	-74.7(3)
N(1)-C(2)-C(40)-C(41)	171.2(2)	C(48)-C(49)-C(50)-C(51)	-179.6(2)
C(3)-C(2)-C(40)-C(41)	-10.0(4)	C(49)-C(50)-C(51)-C(52)	176.3(3)
C(39)-C(40)-C(41)-C(42)	89.3(3)	C(50)-C(51)-C(52)-C(53)	179.6(3)
C(2)-C(40)-C(41)-C(42)	-87.7(3)	C(51)-C(52)-C(53)-C(54)	-177.3(3)
C(39)-C(40)-C(41)-C(46)	-90.3(3)	C(52)-C(53)-C(54)-C(55)	-180.0(3)
C(2)-C(40)-C(41)-C(46)	92.6(3)	C(53)-C(54)-C(55)-C(56)	-177.6(2)
C(46)-C(41)-C(42)-C(43)	-0.2(4)	C(54)-C(55)-C(56)-C(57)	177.0(2)
C(40)-C(41)-C(42)-C(43)	-179.9(2)	C(55)-C(56)-C(57)-Br	178.9(2)

Table 6. Hydrogen bonds, in Ångstroms and degrees.

D-H...A	d(D-H)	d(H...A)	d(D...A)	<(DHA)
C(62)-H(62B)...Br#1	0.98	3.10	4.043(4)	162.4
O(61)-H(61)...N(20)#2	0.791(18)	1.914(19)	2.699(3)	172(3)

Symmetry transformations used to generate equivalent atoms:
#1 : x-1, y, z+1 #2 : -x, 1-y, 2-z

Crystal structure analysis of
[Mg (MeOH) {$(C_8H_4N_2)_3$-C_8H_4NC-C_6H_4-$O(CH_2)_{10}Br$}], *ca* 9.45(C)

Crystal data: $C_{50}H_{44}BrMgN_7O_2$, *ca* 9.45C, M = 992.63. Triclinic, space group P-1 (no. 2), a = 13.3934(2), b = 13.4734(3), c = 14.5663(2) Å, α = 108.1449(17), β = 101.9951(14), γ = 95.1688(15) °, V = 2409.18(8) $Å^3$. Z = 2, Dc = 1.368 g cm^{-3}, F(000) = 1025, T = 100.01(10) K, μ(Cu-Kα) = 17.1 cm^{-1}, λ(Cu-Kα) = 1.54184 Å.

The crystal was a dark blue rhombus. From a sample under oil, one, *ca* 0.46 x 0.22 x 0.06 mm, was mounted on a small loop and fixed in the cold nitrogen stream on a Rigaku Oxford Diffraction XtaLAB Synergy diffractometer, equipped with Cu-Kα radiation, HyPix detector and mirror monochromator. Intensity data were measured by thin-slice ω-scans. Total no. of reflections recorded, to θ_{max} = 70.0°, was 31,099 of which 8979 were unique (Rint = 0.057); 7881 were 'observed' with $I > 2\sigma_I$.

Data were processed using the CrysAlisPro-CCD and -RED (1) programs. The structure was determined by the intrinsic phasing routines in the SHELXT program (2A) and refined by full-matrix least-squares methods, on F^2's, in SHELXL (2B). The Mg complex molecule is well-defined, but several solvent molecules, principally MeOH, were disordered chaotically in the gaps between layers of the Mg complex. The non-hydrogen atoms of the complex were refined with anisotropic thermal parameters. The hydrogen atom on O(61) was located in a difference map and was refined with a distance restraint. The remaining hydrogen atoms in the complex were included in idealised positions and their Uiso values were set to ride on the Ueq values of the parent carbon atoms. The disordered solvent atoms were included as carbon atoms in sites of significance in difference maps, and refined anisotropically or isotropically, varying the site occupancy to give a fairly even set of thermal parameters across the solvent region. At the conclusion of the refinement, wR_2 = 0.165 and R_1 = 0.063 (2B) for all 8979 reflections weighted $w = [\sigma^2(F_o^2) + (0.1014\ P)^2 + 1.8884\ P]^{-1}$ with $P = (F_o^2 + 2F_c^2)/3$; for the 'observed' data only, R_1 = 0.057.

In the final difference map, the highest peak (*ca* 0.9 $eÅ^{-3}$) was near the Mg atom.

Scattering factors for neutral atoms were taken from reference (3). Computer programs used in this analysis have been noted above, and were run through WinGX (4) on a Dell Optiplex 780 PC at the University of East Anglia.

References

(1) Programs CrysAlisPro, Rigaku Oxford Diffraction Ltd., Abingdon, UK (2018).

(2) G. M. Sheldrick, Programs for crystal structure determination (SHELXT), *Acta Cryst.* (2015) A**71**, 3-8, and refinement (SHELXL), *Acta Cryst.* (2008) A**64**, 112-122 and (2015) C**71**, 3-8.

(3) *'International Tables for X-ray Crystallography'*, Kluwer Academic Publishers, Dordrecht (1992). Vol. C, pp. 500, 219 and 193.

(4) L. J. Farrugia, *J. Appl. Cryst.* (2012) **45**, 849–854.

Legends for Figures

Figure 1. View of the magnesium complex molecule, indicating the atom numbering scheme. Thermal ellipsoids are drawn at the 30% probability level.

Figure 2. View of the hydrogen-bonded dimer of the Mg complex.

Figure 3. The packing of molecules, viewed along the *c* axis. Molecules are linked in pairs through O-H…N hydrogen bonds about centres of symmetry at 0, ½, 1, etc.

Notes on the structure

The asymmetric unit, i.e. the unique unit, of the crystals is composed of a methanol-magnesium-phthallocyanine-like complex with several solvent molecules. The magnesium complex is well-defined and has been refined to convergence, Figure 1. The solvent molecules, probably all methanol molecules, are randomly disordered and lie in channels between the complex molecules. The refinement of the solvent region was limited to assigning partially occupied carbon atoms in sites where successive difference maps show electron density remaining; these ‘partial-carbon atoms’ were assigned occupancies which were refined in cycles alternately with their thermal parameters; the aim was to describe the solvent region with electron density which would relate to a network of solvent/methanol molecules, but no recognisable pattern was found.

The magnesium centre is five-coordinate with a square pyramidal configuration, Figure 1. The methanol ligand occupies the apical site, and the N_4 coordinating atoms of the phthalocyanine ring form a good plane; the magnesium ion is displaced 0.4081(14) Å from that mean-plane.

The unique bridging C-atom in the phthalocyanine ring, C(40), is bonded to a planar phenoxy group, hence to a decyl chain and terminal bromine atom; the carbon atoms of the all-*trans* C_{10} chain are close to planar and the bromine atom is not far from that plane. The hydroxyl group of the coordinated methanol ligand forms a good hydrogen bond to N(20) of a molecule related by a centre of symmetry, thus forming a hydrogen-bonded dimer about that centre.